Essays on Monetary Policy, Inflation and Financial Markets in the euro area

Aymeric Ortmans

université PARIS-SACLAY

Essays on Monetary Policy, Inflation and Financial Markets in the euro area

Essais sur la politique monétaire, l'inflation et les marchés financiers en zone euro

Thèse de doctorat de l'université Paris-Saclay

École doctorale n° 630: Droit, Économie, Management (DEM)

Spécialité de doctorat: Sciences Économiques

Graduate School : Économie - Management

Référent : Université d'Évry Val d'Essonne

Thèse préparée dans l'unité de recherche EPEE (Université Paris-Saclay, Univ Evry), sous la direction de **Fabien TRIPIER**, Professeur des universités

Thèse soutenue à Paris-Saclay, le 1er décembre 2023, par

Aymeric ORTMANS

Composition du jury

Membres du jury avec voix délibérative

Jérôme HÉRICOURT	Président
Professeur des universités, Université Paris-Saclay	
Laurent FERRARA	Rapporteur
Professeur d'économie internationale, SKEMA Business School	
Valérie MIGNON	Rapporteur
Professeur des universités, Université Paris Nanterre	
Giovanni RICCO	Examinateur
Professeur, Ecole Polytechnique et Université de Warwick	
Jean-Guillaume SAHUC	Examinateur
Chercheur conseiller senior, Banque de France	

THESE DE DOCTORAT

NNT : 2023UPASI010

université PARIS-SACLAY | ÉCOLE DOCTORALE Droit, Économie, Management (DEM)

Title: Essays on monetary policy, inflation and financial markets in the euro area

Keywords: ECB monetary policy; Euro ara; Business cycle; Inflation; Macroeconomic risks; Financial crises

Summary: This thesis is composed of three essays which analyze the implications of macroeconomic and financial risks for monetary policy, using the euro area as a laboratory.

Chapter 1 shows how the conduct of euro area monetary policy has evolved in the aftermath of the Great Recession of 2007-09 with respect to that implemented in the U.S., and what have been the macroeconomic effects of this shift. I use a vector autoregression with time-varying parameters to estimate a monetary policy rule with drifting response coefficients to inflation and real economic activity. The results show that the conduct of monetary policy in the euro area has evolved differently than in the U.S. after the 2008 crisis. Whereas the estimated U.S. policy rule does not suggest any significant change in the Fed's systematic reaction to macroeconomic fluctuations after 2008, euro area reaction function reveals important changes in ECB's monetary policy, which has considerably increased the weight it placed on stabilizing inflation. A counterfactual analysis shows that the shift in ECB monetary policy appears to be a key determinant of the level of inflation in the euro area at the ZLB, that would have suffered successive deflationary episodes from 2014 onward.

Chapter 2 studies the role of the ECB in stopping the spread of the coronavirus pandemic to financial markets in the euro area. We use non-linear local projections to measure the reaction of sovereign spreads to new COVID cases and examine how it evolved around the dates of ECB interventions in March 2020. The results show that despite the controversy generated by the "we are not here to close spreads" declaration of Christine Lagarde, the ECB actually stopped the spread of the pandemic-sparked crisis to the euro area sovereign debt markets on March 12, before the announcement of the PEPP and the conduct of market operations that occurred on March 18, leading to the reversal of sovereign spreads. A counterfactual analysis indicates that without ECB's interventions, sovereign spreads in the euro area would have reached levels

comparable to those observed during the 2010-12 sovereign debt crisis.

Chapter 3 assesses inflation differentials in the euro area, and how it should be assessed through the lens of risk of inflation. We aim at providing a more complete picture of inflation differentials across euro area countries by delivering time-varying measures of inflation risks dispersion. To do so, we construct measures of risk of inflation dispersion based on the cross-country standard deviation of predictive inflation distribution estimated with a quantile Phillips curve. We find that whereas the dispersion was concentrated on upside inflation risks until 2008, it has been stronger for the lower tail of the distribution after 2008. The results also show that inflation dispersion has been driven by successive episodes of downside and upside inflation risks over the post-COVID period. A counterfactual analysis highlights financial stress as being a key determinant of the dispersion of downside inflation risks, and supply chains disruptions a being an important driver of the dispersion of upside risk to inflation. Estimation results also reveal noticeable Phillips curves heterogeneity across countries, and underline the role of heterogeneous Phillips curve coefficients in the dispersion of inflation in the euro area.

université PARIS-SACLAY | ÉCOLE DOCTORALE Droit, Économie, Management (DEM)

Titre: Essais sur la politique monétaire, l'inflation et les marchés financiers en zone euro

Mots clés: Politique monétaire de la BCE; Zone euro; Cycle économique; Inflation; Risques macroéconomiques; Crises financières

Résumé: Cette thèse se compose de trois essais qui analysent les implications des risques macroéconomiques et financiers pour la politique monétaire, en utilisant la zone euro comme laboratoire.

Le chapitre 1 montre comment la conduite de la politique monétaire de la zone euro a évolué au lendemain de la Grande Récession de 2007-09 par rapport à celle mise en œuvre aux États-Unis, et quels ont été les effets macroéconomiques de cette évolution. J'utilise un modèle vecteur autorégressif avec des paramètres variables dans le temps pour estimer une règle de politique monétaire avec des coefficients dérivants de réponse à l'inflation et à l'activité économique réelle. Les résultats montrent que la conduite de la politique monétaire dans la zone euro a évolué différemment qu'aux États-Unis après la crise de 2008. Alors que la règle de politique américaine estimée ne suggère aucun changement significatif dans la réaction systématique de la Fed aux fluctuations macroéconomiques après 2008, la fonction de réaction de la zone euro révèle des changements importants dans la politique monétaire de la BCE, qui a considérablement accru l'importance accordée à la stabilisation de l'inflation. Une analyse contrefactuelle montre que le changement de politique monétaire de la BCE semble être un déterminant clé du niveau d'inflation dans la zone euro en ZLB, qui aurait subi des épisodes déflationnistes successifs à partir de 2014.

Le chapitre 2 étudie le rôle de la BCE dans l'arrêt de la propagation de la pandémie de coronavirus sur les marchés financiers de la zone euro. Nous utilisons des projections locales non-linéaires pour mesurer la réaction des spreads souverains aux nouveaux cas de COVID et examinons son évolution autour des dates d'interventions de la BCE en mars 2020. Les résultats montrent que malgré la controverse générée par la déclaration « nous ne sommes pas là pour réduire les spreads » de Christine Lagarde, la BCE a effectivement stoppé la propagation

de la crise déclenchée par la pandémie aux marchés de la dette souveraine de la zone euro le 12 mars, avant l'annonce du PEPP et la conduite des opérations de marché survenues le 18 mars, conduisant au retournement des spreads souverains. Une analyse contrefactuelle indique que sans les interventions de la BCE, les spreads souverains dans la zone euro auraient atteint des niveaux comparables à ceux observés lors de la crise de la dette souveraine de 2010-12.

Le chapitre 3 évalue les écarts d'inflation dans la zone euro, et la manière dont ils devraient être évalués à travers le prisme du risque d'inflation. Notre objectif est de fournir une image plus complète des écarts d'inflation entre les pays de la zone euro en fournissant des mesures variables dans le temps de la dispersion des risques d'inflation. Pour ce faire, nous construisons des mesures du risque de dispersion de l'inflation sur la base de l'écart type entre pays de la distribution prédictive de l'inflation estimée à l'aide d'une courbe de Phillips quantile. Nous constatons que si la dispersion était concentrée sur les risques d'inflation à la hausse jusqu'en 2008, elle a été plus forte pour la queue inférieure de la distribution après 2008. Les résultats montrent également que la dispersion de l'inflation a été alimentée par des épisodes successifs de risques d'inflation à la baisse au début de la crise du COVID et des risques d'inflation à la hausse au cours de la période post-COVID. Une analyse contrefactuelle souligne que les tensions financières sont un déterminant clé de la dispersion des risques d'inflation à la baisse, et que les perturbations des chaînes d'approvisionnement sont un facteur important de la dispersion des risques d'inflation à la hausse. Les résultats des estimations révèlent également une hétérogénéité importante des courbes de Phillips entre les pays et soulignent le rôle des coefficients hétérogènes de la courbe de Phillips dans la dispersion de l'inflation en zone euro.

Remerciements

Cette thèse doit beaucoup à toutes celles et ceux qui m'ont accompagné ces dernières années.

Mes premiers remerciements vont à mon directeur de thèse, Fabien Tripier, pour sa bienveillance, sa disponibilité, sa rigueur et sa curiosité intellectuelle. Son goût prononcé pour les questions de politique économique et sa capacité à y répondre en mêlant exigence scientifique et vulgarisation ont énormément contribué à cette thèse, et plus généralement à ma volonté de devenir un jeune chercheur.

Je tiens aussi à exprimer toute ma reconnaissance envers Laurent Ferrara et Valérie Mignon, qui m'ont fait l'immense honneur de rapporter cette thèse. Leurs commentaires avisés et bienveillants ont été plus que précieux à l'amélioration de ce manuscrit. Merci également aux autres membres du jury, Jérôme Héricourt, Giovanni Ricco et Jean-Guillaume Sahuc, dont l'expertise et l'expérience ont permis des discussions passionnantes sur les questions traitées dans cette thèse.

J'aimerais remercier les personnes qui, à travers leurs échanges et leur disponibilité, m'ont permis de mener ce travail à bien. Merci à Paul Hubert pour ses conseils et ses relectures, et ce depuis mon passage à l'OFCE. Merci à Stéphane Lhuissier, là aussi pour sa bienveillance et sa disponibilité. Cette thèse leur doit beaucoup. Merci aussi à ceux dont les remarques et l'aide ont été cruciales lors de cette dernière année. Merci à Nicolas Groshenny, pour nos longues discussions sur la politique monétaire et sa gentillesse. Merci à Eric Mengus, de m'avoir aidé à travailler et à retravailler mon speech pour les entretiens.

La réalisation de cette thèse n'aurait jamais été possible sans toutes les personnes que j'ai eu la chance de côtoyer tout au long de ces années. Tout d'abord, je remercie Brendan Harnoys-Vannier et Jean-Bernard Chatelain de m'avoir orienté, plus ou moins volontairement, vers la voie du doctorat. Ensuite, au laboratoire EPEE, j'aimerais commencer par remercier les directeurs successifs depuis mon arrivée, d'abord Eleni, puis Grégory, dont la porte est toujours restée ouverte. Merci aussi à Patricia, puis à Christelle surtout, pour leur gentillesse

et leur disponibilité. Leur aide plus que précieuse sur les points logistiques et administratifs a été cruciale à la préparation de cette thèse. Merci à Samuel pour avoir géré les points informatiques de dernière minute avec autant de patience et de professionnalisme. Merci à celles et ceux du labo qui ont toujours été à l'écoute et de bon conseil. Je tiens tout d'abord à remercier Damien, dont la bonne humeur a su faire oublier mes questionnements et mes coups de gueule. Merci à Fabrice et Marlène: votre écoute, votre aide et vos conseils avisés, notamment pendant la dernière année, ont énormément contribué à la finalisation de cette thèse. Merci à Michel Guillard, Jean De Beir et Margarita López Forero, qui, chacun à sa manière, ont su animer la vie du labo et du département dans le cadre de Paris-Saclay. Enfin, j'aimerais exprimer ma reconnaissance envers mes amis doctorants, avec qui nous avons partagé de nombreux déjeuners, verres, et parfois nos doutes. La route a été longue, mais elle valait le coup en votre compagnie. Merci tout d'abord à Sylvain et Ibrahima, mes ainés de thèse, de m'avoir si bien accueilli à l'EPEE. Merci à mon ami Thomas, pour sa complicité et ces moments passés ensemble à discuter aussi bien des implications financières du risque climatique que du match de la veille. Merci Juho, collègue et ami de ce bureau que nous avons partagé pendant cinq ans. J'ai beaucoup appris de nos discussions, y compris sur la Finlande bien évidemment. Enfin, merci aux doctorantes et aux doctorants de Paris-Saclay. Vous avez, ici encore, été là, dans les bons comme dans les moments plus difficiles. Merci à Juan Daniel, Malak, Mathilde, Imen, et Raphaël.

Ces années de thèse ont aussi été l'occasion pour moi de faire de belles rencontres en dehors même du cadre de Paris-Saclay. Je tenais à exprimer toute ma gratitude envers Haroon Mumtaz, qui m'a accueilli en visiting outre-Manche, à Queen Mary. Merci pour ses conseils et sa disponibilité sur le campus, dans une période marquée par la pandémie. Merci aussi de m'avoir accompagné pendant les années qui ont suivi mon séjour londonien, qui n'aurait jamais été aussi heureux sans mes amis doctorants sur place. Merci infiniment à Leo, Chiara, Gabriel Chaves, Ezgi, Andrea, Giulia, Laura, Paula, Giacomo, Eugenio, Gabriel Bracons, Sofia, Elisabet, Ioannis. Enfin, j'aimerais remercier celles et ceux qui ont accompagné pendant mes deux dernières années de thèse au département d'économie de Sciences Po, notamment les irréductibles doctorants en macroéconomie monétaire: Alaïs, Diego et Naomi. Merci pour leur accueil dans cet endroit mythique que représente les Combles de la rue des Saints-Pères. Merci aussi aux professeurs Emeric Henry et Nicolas Cœurdacier de m'avoir fait confiance et d'avoir su prêter une oreille attentive à la préparation des cours.

Parmi les personnes qui me sont chères, il m'est impossible de ne pas penser à ma famille, qui m'a toujours si bien entouré, et ce depuis mon plus jeune âge. Mille mercis à mes parents, pour leur amour et leur soutien, si précieux depuis toujours, au-delà même de ces années de thèse. Merci aussi à mon frère, Geoffroy, et à mes sœurs, Astrid et Bertille, qui m'ont tant appris et tant donné, là encore depuis tant d'années. Cette thèse n'aurait jamais été possible sans vous tous. J'aimerais aussi remercier ma grand-mère, Granny, pour ses encouragements tout au long de ces années de scolarité. Gérard, merci à toi aussi, pour ton écoute et l'exemple de rigueur que tu incarnes. Enfin, j'ai une pensée émue pour ma grand-mère Monique et mon cousin Xavier: le jeune étudiant que j'étais à l'époque ne s'attendait probablement pas à un si long chemin, mais le souvenir de nos conversations m'a toujours redonné la force d'aller jusqu'au bout. Cette thèse est aussi la vôtre.

Aussi, j'aimerais remercier chaleureusement mes amis les plus proches, compagnons de route fidèles de la première heure, et témoins de mes doutes. Merci à toute la Clique–Anthelme, Cyprien, Gabriel, Jules, Louis, Rémi, Séverin, et Thomas–d'avoir été présents quand il le fallait, en plus d'avoir rendu mon quotidien plus léger, que ce soit sur un terrain de foot ou lors de nos soirées. Ces années de thèse n'auraient pas non plus été les mêmes sans mes amis perrosiens–Émile, Lucie, Nils et Yann–qui m'accompagnent depuis tant de belles années, aussi bien dans la vie parisienne que lors de nos virées bretonnes sur la Côte de Granit Rose, éternel point de ralliement d'une amitié qui m'est si chère. Je tiens aussi à remercier mon pote Loulou, qui n'a cessé d'être présent depuis nos premières années, et dont la contribution a cette thèse est bien plus importante qu'il ne l'imagine. Caroline, merci à toi aussi: si tes qualités d'écoute et d'empathie ont été importantes pour moi, nul doute qu'elles le seront tout autant dans ta vie de jeune maman. Un grand merci aussi à mes cousins Fleur, Louis et Matthieu. Votre esprit de famille, votre convivialité et votre humour ont énormément compté pendant toutes ces années.

Enfin, mes derniers mots vont à celle dont la force et la tendresse m'ont permis de trouver les ressources nécessaires à l'accomplissement de ce doctorat. Isaure, je n'aurais pas imaginé une seule seconde que ces dernières années de thèse soient aussi les plus heureuses. Merci.

Contents

List of Figures

List of Tables

Introduction

The euro area has evolved considerably since its creation in 1999. As an important feature of the Economic and Monetary Union (EMU), the euro—as a common currency—was initially adopted by eleven countries to foster economic cooperation, facilitate firms' cross-border trade, bring economic stability, and improve consumers' well-being. Since then, the euro area has also greatly expanded through a series of enlargements to twenty countries as of January 2023. However, along with the above-mentioned advantages offered by the adoption of a single currency and despite prolonged periods of economic expansion, the Eurozone has experienced an increasing number of crises of various kinds over the last few years. The downturn in the U.S. housing market and the collapse of Lehman Brothers in September 2008 led to the so-called Global Financial Crisis—hereafter, GFC—characterized by unprecedented financial turmoil all around the world, including the euro area. In early 2010, the sovereign debt crisis, triggered by the Greek crisis, was marked by soaring borrowing costs in all euro area member countries, threatening the European monetary union as a whole. Ten years later, in late 2019, the health and sanitary crisis caused by the COVID-19 pandemic outbreak has generated a noticeable episode of turbulences in the global, and inevitably, the European financial markets. More recently, in 2021, the world economy has also faced a global energy crisis, resulting in record high levels of inflation in the euro area.

Importantly, each of those crises has turned into substantial financial downturn, giving rise to downward pressure on real economic activity, and sparking (a risk of) recession in the euro area. In this context, both macroeconomic and financial risks had huge policy implications, especially regarding monetary policy. To face new challenges posed by this risky and uncertain economic environment, the European Central Bank (ECB) needed to adapt its policy framework and hence reviewed its strategy in July 2021. The points discussed below closely articulate with some of the key elements raised in ECB's strategy review, namely the conduct

of monetary policy at the zero lower bound—hereafter, ZLB—in an inflation targeting framework, the importance of monetary policy communication and the inclusion of financial stability considerations, or the need for a regular and robust assessment of the risks to price stability and the macroeconomic outlook. Each of them is backed by seminal academic papers that gave the ground for a new reflexion to help improving the conduct and the effectiveness of monetary policy. More specifically, the aim is to use this literature to introduce the topics discussed in this thesis, in line with the above-mentioned elements specified in the strategy review of 2021. The present thesis addresses three distinct themes, each depicting a major turning point in euro area monetary policy over the last years.

In the wake of periods of high macroeconomic and financial instability, lots of central banks needed to adjust their policy framework. In the euro area, the deteriorating macroeconomic environment during troubled times has forced the ECB to take major policy decisions in order to fulfill its mandate of price stability. This has induced the implementation of accommodative policies, mainly through lower interest rates, and non-standard monetary policy measures such as asset purchases. A large part of academic research in monetary economics has been devoted to studying the reaction of the central bank to macroeconomic fluctuations.

Evidence of central bank's systematic response to economic conditions has been raised by Professor John Taylor in his landmark paper of 1993 (see Taylor, 1993). Taylor proposes a specification that describes U.S. monetary policy between 1987 and 1992. According to the rule, the Federal Reserve (Fed) sets its policy rate in response to inflation rate and economic activity measured as the percent deviation of real GDP from a long-term trend. Since then, the *Taylor rule* has become a popular tool to gauge how central banks systematically respond to inflation and output fluctuations. Furthermore, the systematic component of monetary policy has been shown to change over time. Clarida et al. (2000) study how the estimated monetary policy reaction function differed before and after Paul Volcker's appointment as Fed Chair in 1979. Their results suggests that the Volcker-Greenspan rule has been highly sensitive to changes in inflation and then stabilizing, compared to the pre-Volcker rule.

The systematic component of monetary policy has been broadly used in multivariate analysis such as Vector Autoregresssions (VARs) models. Estimating central banks' reaction function in such frameworks provides a broader and more accurate picture of the role of monetary policy in macroeconomic fluctuations. In the spirit of the previous paper, the question of changes in

systematic monetary policy over time has also been raised in VAR models, which bring considerable flexibility regarding estimates of regime-dependent policy rule coefficients. Seminal works using such methodologies include Cogley and Sargent (2005), Primiceri (2005), Sims and Zha (2006a,b).

Previous literature underlines how changes in central banks' systematic responses to macroeconomic conditions could avoid large fluctuations. However, the growing and evolving role of monetary policy as a stabilization tool has also been widely studied through financial markets reaction to central banks' policies. Since financial markets have become the cornerstone of the global economic development over the last decades, their fluctuations matter for the transmission of monetary policy. In this respect, central banks' policy communication and their impact on financial markets now represent a key feature of the conduct of monetary policy, especially during financial downturns.

Most of this literature has been devoted to the analysis of asset price movements in a time window around monetary policy announcements. The economists Timothy Cook and Thomas Hahn were among the first to shed light on this topic in their benchmark paper of 1989 (see Cook and Hahn, 1989). They measure the reaction of market interest rates on days of changes in the Fed's policy instrument in the period from September 1974 to September 1979, and find that target changes significantly affect interest rates all along the yield curve, with larger movements in short-term rates.

Then, the effects of monetary policy on asset prices has been widely studied in the literature using high-frequency event-study analysis. A large strand of the literature started with Kuttner (2001) and including Bernanke and Kuttner (2005) and Gürkaynak et al. (2005) assesses the response of asset prices to financial market surprises around key monetary policy announcements. These papers highlight the major role played by communication in monetary policy making, mainly through its direct effect on financial markets.

Recent evidence of euro area monetary policy using these techniques include Altavilla et al. (2019), Andrade and Ferroni (2021), Leombroni et al. (2021).

Assessing macroeconomic and financial risks is essential for central banks, whose policy decisions mostly depend on current and future economic conditions. The successive crises that have affected the world economy since 2008 have encouraged academics and policy-makers to

rethink the role of monetary policy in business and financial cycles fluctuations. Precisely, it aims at considering a new monetary policy framework based on the central bank's assessment of the risks to the economic outlook.

This relates to the concept of *risk-management approach to monetary policy-making* developed by the then Fed Chair, Alan Greenspan, in 2004 (see Greenspan, 2004). For the policy-makers, it consists in identifying the sources of risk and uncertainty surrounding the economy, quantifying those risks, and assessing the associated costs that are likely to threaten central banks' ability to achieve its goals. This concept has also been used in the context of financial crises by Mishkin (2009), and in the context of ZLB on nominal interest rates Evans et al. (2015). Interestingly, each of those papers define the risk-management approach as the way the policy-maker takes into account all future possible outcomes in its decision.

Hence, measuring macroeconomic tail-risks by assessing the full distribution of future macroeconomic series is crucial for the policy-makers. The close interplay between growth vulnerability and financial stress supports the view of central banks as risk managers, assessing the balance of macroeconomic risks based on the range of possible outcomes. In this respect, Adrian et al. (2019) use quantile regressions to measure the predictive power of financial conditions for real economic activity. Their main results point a nonlinear relationship between financial conditions and the conditional distribution of GDP growth. While the estimated upper quantiles of distribution of future GDP growth are stable, the lower quantiles exhibit are strongly responsive to current financial conditions.

Evidence on *growth-at-risk* in the euro area can be found in Figueres and Jarociński (2020), Lhuissier (2022), and Ferrara et al. (2022).

Today, monetary policy is at the crossroads in the euro area, and its role as a stabilization policy tool has never been so essential. Over the years, the ECB has shown its ability to stimulate inflation in order to maintain its primary objective of price stability. Additionally, ECB's interventions has proved to be effective in fending off financial turmoil, especially since the GFC. The growing link between financial stability and macroeconomic performance in the euro area has also rationalized ECB's increased emphasis on managing risks when it comes to implementing monetary policy.

My thesis lies at the intersection of these three distinct facts and empirically shows the need for the ECB to constantly adapt the design of its monetary policy operational framework to

face new challenges. The thesis is divided into three chapters. Each of the chapters illustrates an episode which represented a challenge for the ECB with important implications for monetary policy in the euro zone. Of course, this thesis does not cover all the challenges that the ECB has faced in recent years. The first chapter studies the macroeconomic effects of changes in the conduct of monetary policy in the U.S. and the euro area since the Great Recession. The second chapter investigates the role of ECB's announcements in the early stage of the COVID-19 crisis in the evolution of the spread of the pandemic to the European sovereign debt market. The third chapter assesses the extent to which inflation differentials in the euro area should be addressed through the lens of inflation risks and its main determinants.

The first chapter is single-authored and is named '*Evolving Monetary Policy in the Aftermath of the Great Recession*'. It raises the question of the evolution of monetary policy during and after the Great Recession. Worsening macroeconomic conditions and inflation risks forced central banks to decrease drastically their main policy rates after the GFC. Hitting the ZLB on short-term nominal interest rates, lots of them decided to use a set of new tools, known as unconventional monetary policies. The implementation of unconventional measures have been justified by many central banks as a means to reach price stability and foster economic activity by going beyond the traditional use of short-term interest rates as the main policy instrument. In this context, this study attempts to address the challenge posed by the ZLB and focuses on the evolution of monetary policy over a sample period including the post-GFC period, and hence unconventional times. The evolution of monetary policy is captured by changes in central banks' rule-like behavior, determined by possible shifts in central banks' reaction to inflation and real activity. This *Taylor rule-like behavior* has been shown to constantly change over time, and has been often used to describe the evolution of Federal Reserve's behavior during the Great Moderation and Volcker's disinflation in the 1980s. However, there is little evidence of shifts in monetary policies after the GFC, and especially in the euro area. Has the conduct of Fed and ECB monetary policy evolved in the aftermath of the Great Recession? How has it affected macroeconomic performances in the United States and the euro area? As a whole, this chapter investigates the extent to which changes in central banks' behavior may explain monetary policy decisions since the Great Recession by comparing the ECB with the Fed, and how it may have affected differently macroeconomic performances in the U.S. and the euro area.

To do so, I follow Belongia and Ireland (2016) and use a small-scale time-varying parameter vector autoregressive (TVP-VAR) model with stochastic volatility combined with sign restrictions on impulse responses to estimate a Taylor-type rule with drifting coefficients. Thus, time-variation in the parameters of the policy rule captures changes in the whole behavior of the central bank. More precisely, it allows to assess expected changes in the conduct of monetary policy through drifting response coefficients to inflation and real economic activity. Also, and importantly, to get rid of flat rates challenging monetary policy rule estimations in the ZLB era, I use an estimated shadow rate as a proxy for the short-term nominal interest rate that captures the overall stance of monetary policy at the ZLB taking into account unconventional policy actions. Hence, a shadow Taylor rule with time-varying parameters is estimated on a sample period including the ZLB. The model is estimated on quarterly data starting from 1960 in the U.S., and 1971 in the euro area. The sample period of estimation ends before the COVID crisis, in end-2019.

This paper is close to Debortoli et al. (2020) and Ellington (2022) who also estimate a structural VAR with time-varying coefficients including a shadow rate to deal with the evolution of monetary policy during the post-2008 decade. However, the present paper departs from previous studies in several ways. Since Debortoli et al. (2020) and Ellington (2022) focus exclusively on U.S. monetary policy, they do not compare the Fed and the ECB, as I do. As a whole, the contribution of my paper mainly consists in providing further evidence of the evolution of monetary policy in the U.S. and in the euro area before and after the Great Recession. Surprisingly, and to my knowledge, no attempt has been made to try to compare changes in U.S. and euro area monetary policies over a long period of time including the ZLB. Moreover, the present paper investigates the evolution of (non)-systematic components of ECB and Fed monetary policy, and hence provides further evidence on rule-based monetary policy in the U.S. and in the euro area after 2008. Focusing on changes in the conduct of monetary policy through the lens of time-varying reaction function allows to go further into the empirical analysis. Indeed, another contribution of this paper also lies in the conduct of an in-depth counterfactual analysis to gauge the macroeconomic effectiveness of changes in monetary policies.

The results show that the conduct of monetary policy in the euro area has evolved differently than in the U.S. after the 2007-08 financial crisis. Despite a slight decrease in the long-run response to inflation, the estimated U.S. policy rule does not suggest any significant change

in the Fed's systematic reaction to macroeconomic fluctuations after 2008. The results rather tend to highlight the role of the non-systematic component of Fed's monetary policy: U.S. monetary policy shocks explain a relatively small share of inflation and output fluctuations but a non-negligible part of the evolution of the policy rate over the period. These departures from the rule-based monetary policy are interpreted as Fed's discretionary policy-making. On the other hand, the estimated monetary policy rule in the euro area reveals that the ECB has considerably increased the weight it placed on stabilizing inflation, and has also regularly but briefly departed from the rule-like behavior since 2008. These results suggest important changes in the conduct of ECB's monetary policy, mainly through its systematic component. A counterfactual analysis shows that this shift appears to be a key determinant of the level of inflation in the euro area at the ZLB, that would have suffered successive deflationary episodes from 2014 onward.

Those results raise some important policy implications. First, model-based inflation targets highlight the need for adapting inflation targeting framework, especially in the euro area. Second, counterfactual results highlight the benefits of adopting a rule-based approach to monetary policy-making.

The second chapter of the thesis, '*COVID-induced sovereign risk in the euro area: When did the ECB stop the spread?*', is a joint work with my thesis supervisor Fabien Tripier, and studies the role of ECB's policy response to the coronavirus pandemic. Started officially in China in end-December 2019, the COVID-19 virus pandemic reached Europe in early 2020. As a threat to the economy, the rapid spread of the virus led to a sizeable financial turmoil, and especially in Italy, the most heavily affected European country. On March 12, the ECB announced a set of monetary policy measures to support the economy in the wake of the pandemic. The announcement of those measures gave rise to controversy over ECB president Christine Lagarde's announcement that the ECB would certainly use "all the flexibilities that are embedded in the framework of the asset purchase programme", but also that the central bank was "not here to close spreads". This last sentence has been widely cited as a communication failure, contrasting with the famous "whatever it takes" of her predecessor Mario Draghi. On March 18, the ECB conducted an exceptional longer-term refinancing operation (LTRO) to provide liquidity and announced the launch of a massive intervention program known as the Pandemic Emergency Purchase Programme (PEPP), which led to a turnaround in sovereign rates and a reboot in

stock prices. While the COVID-19 pandemic continued to spread in Europe, its transmission to financial markets stopped in Italy and the rest of the euro area. What was the role of these successive ECB interventions in stopping the spread of the pandemic to financial markets? What would have happened without these interventions? As a whole, this chapter investigates how ECB's policy announcements stopped the spread of the COVID-19 pandemic to the euro area sovereign debt market.

To answer those questions, we measure the reaction of sovereign spreads to new COVID cases and examine how it evolved around the time of ECB interventions. Using local projection method developed by Jordà (2005), we measure the effect on impact and over a five-day ahead horizon. We then use state-dependent local projections following Ramey and Zubairy (2018) by splitting the sample period of estimation into two subsamples divided at a reference date falling between March 5 and March 25. This state-dependent framework offers a flexible approach to study possible non-linearities in the sovereign spread reaction to the pandemic. Importantly, it allows to run split sample estimates according to dates which include key ECB's policy interventions of March 12 and March 18. We include national stock indices and both country and time fixed effects to capture an unbiased measure of the time-varying impact of COVID-19 severity on euro area sovereign risk. Both linear and non-linear models are estimated on daily data over the sample period from January 2 to May 29, 2020. Our panel includes fifteen euro area countries: Austria, Belgium, Cyprus, Finland, France, Greece, Ireland, Italy, Lithuania, Malta, Netherlands, Portugal, Slovakia, Slovenia, and Spain.

This paper provides empirical evidence of Arellano et al.'s (2023) theoretical insights on the link between the severity of the pandemic and the increasing risk of default in emerging economies. In the paper, we explore the effect of the pandemic outbreak on sovereign risk in a panel of euro area countries. From this perspective, this paper is close to Augustin et al. (2022) who study the sensitivity of sovereign default risk to the intensity of the coronavirus pandemic in developed countries, including the euro area. However, we depart from the latter paper by considering the dynamic response of the sovereign debt and the stock markets to the pandemic. Moreover, our purpose is to assess the break in the transmission of the pandemic to the euro area financial markets. More precisely, we track how financial markets' reaction to the COVID-19 pandemic has changed according to ECB's policy decision timeline. Additionally, we assess possible spillovers from the pandemic outbreak in Italy—the most affected European country in the early stage of the pandemic—to domestic financial markets. Finally, based on

our estimation, we provide a counterfactual analysis by simulating the path of sovereign spreads that would have occurred without the change in the sensitivity of bond spreads to the COVID crisis.

The results show that despite the controversy generated by the "we are not here to close spreads" declaration of Christine Lagarde, the ECB actually stopped the spread of the pandemic-sparked crisis to the euro area sovereign debt markets on March 12, before the announcement of the PEPP and the conduct of market operations that occurred on March 18, leading to the reversal of sovereign spreads. Our results support the view that ECB's unprecedented monetary policy responses to the COVID-19 pandemic were very effective in disrupting the explosive path of sovereign default risk within eurozone countries. Indeed, a counterfactual analysis indicates that without these interventions, sovereign spreads in the euro area would have reached levels comparable to those observed during the 2010-12 sovereign debt crisis.

The results highlight some policy implications for central bankers, especially regarding the effectiveness of central bank's communication as a powerful tool to mitigate financial downturn. However, the COVID crisis had huge and long lasting consequences for public finances, and raised additional challenges for policy-makers in Europe and all around the world in managing the public debt induced by the COVID crisis.

The third chapter is entitled '*The Risk of Inflation Dispersion in the Euro Area*' and has been co-written with Stéphane Lhuissier and Fabien Tripier. It investigates the topic of inflation differentials in the euro area. With the return of global inflation in early 2021, euro area inflation has hit all-time high levels month after month. This has been accompanied by large heterogeneity of inflation rates across euro area countries. The dispersion of the conditional mean of inflation across countries is a well-known phenomenon, but the study of the divergences in the tails of inflation distribution remains completely unexplored. Looking at historical data, we first document that the dispersion of inflation rates across euro area member states varies over time. A second stylized fact indicates that the tails of inflation historical distribution are more dispersed than the median. As for inflation itself, it is critical for the policy-makers to know what type of tail risks (upside or downside) are causing the dispersion of inflation, especially in a monetary union. The conduct of a single monetary policy, with a common inflation target, could be costly for countries experiencing extreme inflation rates. From this perspective, we think that inflation differentials in the euro area deserve further consideration,

and we propose to go beyond the mean of inflation dispersion. We then try to answer the following questions of interest for the policy-makers: Where does the dispersion of inflation come from? What are the main determinants of the risk of inflation dispersion? In this paper, we aim at providing a more complete picture of inflation differentials across euro area countries by delivering time-varying measures of inflation dispersion associated to the different quantiles of predictive inflation distributions, and at identifying their main drivers.

To construct our measures of risk of inflation dispersion, we proceed in two steps. First, we compute the predictive inflation distribution at the country level by estimating a quantile Phillips curve. The methodology employed closely follows López-Salido and Loria (2022), who also use Phillips curve quantile regressions based on Adrian et al.'s (2019) seminal work dealing with U.S. GDP growth. As in aforementioned papers, conditional quantiles vary over time according to the evolution of key economic and financial variables considered as being inflation predictors, including past and expected inflation rates, unemployment gap, financial stress, oil inflation, and supply chain pressures. Second, for each date, we compute the standard deviation of quantiles across countries as a measure of dispersion. By looking at the 10^{th} and the 90^{th} quantiles, we can then evaluate the cross-country dispersion of inflation-at-risk at the bottom (i.e., risk of low inflation or deflation) and at the top of the distribution (i.e., risk of excessive inflation), respectively. The model is estimated on monthly data over the sample period from January 1999 to January 2023. Our panel includes the twelve first euro area countries: Austria, Belgium, Finland, France, Germany, Greece, Ireland, Italy, Luxembourg, Netherlands, Portugal, and Spain.

Our paper is thus close to López-Salido and Loria (2022) whose approach builds on the concept of Inflation-at-Risk—thereafter, IaR—developed earlier by Andrade et al. (2014). In the spirit of Adrian et al. (2019) who assess how financial conditions affect the predictive distribution of real GDP growth in the U.S., López-Salido and Loria (2022) provide an in-depth analysis of the evolution and the determinants of inflation tails both in the U.S. and the euro area. However, we go further by running quantile Phillips curve estimates for each euro area country included in our sample. We then compute the dispersion of inflation risks by considering cross-country differences in the tails of national predictive inflation distribution.

Tracking the dispersion of inflation tail risks over the sample period of estimation, we find that the dispersion was concentrated on upside inflation risks until 2008. Our measures of dispersion then indicate that it has been stronger for the lower tail of the distribution after

2008. The results show that inflation dispersion has been driven by successive episodes of downside inflation risks at the early stage of the COVID crisis and upside inflation risks over the post-COVID period. A counterfactual analysis highlights financial stress as being a key determinant of the dispersion of downside inflation risks during the post-2008 decade. On the other hand, the results also suggests that the disperison of upside inflation risks observed during the post-COVID era would have been much lower without supply chains disruptions. Estimation results also reveal huge Phillips curve heterogeneity across countries, and underline the role of heterogeneous Phillips curve coefficients in the dispersion of inflation across euro area countries.

Previous results stress the need for the policy-makers to take into account inflation-at-risk when assessing inflation differentials across countries in a monetary union. The methodology used in this paper is also useful for identifying the determinants of the evolution of inflation dispersion over time, which are shown to be different from one tail of inflation distribution to the other. Overall, disregarding the risk of inflation and its origins could seriously jeopardize central bankers' ability to face the challenge posed by inflation differentials in a monetary union.

Chapter I

Evolving Monetary Policy in the Aftermath of the Great Recession

Abstract. *A Taylor-type rule is estimated using a time-varying parameter vector autoregressive model to assess changes in the conduct of monetary policy since the Great Recession. Based on U.S. and euro area data, the results suggest different evolution across monetary policies after the 2007-08 financial crisis. Whereas the estimated U.S. policy rule tends to support the view of a discretionary Fed's policy, empirical investigation in the euro area reveals a more aggressive monetary policy response towards inflation stabilization. A counterfactual analysis shows that this shift in ECB's systematic component has been crucial to avoid successive deflationary episodes in the euro area.*

> *"My colleagues on the FOMC and I are regularly reviewing the asset purchase program in light of incoming information, and* ***we will adjust the program as needed to promote our statutory mandate of maximum employment and stable prices****."*
> Yellen (2011)

> *"As the scope for further interest rate cuts was now limited, it became increasingly clear that* ***our reaction function needed to evolve to address these new challenges****."*
> Draghi (2019)

I.1 Introduction

Central banks are in the spotlight since the 2007-08 financial crisis and the resulting 'Great Recession'. The global economic downturn spurred the main central banks to take drastic decisions, as cutting short-term interest rates to zero. Hitting the so-called zero lower bound (hereafter ZLB) on nominal interest rates, lots of them decided to use a large set of new monetary policy tools, including negative interest rate policy (NIRP), asset purchases from the open market–known as quantitative easing (QE), lending facilities to financial institutions, or forward guidance (FG) to communicate about the path of future short-term interest rates. Those unconventional measures have been conducted to foster economic activity by going beyond the traditional use of nominal short-term interest rates as the main policy instrument. By focusing on the evolution of monetary policy over a sample period including unconventional times, this study attempts to address the challenge posed by the ZLB and investigates how the conduct of monetary policy has evolved in terms of reaction to its fundamental economic objectives and discretionary decisions after the 2007-08 financial crisis.

As depicted in Figure I.1.1, policy rates and central banks' balance sheets have experienced tremendous changes since the pre-crisis era. Notwithstanding target nominal interest rates near or at zero, explosive balance sheets show how the Federal Reserve and the European Central Bank (hereafter Fed and ECB, respectively) kept acting strongly to lower long-term interest rates during the ZLB, for the purpose of stimulating the real economy.[1] However, this figure also highlights the difference in the timing of monetary policy decisions between the U.S. and the euro area. While the Fed has reacted quickly by continuously decreasing the fed funds target rate from 5.25% in August 2007 to 0.125%–its lowest level–in December 2008, the ECB decreased the main refinancing rate from 4.25% in September 2008 to reach zero only in March 2016, after having temporarily increased it in July 2008 and April 2011. The contrast is even starker when comparing the path of balance sheets that mostly reflects the implementation of unconventional monetary policies both in the U.S. and in the euro area.

Despite their exceptional nature, and as stated by then-Fed Vice-Chair Janet Yellen, these policies have been launched in order to pursue the standard objectives of maximum employment and stable prices. However, worsening macroeconomic conditions and unprecedented downside inflation risks have posed serious challenges for the conduct of monetary policy at

[1] The narrative and the timing of Fed and ECB unconventional monetary policies are detailed in Section I.3.

Figure I.1.1 – Policy rates and balance sheets

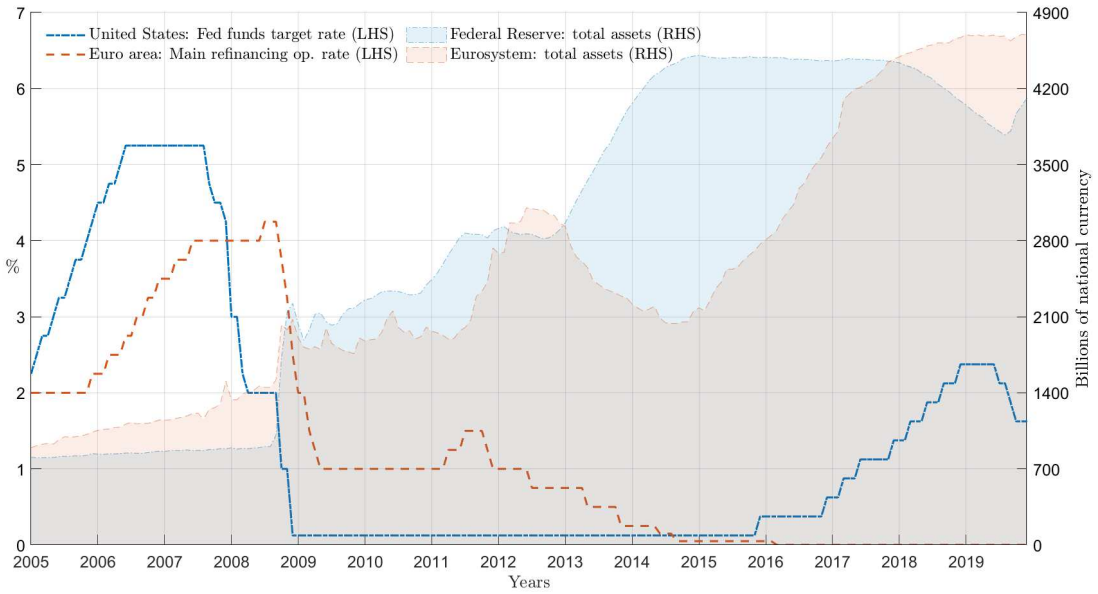

Note: Both policy rates are given in percentage (left-hand side). Central banks' total assets are given in billions of U.S. dollars for the Federal Reserve, and in billions of euros for the Eurosystem (right-hand side).
Source: Monthly data from Federal Reserve and European Central Bank.

the ZLB. In the U.S., the Fed has taken a series of unconventional measures starting from 2008 and 2009 "to provide further support for the economic recovery while maintaining price stability".[2] On the other hand, and despite growing concerns about economic growth, the focus was more on inflation in the euro area. In 2015, the ECB has expanded the amount of asset purchases mentioning that it will be conducted until reaching a "sustained adjustment in the path of inflation", consistent with ECB's primary objective of price stability.[3] Therefore, the implementation of U.S. and euro area monetary policy may have evolved in a sense that both central banks could have adapted their response to changing macroeconomic conditions after the crisis, in line with the declaration of then-ECB President Mario Draghi reported above. How has ECB monetary policy differed from that of the Fed since the Great Recession? How has it affected macroeconomic performances in the U.S. and in the euro area?

The present paper draws on the seminal work of Taylor (1993) and the well-known 'Taylor rule', according to which the central bank sets the policy rate considering inflation and output fluctuations. Since then, a huge literature has emerged to give further insights into central banks' behavior.[4] As a whole, this paper investigates to which extent changes in ECB and

[2]See Bernanke's (2010) remarks at Jackson Hole.
[3]See the introductory statement to ECB's January 22, 2015 Press Conference.
[4]Bernanke and Mishkin (1992) use the expression "central bank behavior" to mention both the conduct and the effectiveness of monetary policy. In the spirit of the standard Taylor rule, central bank's behavior may

Fed's behavior may have explained monetary policy decisions since the Great Recession, and how it may have influenced inflation and economic growth. To do so, I use a small-scale time-varying parameters vector autoregressive (TVP-VAR) model with stochastic volatility to estimate a Taylor-type rule with drifting coefficients. Thus, time-variation in the parameters of the policy rule captures changes in the whole behavior of the central bank. More specifically, it allows to assess not only expected changes in the conduct of monetary policy through drifting Taylor rule coefficients, but also unexpected changes of monetary policy through shifts in the volatility of monetary policy shocks. Also, and importantly, to get rid of flat rates challenging monetary policy rule estimations in the ZLB era, I use the shadow rate constructed by Wu and Xia (2016) as a proxy for the short-term nominal interest rate that captures the overall stance of monetary policy at the ZLB taking into account unconventional policy actions. Hence, a shadow Taylor rule with time-varying parameters is estimated on a sample period including the ZLB.[5]

Estimation results show that the conduct of monetary policy in the euro area has evolved differently than in the U.S. after the 2007-08 financial crisis. Despite a slight decrease in the long-run response to inflation, the estimated U.S. policy rule points no noticeable change in the Fed's reaction to macroeconomic fluctuations after 2008. In fact, the results highlight the role of the non-systematic component of Fed's monetary policy: U.S. monetary policy shocks explain a relatively small share of inflation and output fluctuations but a non-negligible part of the evolution of the policy rate over the period. These departures from the rule-based monetary policy are interpreted as Fed's discretion in policy making. On the other hand, the estimated monetary policy rule in the euro area reveals that the ECB has considerably increased the weight it placed on stabilizing inflation and has also regularly but briefly departed from the rule-based behavior since 2008. These results suggest important changes in the conduct of ECB's monetary policy, mainly through its systematic component.

A counterfactual analysis shows that this shift in the systematic component of monetary policy appears to be a key determinant of the level of inflation in the euro area at the ZLB,

be defined by its emphasis on stabilizing inflation and output, but also by its willingness to depart from the behavior prescribed by the policy rule. More formally, the word "behavior" is used here to refer to Taylor rule coefficients on the one hand, and to (the volatility of) monetary policy shocks on the other hand.

[5]See pioneering papers using shadow rates in VARs (Wu and Xia, 2016) or DSGE models (Wu and Zhang, 2019). Based on the latter paper, the relevance of shadow Taylor rules as a description of monetary policy at the ZLB is discussed in Online Appendix I.B (Section I.3 contains more references). See also recent papers using SVARs with an occasionally-binding constraint that generates a censored nominal interest rate as a dependent variable (Aruoba et al., 2022, Mavroeidis, 2021, among others). More references are given below.

that would have suffered deflationary episodes from 2014:3 to 2016:4 and starting from 2019:3 without any change in ECB's response to macroeconomic conditions after the 2007-08 crisis. However, the situation could have been even worse when ignoring the role of the non-systematic component of ECB's monetary policy, where the euro area would have experienced periods of deflation from 2014:3 to 2016:4, from 2017:3 to 2018:1 and starting from 2019:1.

This paper is close to Debortoli et al. (2019) and Ellington (2022) who also estimate an SVAR with time-varying coefficients including a shadow rate in the U.S., and contribute to the literature by dealing especially with the post-2008 decade. However, the present paper departs from previous studies in several ways. Since Debortoli et al. (2019) and Ellington (2022) focus exclusively on U.S. monetary policy, they do not compare the Fed and the ECB, as I do. As a whole, the contribution of my paper mainly consists in providing further evidence of the evolution of monetary policy in the U.S. and in the euro area before and after the Great Recession. Surprisingly, and to my knowledge, no attempt has been made to try to compare changes in U.S. and euro area monetary policies over a long period of time including the ZLB. Moreover, the present paper investigates the evolution of (non)-systematic components of ECB and Fed monetary policy, and hence provides further evidence on rule-based monetary policy in the U.S. and in the euro area after 2008. Focusing on changes in the conduct of monetary policy through the lens of time-varying reaction function allows to go further into the empirical analysis. Indeed, another contribution of this paper also lies in the conduct of an in-depth counterfactual analysis to gauge the macroeconomic effectiveness of changes in monetary policies. Along with impulse responses and variance decomposition analyses, the paper therefore compares the effectiveness of changes in the conduct of Fed's and ECB's monetary policy on U.S. and euro area macroeconomic performances at the ZLB.

Related literature. The present paper relies on three different strands of the literature. First, it supplements works assessing the effectiveness of the conduct of monetary policy through reaction function estimates both in the U.S. and in the euro area. Second, the paper is in line with the vast literature employing VARs for the purpose of empirical monetary analysis. Third, it is related to the literature dealing with monetary policy shocks identification at the ZLB.

Monetary policy rules have been used to identify changes in Fed's behavior across different monetary policy regimes in the U.S., by disentangling pre-Volcker (before Paul Volcker's

appointment as Fed Chairman in 1979) and post-Volcker (including Paul Volcker's tenure) periods. Clarida et al. (2000) advocate that a shift in the systematic component of monetary policy has been the main source of macroeconomic stability during the post-Volcker period. Lubik and Schorfheide (2004) conduct a test for indeterminacy in the pre-Volcker and Volcker-Greenspan periods and confirm this result. Favero and Rovelli (2003), Ozlale (2003), Dennis (2006), and Surico (2007a) provide additional support for these findings, with a specific attention on interest rate smoothing in the reaction function.[6] Similarly, Stock and Watson (2002), Galí et al. (2003) and Ahmed et al. (2004) support the view that better Fed's performances has considerably reduced macroeconomic volatility during the Great Moderation. Interestingly, Coibion (2012) attributes a leading role to monetary policy shocks measured from estimated Taylor rules in significantly contributing to real economic fluctuations during the 1970s and early 1980s. Nikolsko-Rzhevskyy et al. (2014) identify monetary policy regimes according to rules-based or discretionary eras. They provide further evidence of improving economic performance when central banks adhere to a monetary policy rule.

Since all of the papers cited above focus on Fed's behavior, other studies focus on the ECB (Taylor, 1999, Gerlach and Schnabel, 2000).[7] Relying on estimates of reaction functions, Gerdesmeier and Roffia (2004), Garcia-Iglesias (2007) and Surico (2007b) find a stronger interest rate response to inflation than to output fluctuations. However, other studies find a relatively high contemporaneous coefficient on output stabilization in a Taylor rule applied to the eurozone (see Fourçans and Vranceanu, 2007, Sauer and Sturm, 2007 for estimations on ex-post data, and Castelnuovo, 2007 and Gorter et al., 2008 for forward-looking estimations of monetary policy rules). Other papers do the same exercise including the ZLB and the financial crisis, as Gorter et al. (2010), Gerlach (2011), and more recently Gerlach and Lewis (2014a,b). Hutchinson and Smets (2017) advocate that the ECB has launched unconventional measures to respond to its communicated reaction function and fulfill its mandate, that is a key point in the present analysis using a simple estimated monetary policy rule. Recently, Coenen et al. (2021) highlight the role of nonstandards monetary policy instruments in mitigating the costs caused by the effective lower bound on macroeconomic performances in the euro area.

However, only a small strand of the literature proposes a comparative analysis of the conduct

[6] Higher persistence of lagged interest rate in the conduct of monetary policy can be justified by misspecifications of the macroeconomic dynamics, as highlighted by Rudebusch (2001), Castelnuovo and Surico (2004), Castelnuovo (2006) and Givens (2012).

[7] More recently, Hartmann and Smets (2018) look at the evolution of ECB's behavior during its first twenty years.

of monetary policy between the U.S. and the euro area. Empirical estimates include Ullrich (2005) and Belke and Polleit (2007). In the latter, the authors find that the standard Taylor rule is a better tool for modelling Fed's monetary policy than ECB's. They also find a lower emphasis on inflation relative to the output gap in the euro area. Belke and Klose (2013) propose the same exercise during the Great Recession. Nevertheless, vector autoregressive (VAR)-based analyses such as the one conducted earlier in Peersman and Smets (2003) find similar euro area macroeconomic effects of an area-wide monetary policy impulse to those estimated in the U.S. Based on dynamic stochastic general equilibrium (DSGE) models and in accordance with Smets and Wouters (2005), Christiano et al. (2008) and Sahuc and Smets (2008) show that differences in shocks largely explain the gap between Fed's and ECB's interest rate setting.

A large set of VAR specification has been developed to capture the non-linear dynamics of the whole central banks' behavior over a given sample period, including vector autoregressions with time-varying parameters and stochastic volatility (TVP-VAR).

TVP-VAR models allow for smooth and gradual changes in the parameters of the estimated monetary policy rule. In a seminal paper, Primiceri (2005)[8] wonders whether monetary policy in the U.S. has been less active against inflationary pressure during the Martin-Burns period than during the Volcker-Greenspan era. He finds that the non-systematic part of U.S. monetary policy was higher in the 1960s and 1970s, although monetary policy was more systematic under Greenspan in the U.S. Other influential studies such as Cogley and Sargent (2005), Boivin (2006), Kim and Nelson (2006), Benati and Mumtaz (2007) use a VAR with drifting coefficients and stochastic volatilities to analyze Fed's behavior during the post-World War II period in the U.S. Altogether, these papers agree on the improvement in the systematic component of monetary policy after Volcker's appointment. As a whole, time-varying parameters VAR methodology has been widely employed in monetary policy analyses. Benati and Surico (2008), Canova and Gambetti (2009), Cogley et al. (2010), Baxa et al. (2014) and Creel and Hubert (2015) use TVP-VARs to examine the evolution of inflation persistence and predictability. Mumtaz and Surico (2009) and Baumeister and Benati (2013) include the yield curve in their model. Koop et al. (2009), Canova and Pérez Forero (2015), Amir-Ahmadi et al. (2016) investigate possible structural breaks in the economy, and attribute large macroeconomic implications to time-varying monetary policy shocks. Recently, Aastveit et al. (2021) also use a

[8]See Del Negro and Primiceri, 2015 for a corrigendum

TVP-VAR with stochastic volatility and focus especially on the role of the systematic monetary policy when including stock and house prices in the VAR-based policy rule.

The present paper firstly replicates the results raised in Belongia and Ireland (2016) on the common sample period of estimation using U.S. data, according to which the Fed decreased the weight it placed on stabilizing inflation from 2000 to 2007, and deviated persistently from the estimated policy rule that had important implications for output and inflation. Then, it brings new evidence on the evolution of monetary policy in the U.S. and in the euro area in the wake of the Global Financial Crisis (GFC). From this point of view, it is close to Debortoli et al. (2019) and Ellington (2022), who also estimate an SVAR with exogenous time-varying coefficients and find no noticeable evidence that macroeconomic responses to monetary policy shocks have been affected by the ZLB–known as the *ZLB empirical 'irrelevance hypothesis'*.[9]

This paper employs an identification method based on sign restrictions on impulse responses using Bayesian methods developed by Rubio-Ramirez et al. (2010) and Arias et al. (2018), and applied in TVP-VARs by Benati (2011) and Belongia and Ireland (2016). The VAR with time-varying coefficient includes a shadow rate to investigate possible differences between macroeconomic responses to monetary policy shocks away and at the ZLB. As pointed out by Rossi (2021), alternative identification schemes–including the use of shadow rate instead of short-term interest rates–are suitable at the ZLB to overcome the problem of the zero bound on nominal interest rates. For instance, Inoue and Rossi (2021) use a functional VAR to use information contained in short- and long-term interest rates by directly capturing movements in the whole-term structure. Note that shadow rate models and functional VARs are very similar, in a sense that both methods use information contained in the term structure of interest rates.

Importantly, this paper also supplements the small, but burgeoning literature suggesting that the use of shadow rate VARs to identify monetary policy shocks at a relatively low fre-

[9]They echo Swanson and Williams (2014) and Swanson (2018), who also support the view that macroeconomic performances were not affected by the binding ZLB constraint through the effectiveness of Fed's unconventional monetary policy and its ability to influence interest rates all along the yield curve. Other recent papers suggest that the ZLB was not such a constraint on policy, such as Garín et al. (2019), Wieland (2019), Wu and Zhang (2019) and Lhuissier et al. (2020) for instance. This is consistent with earlier literature on unconventional monetary policy as a relatively effective substitute for the federal funds rate at the ZLB, including Vissing Jorgensen and Krishnamurthy (2011) for QE and Campbell et al. (2012) for FG, among many others. Recently, Kim et al. (2020) and Kortela and Nelimarkka (2020) use a structural VAR and support this view for the U.S. and the euro area, respectively, while Sims and Wu (2020) use a DSGE approach. Kiley and Roberts (2017) also use the Fed's large scale econometric model FRB/US to investigate the frequency and the costs of ZLB episodes in a low nominal interest rates era. In line with Reifschneider and Williams (2000), they advocate that adjustments to monetary policy strategies based on simple policy rules are required to improve economic performances when the equilibrium interest rate is low.

quency provide crucial evidence of the propagation of monetary policy shocks and the role of central banks in improving macroeconomic performances at the ZLB, and supporting Debortoli et al.'s (2019) view that there is little empirical evidence against the irrelevance hypothesis. In line with Iwata and Wu (2006), recent works including Aruoba et al. (2022), Ikeda et al. (2020), Johannsen and Mertens (2021), and Mavroeidis (2021), employ quarterly multivariate time series models with a censored interest rate variable to capture the ZLB constraint on short-term nominal interest rates.[10] The present paper is even more closely related to Aruoba et al. (2022) and Mavroeidis (2021). Interestingly, the model used in the former paper allows the coefficients to switch when the economy reaches the ZLB. Also, this paper is close to Johannsen and Mertens (2021), in which monetary policy shocks are identified by short-run restrictions on shadow-rate surprises.

Structure of the paper. The rest of the paper is organized as follows. Section I.2 describes the methodology used for the modelling framework. Section I.3 presents the data used in the benchmark model. Section I.4 is devoted to estimation results. Section I.5 contains policy counterfactuals based on those results. Section I.6 examines the robustness of the findings to various changes in the specification of the baseline model. Some policy implications of the results are raised in Section I.7. Finally, Section I.8 concludes.

I.2 Methodology

The model. The methodology is close to Belongia and Ireland (2016). Indeed, a vector autoregressive model with time-varying parameters and stochastic volatility (TVP-VAR) is used to study the evolution of monetary policy on the period of estimation.[11] The empirical procedure is reproduced in this section and detailed in Online Appendix I.A. As a whole, the model is based on Primiceri (2005) and Cogley and Sargent (2005)[12], and its baseline version can be

[10] Carriero et al. (2021) use monthly data to construct point and density forecasts for censored short- and long-term interest rates from a shadow-rate VAR.

[11] Stability of the simple VAR model is checked in Online Appendix I.C. Aastveit et al. (2017) examine the stability of VARs in the period since the Great Recession and provide evidence against stability of parameters.

[12] I am aware of Bognanni's (2018) criticism that vector autoregressive time series models with time-varying parameters and stochastic volatility developed by Primiceri (2005) and Cogley and Sargent (2005) could suffer from a fundamental ordering problem that makes it ill-suited for the structural analysis. However, as shown later in this section, the methodology employed in the present paper is slightly different. Following Benati (2011) and Belongia and Ireland (2016), the choice of the calibration of prior distribution of coefficients and the identification strategy of structural disturbances are different from that of the baseline methodology.

written as follows:

$$\mathbf{y}_t = \begin{bmatrix} \Pi_t & G_t & R_t^s \end{bmatrix}' \tag{1}$$

where Π_t is the inflation rate, G_t is the output gap and R_t^s is the shadow rate at period t. The analysis does not include financial measures that were likely to have played an important role in the transmission of monetary policy during and in the aftermath of the Great Recession, such as credit spreads (Caldara and Herbst, 2019). However, as raised above, the estimated monetary policy rule of the original Taylor type only includes inflation and output objectives. Under these circumstances, I assume that the Fed and the ECB eased monetary policy and launched unconventional measures purely in order to trigger inflation and to boost economic growth, according to their respective mandate.[13] The three endogenous variables are collected in the 3×1 vector $\mathbf{y}_t$. The model is assumed to follow a second-order vector autoregression with time-varying parameters in the reduced form:

$$\mathbf{y}_t = \mathbf{b}_t + \mathbf{B}_{1,t}\mathbf{y}_{t-1} + \mathbf{B}_{2,t}\mathbf{y}_{t-2} + \mathbf{u}_t \tag{2}$$

where $\mathbf{b}_t$ is a 3×1 vector of time-varying intercepts, $\mathbf{B}_{i,t}$ for $i = 1, 2$ are 3×3 matrices of time-varying autoregressive coefficients, and $\mathbf{u}_t$ is a 3×1 vector of heteroskedastic shocks with time-varying covariance matrix $\mathbf{\Omega}_t$, such that $\mathbb{E}\{\mathbf{u}_t\mathbf{u}_t'\} = \mathbf{\Omega}_t$. The robustness of the results when considering three lags in the estimates is checked in Online Appendix I.F.3.

Both intercepts and autoregressive coefficients in the 21×1 vectorized form are obtained from equation (2):

$$\mathbf{B}_t = \text{vec}\left(\begin{bmatrix} \mathbf{b}_t' \\ \mathbf{B}_{1,t}' \\ \mathbf{B}_{2,t}' \end{bmatrix}\right)$$

and decompose the covariance matrix $\mathbf{\Omega}_t$ by applying a Cholesky factorization as

$\mathbf{\Omega}_t = \mathbf{A}_t^{-1}\mathbf{\Sigma}_t\mathbf{\Sigma}_t'(\mathbf{A}_t')^{-1}$

[13] Gavin et al. (2015) and Debortoli et al. (2019) investigate the conduct and the effectiveness of U.S. monetary policy through the lens of a dual mandate monetary policy rule. Moreover, along with its objective of price stability, "the ECB typically should avoid generating excessive fluctuations in output and employment if this is in line with the pursuit of its primary objective" (see ECB's objective of monetary policy).

where the 3×3 matrix $\mathbf{A}_t$ is lower triangular with ones along its diagonal, and the 3×3 matrix $\mathbf{\Sigma}_t$ is diagonal.

Hence, the reduced form of equation (2) can be rewritten in a matrix form as:

$$\mathbf{y}_t = \mathbf{X}_t' \mathbf{B}_t + \mathbf{A}_t^{-1} \mathbf{\Sigma}_t \varepsilon_t$$

where $\mathbf{X}_t = \mathbf{I}_3 \otimes \begin{bmatrix} 1 & \Pi_{t-1} & G_{t-1} & R^s_{t-1} & \Pi_{t-2} & G_{t-2} & R^s_{t-2} \end{bmatrix}$, and $\mathbb{E}\{\varepsilon_t \varepsilon_t'\} = \mathbf{I}_3$, where $\mathbf{I}_3$ is a 3×3 identity matrix.

Let $\alpha_t = \begin{bmatrix} \alpha_{g\pi,t} & \alpha_{r\pi,t} & \alpha_{rg,t} \end{bmatrix}'$ be 3×1 vector containing the elements of $\mathbf{A}_t$ different from zero or one, and $\sigma_t = \begin{bmatrix} \sigma_{\pi,t} & \sigma_{g,t} & \sigma_{r,t} \end{bmatrix}'$ be 3×1 vector collecting diagonal elements of $\mathbf{\Sigma}_t$. The dynamics of the time-varying parameters are governed by the following process:

$\mathbf{B}_t = \mathbf{B}_{t-1} + \nu_t$

$\alpha_t = \alpha_{t-1} + \zeta_t$

and

$log\ \sigma_t = log\ \sigma_{t-1} + \eta_t,$

where all the uncorrelated innovations are assumed to be jointly normally distributed, with the following assumptions on the variance covariance matrix:

$$\mathbf{V} = \mathbb{V}\mathrm{ar} \left(\begin{bmatrix} \varepsilon_t \\ \nu_t \\ \zeta_t \\ \eta_t \end{bmatrix} \right) = \begin{bmatrix} \mathbf{I}_3 & \mathbf{0} & \mathbf{0} & \mathbf{0} \\ \mathbf{0} & \mathbf{Q} & \mathbf{0} & \mathbf{0} \\ \mathbf{0} & \mathbf{0} & \mathbf{S} & \mathbf{0} \\ \mathbf{0} & \mathbf{0} & \mathbf{0} & \mathbf{W} \end{bmatrix}$$

where $\mathbf{0}$ denotes matrices of zeros, $\mathbf{Q}$ is 21×21, $\mathbf{S}$ is 3×3 and block-diagonal, and $\mathbf{W}$ is 3×3 and diagonal with elements $w_{i,i}$ for $i = 1, 2, 3$.

As a whole, $\mathbf{Q}$ has 231 distinct elements, $\mathbf{S}$ has four distinct non-zero elements, and $\mathbf{W}$ has three distinct non-zero elements.

Estimation strategy. Bayesian methods are often used to estimate large numbers of parameters in classical VAR models because of their strong explanatory and predictive powers. In this paper, I follow the same approach than in Primiceri (2005) and Cogley and Sargent (2005) to be able to deal with autoregressive models with time-varying coefficients. The aim

of the estimation strategy is to assess the posterior distribution of the parameters, based on prior distributions calibrated with simple estimates on a training sample period consisting of the first ten years of data (equivalent to the first forty quarters) to a time-invariant coefficients version of the reduced form model presented above. The, posterior distributions of parameters can be simulated by Markov Chain Monte Carlo (MCMC) algorithm, as detailed in Primiceri (2005), Cogley and Sargent (2005) and in Online Appendix I.A. Following the same approach, prior distributions of parameters are obtained by running a constant-parameter version of the model in the form:

$$\mathbf{y}_t = \mathbf{X}_t'\mathbf{B} + \mathbf{A}^{-1}\mathbf{\Sigma}\varepsilon_t$$

Applying ordinary least squares (OLS) to each equation in this system, an estimate $\hat{\mathbf{B}}$ of the parameter vector $\mathbf{B}$ is obtained, and the same Cholesky decomposition as shown previously to the covariance matrix of least-squares residuals is used to obtain estimates $\hat{\alpha}$ and $\hat{\sigma}$ of the parameter vectors α and σ.

Then, normal priors for the initial values of the coefficients are given by:

$\mathbf{B}_0 \sim \mathcal{N}(\hat{\mathbf{B}}, 4\hat{V}_{\mathbf{B}})$

$\alpha_0 \sim \mathcal{N}(\hat{\alpha}, 4\hat{V}_{\alpha})$

and

$log\ \sigma_0 \sim \mathcal{N}(log\ \hat{\sigma}, I)$

based on those used by Primiceri (2005). For the block elements of the variance-covariance matrix of innovations $\mathbf{V}$, inverse Wishart priors are defined as follows:

$\mathbf{Q} \sim \mathcal{IW}(22k_{\mathbf{Q}}^2\hat{V}_{\mathbf{B}}, 22)$

$\mathbf{S}_1 \sim \mathcal{IW}(2k_{\mathbf{S}}^2\hat{V}_{\alpha,1}, 2)$

$\mathbf{S}_2 \sim \mathcal{IW}(3k_{\mathbf{S}}^2\hat{V}_{\alpha,2}, 3)$

and

$w_{i,i} \sim \mathcal{IW}(2k_w^2, 2)$

for $i = 1, 2, 3$, where $\hat{V}_{\alpha,1}$ and $\hat{V}_{\alpha,2}$ are diagonal blocks of $\hat{V}_{\alpha}$. Also, the settings are taken from Belongia and Ireland (2016), where $k_{\mathbf{Q}}^2 = 0.00035$, $k_{\mathbf{S}}^2 = 0.01$ and $k_{\mathbf{W}}^2 = 0.0001$. The robustness of the results using different priors is checked in Online Appendix I.F.3. Then, a Metropolis-within-Gibbs sampling algorithm is used on the remaining sample period starting from the priors given previously to compute blocks of parameters from their conditional posterior distri-

bution. Again, the subsequent steps to obtain estimations for each parameter are well-described in Belongia and Ireland (2016) and in Online Appendix I.A. Draws for the parameters in $\mathbf{Q}$, $\mathbf{S}$ and $\mathbf{W}$ are taken from their inverse Wishart conditional posterior distribution.

This procedure is repeated 100,000 times in a burn-in period. The model is estimated with 50,000 draws of each parameter for the Gibbs sampling. To assess the convergence of the Markov Chain, draws' inefficiency factors are computed across the four blocks of parameters in the sequences $\mathbf{B}^T$, $\mathbf{A}^T$, $\mathbf{\Sigma}^T$, and in the elements from $\mathbf{V}$. For each individual parameter θ, the ineffciency stastistic is defined as the inverse of the measure of relative numerical efficiency following (Geweke, 1992). According to Primiceri (2005) and Benati (2011), inefficiency factors are said acceptable at or below 20. The statistics for hyperparameters in $\mathbf{V}$ are slightly higher than that upper bound, but those for the parameters and shock covariances and volatilities are largely below it. Tables I.D.1 and I.D.2 containing the results are given in Online Appendix I.D.

Structural shocks identification. An approach based on sign restrictions on impulse responses is applied to identify structural disturbances. The technique is based on Rubio-Ramirez et al. (2010) and Arias et al. (2018), and has been applied to VAR models with time-varying coefficients in Benati (2011). Sign restrictions on the impact of structural disturbances are directly given in Table I.2.1. They are imposed on the impulse response of variables to each structural shock: an aggregate supply shock, an aggregate demand shock, and a monetary policy shock. Aggregate supply shock is assumed to be contractionary: inflation increases but output decreases, and thus left the response of monetary policy unconstrained. Aggregate demand shock is expansionary, and is associated to an increase in output, inflation and interest rate. Finally, monetary policy (or interest rate) shock is assumed to be contractionary: it decreases inflation and output. The robustness of the results using different identification strategy is checked in Online Appendix I.F.3.

Table I.2.1 – Sign restrictions on the impact effects of structural shocks

Impact effect on	Structural shocks		
	Aggregate supply	Aggregate demand	Monetary policy
Inflation	+	+	-
Output gap	-	+	-
Shadow rate	?	+	+

Note: The symbol ? indicates that the response is left unconstrained.

As a result, the reduced form covariance matrix is factored as:

$\mathbf{\Omega}_t = \mathbf{C}_t^{-1}\mathbf{D}_t\mathbf{D}_t'(\mathbf{C}_t')^{-1}$

where the 3×3 matrix is no more lower triangular, but still with ones along its diagonal, and the 3×3 matrix is still diagonal.

Consequently, the structural model can be written is as:

$$\mathbf{C}_t\mathbf{y}_t = \boldsymbol{\gamma}_t + \mathbf{\Gamma}_{1,t}\mathbf{y}_{t-1} + \mathbf{\Gamma}_{2,t}\mathbf{y}_{t-2} + \mathbf{D}_t\xi_t$$

where $\boldsymbol{\gamma}_t = \mathbf{C}_t\mathbf{b}_t$, $\mathbf{\Gamma}_{i,t} = \mathbf{C}_t\mathbf{B}_{i,t}$, for $i = 1, 2$, and $\xi_t = \begin{bmatrix}\xi_t^{as} & \xi_t^{ad} & \xi_t^{mp}\end{bmatrix}'$ is a 3×1 vector of structural disturbances to aggregate supply, aggregate demand and monetary policy, with $\mathbb{E}\{\xi_t\xi_t'\} = \mathbf{I}_3$, and $\mathbf{I}_3$ is a 3×3 identity matrix.

Time-varying monetary policy rule. With above-described estimation strategy and sign restrictions, the third row of the above-mentioned three-equation structural model is presented as a Taylor-type monetary policy rule:

$$\begin{aligned} R_t^s = {} & \gamma_{r,t} + c_{r\pi,t}\Pi_t + \gamma_{1,r\pi,t}\Pi_{t-1} + \gamma_{2,r\pi,t}\Pi_{t-2} \\ & + c_{rg,t}G_t + \gamma_{1,rg,t}G_{t-1} + \gamma_{2,rg,t}G_{t-2} + \gamma_{1,rr,t}R_{t-1}^s + \gamma_{2,rr,t}R_{t-2}^s + \delta_{r,t}\xi_t^{mp} \end{aligned} \tag{3}$$

This Taylor-type rule prescribes a setting for the policy rate regarding to changes in current and lagged inflation and output gap variables. It also includes lagged values of interest rate terms to capture central banks' tendency to smooth short-term interest rates movements over time. The time-varying estimation of the intercept $\gamma_{r,t}$ and of the coefficients from matrices $\mathbf{\Gamma}_{1,t}$

and $\mathbf{\Gamma}_{2,t}$ allows to assess changes in the conduct of monetary policy that might have occurred on the sample period. ξ_t^{mp} represents identified monetary policy shocks that capture deviations in the actual policy rate from the value dictated by the estimated monetary policy rule. Importantly, equation (3) allows for time-variation in all of the response coefficients but also in the standard deviation $\delta_{r,t}$ of the monetary policy shocks. Hence, this estimation permits disentangling changes in central bank's responses to inflation versus output gap stabilization and the extent to which the central bank departs from its rule-based behavior. As a whole, the estimated monetary policy rule given in equation (3) may be decomposed into central banks' response to macroeconomic conditions and smoothing behavior–i.e. the *systematic* component of monetary policy–and monetary policy shocks–i.e. the *non-systematic* component of monetary policy. The model is estimated with data described in the following section.

I.3 Data

Monetary policy rules in normal times. Using a TVP-VAR model, the present paper tracks the evolution of U.S. and euro area monetary policies based on results derived from historical data. U.S. quarterly data are extracted from the Federal Reserve Economic Data (FRED) database, and run from 1960:1 to 2019:4. The nominal interest rate is the federal funds rate. PCE price index is taken as a relevant measure of inflation in the estimation[14], and is given as a percentage annual change. The output gap is computed following the Congressional Budget Office (CBO).[15] Prior distribution of the coefficients is obtained from the training sample period from 1960:1 to 1969:4. Then, the Taylor rule is estimated by the TVP-VAR model with stochastic volatility from 1970:1 to 2019:4.

Concerning euro area data, interest rate, inflation and output gap quarterly series are from

[14]John Taylor claims that the Fed has not followed the prescription of the Taylor rule by keeping the interest rate too low from 2003 to 2005 and hence generated the housing bubble in the U.S. Ben Bernanke disagreed with that by justifying that the Fed set the interest rate according to the Taylor rule by targeting core PCE inflation, and not GDP deflator as in Taylor's estimations. For more details, see Bernanke's Brookings post of April 28, 2015 titled "The Taylor Rule: A benchmark for monetary policy?". See also Janet L. Yellen's speech of March 27, 2015 on "Normalizing Monetary Policy: Prospects and Perspectives", or Doko Tchatoka et al. (2017) for additional evidence of Taylor-type policy rule estimated with headline or core PCE inflation.

[15]The output gap (in percentage) is constructed following the basic formula $y_t^{gap} = 100 \times \frac{Y_t - Y_t^*}{Y_t^*}$ that can be approximated by $y_t^{gap} = 100 \times log(Y_t) - log(Y_t^*)$, where Y_t is the real output and Y_t^* is the real potential output at time t. In accordance with the original Taylor rule (Taylor, 1993), including the output gap rather than real GDP growth in the estimates may help the TVP-VAR control for the effects of technology shocks affecting both real and potential GDP, as discussed in Giordani (2004).

two major sources. The first one is the Area-Wide Model database (AWM, Fagan et al., 2005) that contains historical data from 1970:1 to 2017:4. Then, the data are updated to 2019:4 with Eurostat. The main policy rate is the Euribor 3-month. Inflation is the Harmonized Index of Consumer Prices (HICP), and the real potential GDP is estimated with the HP filter (Hodrick and Prescott, 1997) to compute the output gap following the basic formula mentioned above.[16] The period 1971:1 to 1980:4 is used as the training sample. The model is estimated from 1981:1 to 2019:4.

Figure I.3.2 – Inflation, output gap and policy rate

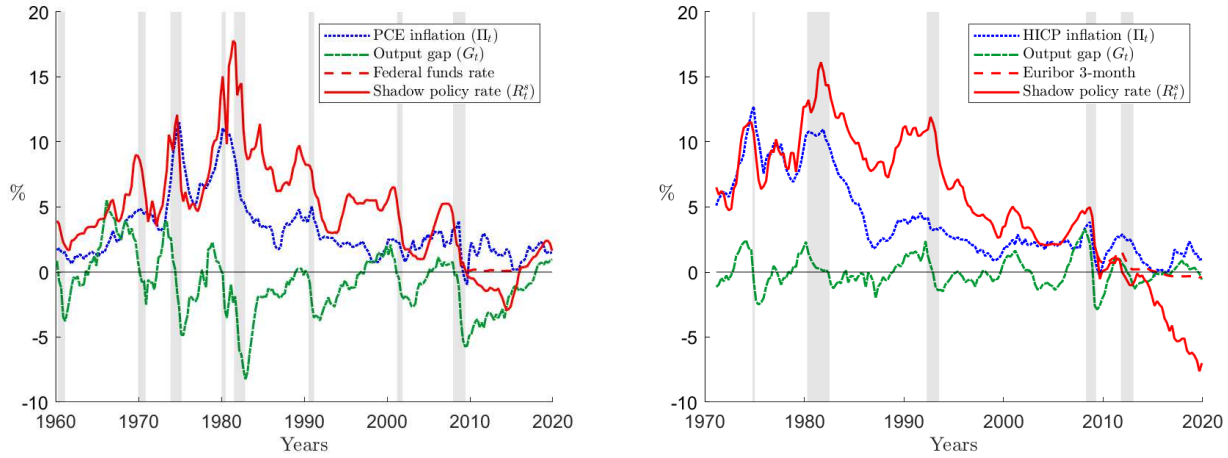

(a) U.S. (b) Euro area

Note: Grey bands represent NBER-dating recessions in the U.S. and CEPR-based recession dates in the euro area. The U.S. shadow policy rate R_t^s is proxied by the federal funds rate and replaced by the shadow rate from November 2008 to November 2015. In the euro area, it tracks the Euribor 3-month over the period and is replaced by the shadow rate in July 2009. Shadow rates are from Wu and Xia (2016).

Figure I.3.2 shows the evolution of inflation, output gap and policy rates since 1960:1 in the U.S. and 1971:1 in the euro area. Both interest rate and inflation have been lastingly decreasing over the sample period in the U.S. and in the euro area. From a two-digit rate level around the 1970s, U.S. PCE inflation rate has substantially decreased to stabilize before the 2000s. The federal funds rate has been evolving along a similar path over the sample period, before hitting the ZLB at the end of 2008. The interpretation of the data is quite the same for the euro area, where both the HICP and Euribor 3-month have been trending down since the 1980s. However, Figure I.3.2 also shows that, unlike the U.S., the euro area has struggled to recover from the 2007-08 crisis, suffering another recession induced by the 2010-2012 sovereign debt crisis and successive deflationary periods in 2015 and 2016.

[16] Following Hamilton's (2018) recent criticism of the use of Hodrick-Prescott filter, real potential GDP in the euro area is estimated with alternative filters to check the robustness of the results in Online Appendix I.F.2.

Unconventional monetary policies and shadow rates. Since the data cover the period up to 2019:4, the estimation results capture both conventional and unconventional monetary policies. Therefore, a major concern is the constrained policy rate at the zero level during periods of unconventional measures. Because of flat interest rates at the ZLB, and along with the launch of non-standard measures, traditional data on policy rate do not entirely reflect central banks' actions during unconventional times and may lead to biased monetary policy rule estimation. Unconventional measures have been characterized by the use of 'non-standard' instruments–i.e. other than the policy rate–consisting mainly in large-scale asset purchases (LSAP) or forward guidance, to fulfill the main objectives stated in central banks' mandate. Consequently, and to be able to estimate the Taylor-type rule up to 2019:4, the policy rate instrument is proxied by the shadow rate from Wu and Xia (2016)[17], constructed as an extrapolation of the yield curve in the negative territory, and hence taking into account unconventional measures that are likely to have affected interest rates at different maturities.

Table I.3.2 – Outlines of monetary policy since the Great Recession

	United States	Euro area
First asset purchase after the GFC	Nov. 2008	July 2009
Tapering	Dec. 2013	Dec. 2016
Period of ZLB	Dec. 2008 - Dec. 2015	Mar. 2016 - —

Note: The symbol — means that the euro area is still stuck at the ZLB in December 2019.
Source: Federal Reserve, European Central Bank, Chen et al. (2017).

Table I.3.2 gives the outlines of U.S. and euro area monetary policies since the 2007-08 crisis.[18] It shows periods when the Fed and the ECB have launched their main non-standard measures, and periods during which they decided to reduce the magnitude of these measures. The Fed has reacted quickly to the financial crisis by implementing its first assets purchases programme (QE1, for 'Quantitative easing 1') of $600 billion. In the euro area, the ECB has enhanced credit support in October 2008 and lengthened the maturity of its LTROs in June 2009. However, the ECB has implemented its first asset purchase programme in July 2009

[17]U.S. and euro area shadow rates data are available on Jing Cynthia Wu's webpage.

[18]From 2008 to 2014, the Fed has implemented three successive QE programmes (Dec. 2008, Nov. 2010 and Sep. 2012). In late 2015, it began to normalize U.S. monetary policy by raising the key policy rate, and by reducing its balance sheet in late 2017. The ECB decided to improve credit support and bank lending (Oct. 2008 and June 2009), and launched its first asset purchase programme (APP) in July 2009. However, its balance sheet expanded a lot in 2012 due to very longer-term refinancing operations (VLTROs), and especially in 2015 when it implemented an APP including both sovereign bonds and private-sector securities purchases.

(CBPP1, for 'Covered-bond purchase programme 1'). As of 2016, the ECB has gradually lowered interest rates to their lowest level, while the Fed was keeping normalizing its monetary policy at this time. Indeed, the Fed announced slowing down assets purchases in December 2013, before raising its policy rate in December 2015. On the other hand, the ECB announced tapering in end-2016. But in late 2019, monetary policy in the euro area was still at the ZLB.

The shadow rate from Wu and Xia (2016) is used as a proxy for unconventional measures of monetary policy in the TVP-VAR specification (Figures I.3.2 and I.3.3).[19] Nominal interest rates used as policy rates in the model are replaced by shadow rates at the ZLB to get a consistent measure of the stance of monetary policy over the full sample period. In the U.S., the federal funds rate is replaced by the shadow rate from November 2008 to November 2015. In the euro area, the Euribor 3-month is replaced by the shadow rate in July 2009. As mentioned previously, the key policy rate cannot be proxied by the shadow rate only once the euro area reached the ZLB in 2016, since the shadow rate starts to diverge from the Euribor 3-month in mid-2009 due to the launch of unconventional measures. Both for the U.S. and the euro area, these dates closely correspond to information reported in Table I.3.2. Moreover, regarding Figure I.3.3, at least two comments can be made to compare the timeline of Fed's and ECB's policy decisions. First, despite the fact that both the Fed and the ECB have simultaneously adopted unconventional measures to face the Great Recession, the Fed was entering the ZLB period while implementing its early non-standard policy, whereas the policy rate in the euro area was around 1% at that time. Second, the Fed exited from the ZLB a couple of months before the ECB finally entered the zero-rate era.

To fit the frequency of the shadow rate series with the rest of the data, quarterly rates are constructed as a three-month average. Also, as discussed in Christensen and Rudebusch (2015), Halberstadt and Krippner (2016), Bauer and Rudebusch (2016) and Krippner (2020), shadow rate estimates are very sensitive to several factors, such as the calibration of the lower bound

[19]Several papers highlight the plausibility to use the shadow rate in a VAR model as a measure of the stance of monetary policy at the ZLB. For instance, Wu and Xia (2016), Lombardi and Zhu (2018), Keating et al. (2019), Krippner (2020) and Francis et al. (2020) show how shadow rate-based monetary policy shocks provide a realistic picture of the post-crisis macroeconomic situation. Basu and Bundick (2017) and Caggiano et al. (2017) investigate the macroeconomic effect of uncertainty at the ZLB. Forbes et al. (2018), Rogers et al. (2018) and Pasricha et al. (2018) find empirical evidence of monetary policy effects at the international level. Georgiadis (2016), Horvath and Voslarova (2016), Potjagailo (2017) focus on global spillovers of unconventional monetary policies in the U.S. and in the euro area. Recently, Diegel and Nautz (2021) use a shadow rate in a structural VAR to assess the role of long-term inflation expectations in the transmission of monetary policy shocks. Plante et al. (2017), Caraiani and Călin (2018) and Crespo Cuaresma et al. (2019) incorporate shadow rates in a TVP-VAR model. Similarly, shadow rates can also be used in estimated DSGE models, as in Mouabbi and Sahuc (2019).

Figure I.3.3 – Policy and shadow rates

(a) U.S.

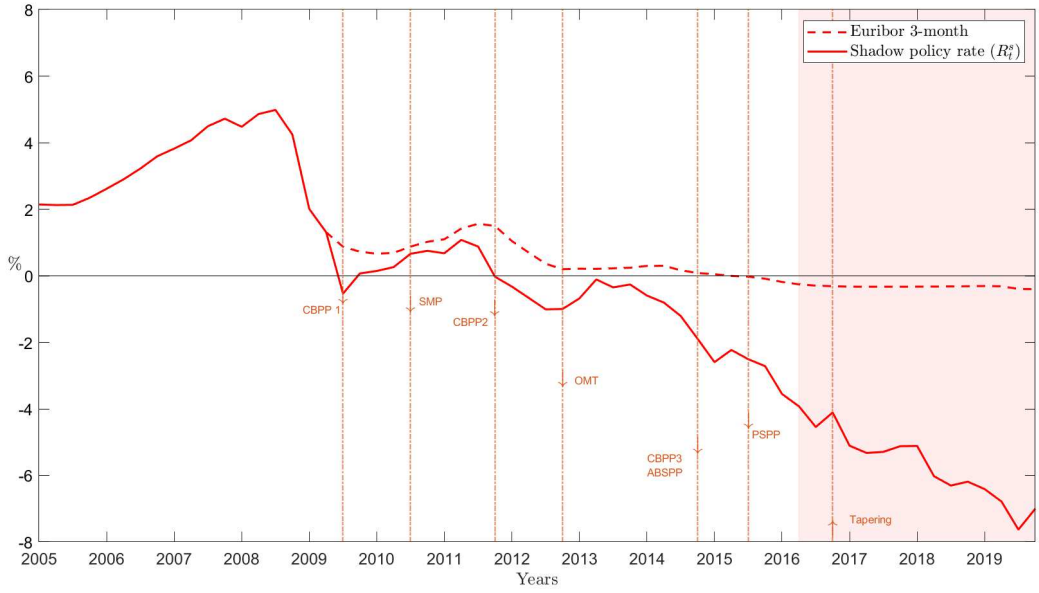

(b) Euro area

Note: Shaded areas depict the ZLB periods. The U.S. shadow policy rate R_t^s is proxied by the federal funds rate and replaced by the shadow rate from November 2008 to November 2015. In the euro area, it tracks the Euribor 3-month over the period and is replaced by the shadow rate in July 2009. Shadow rates are from Wu and Xia (2016).

or the range of rates included in the dataset. The robustness of the results using shadow short rates from Krippner (2013, 2020) is checked in Online Appendix I.F.1.

I.4 Results

Response coefficients of the time-varying reaction function. The baseline model is estimated with the data mentioned previously.[20] Figure I.4.4 compares the evolution of long-run responses of the policy rate to macroeconomic fluctuations in the United States and the euro area. Considering the dual-mandate reaction function, long-run response coefficients can be interpreted as the response of the policy rate to a permanent increase in inflation or output. In this regard, they correspond better to the parameters specified in the theoretical counterpart of empirical monetary policy rules. Figure I.4.4a shows the evolution of long-run coefficients on inflation from 1995:1 to 2019:4. The estimated coefficient in the U.S. has slightly decreased during the Great Recession. The median coefficient on inflation dropped from 0.91 in 2009:1 to 0.34 in 2013:1, and stayed roughly at the same level thereafter (0.37 in 2017:1). The coefficient also shows that the Fed's long-run response to inflation became lower than the unit in the early 2000s, and even non-significantly different from zero in 2008.[21] This result suggests a less aggressive response of U.S. monetary policy to inflation fluctuations over the last decades. However, and importantly, this result does not provide evidence of a strong change in Fed's response to inflation after 2008. On the other hand, results in the euro area indicate that ECB's monetary policy has been much more aggressive towards inflation since 2008, where the long-run response coefficient has considerably increased at the ZLB. Indeed, the median response coefficient increased from 1.84 in 2009:1 to 2.13 in 2013:1 before reaching 3.15 in 2017:1. Moreover, 68% credible intervals show significant difference between the long-run coefficient on inflation in the U.S. and the euro area after the 2007-08 crisis. Figure I.4.4b tracks changes in the long-run response to output gap over time. Estimated coefficients in the U.S. and in the euro area overlapped after 2008 and show no significant change in the response of the Fed and the ECB to output gap fluctuations during the Great Recession, despite a moderate larger increase in the U.S. than in the euro area (the median coefficient in 2017:1 is at 2.14 in the U.S. against 1.88 in the euro area). Moreover, very wide depicted 68% credible intervals associated to the coefficients show how estimated long-run responses to output gap are subject to uncertainty in the U.S. and in the euro area at the end of the sample period of estimation.

[20] Further measures of inflation and real economic activity are employed in the model to check the robustness of the results. The response coefficients of these alternative specifications are shown in Online Appendix I.F.2.

[21] The fact that the Taylor principle is no more satisfied since the 2000s may have had huge implications in terms of indeterminacy and volatilities of variables of interest. However, this analysis would have required additional structure in the model and is beyond the scope of this paper.

Nevertheless, there is no evidence of significant shifts in the long-run response coefficient on output gap within and between the U.S. and the euro area.

Figure I.4.4 – Long-run coefficients from the estimated monetary policy rule

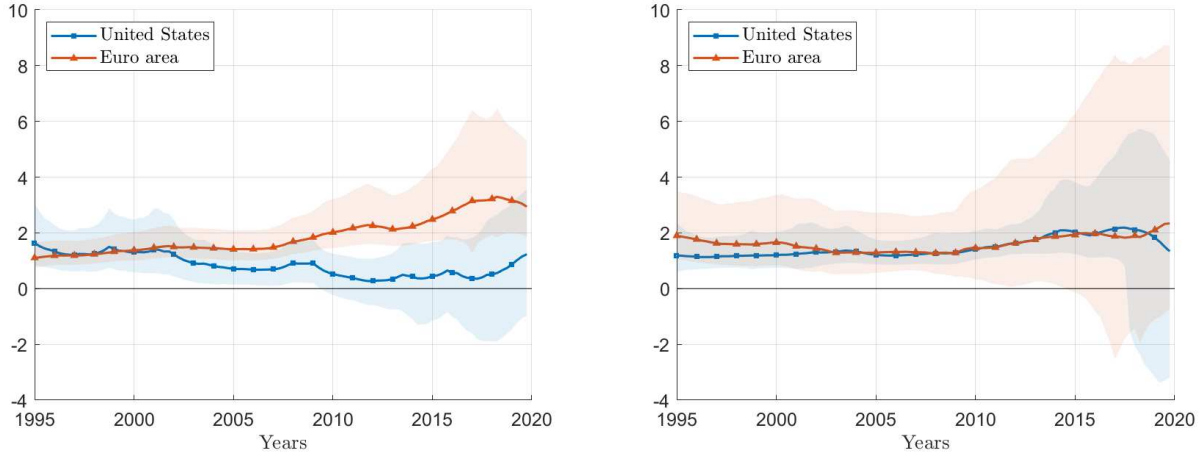

(a) Long-run coefficient on inflation (b) Long-run coefficient on output gap

Note: Long-run coefficients on inflation and output gap are respectively given by $(c_{r\pi,t}+\gamma_{1,r\pi,t}+\gamma_{2,r\pi,t})/(1-\gamma_{1,rr,t}-\gamma_{2,rr,t})$ and $(c_{rg,t}+\gamma_{1,rg,t}+\gamma_{2,rg,t})/(1-\gamma_{1,rr,t}-\gamma_{2,rr,t})$ in equation (3). Median (solid lines) and 68% credible interval (shaded areas) of the posterior distribution of coefficients are plotted for each indicated variable.

Figure I.4.5 plots the time-varying standard deviations of structural monetary policy disturbances in the U.S. and in the euro area. In the U.S., monetary policy shock volatility has peaked when the Fed hit the ZLB and decreased immediately thereafter. Besides no noticeable and significant changes in the long-run response to macroeconomic fluctuations, this spike in the volatility of U.S. monetary policy shocks may be interpreted as an illustration of the 'constrained discretion' approach raised by Bernanke (2003) to describe Fed's monetary policy.[22] In the euro area, monetary policy shock volatility has increased with ECB's early reaction to the 2007-08 crisis. Once again, this figure underlines differences in the conduct of monetary policy in the U.S. and the euro area. As a possible explanation, lags in the implementation of unconventional monetary policy in the euro area compared to the U.S. may have led to a gap between the timing of ECB's and Fed's monetary policy shock volatilities. The coefficient from the ECB monetary policy rule reached an all-time high at the end of the period of esti-

[22] According to Bernanke, the Fed has adopted a flexible behavior such that the inflation targeting objective may be de-emphasized in an output stabilization purpose under some circumstances. As he mentioned in his speech, "under constrained discretion, the central bank is free to do its best to stabilize output and employment in the face of short-run disturbances, with the appropriate caution born of our imperfect knowledge of the economy and of the effects of policy". Contemporaneous coefficients depicted in Figure I.E.1 (see Online Appendix I.E) show a small increase in Fed's short-run response to output gap in 2008-2009 and support the view of the constrained discretion approach to Fed's monetary policy. However, the credible interval associated to this coefficient does not provide any statistical evidence of any significant change in Fed's contemporaneous responses to real economic activity.

mation, whereas it came back to a pre-crisis level in the U.S. This result may be interpreted as the difference in the timing of policy normalization in the U.S. and in the euro area: the Fed began normalizing the stance of monetary policy at a time when the ECB had not yet reached the ZLB. Note that 68% Bayesian credible sets associated to $\delta_{r,t}$ coefficients highlight strong significant changes in the volatility of monetary policy shocks over the sample period.

Figure I.4.5 – Monetary policy shock volatility from the estimated monetary policy rule

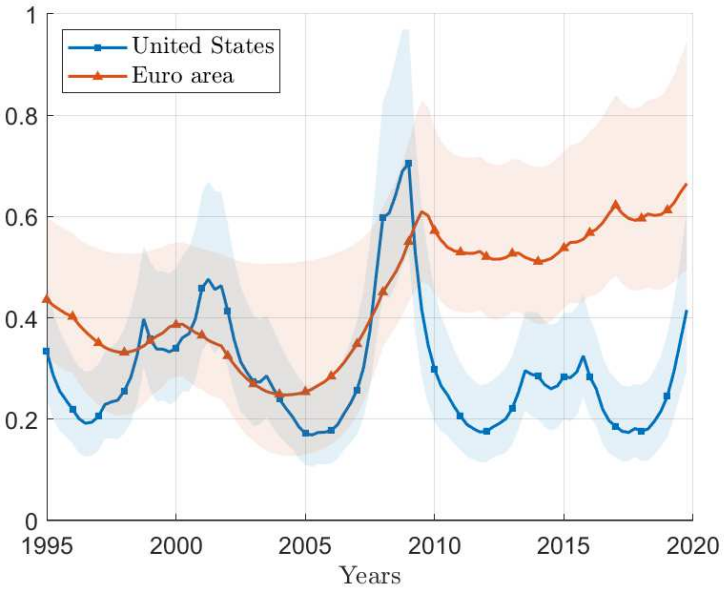

Note: The volatility of monetary policy shocks is captured by $\delta_{r,t}$ in equation (3). Median (solid lines) and 68% credible interval (shaded areas) of the posterior distribution of coefficients are plotted for the indicated variable.

The evolution of monetary policy shocks volatility shows that unconventional monetary policy decisions at the ZLB have been characterized by large departures of the Fed and the ECB from the policy rate prescribed by the Taylor rule. QE has largely contributed to lower expected future short-term rates through the signaling channel, that can be interpreted as additional discretionary monetary policy, whereas FG is commonly defined as the commitment to deviate from the monetary policy rule in the future, resulting in more discretionary policy.[23] Based on these results and on the whole influential related literature, Fed's and ECB's unconventional monetary policy tools such as QE and FG may have undoubtedly led to statistically different and persistent deviations from the baseline Taylor-type policy rule at the ZLB in the U.S. and in the euro area. By definition, these departures from rule-like behavior are interpreted as more discretionary policy at the ZLB. In that case, the central bank is not systematic–or

[23]See Vissing Jorgensen and Krishnamurthy (2011) and Bauer and Rudebusch (2014) for evidence of the signaling role of QE, and Campbell et al. (2012) and Woodford (2012) for the effects of FG.

predictable–in reacting to changes in the economy.

Macroeconomic effects of non-systematic monetary policy. Figure I.4.6 shows the evolution of realized monetary policy shocks since 1995. It reveals that the Fed and the ECB have departed a lot from the behavior prescribed by their estimated policy rule at the ZLB, and that these monetary policy shocks have been considerably negative when the 2007-08 crisis occurred. A negative monetary policy shock means that the central bank sets interest rate at a level below the rate prescribed by the estimated monetary policy rule. In that case, monetary policy is perceived as expansionary. However, it can be graphically deduced that U.S. and euro area monetary policies have been mostly expansionary during the 2007-08 crisis, describing potentially important deviations from estimated policy rules that also occurred with the launch of unconventional measures at the ZLB.

Figure I.4.6 – Realized monetary policy shocks

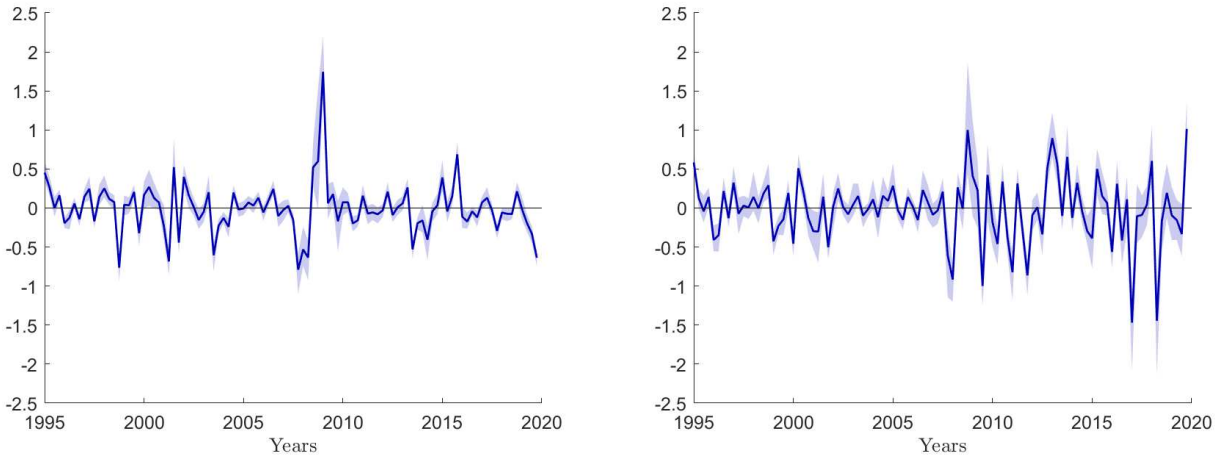

(a) U.S. (b) Euro area

Note: Median (solid lines) and 68% credible interval (shaded areas) of the posterior distribution of the realized monetary policy shock are plotted. A negative monetary policy shock is equivalent to an interest rate setting below the rate prescribed by the estimated monetary policy rule (i.e. expansionary monetary policy).

Then, the purpose is to investigate changes in the macroeconomic impact of monetary policy shocks. Figures I.4.7 and I.4.8 plot impulse responses of each observable variable to monetary policy shocks over a 20 quarter horizon at different dates: 2007:4, 2011:1, and 2015:1. The responses are computed based on draws from the posterior distributions of the parameters estimated for each indicated period. They show how the economy responded to a monetary policy shock at a given point in time. Overall, the signs of the impulse response functions of the TVP-VAR variables to a monetary policy shock do not change at the ZLB.

In the U.S., the responses of inflation and output gap to monetary policy shocks have slightly decreased at the ZLB. However, the policy rate has strongly reacted to monetary policy shocks in 2007:4 and 2015:1, suggesting an important role of the non-systematic component in Fed's monetary policy. In the euro area, the response of inflation to monetary policy shocks has remained quite stable before and after the Great Recession. However, as in the U.S., the response of output gap has gradually decreased since 2007:4. Importantly, the policy rate in the euro area has been more and more responsive to monetary policy shocks since 2007:4. This confirms the view that along with a stronger long-run response to inflation, ECB's monetary policy has been also characterized by a larger non-systematic response to macroeconomic fluctuations during the Great Recession.

Figure I.4.7 – Impulse responses to monetary policy shocks in the U.S.

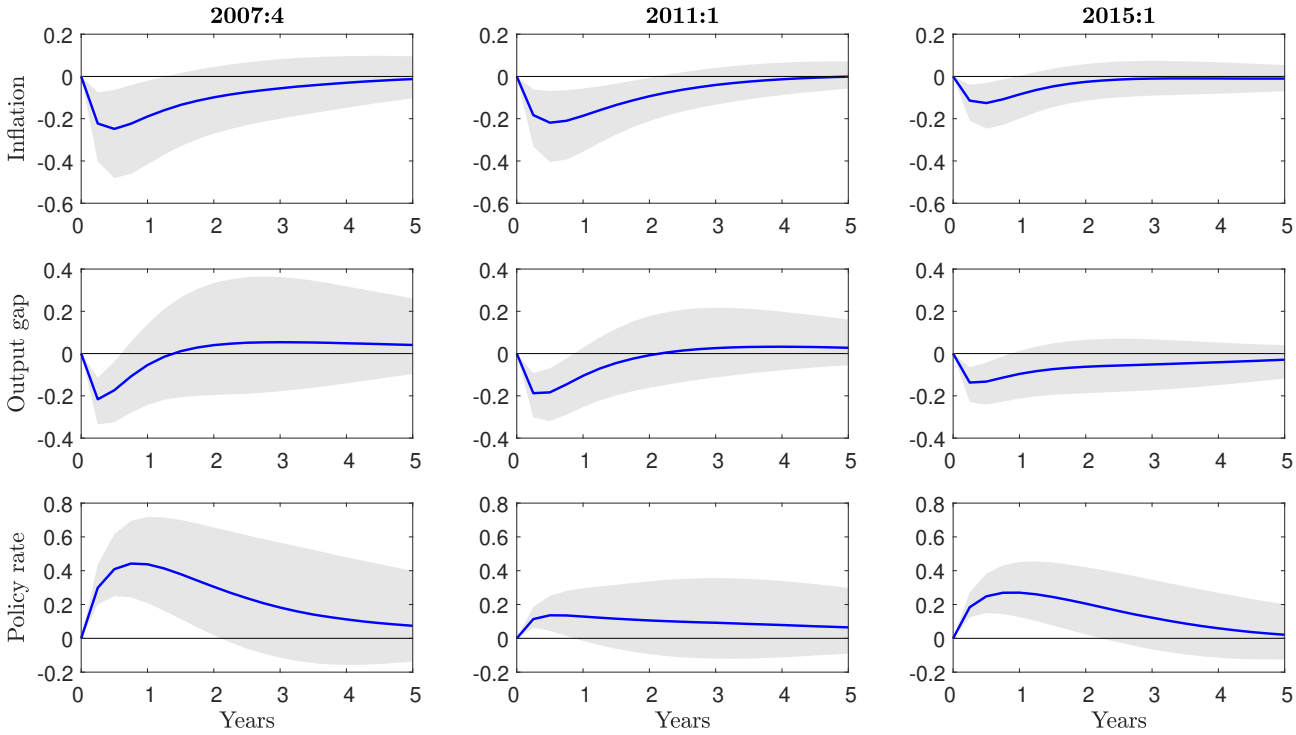

Note: Impulse response of the indicated variable to a contractionary monetary policy shock at the indicated date. Blue lines represent the median and grey shaded areas represent 68% credible intervals of the posterior distribution of each impulse response.

Table I.4.3 reports the percentage share of forecast error variances in endogenous variables attributable to monetary policy shocks for horizons up to 5 years (i.e. 20 quarters). Variance decomposition is based on draws of the model's parameters from their posterior distributions for 2007:4, 2011:1 and 2015:1. As with impulse response functions, the dates are chosen such that the analysis covers both pre-crisis and ZLB periods. The model estimated using U.S. data attributes small fractions of inflation and output gap volatility to monetary policy shocks.

Figure I.4.8 – Impulse responses to monetary policy shocks in the euro area

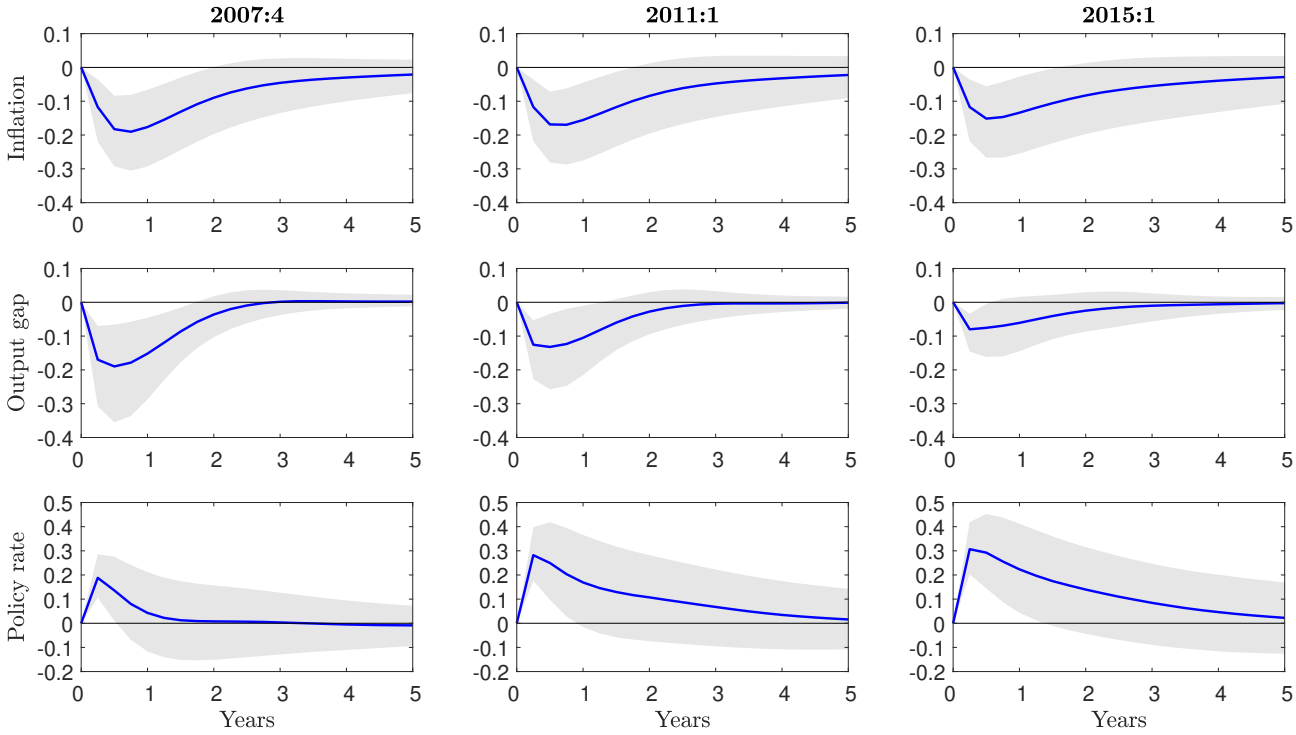

Note: Impulse response of the indicated variable to a contractionary monetary policy shock at the indicated date. Blue lines represent the median and grey shaded areas represent 68% credible intervals of the posterior distribution of each impulse response.

This fraction is about 10% and is quite stable across the three periods. However, monetary policy shocks considerably contribute to the variance of the policy rate in the U.S., confirming previous results from the impulse response analysis of a strong non-systematic component in U.S. monetary policy. In the euro area, monetary policy shocks explain a larger part of inflation volatility than in the U.S., whereas the share of the forecast error variance of the output gap is similar. The contribution of monetary policy shocks to the variance of inflation in the euro area decreases when the economy moves from normal times to the ZLB, while monetary policy shocks explain an increasing part of the variation in the policy rate across the periods. However, this share is lower than in the U.S. These results are consistent with the higher long-run response coefficient for inflation and the increasing role of non-systematic component of monetary policy at the ZLB in the euro area. The 16th and 84th percentiles based on draws from the posterior distributions for each date provide little evidence of significant changes in forecast error variances due to monetary policy shocks. Only median coefficients are reported here.

As a whole, the results presented above show that the ECB has considerably shifted its behavior during the post-2008 decade by responding more aggressively to inflation fluctua-

Table I.4.3 – Variance decomposition

Horizon	% of forecast error variance due to monetary policy shocks					
	U.S.			Euro area		
	2007:4	2011:1	2015:1	2007:4	2011:1	2015:1
Inflation						
1	7.72	9.49	7.49	16.14	14.71	12.78
2	7.78	9.65	7.66	15.08	13.63	11.95
3	8.87	9.98	8.62	14.62	13.63	12.30
4	9.78	10.22	9.39	14.40	13.84	12.86
5	10.33	10.38	10.02	14.29	14.12	13.27
Output gap						
1	8.19	8.23	8.45	9.39	8.60	7.93
2	9.31	7.60	8.90	10.27	10.13	10.83
3	10.49	8.10	10.48	10.61	11.09	12.75
4	11.32	8.47	11.86	10.66	11.38	13.31
5	11.85	8.78	12.73	10.70	11.47	13.48
Policy rate						
1	32.21	10.59	33.35	7.21	16.64	24.61
2	24.12	7.57	23.41	6.55	12.44	17.66
3	21.30	7.53	19.72	7.11	12.21	16.04
4	20.56	7.86	18.85	7.48	12.22	15.25
5	20.37	8.16	18.89	7.69	12.26	14.87

Note: Horizon is the number of years ahead. Variance decomposition is based on draws of the median coefficients from their posterior distributions for 2007:4, 2011:1 and 2015:1.

tions, when its policy rate hit the effective lower bound and when a novel set of unconventional measure was launched. However, the results do not reveal noticeable changes in the conduct of Fed's monetary policy at the ZLB, despite a slightly lower long-run response coefficient on inflation at the ZLB. Nevertheless, estimated response coefficients also suggest dramatic shifts in monetary policy shocks during and after the Great Recession. In the U.S., the volatility of monetary policy shocks peaked when the Fed entered the ZLB and quickly went back to pre-crisis levels, whereas it has slowly increased in the euro area to reach a high level due to ongoing massive expansionary ECB's monetary policy. Impulse response functions and variance decomposition highlight the relative effectiveness of monetary policy shocks in both U.S. and euro area macroeconomic performances at the ZLB. Although they explain a larger part of inflation fluctuations in the euro area than in the U.S., monetary policy shocks have been mostly reflected in the variation of the policy rate in the U.S. and have even played an increasing role

in the evolution of the policy rate in the euro area at the ZLB.

I.5 Policy counterfactuals

The estimated VAR model with time-varying coefficients is used to propose different counterfactual scenarios. The first one focuses mainly on the coefficients of estimated monetary policy rules. Then, the question raised by the second counterfactual scenario is more general and is related to changes in the rest of the estimated model's parameters and in the identified structural shocks. The last counterfactual scenario consists in replacing euro area estimated monetary policy rule coefficients in the model estimated with U.S. data and to study whether U.S. macroeconomic conditions would have been better-off if the Fed followed ECB's policy rule and vice versa.

I.5.1 Do monetary policy changes matter?

The aim is to investigate how changes in the conduct of monetary policy may have affected macroeconomic performances. This experiment gives the path that would have followed inflation, output gap and the policy rate in the U.S. and in the euro area under some circumstances. Counterfactual series for the U.S. and the euro area are presented in Figures I.F.7 and I.F.8, respectively.

The first scenario consists in drawing the coefficients of the policy rule from the posterior distribution from 2007:4. In the U.S., the levels of PCE inflation and output gap would have been slightly lower than those observed after the crisis if the Fed had kept monetary policy rule unchanged since 2007:4. Also, the simulated policy rate would have been only somewhat above its actual level, meaning that monetary policy would have been constantly less accommodative in that scenario than that has actually been over the period. Although they are not statistically significant either, the results are much more striking concerning inflation in the euro area. Changes in ECB's monetary policy had a huge impact on HICP, especially during the Great Recession: unconventional monetary policy has strongly reduced the deflationary risk in the euro area. Overall, both Fed's and ECB's unconventional monetary policies have improved inflation and real economic activity in the U.S. and the euro area.

In the second scenario, the Taylor rule parameters are also drawn from their 2007:4 posterior

distribution, but monetary policy shocks are now assumed to be muted from 2007:4 forward. In that case, counterfactual series also induced a shift in the non-systematic component of monetary policy, and highlight the role of monetary policy shocks when compared to the previous scenario. The interpretation of the results is similar to that has been observed in the first scenario. However, changes in ECB's systematic and non-systematic components of monetary policy led to a significant gap between actual and counterfactual inflation path: without any change in ECB's behavior at the ZLB, the euro area would have suffered a prolonged period of deflation from 2014:3 to 2016:4. In the U.S., this gap widened from 2007:4 onward, more than that observed in the first scenario. But the results still do not suggest significant evidence of the efficiency of Fed's policy shifts on economic performances in the U.S.

Figure I.5.9 – Counterfactual simulations (U.S.)

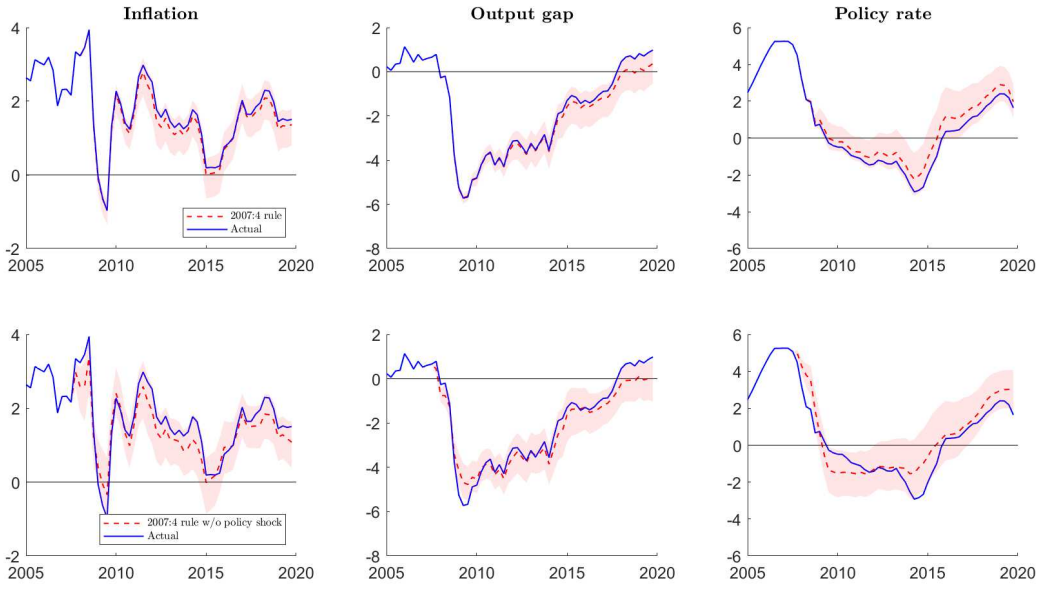

Note: Median counterfactual path (red dashed lines) and 68% credible interval (red shaded areas) are plotted for each indicated variable.

Other counterfactuals are shown in Figures I.E.4 and I.E.5 (see Online Appendix I.E), and give further insights on the macroeconomic implications of changes in the non-systematic component of monetary policy. The top panel reports results when monetary policy shocks are turned off from 2007:4 onward. There is no noticeable difference between the actual and counterfactual paths. Then, it appears that the role of monetary policy shocks considered separately is negligible in the U.S. and the euro area compared to the role of changing policy parameters in explaining macroeconomic performances. The bottom panel focuses on the volatility of monetary policy shocks. The scenario consists in drawing the coefficient on monetary pol-

Figure I.5.10 – Counterfactual simulations (Euro area)

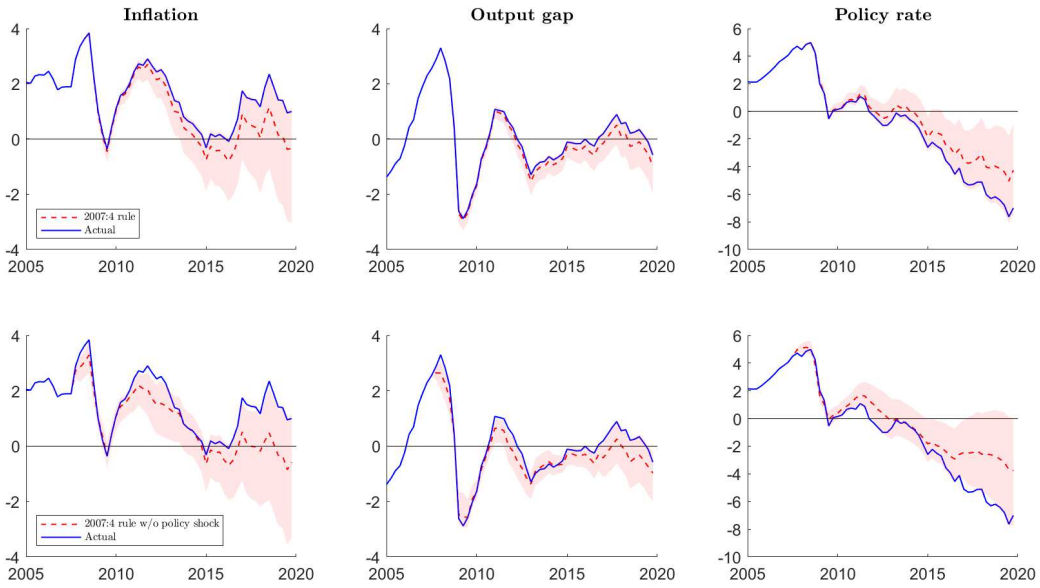

Note: Median counterfactual path (red dashed lines) and 68% credible interval (red shaded areas) are plotted for each indicated variable.

icy shocks volatility from the 2007:4 posterior distribution, and keeping it fixed from 2007:4 forward. Similarly, the results do not suggest any role of monetary policy shocks volatility in macroeconomic performances in the U.S. and in the euro area.

I.5.2 Structure, shocks or policy?

Previous counterfactual results show that macroeconomic fluctuations are partially driven by changes in Fed's and ECB's interest rate setting behavior. Whereas changes in Fed's policy hardly and non-significantly explain the evolution of U.S. inflation and output gap, empirical results in the euro area highlight the role of changing ECB's monetary policy in macroeconomic fluctuations, especially regarding inflation. Those results are obtained by keeping the coefficients of the estimated monetary policy rule, and by additionally muting monetary policy shocks from 2007:4 onward, and therefore are subject to the Lucas critique (Lucas, 1976) according to which the whole structure of the economy is affected by policy changes due to the forward-looking behavior of rational private agents.

To deal with the Lucas critique, a first scenario consists in keeping all the response coefficients fixed from 2007:4 onward. Fixed coefficients now include parameters from the first ("inflation equation") and second ("output gap equation") rows of the structural model presented in Section I.2. As for the so-called Taylor-type rule that stands for the "interest rate

equation", inflation equation is called "Phillips curve" and output gap equation is called "IS curve" in the following exercise.[24] The effect of monetary policy changes on macroeconomic fluctuations is then assessed by comparing those results with previous counterfactual results, where only policy parameters were kept fixed from 2007:4 onward. In a second scenario, all structural shocks (supply, demand, and monetary policy) are then assumed to be muted from 2007:4 onward. The main idea is based on Smets and Wouters (2005), Christiano et al. (2008) and Sahuc and Smets (2008) who show that the gap between the conduct of Fed and ECB monetary policies comes from the difference in shocks hitting the U.S. and the euro area economies. Therefore, in addition to fixed coefficients, all structural shocks are muted from 2007:4 onward.

While Figure I.E.6 in Online Appendix I.E reveals no noticeable change in inflation, output gap and policy rate when keeping fixed all the structural parameters, the path of endogenous variables is different when shocks are muted and coefficients are fixed from 2007:4 onward as depicted in Figures I.E.7 and I.E.8. This is particularly obvious in the case of muted supply shocks and fixed parameters in the inflation equation. Without negative supply shocks and time-variation in the inflation equation's parameters, inflation would have been much lower and the output gap would have dropped less than what has been observed in the wake of the 2007-08 financial crisis, as indicated in Figure I.E.7. The sharp recovery of the U.S. economy and the inflation rate at around its 2% target level would have encouraged the Fed to stop monetary policy easing around 2011. Although they are less noticeable, the results also hold in the case of fixed parameters and muted demand shocks in the output gap equation. Figure I.E.8 reveals that strong negative demand shocks led to U.S. deflation in 2009. Without this shock, the results shows that the Fed would have slightly postponed monetary policy easing, entering the ZLB only around 2011. Although previous results tend to indicate that U.S. macroeconomic fluctuations have been driven by structural shocks rather than changes in the structure of the economy, it is worth mentioning that they should be interpreted cautiously due to weak statistical evidence.

The story seems to be different in the euro area. Empirical results show that changes in the structure of the economy have affected the path of inflation, output gap and hence the policy rate after the 2007-08 crisis, as reported in Figure I.E.11 in Online Appendix I.E. As depicted in Figure I.E.15, changes in the structure of the economy have been driven by changes in the

[24] Of course, the structural specification of the model does not allow to give an empirical estimation of both the Phillips and the IS curves consistent with the literature. For instance, the empirical so-called Phillips curve in this paper contains current and lagged values of the policy rate, which is not the case in any Phillips curve specification from standard macroeconomic textbook models.

parameters of the output gap equation to a great extent. This shift in the parameters of the equation seems to have slightly worsened euro area macroeconomic performances. Without any change in output gap equation's parameters from 2007:4 onward, the output gap would have been mostly positive and inflation would have constantly been on target, even increasing after 2015 to reach around 4%. In this specific case, ECB's monetary policy would have been less accommodative than what has been experienced in the euro area, despite being still at the ZLB. The results are more striking when demand shocks are muted in addition to fixed parameters in the output gap equation from 2007:4 onward. Indeed, Figure I.E.13 shows tighter credible intervals associated to simulated counterfactual series, and less volatile inflation and output gap around demand shocks observed around 2009. Once again, previous results should be interpreted with caution given the large uncertainty surrounding the results.

I.5.3 Should the ECB be a role model for the Fed and vice versa?

Previous results show how changes in the structure of the economy and shocks may have partially explained macroeconomic fluctuations. Whereas structural shocks hitting the economy appear to be a key feature of U.S. macroeconomic conditions, the path of euro area inflation and output gap seems to have been moving in reaction to changes in the structure of the economy. Those changes would have had huge monetary policy implications for both the Fed and the ECB. However, those results are hardly interpretable, since they do not provide any strong statistical evidence of the role of shocks and structures in U.S. and euro area macroeconomic fluctuations. Importantly, other previous counterfactual results show that changes in the conduct of ECB's monetary policy have been very effective in improving macroeconomic performances and particularly inflation in the euro area, which is not as obvious regarding the effectiveness of Fed's time-varying systematic policy.

For this reason, the question raised in this subsection is now the following: what would have happened to U.S. macroeconomic performances if the Fed had followed ECB's monetary policy rule? Based on Benati (2011), this counterfactual investigates whether the U.S. macroeconomic situation would have been better off when "bringing the ECB to the U.S.". Inversely, another counterfactual investigates what would have happened to euro area macroeconomic performances when "bringing the Fed to the euro area", i.e. if the ECB had adhered to Fed's monetary policy rule. To be able to construct these counterfactuals, response coefficients are rescaled to get some consistency before and after 2007:4.

Figure I.5.11 shows that the U.S. shadow policy rate would have been heavily negative in the case where the Fed had adhered to ECB's policy rule from 2007:4 onward, meaning that larger unconventional measures would have been implemented in reaction to the financial crisis. As a result, the U.S. economic recovery would have been sharper, but this strong accommodative policy would have been very costly in terms of inflation that would have largely overshot its target, reaching more than 7% in 2011.

Figure I.5.11 – Counterfactual simulations (U.S.)

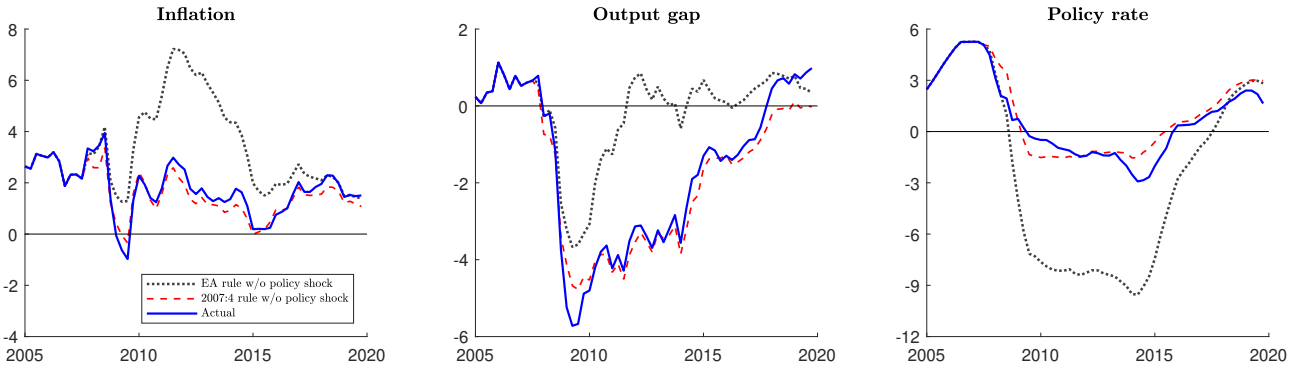

Note: Median counterfactual path (black dotted lines) are plotted for each indicated variable.

Figure I.5.12 shows that inflation in the euro area would have been much lower than what has been observed if the ECB had followed the U.S. policy rule. However, still according to this scenario, ECB monetary policy would have been more accommodative than that has been observed between 2010 and 2017, slightly improving real economic activity and avoiding periods of deflation in the euro area that would have been observed in the scenario with fixed policy rule parameters from 2007:4 onward. Overall, following Fed monetary policy would have been costly regarding ECB's primary objective of price stability, leading to weak inflation in the euro area.

I.6 Sensitivity analysis

I.6.1 Data choice

Shadow rate. The model is re-estimated with the shadow rate extracted from Krippner (2013, 2020).[25] Short- and long-run coefficients are given in Figures I.F.2 and I.F.3 in Online Appendix I.F.1. Although the tables containing median coefficients across different post-crisis

[25]Shadow short rates data are available on Leo Krippner's webpage.

Figure I.5.12 – Counterfactual simulations (Euro area)

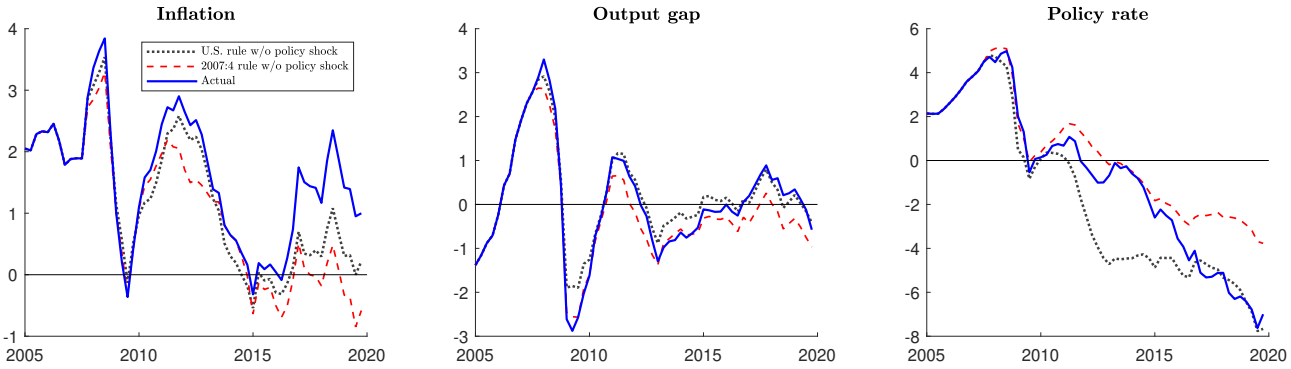

Note: Median counterfactual path (black dotted lines) are plotted for each indicated variable.

periods are not reported, it can be graphically deduced that estimated coefficients using Krippner's shadow short rate follow a similar path than those estimated with Wu and Xia's shadow rate. They also show that the ECB has been increasingly responsive to inflation fluctuations after the 2007-08 crisis, whereas Fed's systematic monetary policy has not changed significantly over that period. However, impulse responses and variance decompositions highlight that the U.S. shadow policy rate absorbs a large part of monetary policy shocks, providing evidence of a strong non-systematic component in Fed's monetary policy. Policy counterfactuals shed light on these results: the euro area would have suffered deflation episodes without a more aggressive ECB's response to inflation, and U.S. monetary policy would have been less accommodative without monetary policy shocks. Note that this tight Fed's monetary policy would not even have been noticeably costly for the U.S. macroeconomy.

Inflation and output series. Alternative specifications of the estimated monetary policy rule using different series are run over the sample. The robustness of the results is tested with different series of ex-post inflation and proxies for real activity. U.S. alternative series are mostly chosen following FOMC's historical prescriptions of targeted policy rules using various economic series.[26] First, the policy rule is assumed to be implemented as responding to the growth rate of core PCE price index rather than to headline PCE inflation. The main reason is that core PCE inflation seems to better predict the medium-term path of headline inflation than headline PCE inflation. Another specification includes real GDP growth rather than the CBO output gap. Also, following Okun's law (Okun, 1962), real GDP growth and output gap can be replaced by unemployment rate and unemployment gap, respectively.

[26] As recently and clearly explained is Part 2 of the Fed's 2021 Monetary Policy Report.

Euro area variables used in this paper are not as abundant as U.S. series, which reduces the possibility to run alternative ECB's reaction function estimates. This is especially true regarding inflation series. The benchmark ECB's policy rule specification includes HICP as an appropriate measure of the price index.[27] However, the euro area policy rule can still be estimated according to different proxies for real activity. As for the U.S., these rules consist in responding to real GDP growth or unemployment rate, rather than to output gap. Also, in line with Hamilton's (2018) criticism of the use of Hodrick-Prescott filter, euro area real potential GDP used to construct the output gap is estimated with Christiano and Fitzgerald (2003) bandpass filter.

As a whole, the results show that estimates of response coefficients are robust to these alternative inflation series and real activity proxies, especially regarding long-run coefficients and the volatility of monetary policy shocks. The time-varying coefficients are depicted in Figures I.F.11 to I.F.22 in Online Appendix I.F.2.

I.6.2 Choice of lag length

Three lags. Based on Primiceri (2005), Cogley and Sargent (2005), Benati and Mumtaz (2007), Gambetti et al. (2008), Canova and Gambetti (2009), and Koop et al. (2009), the baseline model is assumed to follow a second-order vector autoregressive model with time-varying coefficients and a time-varying covariance matrix for its innovations in the reduced form given in equation (2). More generally, the model follows a pth-order TVP-VAR model in the following reduced form: $\mathbf{y}_t = \mathbf{b}_t + \mathbf{B}_{1,t}\mathbf{y}_{t-1} + \ldots + \mathbf{B}_{p,t}\mathbf{y}_{t-p} + \mathbf{u}_t$, where p is the number of lags. The robustness of the results is checked when the number of lags is set at $p = 3$ instead of $p = 2$. The results are shown in Figures I.F.23 and I.F.24 in Online Appendix I.F.3. The interpretation is the same than that of the baseline model, concerning both long-term responses and volatility of monetary policy shocks.

I.6.3 Prior distribution

Calibration. The interpretation of estimation results may depend on the calibration of prior distribution. To test the sensitivity of the results to the specification of priors, the block element $\mathbf{Q}$ of the variance-covariance matrix of innovations $\mathbf{V}$ is now defined as $\mathbf{Q} \sim \mathcal{IW}(d_{\mathbf{Q}} k_{\mathbf{Q}}^2 \hat{V}_{\mathbf{B}}, d_{\mathbf{Q}})$, where $k_{\mathbf{Q}}^2 = 0.0001$ instead of $k_{\mathbf{Q}}^2 = 0.00035$ and $d_{\mathbf{Q}} = 40$ instead of $d_{\mathbf{Q}} = 22$, as specified

[27] As mentioned in the new monetary policy strategy of the ECB.

in Primiceri (2005). Moreover, the first five years are used to calibrate the prior distribution of coefficients, instead of using the first ten years. As a consequence, the sample period of estimation is extended to 1965:1 in the U.S. and 1976:1 in the euro area, instead of 1970:1 and 1981:1 as in the benchmark specification, respectively. Results do not show any significant difference with the benchmark results. They are reported in Figures I.F.25 and I.F.26 in Online Appendix I.F.3.

Horseshoe priors. Another alternative to the baseline TVP-VAR specification *à la* Primiceri (2005) consists in using different priors as recommended by Baumeister and Hamilton (2015, 2018). Since the calibration of the priors used in the traditional specification may suppress some degree of time variation in the VAR coefficients, Prüser (2021) proposes a flexible global-local prior allowing for abrupt rather than smooth changes in the parameters and in systematic monetary policy, and follows the TVP-VAR specification developed in Chan and Eisenstat (2018). Long-run response coefficients are depicted in Figure I.F.27 in the U.S. and Figure I.F.29 in the euro area. Monetary policy shock volatilities are given in Figure I.F.28 in the U.S. and Figure I.F.30 in the euro area in Online Appendix I.F.3. The results show that the monetary policy shocks volatility remains unchanged in the framework using flexible global-local priors.

I.6.4 Structural shocks identification

Cholesky factorization. Then, the robustness of the results is checked when monetary policy shocks are identified using the traditional Cholesky factorization of the variance-covariance matrix. In that case, inflation and output are assumed to react to monetary policy shocks with a one-period lag. The results are shown in Figures I.F.31 and I.F.32 in Online Appendix I.F.3. Using this identification strategy allows reducing uncertainty surrounding long-run coefficients, especially the response to output. As a consequence, long-term responses are more easily interpretable than in the baseline identification scheme. The response coefficient on output is even significantly different between the U.S. and the euro area after 2008, and suggests a much stronger Fed's response to output than before the financial crisis. On the other hand, the long-term response coefficient on output has decreased since 2008, and even became non-significantly different from zero when the crisis occurred.

Unrestricted response of output to a monetary policy shock. As highlighted by Uhlig (2005) and recently discussed by Arias et al. (2019) and Wolf (2020), the response of output gap to a monetary policy shock is left unconstrained to assess the effect of monetary policy on output.[28] Response coefficients of estimated policy rules are shown in Figures I.F.33 and I.F.34, and policy counterfactuals are shown in Figures I.F.35 and I.F.36 in Online Appendix I.F.3. Long-run responses and policy counterfactuals show similar pattern than in the baseline model.

I.7 Policy implications

Inflation targeting and monetary policy strategy. Previous results raise huge policy implications. Figure I.7.13 plots the time-varying inflation targets defined as the stochastic trend towards which inflation would have fluctuated based on draws of the model's parameters for each period, based on Cogley and Sargent (2005) and Cogley et al. (2010). U.S. estimates show evidence of a decline in the inflation objective through the financial crisis, then a stabilization at the 2% level consistent with the Fed's mandate. Then, the estimated target starts to increase just above 2% around the time of the main policy rate lift-off and Fed's policy normalization. Estimated inflation targets in the euro area shows unstable path of inflation objective compared with Fed's. While the ECB targeted a 2% level of inflation around 1999 and the launch of the euro, estimated targets have declined since the early 2000s in the euro area and have sharply dropped around the 2010-2012 sovereign debt crisis. The targets then rose due to strong ECB's unconventional measures to reach the 2% targeted level after 2015, before plummeted at the end of the sample period of estimation. Compared to the U.S., euro area monetary policy did not manage to stabilize its targeted values for inflation around the 2% level as mentioned in its mandate, especially because of these two major shocks that hit the economy in 2008 and 2010-2012. But this also raises the question of the anchoring of private agents' inflation expectations and of the credibility of the ECB to reach the 2% target over the long-run.

Recent evidence of the role of inflation target adjustments as a tool to stabilize macroeconomic fluctuations have been provided by Eo and Lie (2020).

[28] Uhlig (2005) finds no clear evidence of the effects of "contractionary" monetary policy shocks on real GDP.

Figure I.7.13 – Estimated inflation target

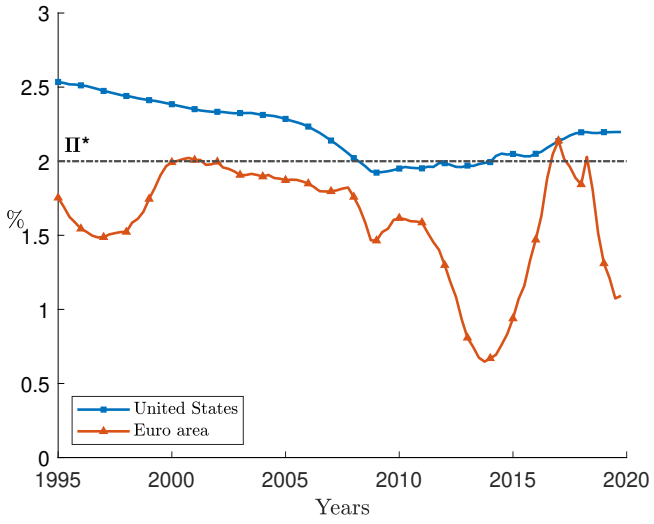

Note: Estimated inflation target is defined as the time-varying long-run mean for inflation. Median (solid lines) of the posterior distribution of the inflation target are plotted. Π^* stands for the 2% inflation target.

Rules versus discretion. Empirical results of estimated time-varying reaction functions also revive the debate over whether the central bank should adopt a rule-based approach to monetary policy-making. Nikolsko-Rzhevskyy et al. (2014) investigate the cost of deviating from Taylor-type policy rules and how it is related to discretionary monetary policy. They consider three types of monetary policy rules: an original, a modified, and an estimated Taylor rule. Interestingly, and in line with the results discussed above, they show that the overall period starting from 1965 has been mostly dominated by discretionary eras in the case of an estimated Taylor rule (from 1974 to 1987, and from 1995 until the end of their sample in 2013). In the TVP-VAR framework used in the paper, deviations from the estimated U.S. monetary policy rule are not caused by changes in the systematic component of monetary policy, which are found to be not statistically significant over time.

I.8 Conclusion

The question of changes in central banks' behavior can be explored by assuming that central banks follow a standard Taylor-type rule to guide monetary policy decisions. According to this framework, the central bank focuses attention on the evolution of macroeconomic fundamentals, such as inflation and output, to determine its target value for the interest rate. The small-scale time-varying parameters vector autoregressive model used in this paper gives some empirical assessments of time-variations in the estimated simple Taylor rule in the U.S. and in

the euro area during the post-2008 decade. It allows a better understanding of monetary policy implementations by assessing changes in Fed's and ECB's behavior over the post-crisis period.

Using a shadow rate to capture the stance of monetary policy at the ZLB, the empirical analysis shows that the conduct of monetary policy in the euro area has evolved differently than in the U.S. after the 2007-08 financial crisis. Despite a slight decrease in the response to inflation, the estimated U.S. policy rule shows no noticeable change in the Fed's reaction to macroeconomic fluctuations after 2008. In fact, the results highlight the role of the non-systematic component of Fed's monetary policy. By reacting in an unpredictable manner to changes in macroeconomic conditions, the Fed has largely departed from the rule-based policy and hence used discretion in policy making. In the euro area, the estimated monetary policy rule reveals that the ECB has been considerably more aggressive towards inflation stabilization and has also regularly but briefly departed from the rule-based policy since 2008. These results suggest important changes in the conduct of ECB's monetary policy, mainly through its systematic component. A counterfactual analysis shows that this shift in the systematic component of monetary policy appears to be a key determinant of the level of inflation in the euro area at the ZLB, that would have suffered deflationary episodes from 2014:3 to 2016:4 and starting from 2019:3 without any change in ECB's response to macroeconomic conditions after the 2007-08 crisis. The situation could have been even worse when ignoring the role of the non-systematic component of ECB's monetary policy.

Estimation results concerning changes in Fed's and ECB's behavior since the Great Recession therefore raise some potential policy implications. Among them, it highlights the need for adapting inflation targeting framework, especially in the euro area.

Also, the shift in the conduct of U.S. and euro area monetary policies challenges the idea of a monetary policy coordination.[29] A cooperation between Fed and ECB monetary policies should rely on strong assumptions, such as similar objectives, common aspects in the transmission mechanisms or synchronized business cycles. All these points could explain differences in U.S. and euro area estimation results presented in this paper, and could also be considered as a possible explanation for the gap in the timing of monetary policy decisions between the Fed and the ECB. From this point of view, a two-country structural model allowing for international spillovers would be welcomed to investigate the relationship between Fed's and ECB's behavior and macroeconomic fluctuations at the ZLB, and to suggest a theoretical framework consistent

[29] See Cœuré (2014) for remarks on policy coordination.

with the empirical findings. Such implications for the conduct of monetary policy are left for future research.

Appendix

Evolving Monetary Policy in the Aftermath of the Great Recession

I.A TVP-VAR methodology

I.A.1 The model

The model is from Primiceri (2005), with the MCMC algorithm corrected as described by Del Negro and Primiceri (2015). This section is a step-by-step guide to use the TVP-VAR methodology, as described in details in Primiceri's (2005) and Belongia and Ireland's (2016) corresponding appendices.

The baseline model is applied to quarterly data on the inflation rate (measured by the PCE inflation rate in the U.S. and the HICP in the euro area), denoted Π_t, output gap (estimated using CBO formula for the U.S. and HP filter for the euro area), denoted G_t, and the short-term shadow rate (federal funds rate in the U.S., 3-month Euribor in the euro area in normal times, and shadow rates at the ZLB), denoted R_t^s. U.S. data run from 1960:1 to 2019:4. Euro area data run from 1971:1 to 2019:4.

These observable endogenous series are combined into the 3×1 vector

$$\mathbf{y}_t = \begin{bmatrix} \Pi_t & G_t & R_t^s \end{bmatrix}', \tag{I.1}$$

which is assumed to follow a second-order vector autoregression with time-varying coefficients

and a time-varying covariance matrix for the innovations. Thus, the model's reduced form is

$$\mathbf{y}_t = \mathbf{b}_t + \mathbf{B}_{1,t}\mathbf{y}_{t-1} + \mathbf{B}_{2,t}\mathbf{y}_{t-2} + \mathbf{u}_t \tag{I.2}$$

where

$$\mathbf{b}_t = \begin{bmatrix} b_{\pi,t} & b_{g,t} & b_{r,t} \end{bmatrix}'$$

is a 3×1 vector of time-varying constant terms,

$$\mathbf{B}_{i,t} = \begin{bmatrix} b_{i,\pi\pi,t} & b_{i,\pi g,t} & b_{i,\pi r,t} \\ b_{i,g\pi,t} & b_{i,gg,t} & b_{i,gr,t} \\ b_{i,r\pi,t} & b_{i,rg,t} & b_{i,rr,t} \end{bmatrix},$$

with $i = 1, 2$, are 3×3 matrices of time-varying coefficients, and

$$\mathbf{u}_t = \begin{bmatrix} u_{\pi,t} & u_{g,t} & u_{r,t} \end{bmatrix}'$$

is a 3×1 vector of heteroskedastic shocks with covariance matrix $\mathbf{\Omega}_t$, such that $\mathbb{E}\{\mathbf{u}_t\mathbf{u}_t'\} = \mathbf{\Omega}_t$.

Without loss of generality, $\mathbf{\Omega}_t$ can be decomposed as

$$\mathbf{\Omega}_t = \mathbf{A}_t^{-1}\mathbf{\Sigma}_t\mathbf{\Sigma}_t'(\mathbf{A}_t')^{-1} \tag{I.3}$$

where $\mathbf{A}_t$ is the lower triangular matrix

$$\mathbf{A}_t = \begin{bmatrix} 1 & 0 & 0 \\ \alpha_{g\pi,t} & 1 & 0 \\ \alpha_{r\pi,t} & \alpha_{rg,t} & 1 \end{bmatrix} \tag{I.4}$$

and $\mathbf{\Sigma}_t$ is the diagonal matrix

$$\mathbf{\Sigma}_t = \begin{bmatrix} \sigma_{\pi,t} & 0 & 0 \\ 0 & \sigma_{g,t} & 0 \\ 0 & 0 & \sigma_{r,t} \end{bmatrix}. \tag{I.5}$$

The reduced form (I.2) can therefore be represented equivalently as

$$\mathbf{y}_t = \mathbf{b}_t + \mathbf{B}_{1,t}\mathbf{y}_{t-1} + \mathbf{B}_{2,t}\mathbf{y}_{t-2} + \mathbf{A}_t^{-1}\mathbf{\Sigma}_t\varepsilon_t, \tag{I.6}$$

where $E\{\varepsilon_t \varepsilon_t'\} = \mathbf{I}_3$. Stacking all the coefficients into the 21×1 vector

$$\mathbf{B}_t = \text{vec}\left(\begin{bmatrix} \mathbf{b}_t' \\ \mathbf{B}_{1,t}' \\ \mathbf{B}_{2,t}' \end{bmatrix}\right),$$

(I.6) can be rewritten as

$$\mathbf{y}_t = \mathbf{X}_t' \mathbf{B}_t + \mathbf{A}_t^{-1} \mathbf{\Sigma}_t \varepsilon_t, \tag{I.7}$$

where

$$\mathbf{X}_t = \mathbf{I}_3 \otimes \begin{bmatrix} 1 & \Pi_{t-1} & G_{t-1} & R_{t-1}^s & \Pi_{t-2} & G_{t-2} & R_{t-2}^s \end{bmatrix}$$

Let

$$\alpha_t = \begin{bmatrix} \alpha_{g\pi,t} & \alpha_{r\pi,t} & \alpha_{rg,t} \end{bmatrix}'$$

be the vector of non-zero and non-one elements of $\mathbf{A}_t$ and

$$\sigma_t = \begin{bmatrix} \sigma_{\pi,t} & \sigma_{g,t} & \sigma_{r,t} \end{bmatrix}'$$

be the vector of diagonal elements of $\mathbf{\Sigma}_t$. The dynamics of the time-varying parameters are specified as

$$\mathbf{B}_t = \mathbf{B}_{t-1} + \nu_t, \tag{I.8}$$

$$\alpha_t = \alpha_{t-1} + \zeta_t, \tag{I.9}$$

and

$$\log \sigma_t = \log \sigma_{t-1} + \eta_t. \tag{I.10}$$

In (I.7)-(I.10), all of the innovations are assumed to be jointly normally distributed with

$$\mathbf{V} = \mathbb{V}\text{ar}\left(\begin{bmatrix} \varepsilon_t \\ \nu_t \\ \zeta_t \\ \eta_t \end{bmatrix}\right) = \mathbb{E}\left(\begin{bmatrix} \varepsilon_t \\ \nu_t \\ \zeta_t \\ \eta_t \end{bmatrix} \begin{bmatrix} \varepsilon_t & \nu_t & \zeta_t & \eta_t \end{bmatrix}\right) = \begin{bmatrix} \mathbf{I}_3 & \mathbf{0}_{3,21} & \mathbf{0}_{3,3} & \mathbf{0}_{3,3} \\ \mathbf{0}_{21,3} & \mathbf{Q} & \mathbf{0}_{21,3} & \mathbf{0}_{21,3} \\ \mathbf{0}_{3,3} & \mathbf{0}_{3,21} & \mathbf{S} & \mathbf{0}_{3,3} \\ \mathbf{0}_{3,3} & \mathbf{0}_{3,21} & \mathbf{0}_{3,3} & \mathbf{W} \end{bmatrix}, \tag{I.11}$$

where $\mathbf{Q}$ is 21×21, $\mathbf{S}$ is 3×3, and $\mathbf{W}$ is 3×3 and diagonal, so that the standard deviations in σ_t evolve as independent geometric random walks. Following Primiceri (2005), it will be

assumed that $\mathbf{S}$ is block-diagonal, with one non-zero element in the first column of the first row and three distinct non-zero elements in the second and third columns of the second and third rows. Hence, $\mathbf{Q}$ has 231 distinct elements, $\mathbf{S}$ has 4 distinct elements and is block-diagonal in the following form:

$$\mathbf{S} = \begin{bmatrix} s_{1,1} & 0 & 0 \\ 0 & s_{2,2} & s_{2,3} \\ 0 & s_{3,2} & s_{3,3} \end{bmatrix}$$

where $s_{i,j}$ are non-zero elements on line-i and row-j of matrix $\mathbf{S}$. Hence, the two diagonal blocks are given by the following matrices:

$$\mathbf{S}_1 = s_{1,1} \text{ and } \mathbf{S}_2 = \begin{bmatrix} s_{2,2} & s_{2,3} \\ s_{3,2} & s_{3,3} \end{bmatrix}, \text{ where } s_{2,3} = s_{3,2}$$

Moreover, $\mathbf{W}$ is diagonal with elements $w_{i,i}$ for $i = 1, 2, 3$, and has three distinct elements.

In all that follows, let

$$\omega^{\tau} = \begin{bmatrix} \omega_1' & \dots & \omega_{\tau}' \end{bmatrix}'$$

denote the history of a generic vector of variables ω_t up to a generic time τ. And for a generic matrix of variables and constant terms $\mathbf{M}_t$, let

$$\mathbf{M}^{\tau} = \begin{bmatrix} m_1' & \dots & m_{\tau}' \end{bmatrix}'$$

where m_t is a column vector constructed from the time varying elements of $\mathbf{M}_t$.

I.A.2 Prior Distributions

Following Cogley and Sargent (2005) and Primiceri (2005), classical estimates of the parameters obtained by applying a training sample consisting of the first ten years of data to a constant-parameter version of the model are used to calibrate the prior means and standard deviations for the time-varying parameters when estimated with the rest of the sample. The

constant-parameter version of the reduced form (I.2) is written as

$$\mathbf{y}_t = \mathbf{b} + \mathbf{B}_1\mathbf{y}_{t-1} + \mathbf{B}_2\mathbf{y}_{t-2} + \mathbf{u}_t,$$

Hamilton (1994) and Lütkepohl (2005) show that estimates of the constant and slope coefficients in $\mathbf{b}$, $\mathbf{B}_1$, and $\mathbf{B}_2$ can be obtained by applying OLS separately to each equation. Stacking these estimated coefficients into the 21×1 vector

$$\hat{\mathbf{B}} = \text{vec}\left(\begin{bmatrix} \hat{\mathbf{b}}' \\ \hat{\mathbf{B}}_1' \\ \hat{\mathbf{B}}_2' \end{bmatrix}\right),$$

and defining

$$\mathbf{x}_t = \begin{bmatrix} 1 & \Pi_{t-1} & G_{t-1} & R^s_{t-1} & \Pi_{t-2} & G_{t-2} & R^s_{t-2} \end{bmatrix},$$

standard errors can be computed using the formulas from Hamilton's (1994) proposition on maximum likelihood estimation of vector autoregressions:

$$\mathbb{V}\text{ar}(\hat{\mathbf{B}}) = \hat{\mathbf{\Omega}} \otimes \left(\sum_{t=1}^{T} \mathbf{x}_t\mathbf{x}_t'\right)^{-1},$$

where

$$\hat{\mathbf{\Omega}} = \frac{1}{T}\sum_{t=1}^{T} \hat{\mathbf{u}}_t\hat{\mathbf{u}}_t'$$

is the estimated covariance matrix for the least squares residuals

$$\hat{\mathbf{u}}_t = \mathbf{y}_t - \hat{\mathbf{b}} - \hat{\mathbf{B}}_1\mathbf{y}_{t-1} - \hat{\mathbf{B}}_2\mathbf{y}_{t-2}$$

The initial states for the coefficients, covariances, and log volatilities as well as the hyper-parameters in $\mathbf{V}$ are assumed to be all independent of each other. The priors for $\mathbf{B}_0$, α_0, and $\log\sigma_0$ are assumed to be normal and the priors for $\mathbf{Q}$, $\mathbf{W}$, and the blocks of $\mathbf{S}$ are assumed to be distributed as independent inverse-Wishart. These assumptions together with (I.6)-(I.8) imply normal priors on the entire sequences $\mathbf{B}^T$, α^T, and $\mathbf{\Sigma}^T$.

Estimates $\hat{\mathbf{A}}$ and $\hat{\mathbf{\Sigma}}$ of $\mathbf{A}$ and $\mathbf{\Sigma}$ can then be obtained by decomposing $\hat{\mathbf{\Omega}}$ as in (I.3):

$$\hat{\mathbf{\Omega}} = \hat{\mathbf{A}}^{-1}\hat{\mathbf{\Sigma}}\hat{\mathbf{\Sigma}}'(\hat{\mathbf{A}}')^{-1}.$$

Standard errors for the non-zero, non-one elements $\hat{\alpha}$ and $\hat{\sigma}$ of $\hat{\mathbf{A}}$ and $\hat{\mathbf{\Sigma}}$ can be computed using the formulas in Lütkepohl's (2005) proposition on the properties of the structural VAR maximum likelihood estimators. Start by rewriting

$$\text{vec}(\mathbf{A}) = R_{\mathbf{A}}\alpha + r_{\mathbf{A}}$$

and

$$\text{vec}(\mathbf{\Sigma}) = R_{\mathbf{\Sigma}}\sigma$$

with $R_{\mathbf{A}}$ and $R_{\mathbf{\Sigma}}$ are 9×3 suitable fixed matrices of zeros and ones, where

$$R_{\mathbf{A}} = \begin{bmatrix} 0 & 1 & 0 & 0 & 0 & 0 & 0 & 0 & 0 \\ 0 & 0 & 1 & 0 & 0 & 0 & 0 & 0 & 0 \\ 0 & 0 & 0 & 0 & 0 & 1 & 0 & 0 & 0 \end{bmatrix}'$$

and

$$R_{\mathbf{\Sigma}} = \begin{bmatrix} 1 & 0 & 0 & 0 & 0 & 0 & 0 & 0 & 0 \\ 0 & 0 & 0 & 0 & 1 & 0 & 0 & 0 & 0 \\ 0 & 0 & 0 & 0 & 0 & 0 & 0 & 0 & 1 \end{bmatrix}'$$

and $r_{\mathbf{A}}$ is a 9×1 vector of fixed parameters allowing for the normalization of diagonal elements of matrix $\mathbf{A}$.

$$r_{\mathbf{A}} = \begin{bmatrix} 1 & 0 & 0 & 0 & 1 & 0 & 0 & 0 & 1 \end{bmatrix}'$$

Next, let $\mathbf{K}_{9,9}$ be the commutation matrix that, for any 3×3 matrix $\mathbf{D}$, is such that

$$\text{vec}(\mathbf{D}) = \mathbf{K}_{9,9}\text{vec}(\mathbf{D}').$$

Then, in particular, $\mathbf{K}_{9,9}$ is a 9×9 matrix of zeros and ones such that

$$\mathbf{K}_{9,9} = \begin{bmatrix} 1 & 0 & 0 & 0 & 0 & 0 & 0 & 0 & 0 \\ 0 & 0 & 0 & 1 & 0 & 0 & 0 & 0 & 0 \\ 0 & 0 & 0 & 0 & 0 & 0 & 1 & 0 & 0 \\ 0 & 1 & 0 & 0 & 0 & 0 & 0 & 0 & 0 \\ 0 & 0 & 0 & 0 & 1 & 0 & 0 & 0 & 0 \\ 0 & 0 & 0 & 0 & 0 & 0 & 0 & 1 & 0 \\ 0 & 0 & 1 & 0 & 0 & 0 & 0 & 0 & 0 \\ 0 & 0 & 0 & 0 & 0 & 1 & 0 & 0 & 0 \\ 0 & 0 & 0 & 0 & 0 & 0 & 0 & 0 & 1 \end{bmatrix}$$

Following Lütkepohl's (2005) proposition

$$\sqrt{T}\left(\begin{bmatrix}\hat{\alpha}\\ \hat{\sigma}\end{bmatrix} - \begin{bmatrix}\alpha\\ \sigma\end{bmatrix}\right) \rightarrow \mathcal{N}\left(0, \mathcal{I}_a\left(\begin{bmatrix}\alpha\\ \sigma\end{bmatrix}\right)^{-1}\right)$$

and hence

$$\mathbb{V}\mathrm{ar}\left(\begin{bmatrix}\hat{\alpha}\\ \hat{\sigma}\end{bmatrix}\right) = \frac{1}{T}\left[\mathcal{I}_a\left(\begin{bmatrix}\alpha\\ \sigma\end{bmatrix}\right)\right]^{-1}$$

where $\mathcal{I}_a(.)$ is the is the asymptotic information matrix that has the form

$$\mathcal{I}_a\left(\begin{bmatrix}\alpha\\ \sigma\end{bmatrix}\right) = \begin{bmatrix} R'_{\mathbf{A}} & \mathbf{0}_{3,9} \\ \mathbf{0}_{3,9} & R'_{\mathbf{\Sigma}} \end{bmatrix} \mathcal{I}_a\left(\begin{bmatrix}\mathrm{vec}(\mathbf{A})\\ \mathrm{vec}(\mathbf{\Sigma})\end{bmatrix}\right) \begin{bmatrix} R_{\mathbf{A}} & \mathbf{0}_{9,3} \\ \mathbf{0}_{9,3} & R_{\mathbf{\Sigma}} \end{bmatrix},$$

and

$$\mathcal{I}_a\left(\begin{bmatrix}\mathrm{vec}(\mathbf{A})\\ \mathrm{vec}(\mathbf{\Sigma})\end{bmatrix}\right) = \begin{bmatrix} \mathbf{A}^{-1}\mathbf{\Sigma} \otimes \mathbf{\Sigma}'^{-1} \\ -(\mathbf{I}_3 \otimes \mathbf{\Sigma}'^{-1}) \end{bmatrix} (\mathbf{I}_9 + \mathbf{K}_{9,9}) \begin{bmatrix} [\mathbf{\Sigma}'\mathbf{A}'^{-1}] \otimes \mathbf{\Sigma}^{-1} & -(\mathbf{I}_3 \otimes \mathbf{\Sigma}^{-1}) \end{bmatrix},$$

Priors can now be selected along the same lines proposed by Cogley and Sargent (2005), Primiceri (2005) and Benati (2011). Specifically, for $\mathbf{B}_0$, α_0, and $\log \sigma_0$, it is assumed that

$$\mathbf{B}_0 \sim \mathcal{N}(\hat{\mathbf{B}}, k_{\mathbf{B}}^2 V_{\mathbf{B}}),$$

$$\alpha_0 \sim \mathcal{N}(\hat{\alpha}, k_\alpha^2 V_\alpha),$$

and

$$\log \sigma_0 \sim \mathcal{N}(\log \hat{\sigma}, k_\sigma^2 \mathbf{I}_3),$$

where choices for the hyperparameters are tabulated below.

Training Sample Prior Hyperparameters

	$k_{\mathbf{B}}^2$	$V_{\mathbf{B}}$	k_α	V_α	k_σ^2
Cogley and Sargent (2005)	1	$\mathbb{V}\mathrm{ar}(\hat{\mathbf{B}})$	10000	$\mathbf{I}_3$	10
Primiceri (2005)	4	$\mathbb{V}\mathrm{ar}(\hat{\mathbf{B}})$	4	$\mathbb{V}\mathrm{ar}(\hat{\mathbf{A}})$	1
Benati (2011)	4	$\mathbb{V}\mathrm{ar}(\hat{\mathbf{B}})$	$\sqrt{10}$	$\mathrm{diag}(\hat{\alpha})$	10

Training sample prior hyperparameters used in the TVP-VAR are calibrated according to Primiceri (2005). Note that (I.8)-(I.10) imply that

$$\mathbf{B}_t | \mathbf{B}_{t-1}, \mathbf{Q} \sim \mathcal{N}(\mathbf{B}_{t-1}, \mathbf{Q}),$$

$$\alpha_t | \alpha_{t-1}, \mathbf{S} \sim \mathcal{N}(\alpha_{t-1}, \mathbf{S}),$$

and

$$\log \sigma_t | \sigma_{t-1}, \mathbf{W} \sim \mathcal{N}(\log \sigma_{t-1}, \mathbf{W}).$$

Hence, priors for the entire sequences $\mathbf{B}^T$, α^T, and $\mathbf{\Sigma}^T$ are

$$p(\mathbf{B}^T | \mathbf{B}_0, \mathbf{Q}) = \prod_{t=1}^{T} p(\mathbf{B}_t | \mathbf{B}_{t-1}, \mathbf{Q}),$$

$$p(\alpha^T | \alpha_0, \mathbf{S}) = \prod_{t=1}^{T} p(\alpha_t | \alpha_{t-1}, \mathbf{S}),$$

and

$$p(\mathbf{\Sigma}^T | \mathbf{\Sigma}_0, \mathbf{W}) = \prod_{t=1}^{T} p(\log \sigma_t | \log \sigma_{t-1}, \mathbf{W}).$$

For $\mathbf{Q}$ and the two blocks of $\mathbf{S}$, the inverse Wishart priors are calibrated as

$$\mathbf{Q} \sim \mathcal{IW}(d_{\mathbf{Q}} k_{\mathbf{Q}}^2 V_{\mathbf{Q}}, d_{\mathbf{Q}}),$$

$$\mathbf{S}_1 \sim \mathcal{IW}(d_{\mathbf{S}1} k_{\mathbf{S}}^2 V_{\mathbf{S}1}, d_{\mathbf{S}1}),$$

and

$$\mathbf{S}_2 \sim \mathcal{IW}(d_{\mathbf{S}2} k_{\mathbf{S}}^2 V_{\mathbf{S}2}, d_{\mathbf{S}2}).$$

Finally, for each diagonal element $w_{i,i}$, $i = 1, 2, 3$, of $\mathbf{W}$, the inverse Gamma prior used by Cogley and Sargent (2005) and Benati (2011) can also be expressed as an inverse Wishart:

$$w_{i,i} \sim \mathcal{IG}\left(\frac{d_{\mathbf{W}}}{2}, \frac{d_{\mathbf{W}} k_{\mathbf{W}}^2}{2}\right) = \mathcal{IW}(d_{\mathbf{W}} k_{\mathbf{W}}^2, d_{\mathbf{W}}).$$

Choices for the hyperparameters are tabulated below. Cogley and Sargent (2005) do not allow for time-variation in the elements of $\mathbf{A}$.

Time-Varying Parameter Prior Hyperparameters

	$k_{\mathbf{Q}}^2$	$V_{\mathbf{Q}}$	$d_{\mathbf{Q}}$	$k_{\mathbf{S}}^2$	$V_{\mathbf{S}1}$	$d_{\mathbf{S}1}$	$V_{\mathbf{S}2}$	$d_{\mathbf{S}2}$	$k_{\mathbf{W}}^2$	$d_{\mathbf{W}}$
Cogley and Sargent (2005)	0.00035	$\mathbb{V}\mathrm{ar}(\hat{\mathbf{B}})$	22	–	–	–	–	–	0.0001	1
Primiceri (2005)	0.0001	$\mathbb{V}\mathrm{ar}(\hat{\mathbf{B}})$	40	0.01	$V_{\alpha}^{1,1}$	2	$V_{\alpha}^{2:3,2:3}$	3	0.0001	2
Benati (2011)	0.00035	$\mathbb{V}\mathrm{ar}(\hat{\mathbf{B}})$	22	0.001	$\hat{\alpha}^1$	2	$\mathrm{diag}(\hat{\alpha}^{2:3})$	3	0.0001	1

where $V_{\alpha}^{1,1}$ is the element from the first row and first column of V_{α}, $V_{\alpha}^{2:3,2:3}$ is the matrix formed from the last two rows and columns of V_{α}, and $\hat{\alpha}^1$ and $\hat{\alpha}^{2:3}$ correspond to the first and the second through third elements of the vector $\hat{\alpha}$. Time-varying parameter model's prior hyperparameters are calibrated according to Cogley and Sargent (2005) and Benati (2011) for matrix $\mathbf{Q}$. Cogley and Sargent (2005) suggest to set out the degree of freedom of inverse Wishart as $d_{\mathbf{Q}} = \dim(\mathbf{B}_t) + 1$. Otherwise, model's prior hyperparameters are calibrated according to Primiceri (2005).

I.A.3 The Markov Chain Monte Carlo Algorithm

The algorithm gets initialized by choosing initial draws for α^T, σ^T, and $\mathbf{V}$ from the prior distributions described above. The Gibbs sampling algorithm then loops through the following steps.

Drawing the Coefficient States

Conditional on $(\alpha^T, \sigma^T, \mathbf{V})$, the observation equation (I.5) in linear and has Gaussian innovations with known variance. As shown in Carter and Kohn (1994a) and Frühwirth-Schnatter

(1994), the density can be factored as

$$p(\mathbf{B}^T|\mathbf{y}^T,\alpha^T,\sigma^T,\mathbf{V}) = p(\mathbf{B}_T|\mathbf{y}^T,\alpha^T,\sigma^T,\mathbf{V})\prod_{t=1}^{T-1} p(\mathbf{B}_t|\mathbf{B}_{t+1},\mathbf{y}^t,\alpha^T,\sigma^T,\mathbf{V}),$$

where

$$\mathbf{B}_t|\mathbf{B}_{t+1},\mathbf{y}^t,\alpha^T,\sigma^T,\mathbf{V} \sim \mathcal{N}(\mathbf{B}_{t|t+1},\mathbf{P}_{t|t+1}),$$

$$\mathbf{B}_{t|t+1} = \mathbb{E}(\mathbf{B}_t|\mathbf{B}_{t+1},\mathbf{y}^t,\alpha^T,\sigma^T,\mathbf{V}),$$

and

$$\mathbf{P}_{t|t+1} = \mathbb{V}\mathrm{ar}(\mathbf{B}_t|\mathbf{B}_{t+1},\mathbf{y}^t,\alpha^T,\sigma^T,\mathbf{V}).$$

The vector of $\mathbf{B}$s can be drawn easily because $\mathbf{B}_{t|t+1}$ and $\mathbf{P}_{t|t+1}$ can be computed using forward and backward recursions on the Kalman filter as follows.

The measurement equation for this step is (I.7), rewritten as

$$\mathbf{y}_t = \mathbf{X}_t'\mathbf{B}_t + \mathbf{u}_t \tag{I.12}$$

where $\mathbf{u}_t = \mathbf{A}_t^{-1}\mathbf{\Sigma}_t\varepsilon_t$, $\mathbb{E}\{\mathbf{u}_t\mathbf{u}_t'\} = \mathbf{\Omega}_t$ and $\mathbf{\Omega}_t = \mathbf{A}_t^{-1}\mathbf{\Sigma}_t\mathbf{\Sigma}_t'(\mathbf{A}_t^{-1})'$, and the state transition equation is given by (I.8) as

$$\mathbf{B}_t = \mathbf{B}_{t-1} + \nu_t$$

where $\mathbb{E}\{\nu_t\nu_t'\} = \mathbf{Q}$. Let

$$\mathbf{B}_{t|s} = \mathbb{E}(\mathbf{B}_t|\mathbf{y}^s,\mathbf{X}^s,\mathbf{\Omega}^s,\mathbf{Q})$$

and

$$\mathbf{P}_{t|s} = \mathbb{V}\mathrm{ar}(\mathbf{B}_t|\mathbf{y}^s,\mathbf{X}^s,\mathbf{\Omega}^s,\mathbf{Q}).$$

Then, given $\mathbf{B}_{0|0} = \hat{\mathbf{B}}$ and $\mathbf{P}_{0|0} = k_{\mathbf{B}}^2 V_{\mathbf{B}}$, the Kalman filter implies

$$\mathbf{B}_{t|t-1} = \mathbf{B}_{t-1|t-1},$$

$$\mathbf{P}_{t|t-1} = \mathbf{P}_{t-1|t-1} + \mathbf{Q},$$

$$\mathbf{K}_t = \mathbf{P}_{t|t-1}\mathbf{X}_t(\mathbf{X}_t'\mathbf{P}_{t|t-1}\mathbf{X}_t + \mathbf{\Omega}_t)^{-1},$$

$$\mathbf{B}_{t|t} = \mathbf{B}_{t|t-1} + \mathbf{K}_t(\mathbf{y}_t - \mathbf{X}_t'\mathbf{B}_{t|t-1}),$$

and

$$\mathbf{P}_{t|t} = \mathbf{P}_{t|t-1} - \mathbf{K}_t \mathbf{X}_t' \mathbf{P}_{t|t-1}.$$

The last elements from these recursions are $\mathbf{B}_{T|T}$ and $\mathbf{P}_{T|T}$, which are the mean and variance of the normal distribution used to make a draw for $\mathbf{B}_t$. The draw for $\mathbf{B}_t$ and the output of the filter can now be used for the first step of the backward recursions

$$\mathbf{B}_{t|t+1} = \mathbf{B}_{t|t} + \mathbf{P}_{t|t}\mathbf{P}_{t+1|t}^{-1}(\mathbf{B}_{t+1} - \mathbf{B}_{t|t}) = \mathbf{B}_{t|t} + \mathbf{P}_{t|t}(\mathbf{P}_{t|t} + \mathbf{Q})^{-1}(\mathbf{B}_{t+1} - \mathbf{B}_{t|t})$$

and

$$\mathbf{P}_{t|t+1} = \mathbf{P}_{t|t} - \mathbf{P}_{t|t}\mathbf{P}_{t+1|t}^{-1}\mathbf{P}_{t|t} = \mathbf{P}_{t|t} - \mathbf{P}_{t|t}(\mathbf{P}_{t|t} + \mathbf{Q})^{-1}\mathbf{P}_{t|t},$$

which are the means and variances used to make the draws for $\mathbf{B}_t$, $t = T-1, T-2, \ldots, 1$.

Drawing Covariance States

The system of equations in (I.7) can be rewritten as

$$\mathbf{A}_t(\mathbf{y}_t - \mathbf{X}_t'\mathbf{B}_t) = \mathbf{A}_t\mathbf{u}_t = \mathbf{\Sigma}_t\varepsilon_t, \tag{I.13}$$

where, taking $\mathbf{B}^T$ as given, $\mathbf{u}_t$ is observable from (I.12). Since $\mathbf{A}_t$ is a lower triangular matrix with ones on the main diagonal, (I.13) can be rewritten as

$$\mathbf{u}_t = \mathbf{Z}_t\alpha_t + \mathbf{\Sigma}_t\varepsilon_t, \tag{I.14}$$

where α_t is defined in (I.9) and $\mathbf{Z}_t$ is the following 3×3 matrix:

$$\mathbf{Z}_t = \begin{bmatrix} 0 & 0 & 0 \\ -u_{\pi,t} & 0 & 0 \\ 0 & -u_{\pi,t} & -u_{g,t} \end{bmatrix}$$

The model given by (I.14) and (I.9) has a Gaussian but nonlinear state space representation. The problem is that the dependent variable of the observation equation, $\mathbf{u}_t$, also appears on the right-hand side in $\mathbf{Z}_t$. Therefore, the vector $\begin{bmatrix} \mathbf{u}_t & \alpha_t \end{bmatrix}$ is not jointly normal and, as a consequence, the conditional distributions cannot be computed using the standard Kalman filter recursions. However, under the additional maintained assumption that $\mathbf{S}$ is block diagonal, this problem

can be solved by applying the Kalman filter and the backward recursion equation by equation.

Thus, consider the second equation from (I.14), which can be written

$$u_{g,t} = \mathbf{Z}_{1t}\alpha_{g\pi,t} + \sigma_{g,t}\varepsilon_{g,t}, \tag{I.15}$$

where $\mathbf{Z}_{1t} = -u_{\pi,t}$ and $\varepsilon_{g,t} \sim iid\mathcal{N}(0,1)$. Taking $\mathbf{B}^T$ and σ^T as given, u_{gt} and $\mathbf{Z}_{1t}$ are observable and $\sigma_{g,t}$ is given as well. Equation (I.15) can serve as the observation equation and the first equation from (I.9),

$$\alpha_{g\pi,t} = \alpha_{g\pi,t-1} + \zeta_{1,t} \tag{I.16}$$

as the state transition equation, where $\xi_{1,t} \sim \mathcal{N}(0, \mathbf{S}_1)$, with $\mathbf{S}_1$ given as well.

Thus, given $\alpha_{g\pi,0|0} = \hat{\alpha}_{g\pi}$ and $\mathbf{P}_{0|0} = k_\alpha^2 V_\alpha^{1,1}$, the Kalman filter implies

$$\alpha_{g\pi,t|t-1} = \alpha_{g\pi,t-1|t-1},$$

$$\mathbf{P}_{t|t-1} = \mathbf{P}_{t-1|t-1} + \mathbf{S}_1,$$

$$\mathbf{K}_t = \mathbf{P}_{t|t-1}\mathbf{Z}_{1t}'(\mathbf{Z}_{1t}\mathbf{P}_{t|t-1}\mathbf{Z}_{1t}' + \sigma_{g,t}^2)^{-1},$$

$$\alpha_{g\pi,t|t} = \alpha_{g\pi,t|t-1} + \mathbf{K}_t(u_{g,t} - \mathbf{Z}_{1t}\alpha_{g\pi,t|t-1}),$$

and

$$\mathbf{P}_{t|t} = \mathbf{P}_{t|t-1} - \mathbf{K}_t\mathbf{Z}_{1t}\mathbf{P}_{t|t-1}.$$

The last elements from these recursions are $\alpha_{g\pi,T|T}$ and $\mathbf{P}_{t|t}$, which are the mean and variance of the normal distribution used to make a draw for $\alpha_{g\pi,T}$. The draw for $\alpha_{g\pi,T}$ and the output of the filter can now be used for the first step of the backward recursions

$$\alpha_{g\pi,t|t+1} = \alpha_{g\pi,t|t} + \mathbf{P}_{t|t}\mathbf{P}_{t+1|t}^{-1}(\alpha_{g\pi,t+1} - \alpha_{g\pi,t|t}) = \alpha_{g\pi,t|t} + \mathbf{P}_{t|t}(\mathbf{P}_{t|t} + \mathbf{S}_1)^{-1}(\alpha_{g\pi,t+1} - \alpha_{g\pi,t|t})$$

and

$$\mathbf{P}_{t|t+1} = \mathbf{P}_{t|t} - \mathbf{P}_{t|t}\mathbf{P}_{t+1|t}^{-1}\mathbf{P}_{t|t} + \mathbf{P}_{t|t} - \mathbf{P}_{t|t}(\mathbf{P}_{t|t} + \mathbf{S}_1)^{-1}\mathbf{P}_{t|t},$$

which are the means and variances used to make the draws for $\alpha_{u\pi,t}$, $t = T-1, T-2, \ldots, 1$.

Now consider the third equation from (I.14), which can be written

$$u_{r,t} = \mathbf{Z}_{2t}\alpha_{2,t} + \sigma_{r,t}\varepsilon_{r,t}, \tag{I.17}$$

where $\mathbf{Z}_{2t} = \begin{bmatrix} -u_{\pi,t} & -u_{g,t} \end{bmatrix}$, $\alpha_{2,t} = \begin{bmatrix} \alpha_{r\pi,t} & \alpha_{rg,t} \end{bmatrix}'$, and $\varepsilon_{r,t} \sim iid\mathcal{N}(0,1)$. Taking $\mathbf{B}^T$ and σ^T as given, u_{rt} and $\mathbf{Z}_{2t}$ are observable and $\sigma_{r,t}$ is given as well. Equation (I.17) can serve as the observation equation and last two equations from (I.9),

$$\alpha_{2,t} = \alpha_{2,t-1} + \xi_{2,t} \tag{I.18}$$

as the state transition equation, where $\xi_{2,t} \sim \mathcal{N}(0, \mathbf{S}_2)$, with $\mathbf{S}_2$ given as well.

Thus, given $\alpha_{2,0|0} = \begin{bmatrix} \hat{\alpha}_{r\pi} & \hat{\alpha}_{rg,t} \end{bmatrix}'$ and $\mathbf{P}_{0|0} = k_\alpha^2 V_\alpha^{2:3,2:3}$, the Kalman filter implies

$$\alpha_{2,t|t-1} = \alpha_{2,t-1|t-1},$$

$$\mathbf{P}_{t|t-1} = \mathbf{P}_{t-1|t-1} + \mathbf{S}_2,$$

$$\mathbf{K}_t = \mathbf{P}_{t|t-1}\mathbf{Z}_{2t}'(\mathbf{Z}_{2t}\mathbf{P}_{t|t-1}\mathbf{Z}_{2t}' + \sigma_{r,t}^2)^{-1},$$

$$\alpha_{2,t|t} = \alpha_{2,t|t-1} + \mathbf{K}_t(u_{r,t} - \mathbf{Z}_{2t}\alpha_{2,t|t-1}),$$

and

$$\mathbf{P}_{t|t} = \mathbf{P}_{t|t-1} - \mathbf{K}_t\mathbf{Z}_{2t}\mathbf{P}_{t|t-1}.$$

The last elements from these recursions are $\alpha_{2,T|T}$ and $\mathbf{P}_{t|t}$, which are the mean and variance of the normal distribution used to make draws for $\alpha_{r\pi,T}$ and $\alpha_{rg,T}$. The draw for $\alpha_{2,T}$ and the output of the filter can now be used for the first step of the backward recursions

$$\alpha_{2,t|t+1} = \alpha_{2,t|t} + \mathbf{P}_{t|t}P_{t+1|t}^{-1}(\alpha_{2,t+1} - \alpha_{2,t|t}) = \alpha_{2,t|t} + \mathbf{P}_{t|t}(\mathbf{P}_{t|t} + \mathbf{S}_2)^{-1}(\alpha_{2,t+1} - \alpha_{2,t|t})$$

and

$$\mathbf{P}_{t|t+1} = \mathbf{P}_{t|t} - \mathbf{P}_{t|t}\mathbf{P}_{t+1|t}^{-1}\mathbf{P}_{t|t} = \mathbf{P}_{t|t} - \mathbf{P}_{t|t}(\mathbf{P}_{t|t} + \mathbf{S}_2)^{-1}\mathbf{P}_{t|t},$$

which are the means and variances used to make the draws for $\alpha_{u\pi,t}$, $t = T-1, T-2, \ldots, 1$.

Drawing Volatility States

Consider next the system of equations

$$\mathbf{A}_t(\mathbf{y}_t - \mathbf{X}_t'\mathbf{B}_t) = \mathbf{y}_t^* = \mathbf{\Sigma}_t\varepsilon_t, \tag{I.19}$$

where, taking $\mathbf{B}^T$ and α^T as given, $\mathbf{y}_t^*$ is observable. This is a system of nonlinear measurement equations, but can be converted into a linear one by squaring and taking logs of every element of (I.19). Due to the fact that $\mathbf{y}_{i,t}^2$ can be very small, an offset constant can be used to make the estimation procedure more robust. This leads to the following approximating state space form:

$$\mathbf{y}_t^{**} = 2h_t + e_t \tag{I.20}$$

and

$$h_t = h_{t-1} + \eta_t, \tag{I.21}$$

where $\mathbf{y}_{i,t}^{**} = \log[(\mathbf{y}_{i,t}^*)^2 + \bar{c}]$, $\bar{c}$ is the offset constant, set equal to 0.001, $e_{i,t} = \log(\varepsilon_{i,t}^2)$, and $h_{i,t} = \log \sigma_{i,t}$. Observe e and η are not correlated, since ε and η are independent.

This system has a linear, but non-Gaussian, state space form because the innovations in the measurement equations are distributed as $\log \chi^2(1)$. In order to further transform the system into a Gaussian one, a mixture of normal approximations of the $\log \chi^2$ distribution is used, as described by Kim et al. (1998). This involves selecting a mixture of seven normal densities with component probabilities q_j, means $m_j - 1.2704$ and variances v_j^2, where the constants are chosen to match a number of moments of the $\log \chi^2(1)$ distribution as reported in Kim et al.'s (1998) paper:

Selection of the mixing distribution to be $\log \chi^2(1)$

ω	$q_j = Pr(\omega = j)$	m_j	v_j^2
1	0.00730	-10.12999	5.79596
2	0.10556	-3.97281	2.61369
3	0.00002	-8.56686	5.17950
4	0.04395	2.77786	0.16735
5	0.34001	0.61942	0.64009
6	0.24566	1.79518	0.34023
7	0.25750	-1.08819	1.26261

Define $s^T = \begin{bmatrix} s_1 & \dots & s_T \end{bmatrix}'$, the matrix of indicator variables selecting at every point in time which member of the mixture of the normal approximation will be used for each element of e. Given $(\mathbf{y}^{**})^T$ and h^T, each $s_{i,t}$ is sampled from the discrete density defined by

$$Pr(s_{i,t} = j | \mathbf{y}_{i,t}^{**}, h_{i,t}) \propto q_j f_N(\mathbf{y}_{i,t}^{**} | 2h_{i,t} + m_j - 1.2704, v_j^2), \qquad i = 1, 2, ..., n \quad j = 1, 2, ..., 7.$$

$j = 1, 2, \ldots, 7$, where $f_N(\cdot|\mu, v^2)$ denotes the probability density function for a normal random variable with mean μ and variance v^2. Conditional on $\mathbf{B}^T$, $\mathbf{A}^T$, $\mathbf{V}$ and s^T, the system has an approximate linear and Gaussian state space form, where each element $e_{i,t}$ of e_t in (I.18) can now be viewed as being distributed as normal with mean $m_j - 1.2704$ and variance v_j^2 if $s_{i,t} = j$.

For each $t = 1, 2, \ldots, T$, let m_t denote the 3×1 vector consisting of the means $m_j - 1.2704$ of each element of e_t as determined above and let $\mathbf{V}_t$ denote the 3×3 matrix with the corresponding variances v_j^2 along its diagonal. Finally, define $\mathbf{X}_t = \mathbf{y}_t^{**} - m_t + 1.2704$. Now (I.20) can be rewritten as the observation equation

$$\mathbf{X}_t = 2h_t + e_t, \tag{I.22}$$

where $e_t \sim \mathcal{N}(0, \mathbf{V}_t)$ and

$$h_t = h_{t-1} + \eta_t$$

remains as the state transition equation given in (I.21), with $\eta_t \sim \mathcal{N}(0, \mathbf{W})$.

Given $h_{0|0} = \log \hat{\sigma}$ and $\mathbf{P}_{0|0} = k_\sigma^2 \mathbf{I}_3$, the Kalman filter implies

$$h_{t|t-1} = h_{t-1|t-1},$$

$$\mathbf{P}_{t|t-1} = \mathbf{P}_{t-1|t-1} + \mathbf{W},$$

$$\mathbf{K}_t = 2\mathbf{P}_{t|t-1}(4\mathbf{P}_{t|t-1} + \mathbf{V}_t)^{-1},$$

$$h_{t|t} = h_{t|t-1} + \mathbf{K}_t(\mathbf{X}_t - 2h_{t|t-1}),$$

and

$$\mathbf{P}_{t|t} = \mathbf{P}_{t|t-1} - 2\mathbf{K}_t\mathbf{P}_{t|t-1}.$$

The last elements from these recursions are $h_{T|T}$ and $\mathbf{P}_{T|T}$, which are the mean and variance of the normal distribution used to make a draw for h_T. The draw for h_T and the output of the filter can now be used for the first step of the backward recursions

$$h_{t|t+1} = h_{t|t} + \mathbf{P}_{t|t}\mathbf{P}_{t+1|t}^{-1}(h_{t+1} - h_{t|t}) = h_{t|t} + \mathbf{P}_{t|t}(\mathbf{P}_{t|t} + \mathbf{W})^{-1}(h_{t+1} - h_{t|t})$$

and

$$\mathbf{P}_{t|t+1} = \mathbf{P}_{t|t} - \mathbf{P}_{t|t}\mathbf{P}_{t+1|t}^{-1}\mathbf{P}_{t|t} = \mathbf{P}_{t|t} - \mathbf{P}_{t|t}(\mathbf{P}_{t|t} + \mathbf{W})^{-1}\mathbf{P}_{t|t},$$

which are the means and variances used to make the draws for h_t, $t = T-1, T-2, \ldots, 1$.

Del Negro and Primiceri (2015) note that, strictly speaking, because the mixture of normal distributions used in the Kim-Shephard-Chib algorithm is only an approximation to the true distribution of the innovations in the measurement equation (I.20), each draw selected using this algorithm should be used as a proposal in a Metropolis-Hastings step, following the general analysis in Stroud et al. (2003). With $\mathbf{y}_t^*$ and $\mathbf{y}_{i,t}^{**}$ defined as above, let $\tilde{\mathbf{\Sigma}}_t$ and $\mathbf{\Sigma}_t^{old}$ be the latest and previous draws for the volatility state for period $t = 1, 2, \ldots, T$, and let $\tilde{\sigma}_{i,t}$ and $\sigma_{i,t}^{old}$ be the ith diagonal elements of $\tilde{\mathbf{\Sigma}}_t$ and $\mathbf{\Sigma}_t^{old}$. Del Negro and Primiceri (2015) show that in the Metropolis step, the new draw should be accepted with probability α, where

$$\alpha = \frac{\left[\prod_{t=1}^{T} F_N(\mathbf{y}_t^* | \mathbf{0}_{3,1}, \tilde{\mathbf{\Sigma}}_t \tilde{\mathbf{\Sigma}}_t')\right] \left[\prod_{t=1}^{T} \prod_{i=1}^{3} \prod_{j=1}^{7} q_j f_N(\mathbf{y}_{i,t}^{**} | 2\sigma_{i,t}^{old} + m_j - 1.2704, v_j^2)\right]}{\left[\prod_{t=1}^{T} F_N(\mathbf{y}_t^* | \mathbf{0}_{3,1}, \mathbf{\Sigma}_t^{old} (\mathbf{\Sigma}_t^{old})')\right] \left[\prod_{t=1}^{T} \prod_{i=1}^{3} \prod_{j=1}^{7} q_j f_N(\mathbf{y}_{i,t}^{**} | 2\tilde{\sigma}_{i,t} + m_j - 1.2704, v_j^2)\right]},$$

and $F_N(\cdot | \mu, \mathbf{V})$ is the probability density function for the multivariate normal distribution with mean μ and covariance matrix $\mathbf{V}$.

Drawing Hyperparameters

The hyperparameters are the diagonal blocks of $\mathbf{V}$, each of which has an inverse-Wishart posterior distribution. Conditional on $\mathbf{B}^T$, α^T, σ^T, and $\mathbf{y}^T$, it is easy to draw from these posteriors because the innovations are observable. Use (I.8) to compute

$$\nu_t = \mathbf{B}_t - \mathbf{B}_{t-1},$$

use (I.16) to compute

$$\zeta_{1,t} = \alpha_{u\pi,t} - \alpha_{u\pi,t-1},$$

use (I.18) to compute

$$\zeta_{2,t} = \alpha_{2,t} - \alpha_{2,t-1},$$

and use (I.10) to compute

$$\eta_t = \log \sigma_t - \log \sigma_{t-1}.$$

Then a new draw for $\mathbf{Q}$ can be taken from the inverse-Wishart posterior distribution with scale matrix

$$d_{\mathbf{Q}} k_{\mathbf{Q}}^2 V_{\mathbf{Q}} + \sum_{t=1}^{T} \nu_t \nu_t',$$

and degrees of freedom $d_{\mathbf{Q}} + T$, a new draw for $\mathbf{S}_1$ can be taken from the inverse-Wishart posterior distribution with scale matrix

$$d_{\mathbf{S}1} k_{\mathbf{S}}^2 V_{\mathbf{S}1} + \sum_{t=1}^{T} \zeta_{1,t} \zeta_{1,t}',$$

and degrees of freedom $d_{\mathbf{S}1} + T$, a new draw for $\mathbf{S}_2$ can be taken from the inverse-Wishart posterior distribution with scale matrix

$$d_{\mathbf{S}2} k_{\mathbf{S}}^2 V_{\mathbf{S}2} + \sum_{t=1}^{T} \zeta_{2,t} \zeta_{2,t}',$$

and degrees of freedom $d_{\mathbf{S}2} + T$, and new draws for each diagonal element of $\mathbf{W}$ can be taken from the inverse-Wishart posterior distributions with scale matrix

$$d_{\mathbf{W}} k_{\mathbf{W}}^2 + \sum_{t=1}^{T} \eta_t \eta_t',$$

which in this case is a scalar, and degrees of freedom $d_{\mathbf{W}} + T$.

Assessing Convergence

To assess the convergence of the MCMC algorithm, Primiceri (2005) recommends initializing the chain from different, randomly selected starting points, to verify that none of the results is affected. A related but slightly more formal approach is suggested by Geweke (1992). For any model statistic θ, which may be an element of $\mathbf{B}^T$, $\mathbf{A}^T$, $\mathbf{\Sigma}^T$, $\mathbf{V}$, or any function of these parameters, calculate the means $\bar{\theta}_A$ and $\bar{\theta}_B$ from two disjoint subsamples of the Gibbs sampling output: Geweke (1992) suggests letting subsample A be formed from the first 10 percent of the draws and subsample B from the last 50 percent of the draws. The numerical standard errors of the means $\bar{\theta}_A$ and $\bar{\theta}_B$ are given by

$$\left(\frac{1}{N_A}\right)[2\pi S_{\theta,A}(0)] \text{ and } \left(\frac{1}{N_B}\right)[2\pi S_{\theta,B}(0)],$$

where $S_{\theta,A}(0)$ and $S_{\theta,B}(0)$ denote the spectral densities of $\hat{\theta}_A$ and $\hat{\theta}_B$ at frequency zero, which can be estimated using Newey and West's (1987) Bartlett weighting scheme as

$$S_{\theta,A}(0) = \frac{1}{2\pi}\left[\upsilon_{\theta,A,0} + 2\sum_{j=1}^{m}\left(1 - \frac{j}{m+1}\right)\upsilon_{\theta,A,j}\right]$$

and

$$S_{\theta,B}(0) = \frac{1}{2\pi}\left[\upsilon_{\theta,B,0} + 2\sum_{j=1}^{m}\left(1 - \frac{j}{m+1}\right)\upsilon_{\theta,B,j}\right],$$

where $\upsilon_{\theta,A,j}$ and $\upsilon_{\theta,B,j}$ are the j-th autocovariances of the draws for θ in subsamples A and B. Geweke's (1992) convergence diagnostic

$$CD(\theta) = \frac{\bar{\theta}_A - \bar{\theta}_B}{\{N_A^{-1}[2\pi S_{\theta,A}(0)] + N_B^{-1}[2\pi S_{\theta,B}(0)]\}^{1/2}} \rightarrow \mathcal{N}(0,1),$$

which, as shown, has the standard normal distribution as $N_A \rightarrow \infty$ and $N_B \rightarrow \infty$.

To gauge the extent to which the chain mixes, Primiceri (2005) and Benati (2011) compute inefficiency factors. The inefficiency factor for any individual statistic θ, which may again be an element of $\mathbf{B}^T$, $\mathbf{A}^T$, $\mathbf{\Sigma}^T$, $\mathbf{V}$, or any function of these parameters, is defined as the inverse of Geweke's (1992) measure of relative numerical efficiency:

$$IF(\theta) = \frac{2\pi S_\theta(0)}{\mathbb{V}\mathrm{ar}(\theta)} = \frac{2\pi S_\theta(0)}{\int_{-\pi}^{\pi} S_\theta(\omega)\mathrm{d}\omega},$$

where $S_\theta(\omega)$ is the spectral density of θ at frequency ω so that, in particular, $S_\theta(0)$ is the spectral density of θ at frequency zero. Primiceri (2005) notes that

$$IF(\theta) = 1 + 2\sum_{j=1}^{\infty}\rho_{\theta,j},$$

where $\rho_{\theta,j}$ is the j-th autocorrelations of the draws for θ. Hence, $IF(\theta)$ will generally be larger than one, and lower values of $IF(\theta)$ reflect less autocorrelation in the draws. In computing $IF(\theta)$, Newey and West (1987) estimator

$$S_\theta(0) = \frac{1}{2\pi}\left[\upsilon_{\theta,0} + 2\sum_{j=1}^{m}\left(1 - \frac{j}{m+1}\right)\upsilon_{\theta,j}\right]$$

can be used for the numerator, while the denominator is simply the variance $\upsilon_{\theta,0}$ across all draws for θ.

I.A.4 Identification of Monetary Policy Shocks

The Identification Problem

Two approaches can be taken to identify monetary policy shocks from the estimated reduced form. The first uses assumptions about the timing with which monetary policy disturbances affect inflation and the gap variable to re-interpret the triangular factorization of the reduced-form covariance matrix shown in (I.3) as a mapping between the reduced-form and structural models–an approach that dates back to Sims (1980). The second uses sign restrictions to identify monetary policy shocks based on their implied impulse responses. Faust (1998), Canova and De Nicolo (2002), and Uhlig (2005) propose and develop the idea that sign restrictions can serve a source of identifying assumptions in VARs, and Benati (2011) implements the particular scheme used here in a similar VAR framework with time-varying parameters.

Details on each of the two identification strategies follows, but each works to factor the reduced-form covariance matrix as

$$\mathbf{\Omega}_t = \mathbf{C}_t^{-1}\mathbf{D}_t\mathbf{D}_t'(\mathbf{C}_t')^{-1}, \tag{I.23}$$

where $\mathbf{C}_t$ and $\mathbf{D}_t$ are 3×3 matrices of the form

$$\mathbf{C}_t = \begin{bmatrix} 1 & -c_{\pi g,t} & -c_{\pi r,t} \\ -c_{g\pi,t} & 1 & -c_{gr,t} \\ -c_{r\pi,t} & -c_{rg,t} & 1 \end{bmatrix} \tag{I.24}$$

and

$$\mathbf{D}_t = \begin{bmatrix} \delta_{\pi,t} & 0 & 0 \\ 0 & \delta_{g,t} & 0 \\ 0 & 0 & \delta_{r,t} \end{bmatrix} \tag{I.25}$$

Equations (I.23)-(I.25) provide the general mapping between the reduced-form equation (I.2) and the structural model, which can now be written as

$$\mathbf{C}_t\mathbf{y}_t = \boldsymbol{\gamma}_t + \mathbf{\Gamma}_{1,t}\mathbf{y}_{t-1} + \mathbf{\Gamma}_{2,t}\mathbf{y}_{t-2} + \mathbf{D}_t\xi_t, \tag{I.26}$$

where $\boldsymbol{\gamma}_t = \mathbf{C}_t\mathbf{B}_t$, $\mathbf{\Gamma}_{i,t} = \mathbf{C}_t\mathbf{B}_{i,t}$ for $i = 1, 2$, and ξ_t is a 3×1 vector of structural disturbances, normally distributed with zero mean and $\mathbb{E}\{\xi_t\xi_t'\} = \mathbf{I}_3$. The third row from (I.26) takes the

form of a monetary policy rule

$$\begin{aligned} R_t^s = {} & \gamma_{r,t} + c_{r\pi,t}\Pi_t + \gamma_{1,r\pi,t}\Pi_{t-1} + \gamma_{2,r\pi,t}\Pi_{t-2} \\ & + c_{rg,t}G_t + \gamma_{1,rg,t}G_{t-1} + \gamma_{2,rg,t}G_{t-2} + \gamma_{1,rr,t}R_{t-1}^s + \gamma_{2,rr,t}R_{t-2}^s + \delta_{r,t}\xi_t^{mp} \end{aligned} \tag{I.27}$$

The dual-mandate reaction function prescribes a setting for the policy rate regarding to changes in current and lagged inflation and output gap variables. It also includes lagged values of interest rate terms to capture central banks' tendency to smooth short-term interest rates movements over time. The time-varying estimation of the intercept $\gamma_{r,t}$ and of the coefficients from matrices $\mathbf{\Gamma}_{1,t}$ and $\mathbf{\Gamma}_{2,t}$ allows to assess changes to monetary policy that might have occurred on the sample period. ξ_t^{mp} represents identified monetary policy shocks that capture deviations in the actual policy rate from the value dictated by the estimated monetary policy rule. Importantly, equation (I.27) allows for time-variation in all of the response coefficients but also in the standard deviation $\delta_{r,t}$ of the monetary policy shocks. Hence, this estimation permits disentangling changes in central bank's responses to inflation versus output gap stabilization and the extent to which the central bank departs from its rule-based monetary policy. As a whole, the estimated monetary policy rule given in equation (I.27) may be decomposed into central banks' response to macroeconomic conditions and smoothing behavior–i.e. the *systematic* component of monetary policy–and monetary policy shocks–i.e. the *non-systematic* component of monetary policy.

Equation (I.27) can then be decomposed and interpreted as follows

$$\begin{aligned} R_t^s = {} & \overbrace{\gamma_{r,t} + \underbrace{c_{r\pi,t}\Pi_t + \gamma_{1,r\pi,t}\Pi_{t-1} + \gamma_{2,r\pi,t}\Pi_{t-2}}_{\text{response to inflation}}}^{\text{systematic}} \\ & \overbrace{+ \underbrace{c_{rg,t}G_t + \gamma_{1,rg,t}G_{t-1} + \gamma_{2,rg,t}G_{t-2}}_{\text{response to output gap}} + \underbrace{\gamma_{1,rr,t}R_{t-1}^s + \gamma_{2,rr,t}R_{t-2}^s}_{\text{interest rate smoothing}}}^{\text{component of monetary policy}} + \overbrace{\delta_{r,t}\underbrace{\xi_t^{mp}}_{\substack{\text{MP} \\ \text{shocks}}}}^{\substack{\text{non-systematic comp.} \\ \text{of monetary policy}}} \end{aligned}$$

Comparing (I.4) and (I.5) to (I.24) and (I.25) highlights the identification problem: together, the matrices $\mathbf{A}_t$ and $\mathbf{\Sigma}_t$ of reduced-form parameters contain 6 elements not equal to zero or one, whereas the matrices $\mathbf{C}_t$ and $\mathbf{D}_t$ of structural parameters have 9 such elements. Each of the two identification schemes described next imposes more structure on the matrix $\mathbf{C}_t$ to solve this problem.

Triangular Identification Based on Timing Assumptions

The factorization of the symmetric, positive definite reduced-form covariance matrix $\mathbf{\Omega}_t$ shown in (I.3)-(I.5) always exists and is unique; hence, the model can be written in this form without any loss of generality. However, under the additional assumptions–made throughout much of the literature on VARs that builds on Sims (1980)–that inflation and the output gap respond to monetary policy shocks only after a one-period lag, the reduced-form parameters from the third rows of (I.3)-(I.5) are linked to structural parameters from the third rows on (I.23)-(I.25) via

$$c_{r\pi,t} = -\alpha_{r\pi,t},$$

$$c_{rg,t} = -\alpha_{rg,t},$$

and

$$\delta_{r,t} = \sigma_{r,t}$$

and the structural monetary policy shock ξ_t^{mp} from (I.26) and (I.27) is identified as the third element of the vector ε_t from (I.6).

Sign Restrictions for the Variables that Respond to Monetary Policy

An alternative approach to identification builds on work by Faust (1998), Canova and De Nicolo (2002), and Uhlig (2005) by associating monetary policy shocks with the effects they have on observable variables. Following Benati (2011), suppose that the first element of ξ_t corresponds to a supply shock that moves inflation and the output gap in opposite directions or inflation and the unemployment rate in the same direction. Suppose that the second element of ξ_t is a non-monetary demand shock, that moves the short-term interest rate and inflation in the same direction and the interest rate and the output gap in the same direction or the interest rate and the unemployment rate in opposite directions. Finally, suppose that the third element of ξ_t corresponds to a monetary policy shock that moves the short-term interest rate and inflation in opposite directions and the interest rate and the output gap in opposite directions or the interest rate and the unemployment rate in the same direction. Rubio-Ramirez et al. (2010) and Arias et al. (2018) emphasize that sign restrictions of this form do not suffice to identify structural disturbances in the classical sense, but develop a Bayesian algorithm for characterizing the set of parameter values implying impulse responses that satisfy these restrictions.

Let the index $i = 1, 2, \ldots, N$ keep track of the number of desired draws. For $i = 1, 2, \ldots, N$, the algorithm loops through the following steps.

1. Draw $(\mathbf{A}^T, \mathbf{\Sigma}^T)$ from their posterior distribution during the Gibbs sampling stage.

2. For each $t = 1, 2, \ldots, T$, construct $\mathbf{A}_t$ and $\mathbf{\Sigma}_t$ based on the draw for $(\mathbf{A}^T, \mathbf{\Sigma}^T)$. Then let $\mathbf{L}_t = \mathbf{A}_t^{-1}\mathbf{\Sigma}_t$, so that the reduced-form error covariance matrix is given by $\mathbf{\Omega}_t = \mathbf{L}_t\mathbf{L}_t'$.

3. Draw $\tilde{\mathbf{X}}$, a 3×3 random matrix with each element having an independent standard normal distribution. Then factor $\tilde{\mathbf{X}} = \mathbf{Q}_\mathbf{X}\mathbf{R}_\mathbf{X}$, where $\mathbf{Q}_\mathbf{X}$ is an orthogonal matrix and $\mathbf{R}_\mathbf{X}$ is upper triangular with positive diagonal elements.

4. Let $\tilde{\mathbf{L}}_t = \mathbf{L}_t\mathbf{Q}_\mathbf{X}'$, and note that

$$\tilde{\mathbf{L}}_t\tilde{\mathbf{L}}_t' = \mathbf{L}_t\mathbf{Q}_\mathbf{X}'\mathbf{Q}_\mathbf{X}\mathbf{L}_t' = \mathbf{L}_t\mathbf{L}_t' = \mathbf{\Omega}_t,$$

   by virtue of the fact that $\mathbf{Q}_\mathbf{X}$ is orthogonal. This highlights that multiplying the structural model (I.26) through by $\mathbf{D}_t^{-1}$ and then $\mathbf{Q}_\mathbf{X}$ results in an observationally-equivalent rotation of the model's three equations. Suppressing for convenience explicit reference to the constant and lagged terms in (I.26), the candidate structural model based on the specific draw for $\mathbf{Q}_\mathbf{X}$ can be written as

$$\mathbf{y}_t = \tilde{\mathbf{L}}_t\xi_t,$$

   since

$$\mathbb{E}[(\tilde{\mathbf{L}}_t\xi_t)(\tilde{\mathbf{L}}_t\xi_t)'] = \mathbb{E}(\tilde{\mathbf{L}}_t\xi_t\xi_t'\tilde{\mathbf{L}}_t') = \tilde{\mathbf{L}}_t\mathbb{E}(\xi_t\xi_t')\tilde{\mathbf{L}}_t' = \tilde{\mathbf{L}}_t\tilde{\mathbf{L}}_t' = \mathbf{\Omega}_t.$$

   Thus, the matrix $\tilde{\mathbf{L}}_t$ contains impact coefficients linking the structural shocks in ξ_t to the observable variables in $\mathbf{y}_t$. The sign restriction used to identify the supply, demand, and monetary policy shocks as the first, second, and third elements of ξ_t require the elements of $\tilde{\mathbf{L}}_t$ to have the sign patterns

$$\tilde{\mathbf{L}}_t = \begin{bmatrix} (+) & (+) & (-) \\ (-) & (+) & (-) \\ (?) & (+) & (+) \end{bmatrix}$$

if the gap variable is measured by the output gap or the real GDP growth and

$$\tilde{\mathbf{L}}_t = \begin{bmatrix} (+) & (-) & (-) \\ (+) & (+) & (+) \\ (?) & (-) & (+) \end{bmatrix}$$

if the gap variable is measured by the unemployment gap or unemployment rate. If these restrictions are not satisfied for any $t = 1, 2, \ldots, T$, the draws for $(\mathbf{A}^T, \mathbf{\Sigma}^T)$ and $\tilde{\mathbf{X}}$ are discarded and the algorithm returns to step one. If the restrictions are satisfied, then $\tilde{\mathbf{L}}_t$ is renormalized as $\tilde{\mathbf{L}}_t = \mathbf{C}_t^{-1}\mathbf{D}_t$, where $\mathbf{C}_t$ and $\mathbf{D}_t$ have the forms shown in (I.24) and (I.25), these draws are saved, and the Gibbs sampling algorithm moves on.

I.A.5 Impulse Response and Forecast Error Variances Decomposition

Once draws are obtained for the structural parameters using one of three identification schemes, impulse responses can be generated from (I.26) after multiplying through by $\mathbf{C}_t^{-1}$. These computations can be simplified by writing the system in companion form as

$$\mathbf{Y}_t - \bar{\mu}_t = \mathbf{B}_{12,t}(\mathbf{Y}_{t-1} - \bar{\mu}_t) + \mathbf{F}_t\xi_t, \tag{I.28}$$

where

$$\mathbf{Y}_t = \begin{bmatrix} \mathbf{y}_t \\ \mathbf{y}_{t-1} \end{bmatrix},$$

$$\mathbf{B}_{12,t} = \begin{bmatrix} \mathbf{B}_{1,t} & \mathbf{B}_{2,t} \\ \mathbf{I}_3 & \mathbf{0}_{3,3} \end{bmatrix}, \tag{I.29}$$

$$\bar{\mu}_t = (\mathbf{I}_6 - \mathbf{B}_{12,t})^{-1} \begin{bmatrix} \mathbf{B}_t \\ \mathbf{0}_{3,1} \end{bmatrix}, \tag{I.30}$$

and

$$F_t = \begin{bmatrix} \mathbf{C}_t^{-1}\mathbf{D}_t \\ \mathbf{0}_{3,3} \end{bmatrix}. \tag{I.31}$$

Following Cogley and Sargent (2005) and Cogley et al. (2010), the first element of the vector $\bar{\mu}_t$ can be interpreted as the targeted level of inflation.

Since (I.28) implies

$$\mathbf{Y}_{t+k} - \mathbb{E}_t \mathbf{Y}_{t+k} = \mathbf{F}_t \xi_{t+k} + \mathbf{B}_{12,t} \mathbf{F}_t \xi_{t+k-1} + \ldots + \mathbf{B}_{12,t}^{k-1} \mathbf{F}_t \xi_{t+1},$$

the k-step ahead forecast error variances for the elements of $\mathbf{Y}_t$ are

$$\mathbb{E}[(\mathbf{Y}_{t+k} - \mathbb{E}_t \mathbf{Y}_{t+k})(\mathbf{Y}_{t+k} - \mathbb{E}_t \mathbf{Y}_{t+k})'] = \mathbf{F}_t \mathbf{F}_t' + \mathbf{B}_{12,t} \mathbf{F}_t \mathbf{F}_t' \mathbf{B}_{12,t}' + \ldots + \mathbf{B}_{12,t}^{k-1} \mathbf{F}_t \mathbf{F}_t' (\mathbf{B}_{12,t}^{k-1})'. \quad \text{(I.32)}$$

Forecast error variances decomposition can be found by using (I.29), (I.31), and (I.32) to compute the total variances and then by using these same equations with the first two diagonal elements of $\mathbf{D}_t$ set equal to zero to find the variances attributable to monetary policy shocks alone.

I.A.6 Counterfactual Monetary Policy Rules

The estimated VAR model with time-varying coefficients is used to propose different counterfactual scenarios. The aim is to investigate how changes in the conduct of monetary policy may have affected macroeconomic performances. Section I.5 gives some counterfactuals based on empirical results. Counterfactual monetary policy rules $\tilde{R}_t^s$ are constructed according to different assumptions on parameters or policy shocks listed below, from 2007:4 onward. Otherwise, they follow the path of the estimated monetary policy rule given in equation (I.27). Running the TVP-VAR over the full sample period gives the path that would have followed inflation, output gap and the policy rate under these assumptions.

2007:4 policy rule. The first scenario consists in drawing the median of the policy rule coefficients from the posterior distribution from 2007:4. Hence, both the time-varying intercept and policy parameters of the systematic component of monetary policy are kept fixed from 2007:4 onward.

$$\tilde{R}_t^s = \begin{cases} \bar{\gamma}_{r,2007:4} + \bar{c}_{r\pi,2007:4}\Pi_t + \bar{\gamma}_{1,r\pi,2007:4}\Pi_{t-1} + \bar{\gamma}_{2,r\pi,2007:4}\Pi_{t-2} & \\ \qquad + \bar{c}_{rg,2007:4}G_t + \bar{\gamma}_{1,rg,2007:4}G_{t-1} + \bar{\gamma}_{2,rg,2007:4}G_{t-2} & \text{if } t \geq 2007:4 \\ \qquad + \bar{\gamma}_{1,rr,2007:4}R_{t-1} + \bar{\gamma}_{2,rg,2007:4}R_{t-2} + \delta_{r,t}\xi_t^{mp} & \\ R_t^s \text{ from equation (I.27)} & \text{otherwise} \end{cases}$$

2007:4 policy rule and no policy shocks. In the second scenario, the Taylor rule parameters are also drawn from their 2007:4 posterior distribution, and monetary policy shocks are assumed to be muted from 2007:4 forward. Hence, compared to the previous scenario, it is assumed that $\xi_t^{mp} = 0$.

$$\tilde{R}_t^s = \begin{cases} \bar{\gamma}_{r,2007:4} + \bar{c}_{r\pi,2007:4}\Pi_t + \bar{\gamma}_{1,r\pi,2007:4}\Pi_{t-1} + \bar{\gamma}_{2,r\pi,2007:4}\Pi_{t-2} \\ \qquad +\bar{c}_{rg,2007:4}G_t + \bar{\gamma}_{1,rg,2007:4}G_{t-1} + \bar{\gamma}_{2,rg,2007:4}G_{t-2} & \text{if } t \geq 2007:4 \\ \qquad + \bar{\gamma}_{1,rr,2007:4}R_{t-1} + \bar{\gamma}_{2,rg,2007:4}R_{t-2} \\ R_t^s \text{ from equation (I.27)} & \text{otherwise} \end{cases}$$

No policy shocks. The third counterfactual scenario (Appendix I.E) reports results when monetary policy shocks are turned off from 2007:4 onward. Parameters are not kept fixed from 2007:4 in this case. However, policy shocks ξ_t^{mp} are still set to 0.

$$\tilde{R}_t^s = \begin{cases} \gamma_{r,t} + c_{r\pi,t}\Pi_t + \gamma_{1,r\pi,t}\Pi_{t-1} + \gamma_{2,r\pi,t}\Pi_{t-2} \\ \qquad +c_{rg,t}G_t + \gamma_{1,rg,t}G_{t-1} + \gamma_{2,rg,t}G_{t-2} & \text{if } t \geq 2007:4 \\ \qquad + \gamma_{1,rr,t}R_{t-1}^s + \gamma_{2,rr,t}R_{t-2}^s \\ R_t^s \text{ from equation (I.27)} & \text{otherwise} \end{cases}$$

2007:4 volatility. Another counterfactual scenario shown in Appendix I.E gives counterfactuals only in the case where the volatility coefficient $\delta_{r,t}$ is drawn from its 2007:4 posterior distribution, allowing the rest of policy rule parameters to be time-varying from 2007:4 forward.

$$\tilde{R}_t^s = \begin{cases} \gamma_{r,t} + c_{r\pi,t}\Pi_t + \gamma_{1,r\pi,t}\Pi_{t-1} + \gamma_{2,r\pi,t}\Pi_{t-2} \\ \qquad +c_{rg,t}G_t + \gamma_{1,rg,t}G_{t-1} + \gamma_{2,rg,t}G_{t-2} & \text{if } t \geq 2007:4 \\ \qquad + \gamma_{1,rr,t}R_{t-1}^s + \gamma_{2,rr,t}R_{t-2}^s + \bar{\delta}_{r,2007:4}\xi_t^{mp} \\ R_t^s \text{ from equation (I.27)} & \text{otherwise} \end{cases}$$

I.B Shadow Taylor rules

Wu and Zhang (2019) argue that the shadow rate is a good proxy for monetary policy at the ZLB. For this purpose, they estimate a simple 'shadow Taylor rule' for the U.S. using Wu and Xia's shadow rate (Wu and Xia, 2016).

This simple monetary policy rule takes the following form:

$$R_t^s = \alpha + \rho R_{t-1}^s + \beta_\Pi \Pi_t + \beta_G G_t + \varepsilon_t \tag{I.33}$$

where Π_t is the inflation rate, G_t is the output gap and R_t^s is the shadow rate at period t, following the notation used in the TVP-VAR model. ε_t is the error term, and can be interpreted as monetary policy shocks. α is an intercept. Also, and importantly, fixed parameters β_Π and β_G are the response coefficients on inflation and output gap, respectively. ρ is the partial adjustment parameter that captures interest rate smoothing in central bank's behavior.

OLS estimation of equation (I.33) is used to construct shadow Taylor rates shown below.

Figure I.B.1 – Shadow Taylor rules (Wu and Xia's shadow rate)

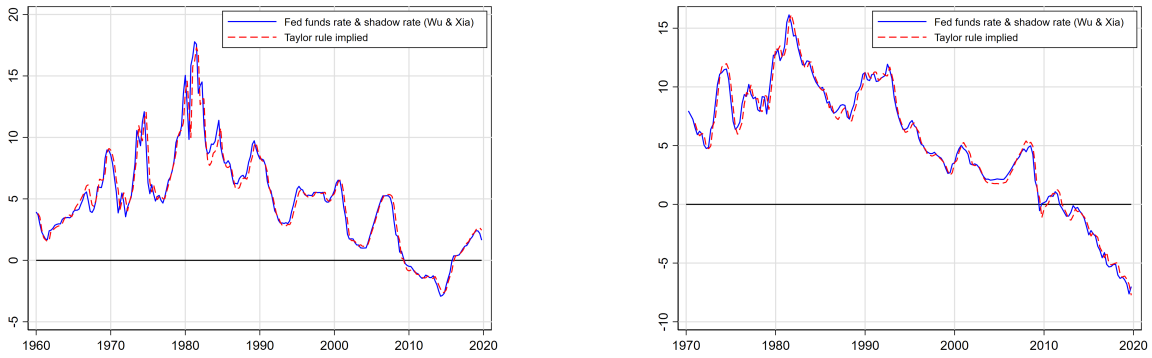

(a) U.S. (b) Euro area

Note: Based on Wu and Zhang (2019). U.S. quarterly data from 1960:1 to 2019:4: Wu and Xia's shadow rate, GDP deflator, CBO output gap. Euro area quarterly data from 1971:1 to 2019:4 are Wu and Xia's shadow rate, HICP, estimated output gap.

As advocated by the authors, *"the Taylor rule seems to be a good description of what actually happens, including the ZLB period"*. Using Wu and Xia's shadow rate (Figure I.B.1), the coefficient on inflation is 1.25 and the coefficient on output gap is 0.23 over the full U.S. sample, consistent with the Taylor principle. For the euro area, the coefficient on inflation is 1.20 and the coefficient on output gap is 0.23.

Figure I.B.2 – Shadow Taylor rules (Krippner's shadow rate)

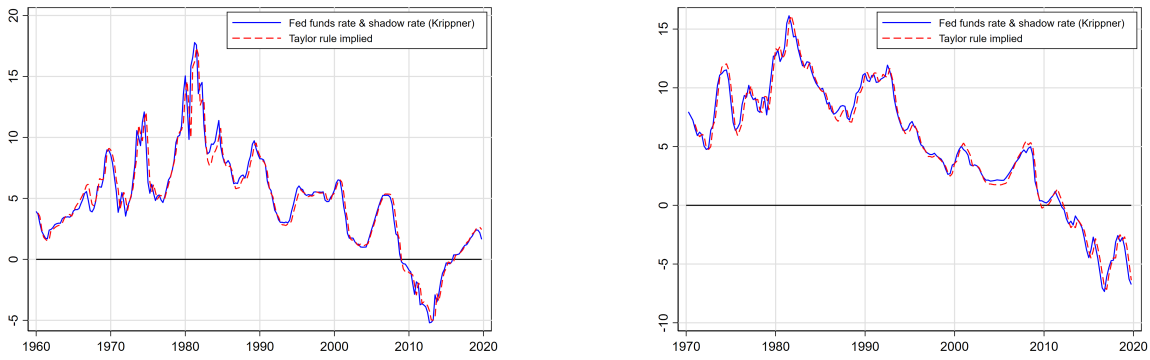

(a) U.S. (b) Euro area

Note: Based on Wu and Zhang (2019). U.S. quarterly data from 1960:1 to 2019:4 are Krippner's shadow rate, GDP deflator, CBO output gap. Euro area quarterly data from 1971:1 to 2019:4 are Krippner's shadow rate, HICP, estimated output gap.

Using Krippner's shadow rate (Figure I.B.2), the coefficient on inflation is 1.29 and the coefficient on output gap is 0.3 over the full U.S. sample. For the euro area, the coefficient on inflation is 1.22 and the coefficient on output gap is 0.28.

These results show that *(i)* the simple Taylor is a good description of the shadow rate dynamics, and that *(ii)* the response coefficients of the simple rule estimation seem to be robust to the choice of the shadow rate, as raised later in Appendix I.F.1.

I.C Stability check for simple VAR analysis

VAR stability

Times series models are usually assumed to be stable over time. Here, the stability of the simple VAR model is checked. First, let us consider a simple VAR(2) model in the form:

$$\mathbf{y}_t = \mathbf{b} + \mathbf{B}_1\mathbf{y}_{t-1} + \mathbf{B}_2\mathbf{y}_{t-2} + \mathbf{u}_t \tag{I.34}$$

where $\mathbf{y}_t = [\Pi_t \quad G_t \quad R_t^s]'$. Then, the companion form of the model can be given as:

$$\tilde{\mathbf{Y}}_t = \mathbf{B}_{12}\tilde{\mathbf{Y}}_{t-1} + \boldsymbol{\nu}_t \tag{I.35}$$

where

$$\tilde{\mathbf{Y}}_t = \begin{bmatrix} \tilde{\mathbf{y}}_t \\ \tilde{\mathbf{y}}_{t-1} \end{bmatrix} \tag{I.36}$$

with $\tilde{\mathbf{y}}_t$ the mean corrected element of $\mathbf{y}_t$,

$$\mathbf{B}_{12} = \begin{bmatrix} \mathbf{B}_1 & \mathbf{B}_2 \\ \mathbf{I}_3 & \mathbf{0}_{3,3} \end{bmatrix} \tag{I.37}$$

is the companion matrix, and

$$\boldsymbol{\nu}_t = \begin{bmatrix} \mathbf{u}_t \\ \mathbf{0}_{3,3} \end{bmatrix}. \tag{I.38}$$

The determinant defining the characteristic equation is defined as $\left|\mathbf{B}_{12} - \lambda\mathbf{I}\right| = \left|\lambda^2\mathbf{I} - \lambda\mathbf{B}_1 - \mathbf{B}_2\right| = 0$.

Hence, the required condition for the stability of the system is that the roots of the previous equation must lie inside the unit circle. The figures showing the results are given below. The six roots lie inside the unit circle insuring the stability of the VAR.

Figure I.C.1 – Roots of VAR(2) models

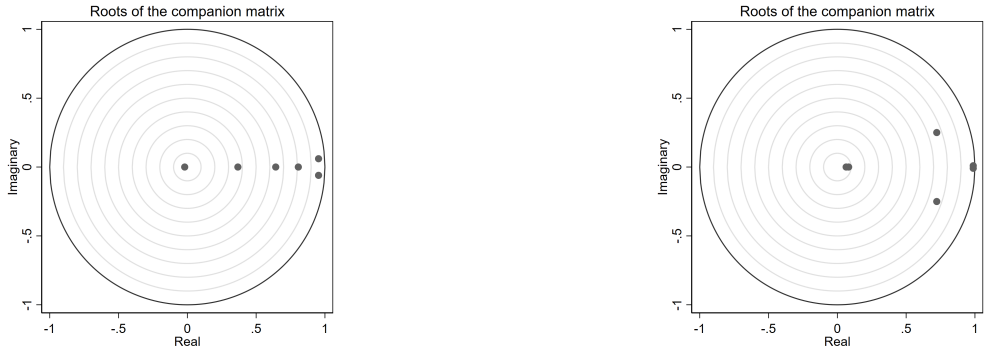

(a) U.S. data

(b) Euro area data

Rolling-window analysis for stability of parameters

A common assumption in time series analysis is that the coefficients are constant with respect to time. Checking for instability allows to assess whether the coefficients are time-invariant. A rolling-window analysis is used to check the stability of the VAR(2) model described above.

First, the size of the rolling window–the number of consecutive observations per rolling window–is set to $m = 40$, that is consistent with the size of the training sample used in the TVP-VAR (40 quarters, i.e. 10 years). Then, the number of increments between successive rolling windows is set to one quarter, in a way that the entire sample is divided into $N = T - m + 1$ subsamples, where T is the sample size such that $t = 1, ..., T$.

Figure I.C.2 gives some insights on the path of coefficients running the VAR(2) with rolling-windows. The coefficients are subject to a high instability.

The use of the VAR model with time-varying parameters is justified by the instability of the coefficients from the VAR with rolling windows (i.e. fixed windows). More precisely, the first difference of each coefficient follows a random walk, validating the assumptions of the process that governs the dynamics of the time-varying coefficients in the TVP-VAR model. Moreover, it seems to be tricky to disentangle regime switches regarding the path of these coefficients on the estimation period. Hence, TVP-VAR estimation is an appropriate tool to investigate changes in the conduct of monetary policy over time. Note that the coefficients are also unstable when the monetary policy rule is estimated with OLS with rolling windows and sequential VAR estimation with recursive windows (i.e. increasing windows). The results are not reported here and are available upon request.

Statistical tests for stability of parameters

Cogley and Sargent (2005) consider classical tests for variation in the parameters of their model. The purpose of this section is to apply some of those tests to U.S. and euro area data used previously to give further insights on the stability of parameters.

Hence, one of the most prominent tests that can easily be implemented after fitting a VAR is the Wald test. It allows to compute the Wald lag-exclusion statistics to test the hypothesis that the endogenous variables at a given lag are jointly zero for each equation and for all equations jointly. Testing stability on an equation-by-equation basis, the hypothesis that all three endogenous variables have zero coefficients at the first lag can be rejected at the 1% level for the three equations. Similarly, we strongly reject the hypothesis that the coefficients on the first and second lags of the endogenous variables are zero in all three equations jointly. The results are not reported here and are available upon request.

Figure I.C.2 – VAR(2) coefficients with rolling-windows

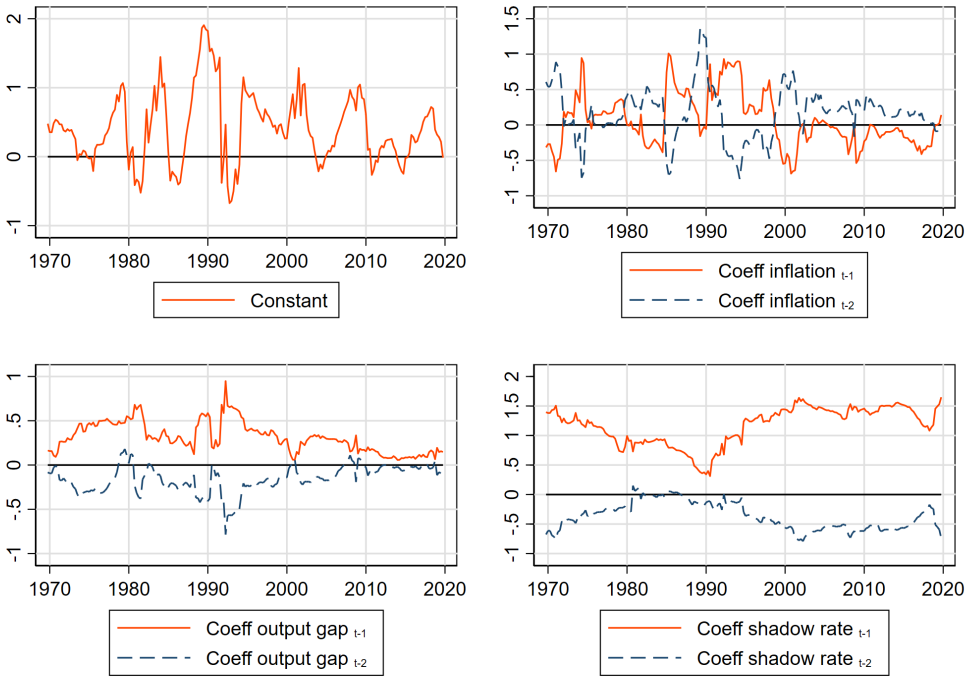

(a) U.S.

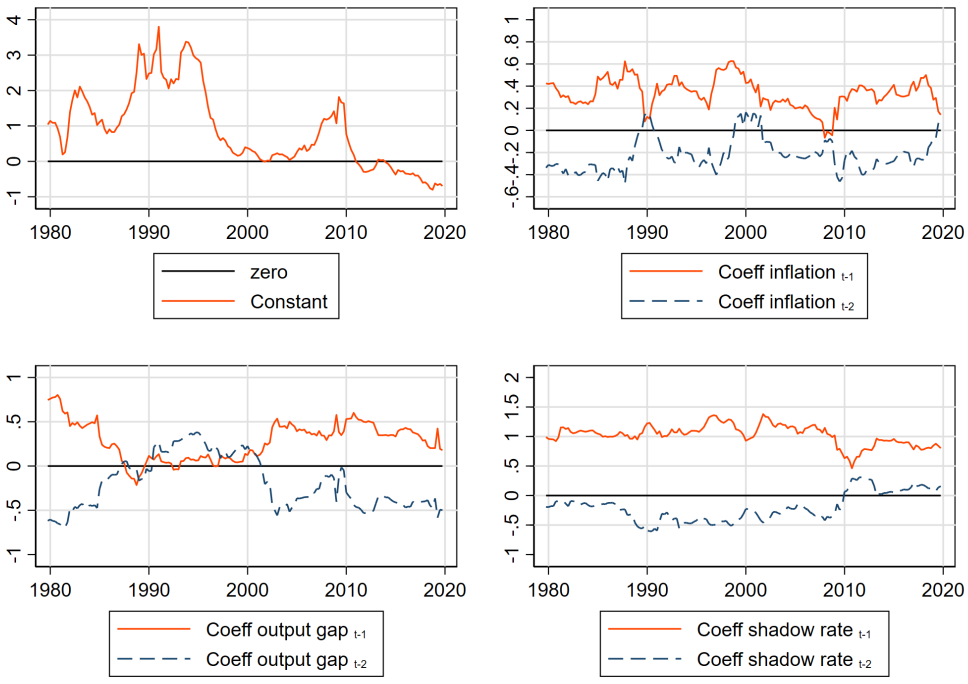

(b) Euro area

I.D Tables

I.D.1 Inefficiency factors

Table I.D.1 – Inefficiency factors (U.S.)

	Median	Mean	Min.	Max.	10th percentile	90th percentile
3150 Coefficients $\mathbf{B}^T$	5.59	5.78	2.51	7.07	3.38	6.65
450 Covariances $\mathbf{A}^T$	3.15	3.35	1.65	3.87	2.06	3.60
450 Volatilities $\mathbf{\Sigma}^T$	6.81	7.24	5.06	7.70	5.60	7.39
238 Hyperparameters $\mathbf{V}$	21.32	21.28	18.27	22.52	20.75	21.78

Table I.D.2 – Inefficiency factors (Euro area)

	Median	Mean	Min.	Max.	10th percentile	90th percentile
3150 Coefficients $\mathbf{B}^T$	5.17	5.57	2.10	10.53	3.00	8.26
450 Covariances $\mathbf{A}^T$	3.35	3.68	2.41	6.11	2.57	5.26
450 Volatilities $\mathbf{\Sigma}^T$	8.22	9.15	5.02	21.84	6.18	11.78
238 Hyperparameters $\mathbf{V}$	21.14	21.14	19.99	22.40	20.68	21.60

I.D.2 Descriptive statistics of the time-varying coefficients

Table I.D.3 – Monetary policy rule parameters in the U.S. (median coefficients)

	2009:1	2013:1	2017:1
Impact coefficient on inflation	0.22	0.12	0.11
Impact coefficient on the output gap	0.50	0.28	0.31
Interest rate smoothing	0.92	0.95	0.97
Long-run coefficient on inflation	0.91	0.34	0.37
Long-run coefficient on the output gap	1.28	1.76	2.14
Monetary policy shock volatility	0.71	0.22	0.19

Table I.D.4 – Monetary policy rule parameters in the U.S. (mean of median coefficients)

	1970:1 - 2019:4		1995:1 - 2019:4		
	Sample	$< 2008{:}1$	Sample	$< 2008{:}1$	$\geq 2008{:}1$
Impact coefficient on inflation	0.52	0.64	0.24	0.32	0.16
Impact coefficient on the output gap	0.44	0.47	0.33	0.33	0.34
Interest rate smoothing	0.96	0.97	0.95	0.94	0.96
Long-run coefficient on inflation	1.10	1.28	0.84	1.10	0.55
Long-run coefficient on the output gap	1.12	0.92	1.48	1.22	1.75
Monetary policy shock volatility	0.64	0.74	0.29	0.29	0.29

Table I.D.5 – Monetary policy rule parameters in the euro area (median coefficients)

	2009:1	2013:1	2017:1
Impact coefficient on inflation	0.67	0.61	0.67
Impact coefficient on the output gap	0.57	0.82	1.07
Interest rate smoothing	0.92	0.93	0.96
Long-run coefficient on inflation	1.84	2.13	3.15
Long-run coefficient on the output gap	1.28	1.76	1.88
Monetary policy shock volatility	0.55	0.53	0.62

Table I.D.6 – Monetary policy rule parameters in the euro area (mean of median coefficients)

	1981:1 - 2019:4		1995:1 - 2019:4		
	Sample	$< 2008{:}1$	Sample	$< 2008{:}1$	$\geq 2008{:}1$
Impact coefficient on inflation	0.66	0.68	0.57	0.50	0.63
Impact coefficient on the output gap	0.65	0.56	0.71	0.58	0.85
Interest rate smoothing	0.91	0.90	0.92	0.91	0.94
Long-run coefficient on inflation	1.54	1.12	1.90	1.37	2.47
Long-run coefficient on the output gap	1.73	1.72	1.61	1.49	1.75
Monetary policy shock volatility	0.48	0.44	0.44	0.33	0.56

I.E Figures

I.E.1 Interest rate smoothing, contemporaneous coefficients and full sample (baseline estimation)

Figure I.E.1 – Interest rate smoothing and contemporaneous coefficients from the estimated monetary policy rule

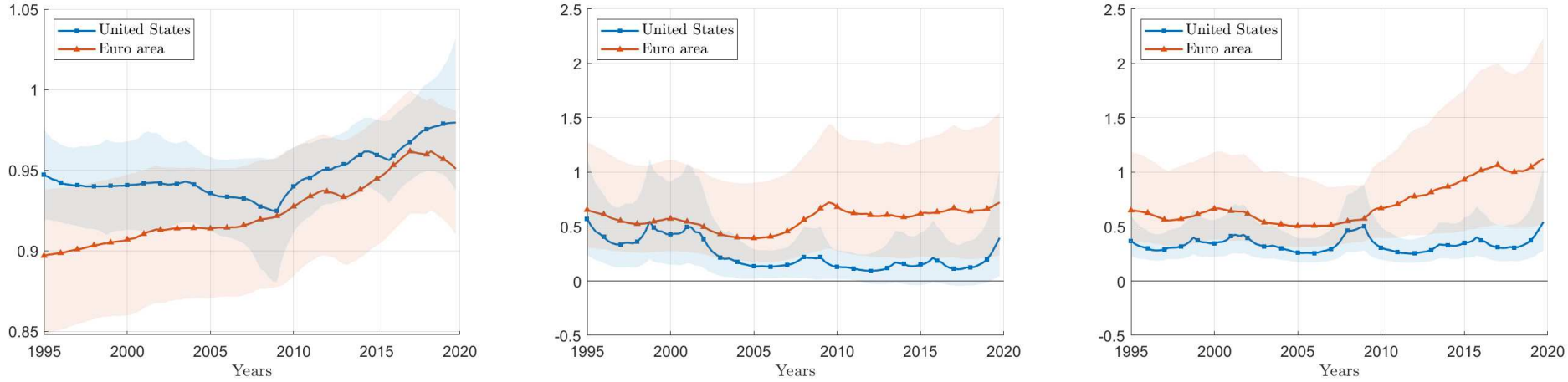

(a) Interest rate smoothing (b) Contemporaneous coefficient on inflation (c) Contemporaneous coefficient on output gap

Note: Interest rate smoothing is given by the sum $\gamma_{1,rr,t} + \gamma_{2,rr,t}$, and contemporaneous coefficients on inflation and output gap are respectively given by $c_{r\pi,t}$ and $c_{rg,t}$ in equation (3). Median (solid lines) and 68% credible interval (shaded areas) of the posterior distribution of coefficients are plotted for each indicated variable.

Figure I.E.2 – Contemporaneous coefficients from the estimated monetary policy rule and monetary policy shock volatility (full sample)

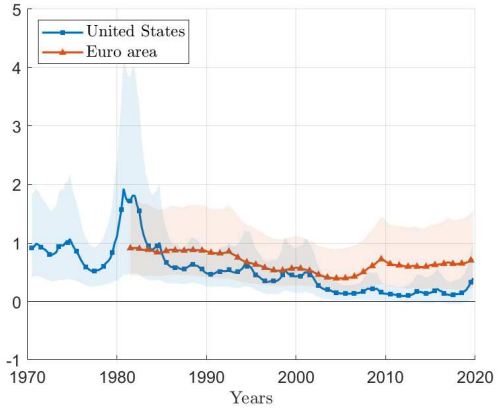

(a) Contemporaneous coefficient on inflation

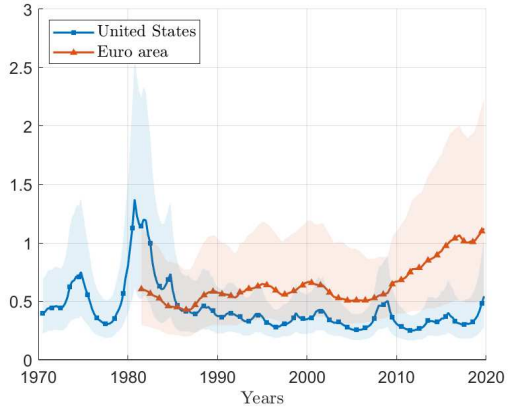

(b) Contemporaneous coefficient on output gap

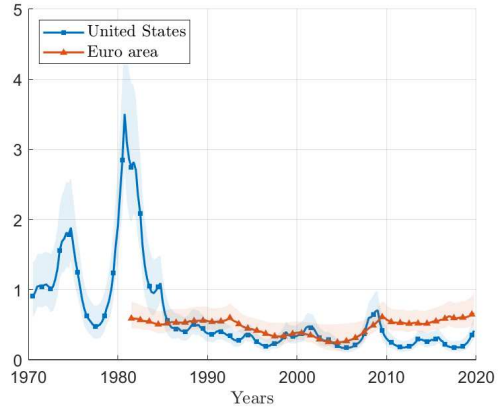

(c) Monetary policy shock volatility

Note: Contemporaneous coefficients on inflation and output gap are respectively given by $c_{r\pi,t}$ and $c_{rg,t}$, and the volatility of monetary policy shocks is captured by $\delta_{r,t}$ in equation (3). Median (solid lines) and 68% credible interval (shaded areas) of the posterior distribution of coefficients are plotted for each indicated variable.

Figure I.E.3 – Interest rate smoothing and long-run coefficients from the estimated monetary policy rule (full sample)

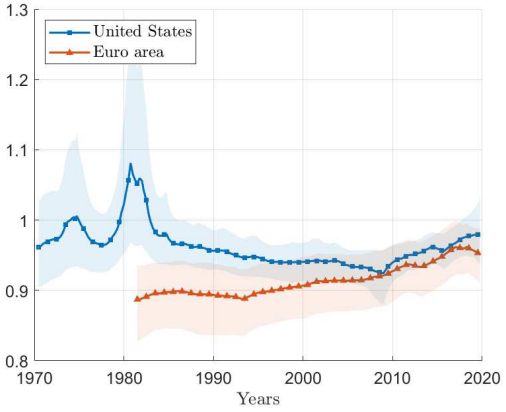

(a) Interest rate smoothing

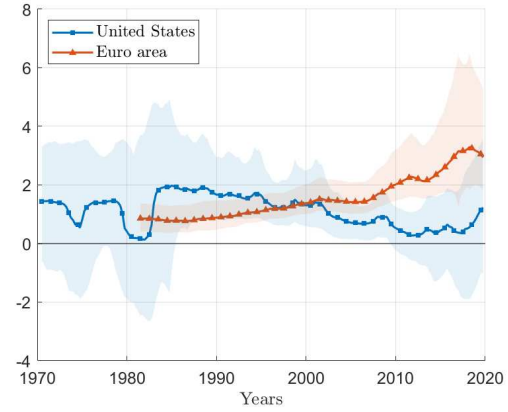

(b) Long-run coefficient on inflation

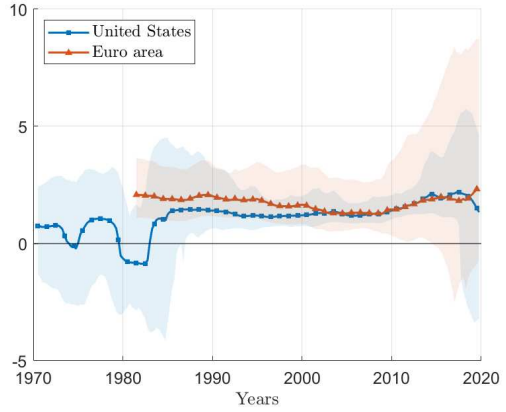

(c) Long-run coefficient on output gap

Note: Interest rate smoothing is given by the sum $\gamma_{1,rr,t}+\gamma_{2,rr,t}$, and long-run coefficients on inflation and output gap are respectively given by $(c_{r\pi,t}+\gamma_{1,r\pi,t}+\gamma_{2,r\pi,t})/(1-\gamma_{1,rr,t}-\gamma_{2,rr,t})$ and $(c_{rg,t}+\gamma_{1,rg,t}+\gamma_{2,rg,t})/(1-\gamma_{1,rr,t}-\gamma_{2,rr,t})$ in equation (3). Median (solid lines) and 68% credible interval (shaded areas) of the posterior distribution of coefficients are plotted for each indicated variable.

I.E.2 Counterfactual analysis (baseline estimation)

Figure I.E.4 – Counterfactual simulations (U.S.)

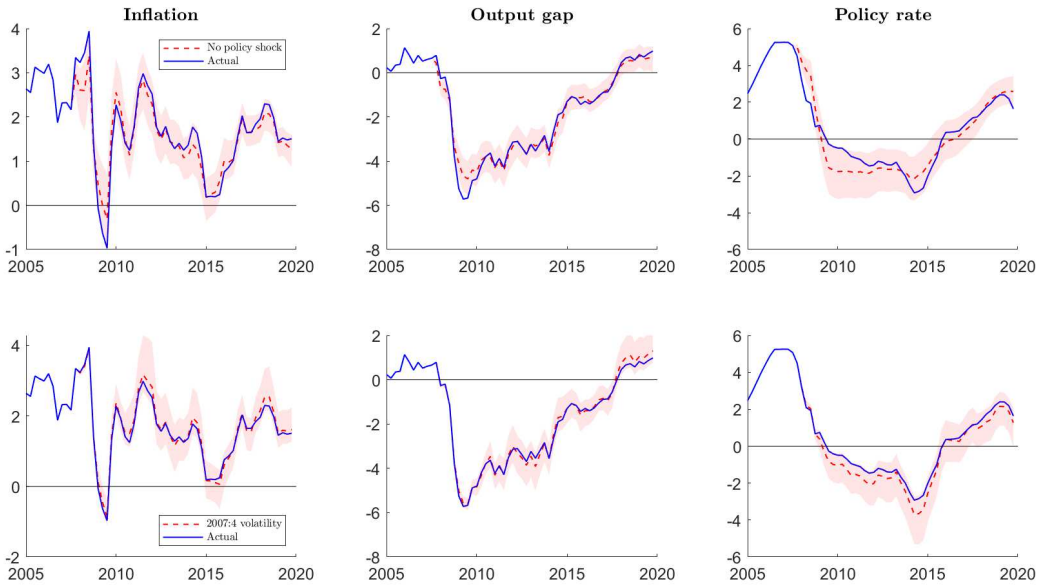

Note: Median counterfactual path (red dashed lines) and 68% credible interval (red shaded areas) are plotted for each indicated variable.

Figure I.E.5 – Counterfactual simulations (Euro area)

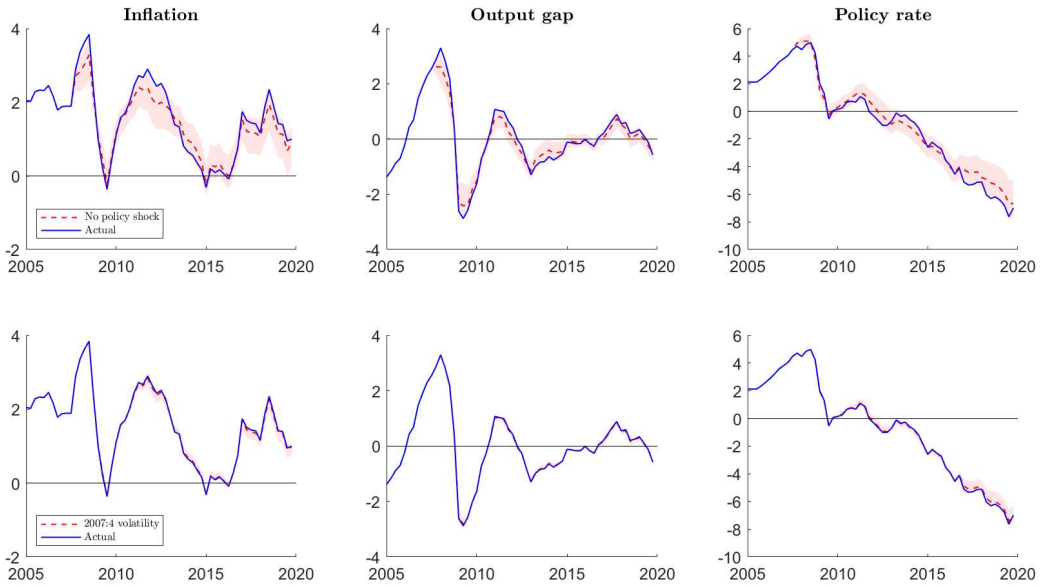

Note: Median counterfactual path (red dashed lines) and 68% credible interval (red shaded areas) are plotted for each indicated variable.

Figure I.E.6 – Counterfactual simulations (U.S.)

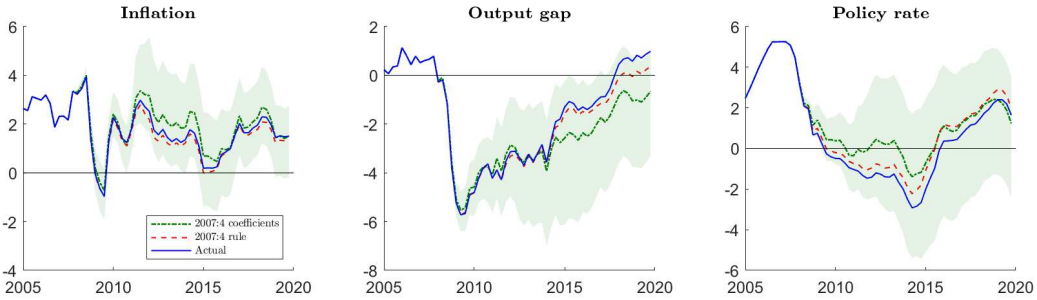

Note: Median counterfactual path (green dashed lines) and 68% credible interval (green shaded areas) are plotted for each indicated variable.

Figure I.E.7 – Counterfactual simulations (U.S.)

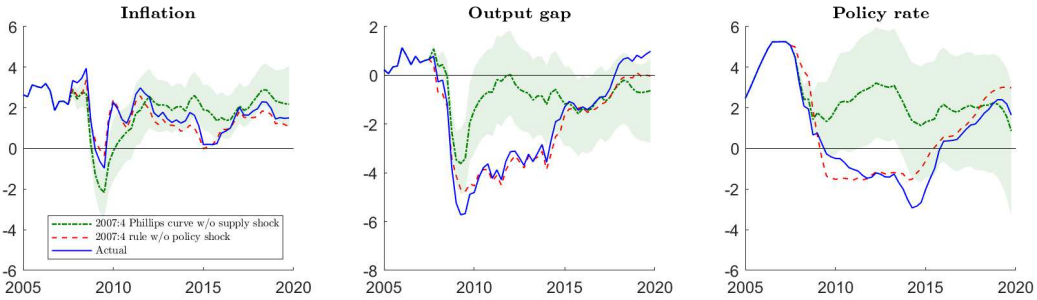

Note: Median counterfactual path (green dashed lines) and 68% credible interval (green shaded areas) are plotted for each indicated variable.

Figure I.E.8 – Counterfactual simulations (U.S.)

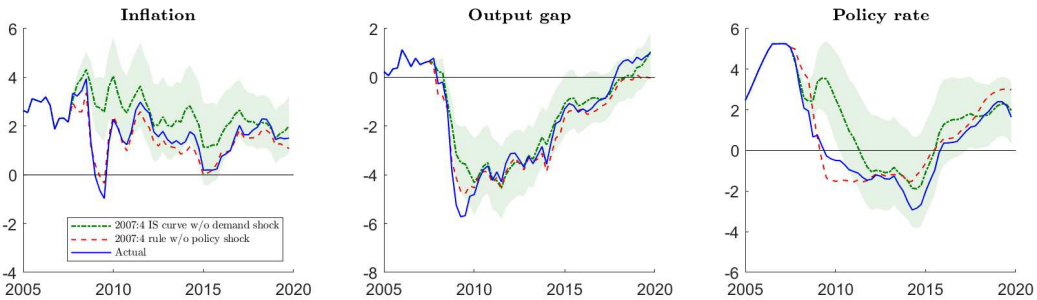

Note: Median counterfactual path (green dashed lines) and 68% credible interval (green shaded areas) are plotted for each indicated variable.

Figure I.E.9 – Counterfactual simulations (U.S.)

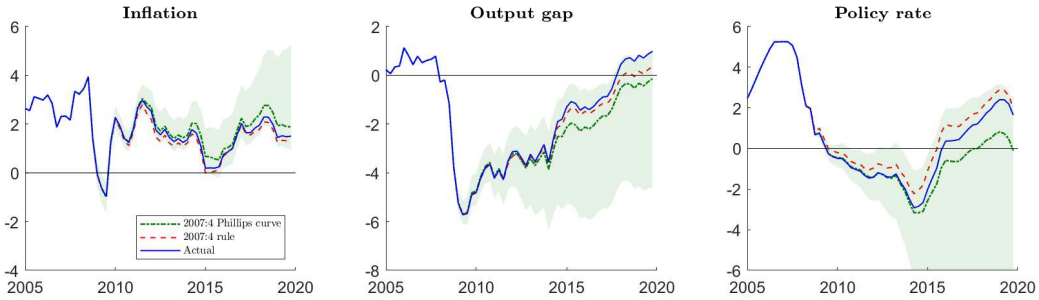

Note: Median counterfactual path (green dashed lines) and 68% credible interval (green shaded areas) are plotted for each indicated variable.

Figure I.E.10 – Counterfactual simulations (U.S.)

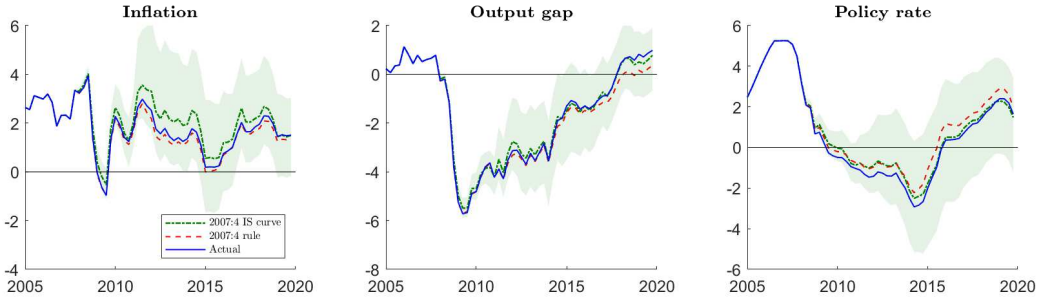

Note: Median counterfactual path (green dashed lines) and 68% credible interval (green shaded areas) are plotted for each indicated variable.

Figure I.E.11 – Counterfactual simulations (Euro area)

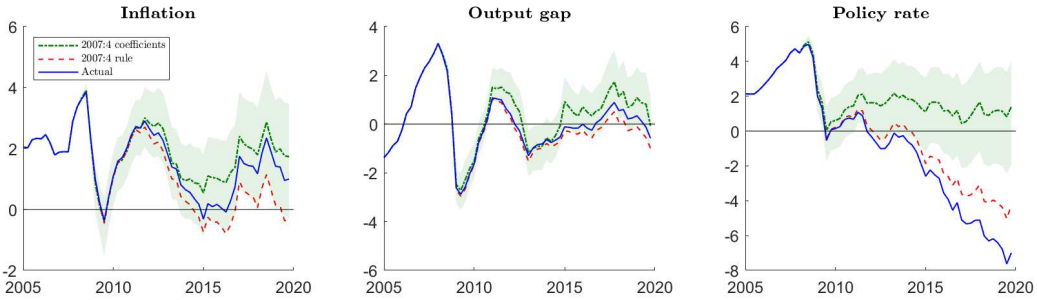

Note: Median counterfactual path (green dashed lines) and 68% credible interval (green shaded areas) are plotted for each indicated variable.

Figure I.E.12 – Counterfactual simulations (Euro area)

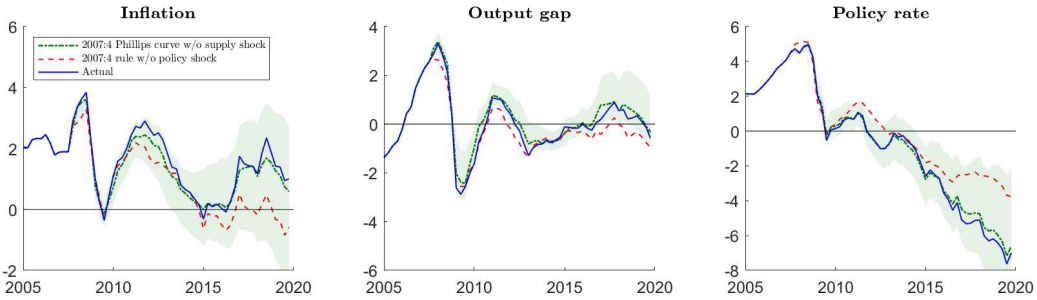

Note: Median counterfactual path (green dashed lines) and 68% credible interval (green shaded areas) are plotted for each indicated variable.

Figure I.E.13 – Counterfactual simulations (Euro area)

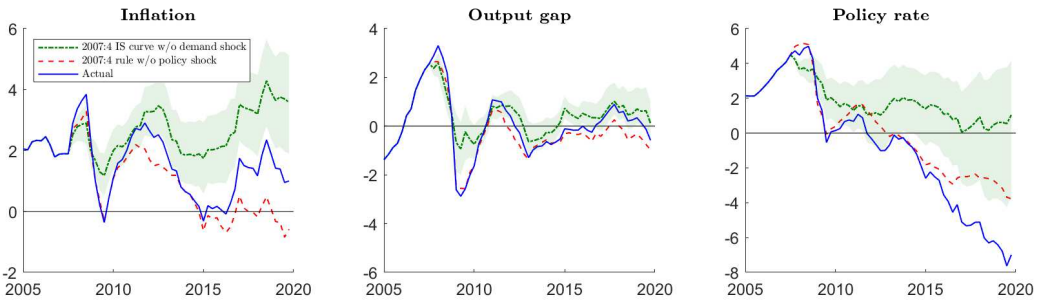

Note: Median counterfactual path (green dashed lines) and 68% credible interval (green shaded areas) are plotted for each indicated variable.

Figure I.E.14 – Counterfactual simulations (Euro area)

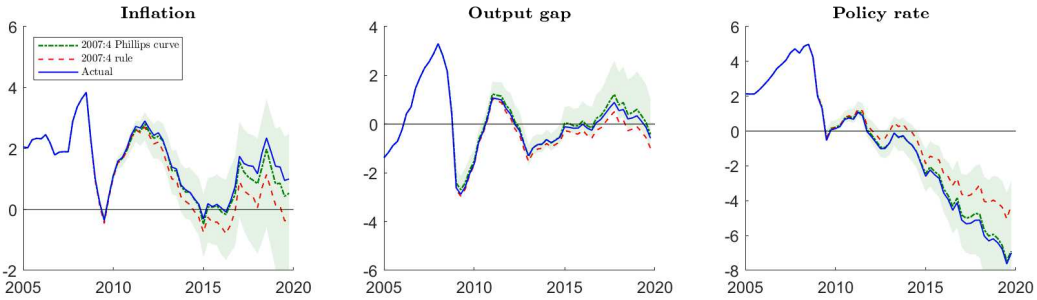

Note: Median counterfactual path (green dashed lines) and 68% credible interval (green shaded areas) are plotted for each indicated variable.

Figure I.E.15 – Counterfactual simulations (Euro area)

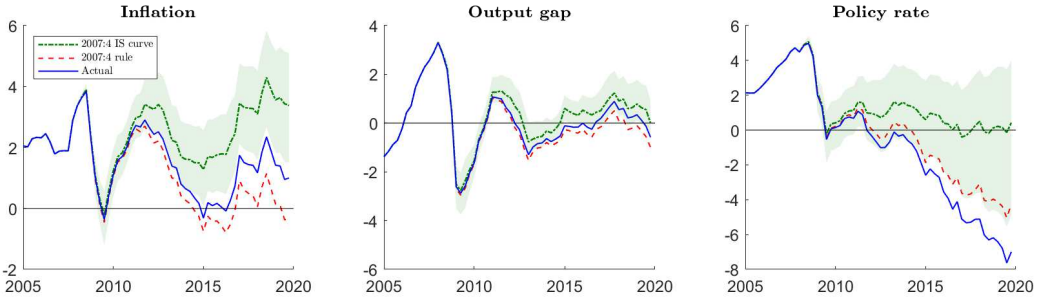

Note: Median counterfactual path (green dashed lines) and 68% credible interval (green shaded areas) are plotted for each indicated variable.

Figure I.E.16 – Counterfactual simulations (U.S.)

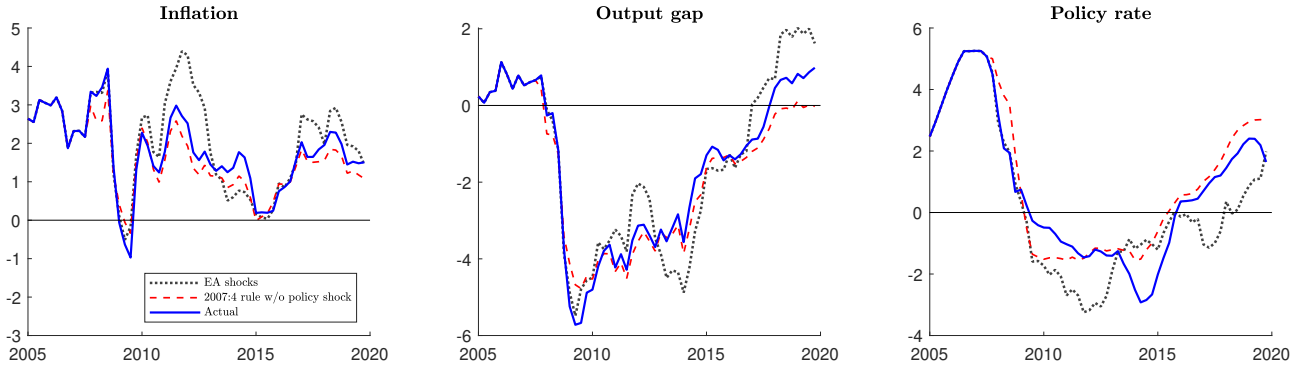

Figure I.E.17 – Counterfactual simulations (Euro area)

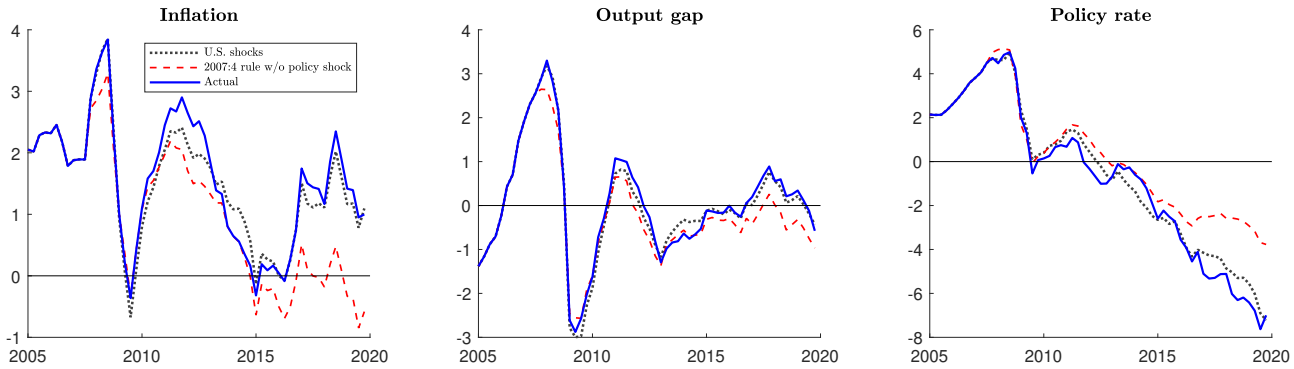

I.F Robustness checks

I.F.1 Shadow rates

As discussed previously in this paper, this shadow rate follows a different path than the shadow rate from Wu and Xia (2016) (see Figure I.F.1). Note that Leo Krippner has recently revised its shadow rate estimates. Hence, "Krippner, 2016" refers to the first version, and "Krippner, 2020" refers to the revised version of the shadow short rate.[30]

[30] Further details can be found in this note.

Figure I.F.1 – Shadow rates

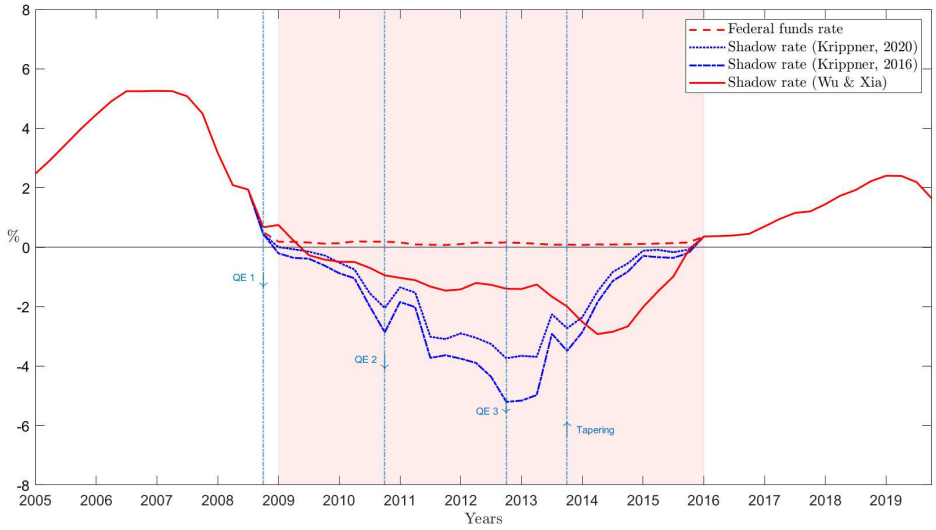

(a) U.S.

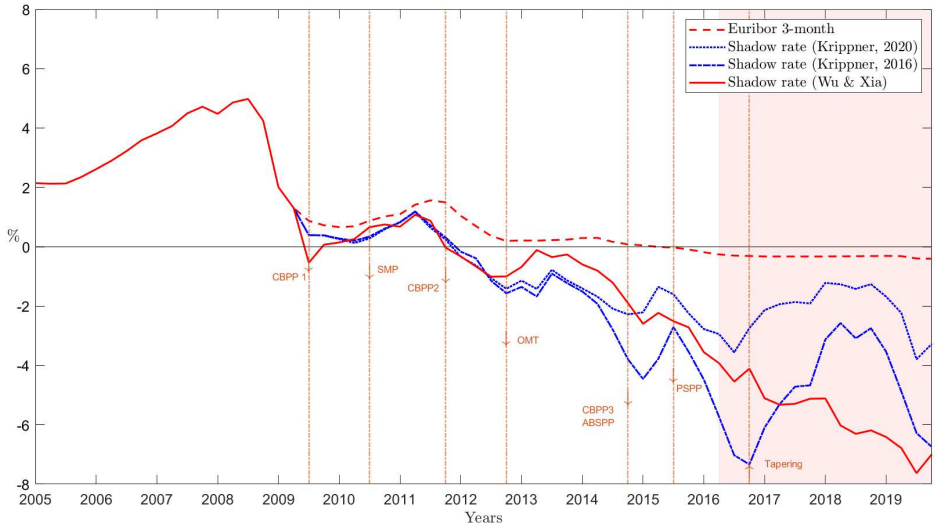

(b) Euro area

Note: U.S. shadow rate series are proxied by the federal funds rate and replaced by the different shadow rates from November 2008 to November 2015. In the euro area, the series track the Euribor 3-month over the period and are replaced by the different shadow rates in July 2009.

Figure I.F.2 – Contemporaneous coefficients from the estimated monetary policy rule and monetary policy shock volatility (Krippner's (2016) shadow rate)

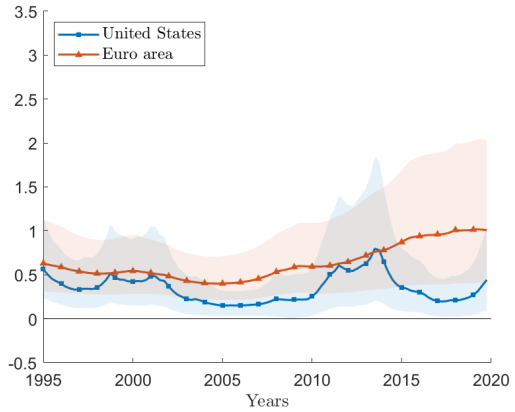

(a) Contemporaneous coefficient on inflation

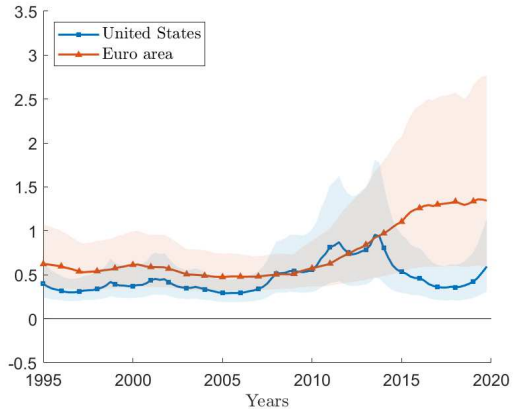

(b) Contemporaneous coefficient on output gap

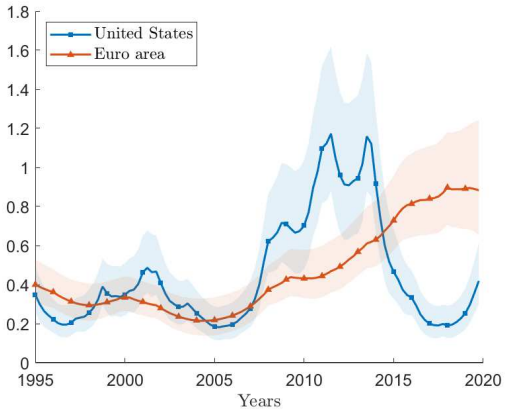

(c) Monetary policy shock volatility

Note: Contemporaneous coefficients on inflation and output gap are respectively given by $c_{r\pi,t}$ and $c_{rg,t}$, and the volatility of monetary policy shocks is captured by $\delta_{r,t}$ in equation (3). Median (solid lines) and 68% credible interval (shaded areas) of the posterior distribution of coefficients are plotted for each indicated variable.

Figure I.F.3 – Interest rate smoothing and long-run coefficients from the estimated monetary policy rule (Krippner's (2016) shadow rate)

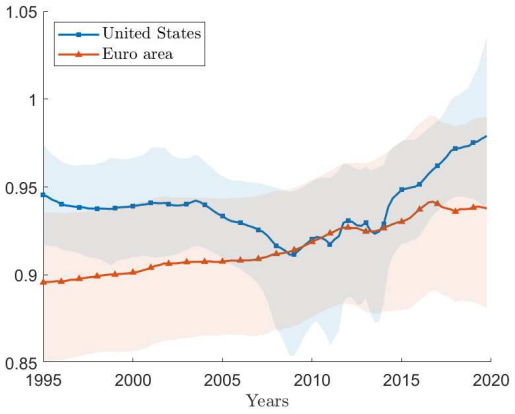

(a) Interest rate smoothing

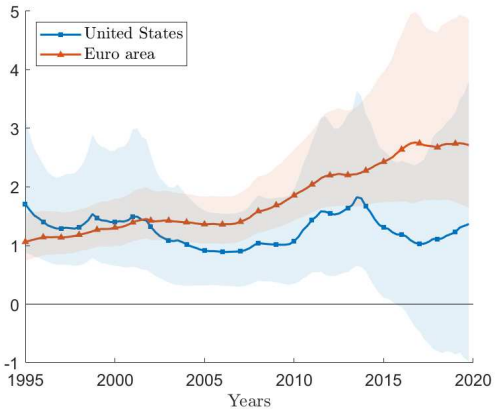

(b) Long-run coefficient on inflation

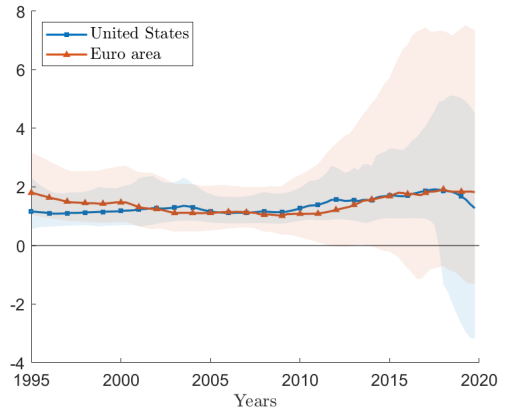

(c) Long-run coefficient on output gap

Note: Interest rate smoothing is given by the sum $\gamma_{1,rr,t}+\gamma_{2,rr,t}$, and long-run coefficients on inflation and output gap are respectively given by $(c_{r\pi,t}+\gamma_{1,r\pi,t}+\gamma_{2,r\pi,t})/(1-\gamma_{1,rr,t}-\gamma_{2,rr,t})$ and $(c_{rg,t}+\gamma_{1,rg,t}+\gamma_{2,rg,t})/(1-\gamma_{1,rr,t}-\gamma_{2,rr,t})$ in equation (3). Median (solid lines) and 68% credible interval (shaded areas) of the posterior distribution of coefficients are plotted for each indicated variable.

Figure I.F.4 – Realized monetary policy shocks (Krippner's (2016) shadow rate)

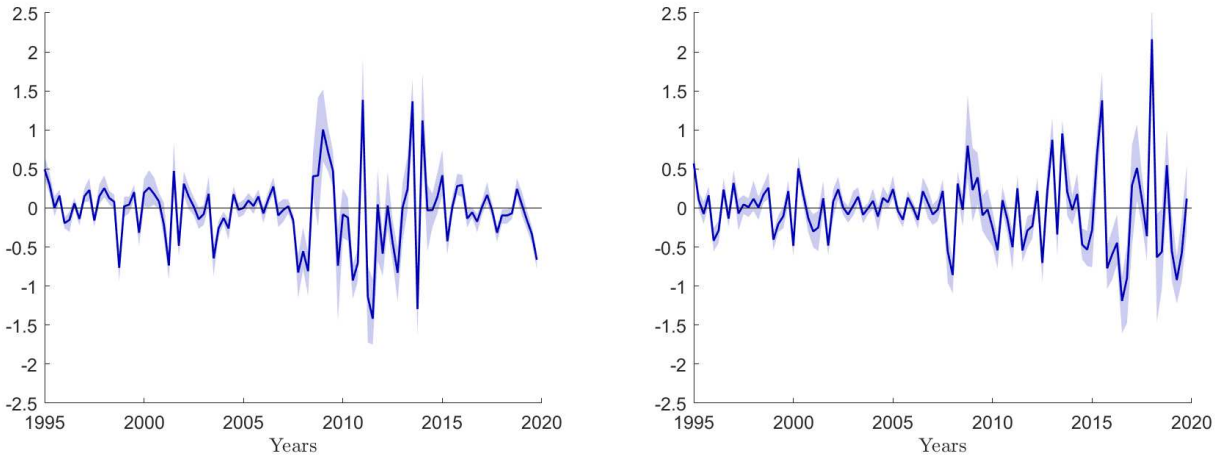

(a) U.S. (b) Euro area

Note: Median (solid lines) and 68% credible interval (shaded areas) of the posterior distribution of the realized monetary policy shock are plotted. A negative monetary policy shock is equivalent to an interest rate setting below the rate prescribed by the estimated monetary policy rule (i.e. expansionary monetary policy).

Figure I.F.5 – Impulse responses to monetary policy shocks in the U.S. (Krippner's (2016) shadow rate)

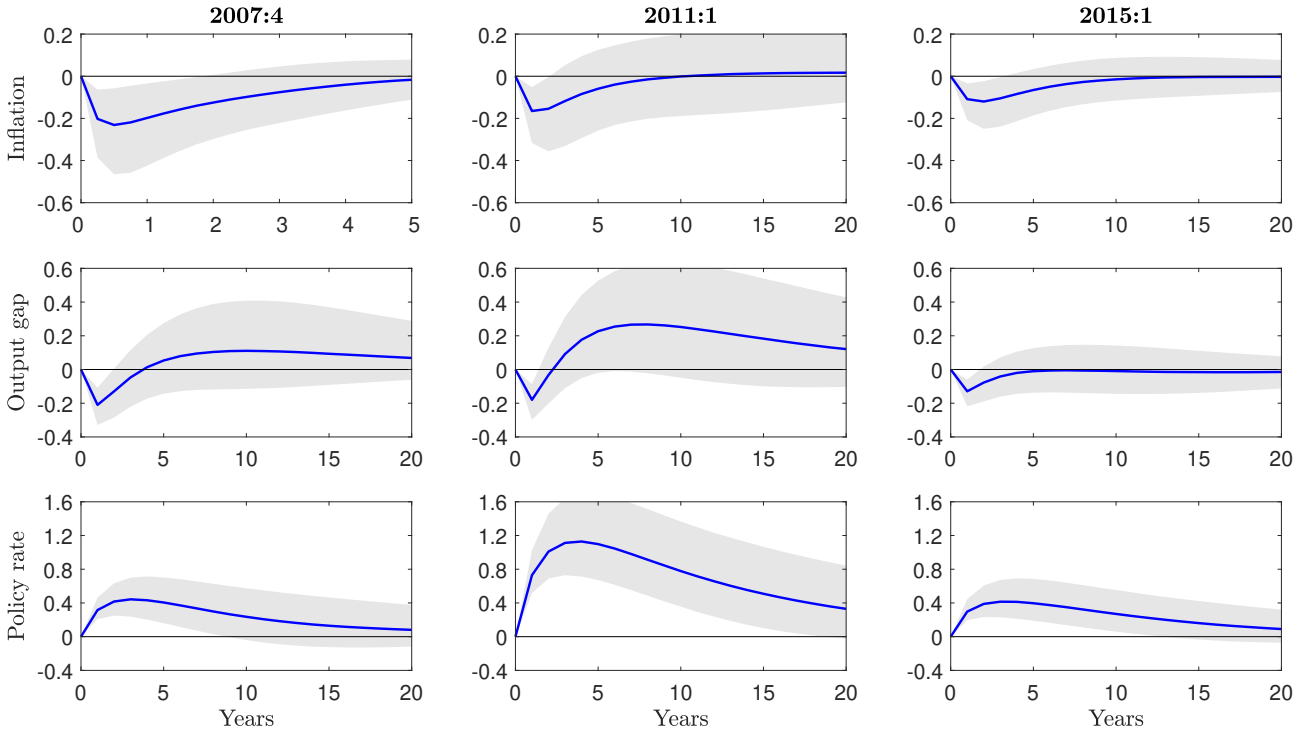

Note: Impulse response of the indicated variable to a contractionary monetary policy shock at the indicated date. Blue lines represent the median and grey shaded areas represent 68% credible intervals of the posterior distribution of each impulse response.

Figure I.F.6 – Impulse responses to monetary policy shocks in the euro area (Krippner's (2016) shadow rate)

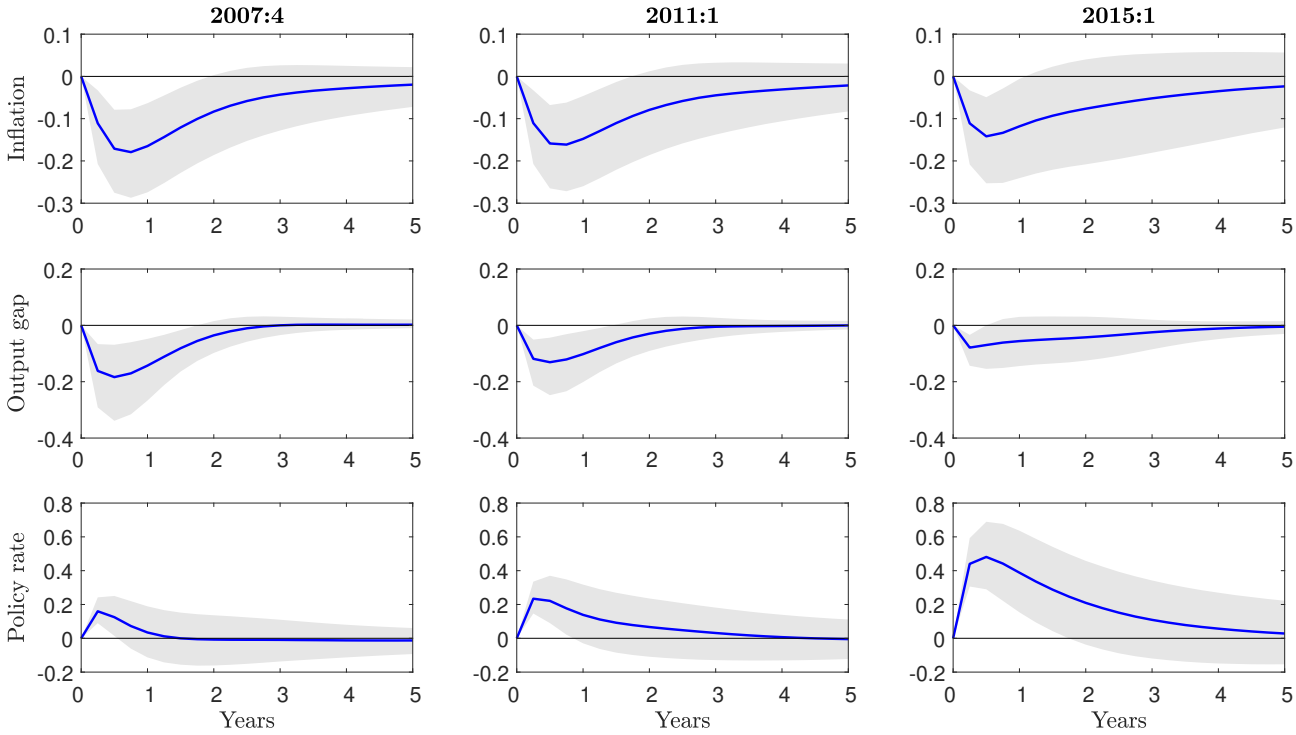

Note: Impulse response of the indicated variable to a contractionary monetary policy shock at the indicated date. Blue lines represent the median and grey shaded areas represent 68% credible intervals of the posterior distribution of each impulse response.

Table I.F.1 – Variance decomposition (Krippner's (2016) shadow rate)

Horizon	% of forecast error variance due to monetary policy shocks					
	U.S.			Euro area		
	2007:4	2011:1	2015:1	2007:4	2011:1	2015:1
Inflation						
1	6.83	5.30	5.88	14.68	13.37	10.76
2	7.07	6.71	6.39	13.51	12.25	10.66
3	8.05	8.91	7.62	12.99	12.12	11.92
4	8.93	10.87	8.65	12.76	12.22	12.87
5	9.50	12.28	9.47	12.65	12.31	13.52
Output gap						
1	7.58	9.55	6.54	9.01	8.73	7.38
2	9.13	14.69	8.05	9.76	10.23	12.12
3	10.50	18.41	9.89	10.08	11.03	14.90
4	11.30	20.77	11.30	10.12	11.21	15.60
5	11.81	22.23	12.29	10.17	11.26	15.79
Policy rate						
1	32.08	55.81	41.48	5.82	13.25	34.44
2	24.24	51.74	34.70	5.72	9.90	26.07
3	21.28	49.67	31.71	6.31	9.96	23.40
4	20.39	48.51	30.14	6.69	10.09	22.32
5	20.16	47.96	29.56	6.90	10.23	21.89

Note: Horizon is the number of years ahead. Variance decomposition is based on draws of the median coefficients from their posterior distributions for 2007:4, 2011:1 and 2015:1.

Figure I.F.7 – Counterfactual simulations (U.S., Krippner's (2016) shadow rate)

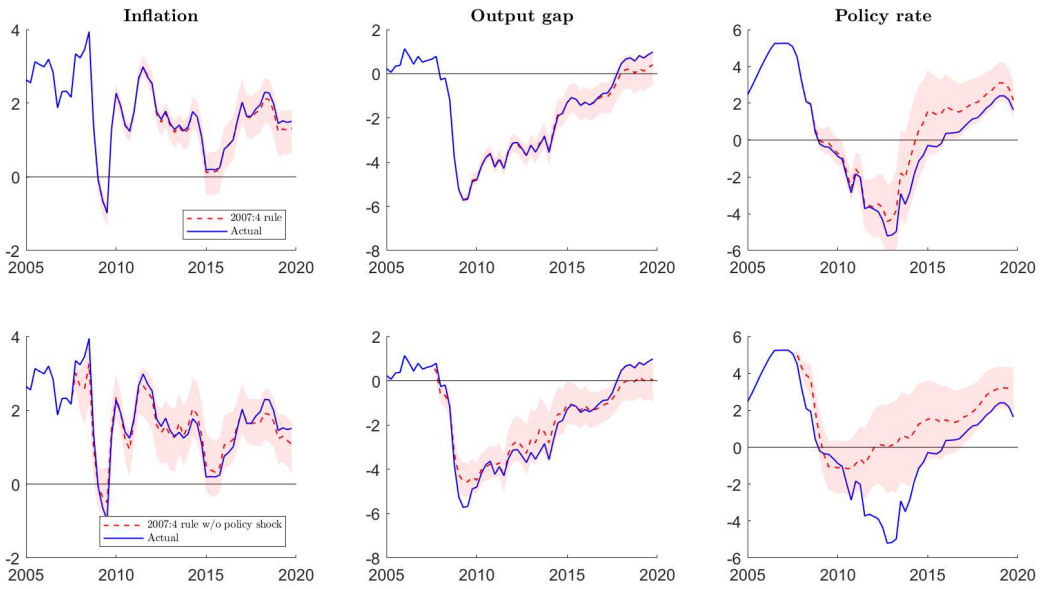

Note: Median counterfactual path (red dashed lines) and 68% credible interval (red shaded areas) are plotted for each indicated variable.

Figure I.F.8 – Counterfactual simulations (Euro area, Krippner's (2016) shadow rate)

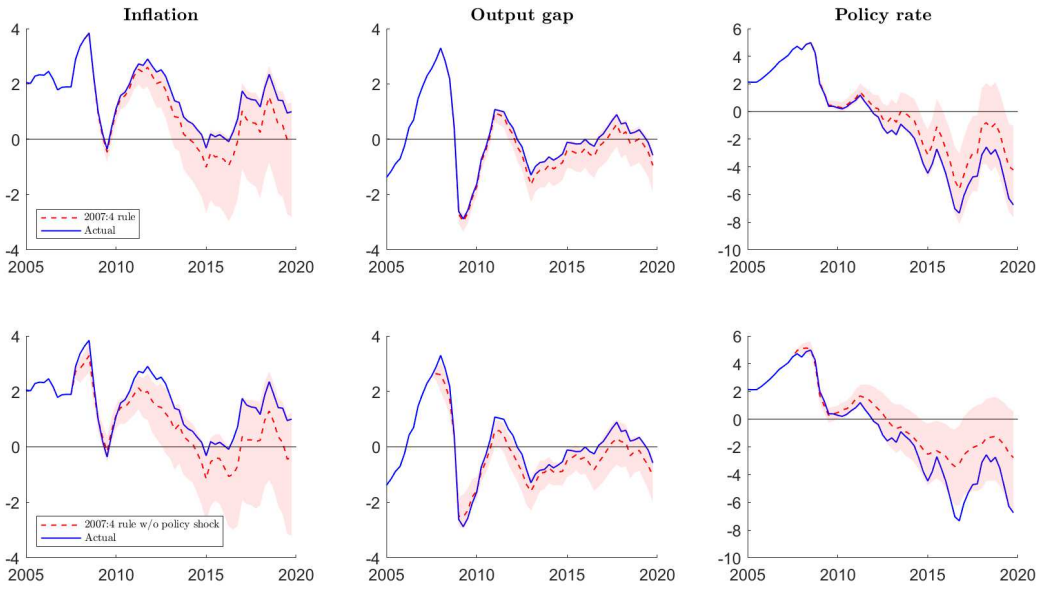

Note: Median counterfactual path (red dashed lines) and 68% credible interval (red shaded areas) are plotted for each indicated variable.

Figure I.F.9 – Contemporaneous coefficients from the estimated monetary policy rule and monetary policy shock volatility (Krippner's (2020) shadow rate)

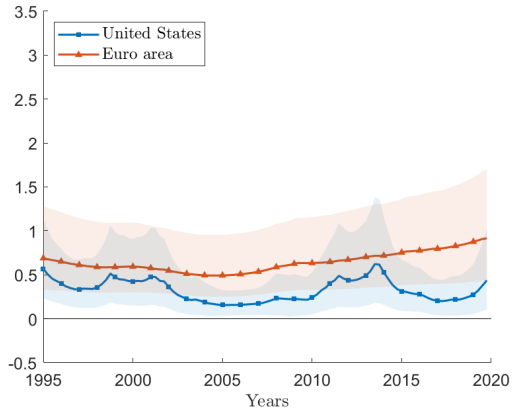

(a) Contemporaneous coefficient on inflation

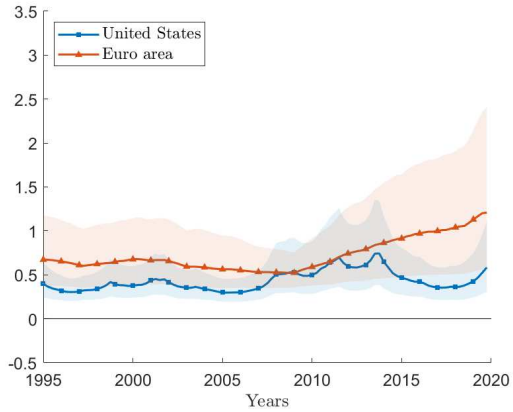

(b) Contemporaneous coefficient on output gap

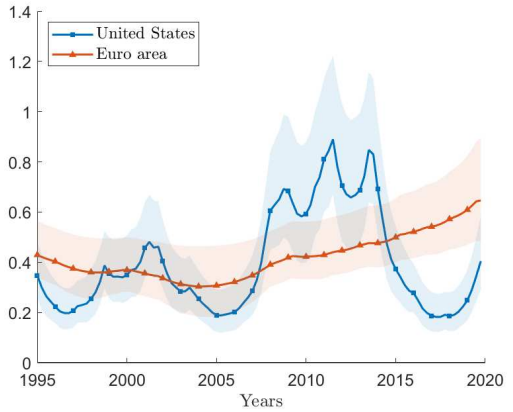

(c) Monetary policy shock volatility

Note: Contemporaneous coefficients on inflation and output gap are respectively given by $c_{r\pi,t}$ and $c_{rg,t}$, and the volatility of monetary policy shocks is captured by $\delta_{r,t}$ in equation (3). Median (solid lines) and 68% credible interval (shaded areas) of the posterior distribution of coefficients are plotted for each indicated variable.

Figure I.F.10 – Interest rate smoothing and long-run coefficients from the estimated monetary policy rule (Krippner's (2020) shadow rate)

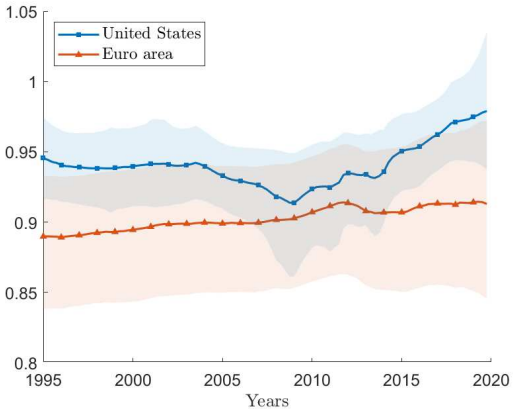

(a) Interest rate smoothing

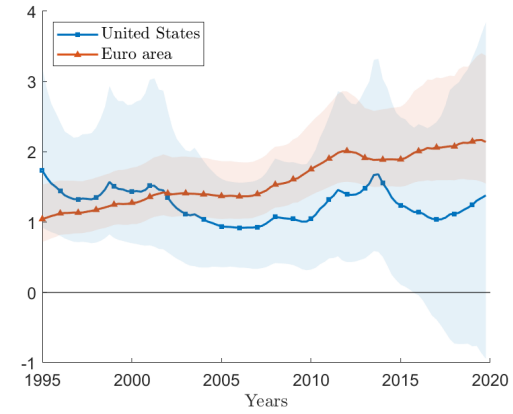

(b) Long-run coefficient on inflation

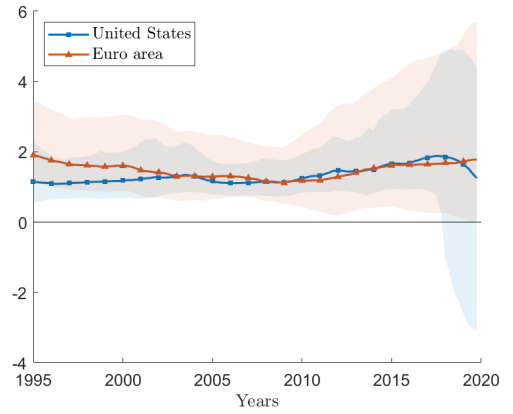

(c) Long-run coefficient on output gap

Note: Interest rate smoothing is given by the sum $\gamma_{1,rr,t}+\gamma_{2,rr,t}$, and long-run coefficients on inflation and output gap are respectively given by $(c_{r\pi,t}+\gamma_{1,r\pi,t}+\gamma_{2,r\pi,t})/(1-\gamma_{1,rr,t}-\gamma_{2,rr,t})$ and $(c_{rg,t}+\gamma_{1,rg,t}+\gamma_{2,rg,t})/(1-\gamma_{1,rr,t}-\gamma_{2,rr,t})$ in equation (3). Median (solid lines) and 68% credible interval (shaded areas) of the posterior distribution of coefficients are plotted for each indicated variable.

I.F.2 Alternative measures of inflation and real activity series

Alternative specifications of the estimated monetary policy rule using different series are run over the sample. The robustness of the results are tested with different series of ex-post inflation (CPI and core PCE price index for the U.S.) and ex-post real activity series (including real GDP growth and unemployment rate for the U.S. and for the euro area, unemployment gap for the U.S. and estimated output gap using Christiano and Fitzgerald (2003) bandpass filter for the euro area). The path of estimated response coefficients are robust to other inflation and real activity series, especially for the long-run coefficients and the volatility of monetary policy shocks.

As made clear by Orphanides (2001, 2003, 2004), real-time and forecast data should also be used in the estimates. Such data are available for the U.S. over a long time span.[31] However, estimates for the euro area with real-time and forecast data are hardly possible because of the lack of observation due to the need for at least 10 years of training sample to calibrate the prior distribution of the time-varying coefficients. This is incompatible with the relatively short period of time covered by those datasets.[32] Hence, to make the comparison between Fed and ECB monetary policy possible, only historical ex-post data are used in the TVP-VAR specification presented in this paper. Croushore and Evans (2006) show that the use of revised data is not a serious limitation for the analysis of monetary policy shocks in recursively identified VARs. However, note that Amir-Ahmadi et al. (2017) employ a TVP-VAR and show that impulse responses to monetary policy shocks is stronger using final data instead of real-time data.

Following Okun's law (Okun, 1962), output gap or real GDP growth are replaced by unemployment gap[33] or simply unemployment rate in the estimate. As a consequence, the strategy based on sign restriction on impulse responses used to identify structural shocks has to be slightly modified as follows:

[31] Real-time data in the U.S. are reported by the Federal Reserve Bank of Philadelphia in the Real-Time Data Set for Macroeconomists, and forecast data are reported in the Survey of Professional Forecasters.

[32] The ECB real-time database (RTD) begins in 1995:1, and the ECB Survey of Professional Forecasters (SPF) only begins in 1999:1.

[33] Unemployment gap is constructed following the formula $u_t^{gap} = u_t - \bar{u}_t$, where u_t is the unemployment rate and $\bar{u}_t$ is the estimated non-accelerating inflation rate of unemployment (NAIRU) at time t.

Table I.F.2 – Sign restrictions on the impact effects of structural shocks

Impact effect on	Structural shocks		
	Aggregate supply	Aggregate demand	Monetary policy
Inflation	+	+	-
Unemployment rate	+	-	+
Shadow rate	?	+	+

Note: The symbol ? indicates that the response is left unconstrained.

Measured by unemployment rate (or unemployment gap), real activity is assumed to react positively to aggregate supply shocks, negatively to aggregate demand shocks and positively to monetary policy shocks. Note also that sign restrictions on impulse responses are the same than those presented in Table I.2.1 when considering real GDP growth instead of output gap in the empirical procedure.

Figure I.F.11 – Contemporaneous coefficients from the estimated monetary policy rule and monetary policy shock volatility (core PCE)

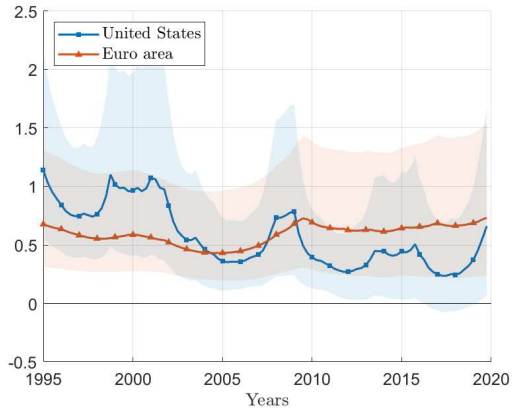

(a) Contemporaneous coefficient on inflation

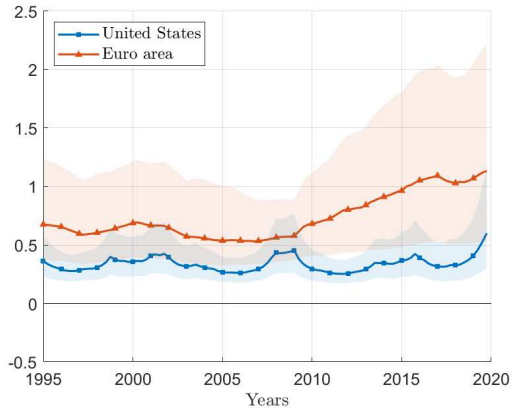

(b) Contemporaneous coefficient on output gap

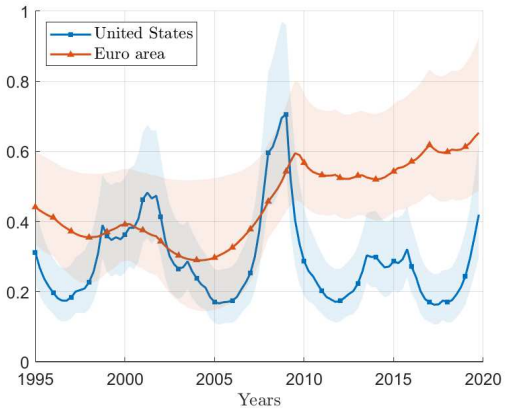

(c) Monetary policy shock volatility

Note: Contemporaneous coefficients on inflation and output gap are respectively given by $c_{r\pi,t}$ and $c_{rg,t}$, and the volatility of monetary policy shocks is captured by $\delta_{r,t}$ in equation (3). Median (solid lines) and 68% credible interval (shaded areas) of the posterior distribution of coefficients are plotted for each indicated variable.

Figure I.F.12 – Interest rate smoothing and long-run coefficients from the estimated monetary policy rule (core PCE)

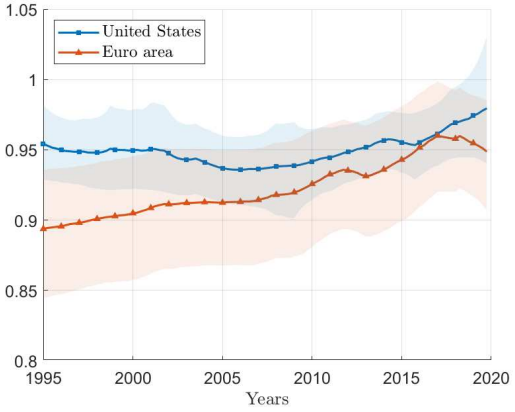

(a) Interest rate smoothing

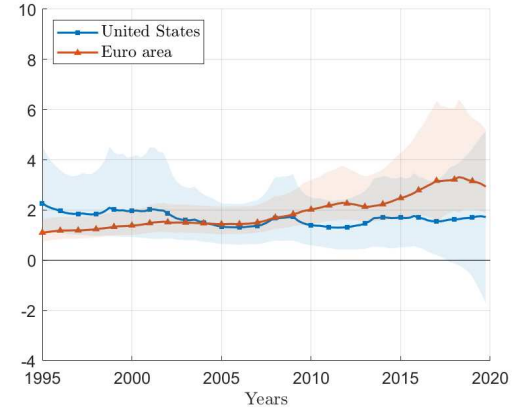

(b) Long-run coefficient on inflation

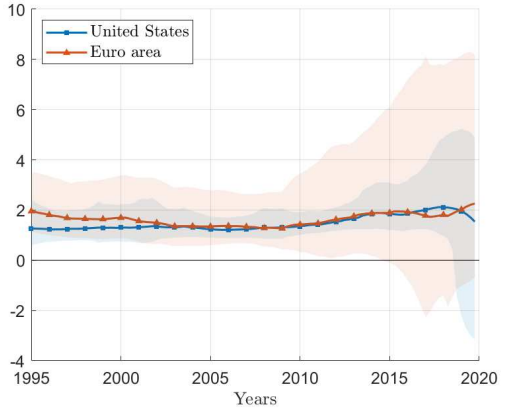

(c) Long-run coefficient on output gap

Note: Interest rate smoothing is given by the sum $\gamma_{1,rr,t}+\gamma_{2,rr,t}$, and long-run coefficients on inflation and output gap are respectively given by $(c_{r\pi,t}+\gamma_{1,r\pi,t}+\gamma_{2,r\pi,t})/(1-\gamma_{1,rr,t}-\gamma_{2,rr,t})$ and $(c_{rg,t}+\gamma_{1,rg,t}+\gamma_{2,rg,t})/(1-\gamma_{1,rr,t}-\gamma_{2,rr,t})$ in equation (3). Median (solid lines) and 68% credible interval (shaded areas) of the posterior distribution of coefficients are plotted for each indicated variable.

Figure I.F.13 – Contemporaneous coefficients from the estimated monetary policy rule and monetary policy shock volatility (real GDP growth)

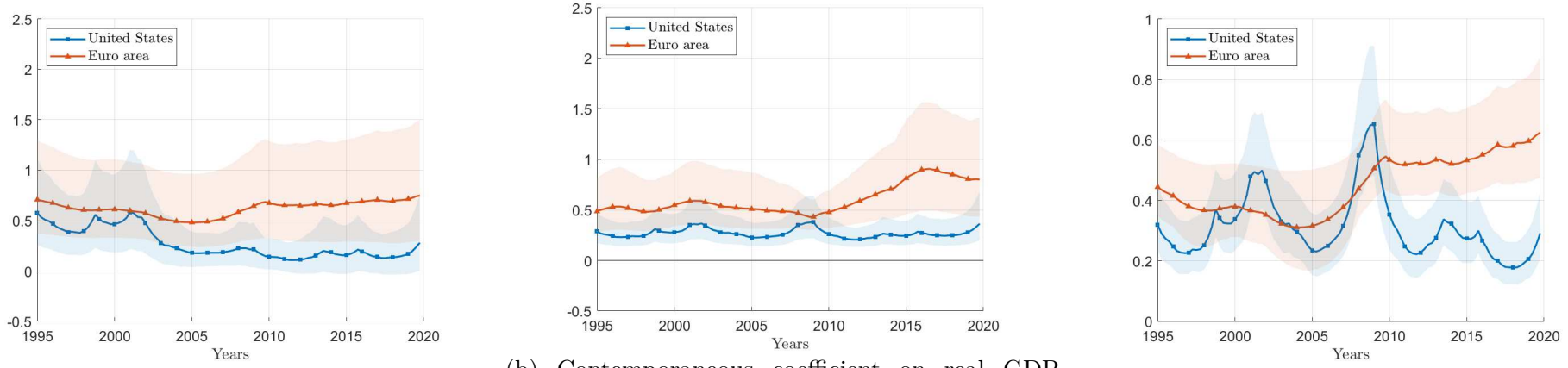

(a) Contemporaneous coefficient on inflation

(b) Contemporaneous coefficient on real GDP growth

(c) Monetary policy shock volatility

Note: Contemporaneous coefficients on inflation and real GDP growth are respectively given by $c_{r\pi,t}$ and $c_{rg,t}$, and the volatility of monetary policy shocks is captured by $\delta_{r,t}$ in equation (3). Median (solid lines) and 68% credible interval (shaded areas) of the posterior distribution of coefficients are plotted for each indicated variable.

Figure I.F.14 – Interest rate smoothing and long-run coefficients from the estimated monetary policy rule (real GDP growth)

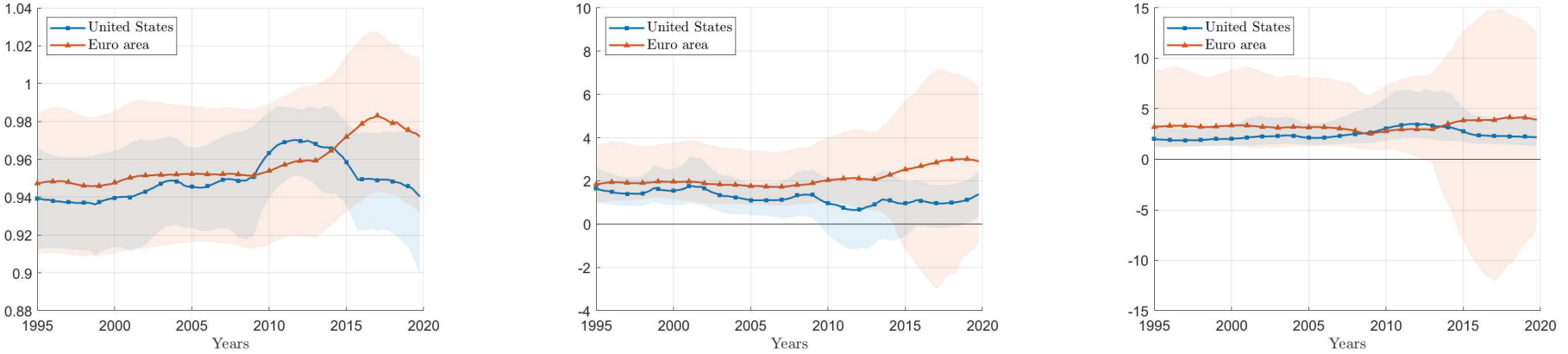

(a) Interest rate smoothing

(b) Long-run coefficient on inflation

(c) Long-run coefficient on real GDP growth

Note: Interest rate smoothing is given by the sum $\gamma_{1,rr,t}+\gamma_{2,rr,t}$, and long-run coefficients on inflation and real GDP growth are respectively given by $(c_{r\pi,t}+\gamma_{1,r\pi,t}+\gamma_{2,r\pi,t})/(1-\gamma_{1,rr,t}-\gamma_{2,rr,t})$ and $(c_{rg,t}+\gamma_{1,rg,t}+\gamma_{2,rg,t})/(1-\gamma_{1,rr,t}-\gamma_{2,rr,t})$ in equation (3). Median (solid lines) and 68% credible interval (shaded areas) of the posterior distribution of coefficients are plotted for each indicated variable.

Figure I.F.15 – Contemporaneous coefficients from the estimated monetary policy rule and monetary policy shock volatility (CPI/HICP and unemployment rate)

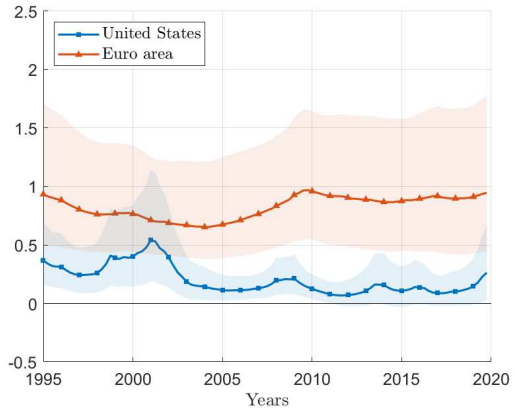

(a) Contemporaneous coefficient on inflation

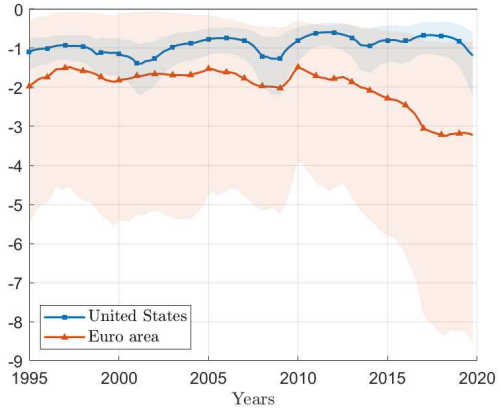

(b) Contemporaneous coefficient on unemployment rate

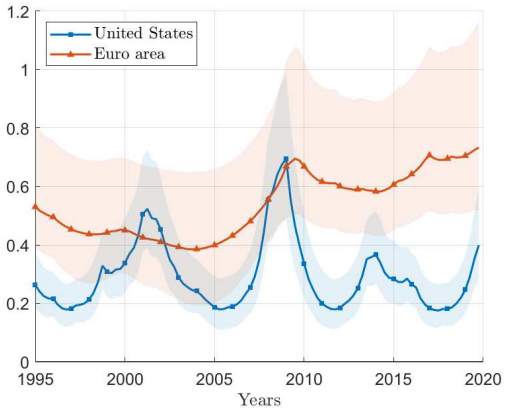

(c) Monetary policy shock volatility

Note: Contemporaneous coefficients on inflation and unemployment rate are respectively given by $c_{r\pi,t}$ and $c_{rg,t}$, and the volatility of monetary policy shocks is captured by $\delta_{r,t}$ in equation (3). Median (solid lines) and 68% credible interval (shaded areas) of the posterior distribution of coefficients are plotted for each indicated variable.

Figure I.F.16 – Interest rate smoothing and long-run coefficients from the estimated monetary policy rule (CPI/HICP and unemployment rate)

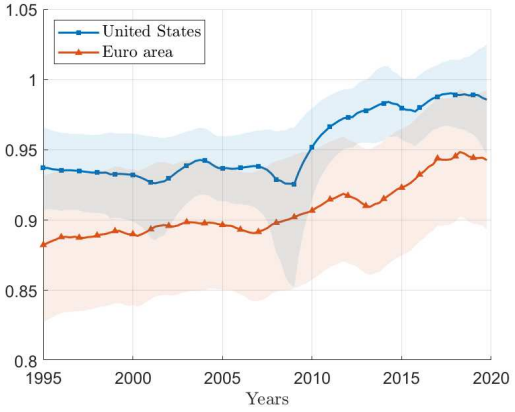

(a) Interest rate smoothing

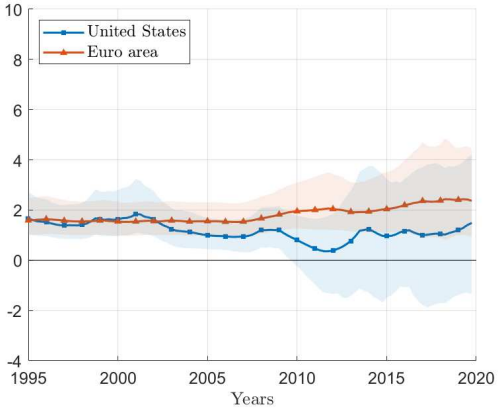

(b) Long-run coefficient on inflation

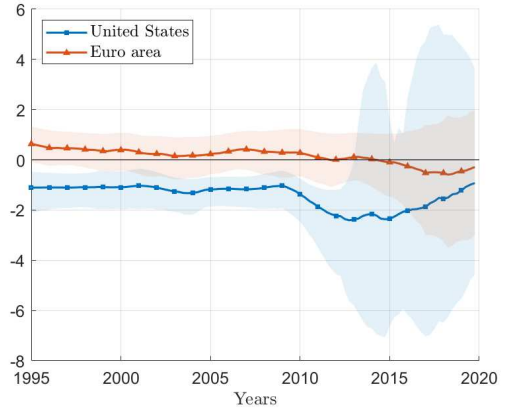

(c) Long-run coefficient on unemployment rate

Note: Interest rate smoothing is given by the sum $\gamma_{1,rr,t}+\gamma_{2,rr,t}$, and long-run coefficients on inflation and unemployment rate are respectively given by $(c_{r\pi,t}+\gamma_{1,r\pi,t}+\gamma_{2,r\pi,t})/(1-\gamma_{1,rr,t}-\gamma_{2,rr,t})$ and $(c_{rg,t}+\gamma_{1,rg,t}+\gamma_{2,rg,t})/(1-\gamma_{1,rr,t}-\gamma_{2,rr,t})$ in equation (3). Median (solid lines) and 68% credible interval (shaded areas) of the posterior distribution of coefficients are plotted for each indicated variable.

Figure I.F.17 – Contemporaneous coefficients from the estimated monetary policy rule and monetary policy shock volatility in the U.S. (unemployment gap)

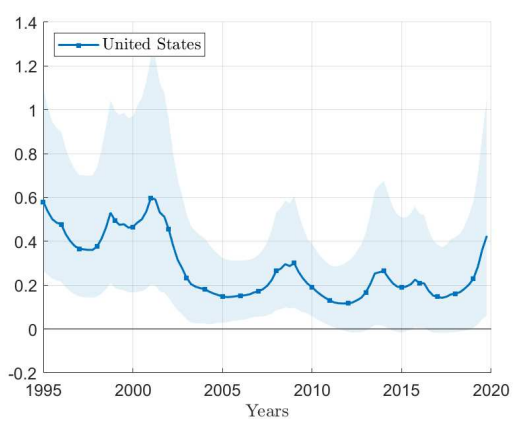

(a) Contemporaneous coefficient on inflation

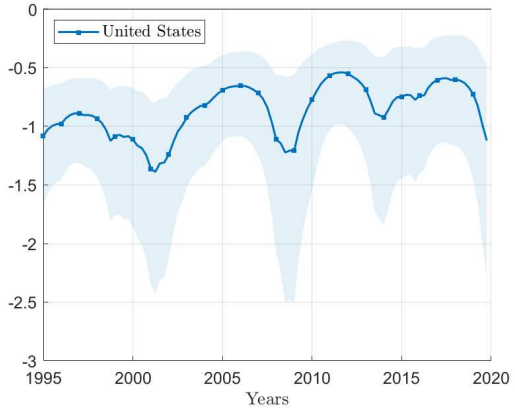

(b) Contemporaneous coefficient on unemployment gap

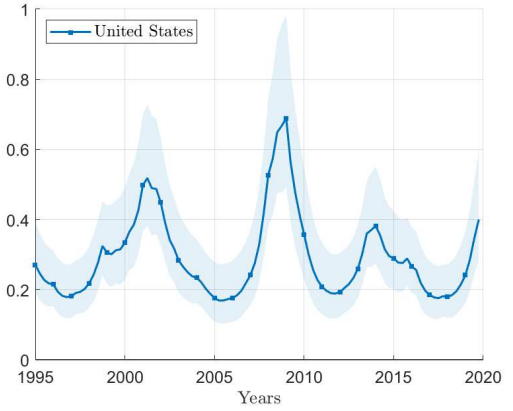

(c) Monetary policy shock volatility

Note: Contemporaneous coefficients on inflation and unemployment gap are respectively given by $c_{r\pi,t}$ and $c_{rg,t}$, and the volatility of monetary policy shocks is captured by $\delta_{r,t}$ in equation (3). Median (solid lines) and 68% credible interval (shaded areas) of the posterior distribution of coefficients are plotted for each indicated variable.

Figure I.F.18 – Interest rate smoothing and long-run coefficients from the estimated monetary policy rule in the U.S. (unemployment gap)

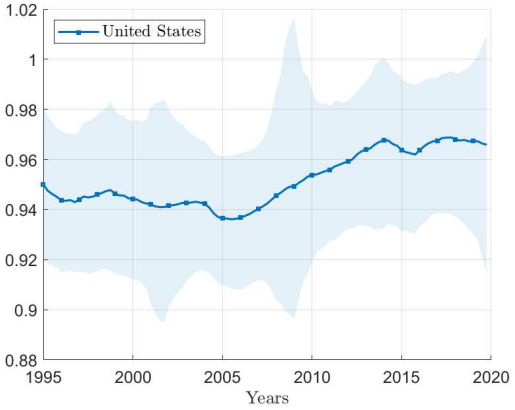

(a) Interest rate smoothing

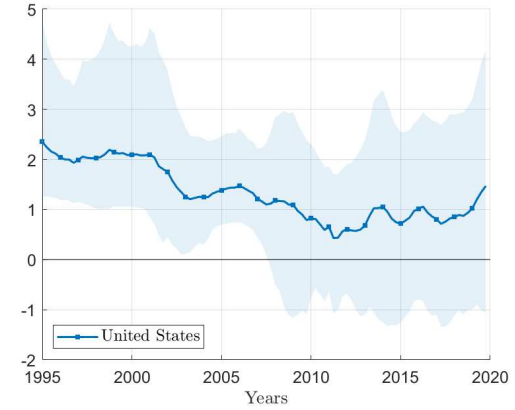

(b) Long-run coefficient on inflation

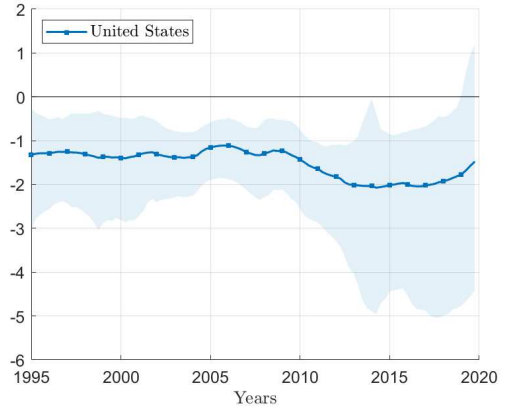

(c) Long-run coefficient on unemployment gap

Note: Interest rate smoothing is given by the sum $\gamma_{1,rr,t}+\gamma_{2,rr,t}$, and long-run coefficients on inflation and unemployment gap are respectively given by $(c_{r\pi,t}+\gamma_{1,r\pi,t}+\gamma_{2,r\pi,t})/(1-\gamma_{1,rr,t}-\gamma_{2,rr,t})$ and $(c_{rg,t}+\gamma_{1,rg,t}+\gamma_{2,rg,t})/(1-\gamma_{1,rr,t}-\gamma_{2,rr,t})$ in equation (3). Median (solid lines) and 68% credible interval (shaded areas) of the posterior distribution of coefficients are plotted for each indicated variable.

Estimating real potential GDP in the euro area with filters

Although it has been universally used in macroeconomics, the Hodrick-Prescott filter may be subject to criticism. According to Hamilton (2018), the HP filter is not a reliable tool to decompose series into a trend and a cycle component, because it introduces spurious dynamic relations and have no basis in the true data-generating process. Therefore, I propose alternative filtering methods commonly used in macroeconomics to estimate euro area real potential GDP. For this purpose, real potential GDP in the euro area is estimated with filtering methods based on Christiano and Fitzgerald (2003), Baxter and King (1999), and following Hamilton (2018) more recently. As a reminder, I briefly give the conceptual framework of Hodrick and Prescott (1997), and raise potential issues implied by the use of the HP filter. Then, other filters are discussed and used to test the robustness of the results.

In accordance with Hodrick and Prescott's (1997) notations, a given time series y_t may be decomposed into a growth (or trend) component g_t and a cyclical component c_t such that:

$y_t = g_t + c_t$

for $t = 1, \dots, T$. As for any filtering methods, the aim of the HP filter is to give a measure of smoothness of the $\{g_t\}$ path. In Hodrick and Prescott (1997), the growth component is determined by the resolution of the following optimization program:

$$\underset{\{g_t\}_{t=-1}^{T}}{\text{Min}} \quad \left\{ \sum_{t=1}^{T} \underbrace{(y_t - g_t)}_{=c_t}^2 + \lambda \sum_{t=1}^{T} [(g_t - g_{t-1}) - (g_{t-1} - g_{t-2})]^2 \right\} \tag{I.39}$$

where $\lambda > 0$ is a 'smoothing parameter' which penalizes variations in the growth component. The larger the value of λ, the smoother is the trend. As a rule of thumb, it is commonly set to 1600 for quarterly data.

However, as highlighted by Hamilton (2018), the HP filter suffers from an end-point bias, and filtered values at the end of the sample are also characterized by spurious dynamics. Also, the author advocates that the value of λ should be data-consistent instead of being calibrated to $\lambda = 1600$ for quarterly data. Hence, Hamilton (2018) suggests an alternative statistical procedure, and proposes running an OLS regression of y_{t+h} on a constant and on the four more recent values as of date t to offer a robust alternative to HP filter:

$$y_{t+h} = \underbrace{\beta_0 + \beta_1 y_t + \beta_2 y_{t-1} + \beta_3 y_{t-2} + \beta_4 y_{t-3}}_{\text{trend component}} + \underbrace{\upsilon_{t+h}}_{\substack{\text{cycle} \\ \text{component}}} \tag{I.40}$$

Hamilton (2018) advocates that for large samples, OLS estimates of equation (I.40) converge to $\beta_1 = 1$ and $\beta_i = 0$ for $i = 0, 2, 3, 4$, and can therefore be written:

$$y_{t+h} = \underbrace{y_t}_{\substack{\text{trend} \\ \text{component}}} + \underbrace{\upsilon_{t+h}}_{\substack{\text{cycle} \\ \text{component}}} \tag{I.41}$$

that gives how much the series y_{t+h} change over a given h horizon.

Euro area output gaps implied by filtered real GDP based on Hamilton's (2018) procedure are presented in the following Figure I.F.19.

Figure I.F.19 – Regression and 8-quarter-change filters applied to euro area real GDP following Hamilton (2018)

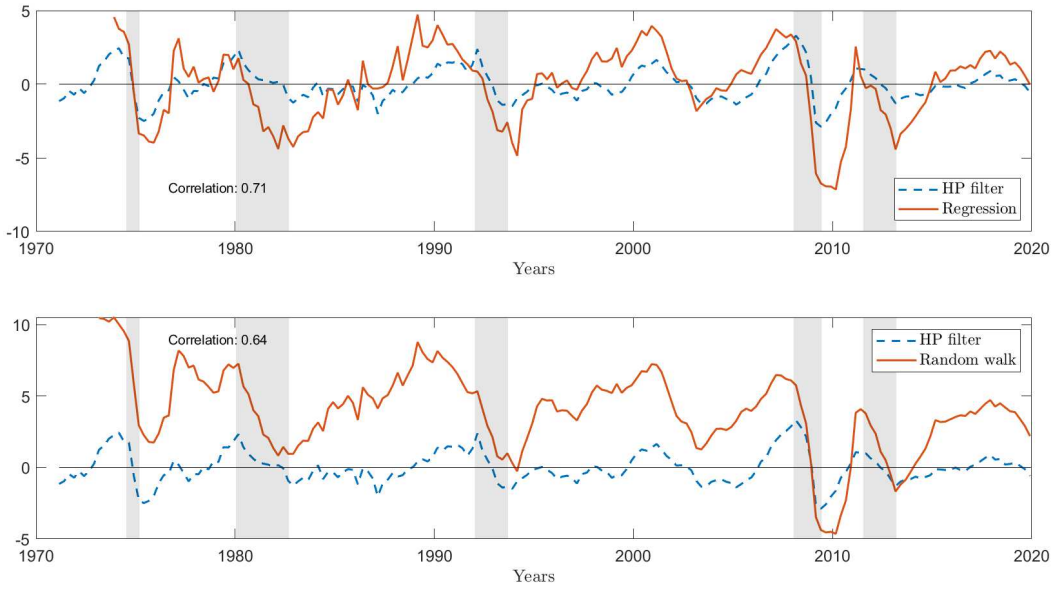

Note: Dashed line shows euro area output gap constructed with real potential GDP estimated by an Hodrick-Prescott filter. Top: solid line plots $\upsilon_t = y_t - \hat{\beta}_0 - \hat{\beta}_1 y_{t-8} - \hat{\beta}_2 y_{t-9} - \hat{\beta}_3 y_{t-10} - \hat{\beta}_4 y_{t-11}$, following equation (I.40). Bottom: solid line plots $\upsilon_t = y_t - y_{t-8}$, following equation (I.41).

Other filtering methods have been widely used in empirical macroeconomics, such as Baxter and King (1999) or Christiano and Fitzgerald (2003) (see Figure I.F.20).

Figure I.F.20 – Band-pass filters applied to euro area real GDP

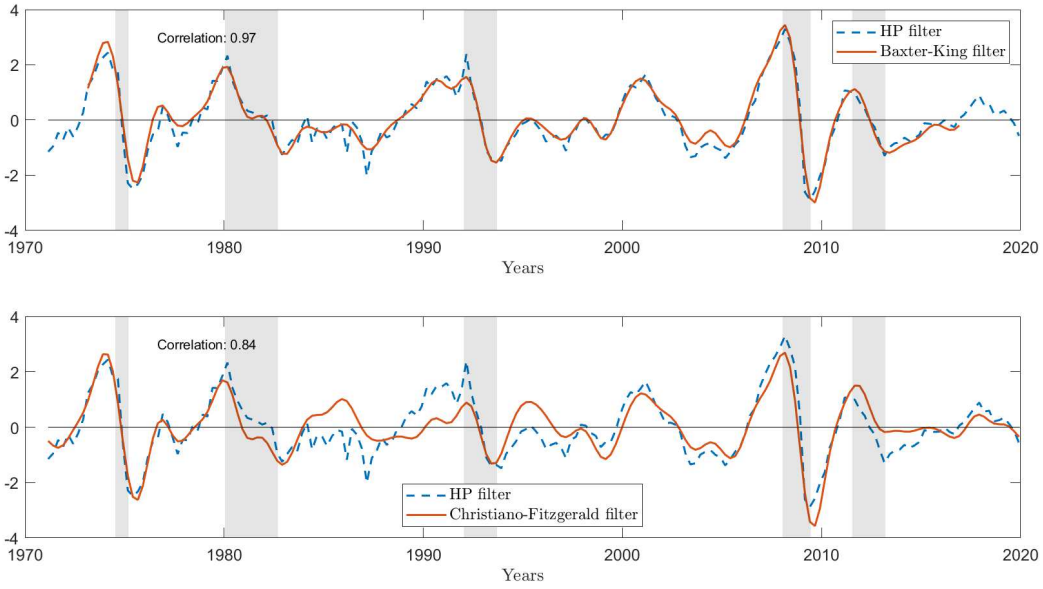

Note: Dashed line shows euro area output gap constructed with real potential GDP estimated by an Hodrick-Prescott filter. Top: solid line plots the cyclical component of euro area real GDP is obtained using a Baxter and King (1999) filter. Bottom: solid line plots the cyclical component of euro area real GDP is obtained using a Christiano and Fitzgerald (2003) filter.

Figure I.F.21 – Contemporaneous coefficients from the estimated monetary policy rule and monetary policy shock volatility in the euro area (HICP and output gap)

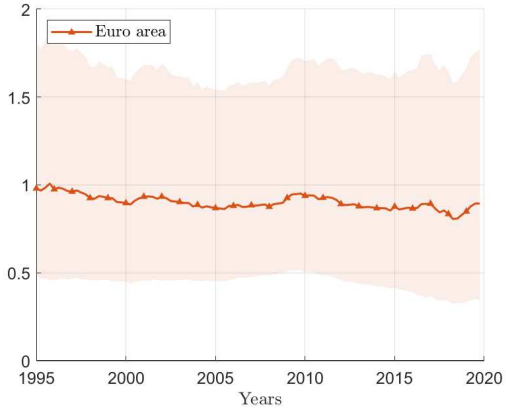

(a) Contemporaneous coefficient on inflation (HICP)

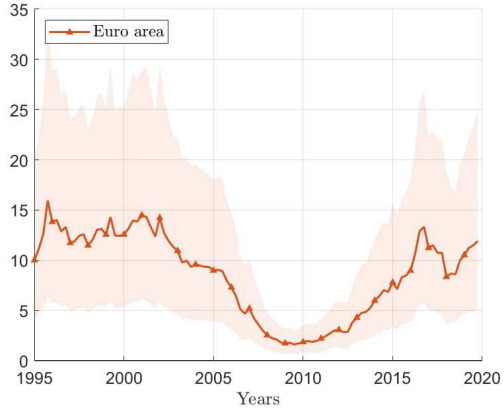

(b) Contemporaneous coefficient on output gap (bandpass filter)

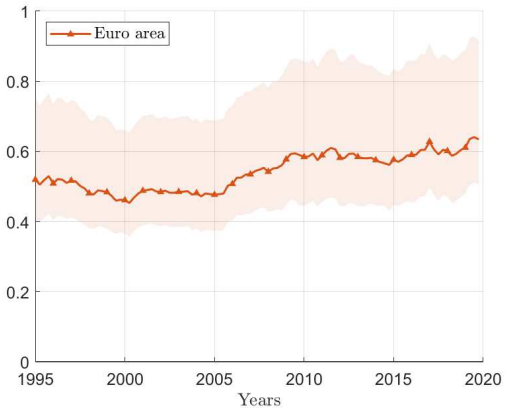

(c) Monetary policy shock volatility

Note: Contemporaneous coefficients on inflation and output gap are respectively given by $c_{r\pi,t}$ and $c_{rg,t}$, and the volatility of monetary policy shocks is captured by $\delta_{r,t}$ in equation (3). Median (solid lines) and 68% credible interval (shaded areas) of the posterior distribution of coefficients are plotted for each indicated variable.

Figure I.F.22 – Interest rate smoothing and long-run coefficients from the estimated monetary policy rule in the euro area (HICP and output gap)

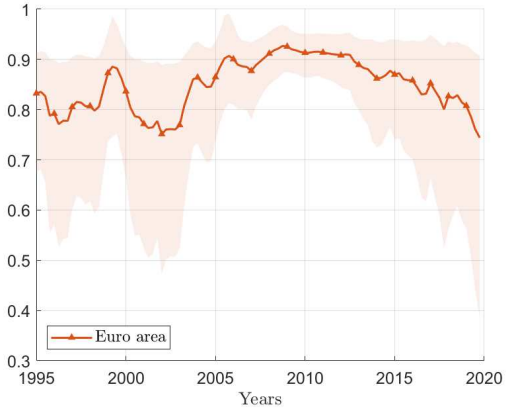

(a) Interest rate smoothing

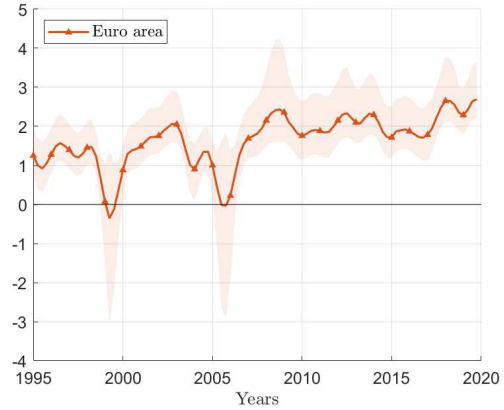

(b) Long-run coefficient on inflation (HICP)

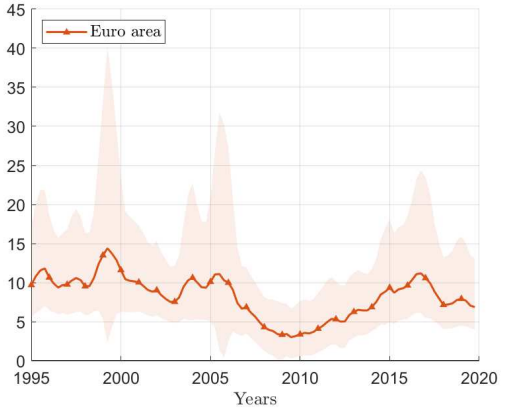

(c) Long-run coefficient on output gap (bandpass filter)

Note: Interest rate smoothing is given by the sum $\gamma_{1,rr,t}+\gamma_{2,rr,t}$, and long-run coefficients on inflation and output gap are respectively given by $(c_{r\pi,t}+\gamma_{1,r\pi,t}+\gamma_{2,r\pi,t})/(1-\gamma_{1,rr,t}-\gamma_{2,rr,t})$ and $(c_{rg,t}+\gamma_{1,rg,t}+\gamma_{2,rg,t})/(1-\gamma_{1,rr,t}-\gamma_{2,rr,t})$ in equation (3). Median (solid lines) and 68% credible interval (shaded areas) of the posterior distribution of coefficients are plotted for each indicated variable.

I.F.3 Alternative TVP-VAR specifications

Further analysis is conducted to check sensitivity of the benchmark results to the VAR specification. As described in Section I.6, *(i)* the choice of lag length (three lags), *(ii)* the choice of prior distributions (calibration and horseshoe priors), and *(iii)* the shocks identification strategy (Cholesky factorization and unrestricted response of output to a monetary policy shock) are modified to check the robustness of the results.

Figure I.F.23 – Contemporaneous coefficients from the estimated monetary policy rule and monetary policy shock volatility ($p = 3$)

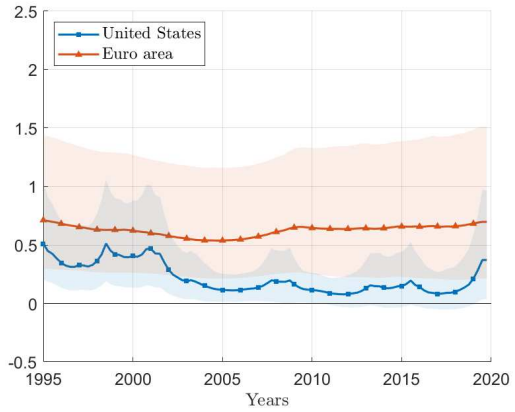

(a) Contemporaneous coefficient on inflation

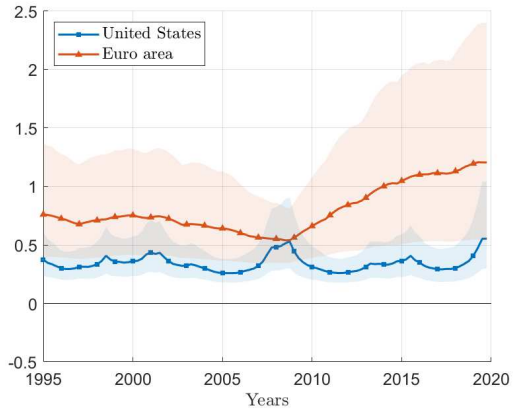

(b) Contemporaneous coefficient on output gap

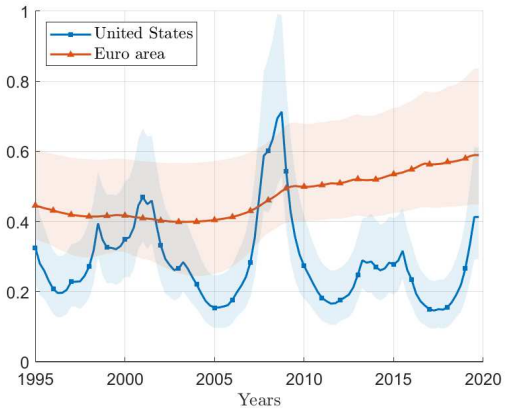

(c) Monetary policy shock volatility

Note: Contemporaneous coefficients on inflation and output gap are respectively given by $c_{r\pi,t}$ and $c_{rg,t}$, and the volatility of monetary policy shocks is captured by $\delta_{r,t}$ in equation (3). Median (solid lines) and 68% credible interval (shaded areas) of the posterior distribution of coefficients are plotted for each indicated variable.

Figure I.F.24 – Interest rate smoothing and long-run coefficients from the estimated monetary policy rule ($p = 3$)

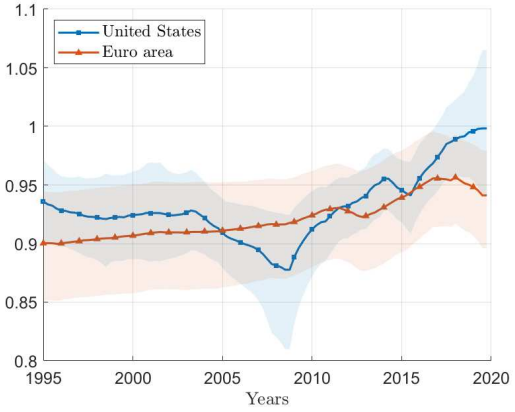

(a) Interest rate smoothing

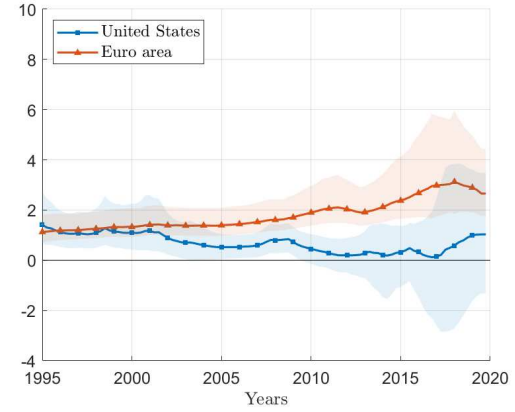

(b) Long-run coefficient on inflation

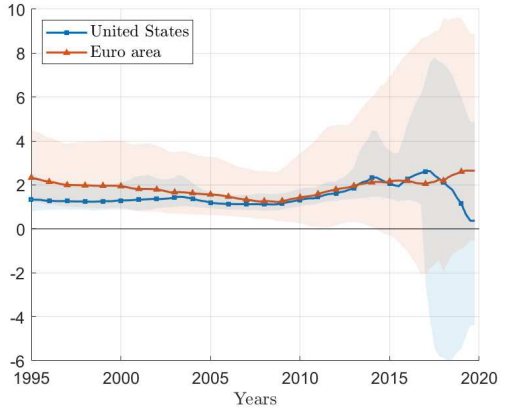

(c) Long-run coefficient on output gap

Note: Interest rate smoothing is given by the sum $\gamma_{1,rr,t}+\gamma_{2,rr,t}$, and long-run coefficients on inflation and output gap are respectively given by $(c_{r\pi,t}+\gamma_{1,r\pi,t}+\gamma_{2,r\pi,t})/(1-\gamma_{1,rr,t}-\gamma_{2,rr,t})$ and $(c_{rg,t}+\gamma_{1,rg,t}+\gamma_{2,rg,t})/(1-\gamma_{1,rr,t}-\gamma_{2,rr,t})$ in equation (3). Median (solid lines) and 68% credible interval (shaded areas) of the posterior distribution of coefficients are plotted for each indicated variable.

Figure I.F.25 – Contemporaneous coefficients from the estimated monetary policy rule and monetary policy shock volatility (calibration of priors)

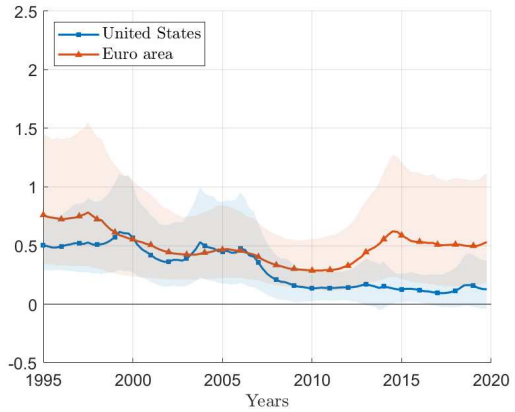

(a) Contemporaneous coefficient on inflation

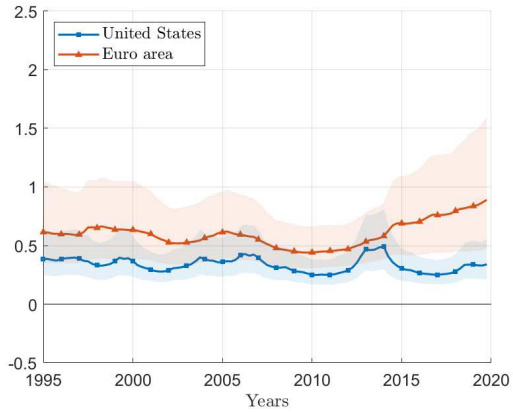

(b) Contemporaneous coefficient on output gap

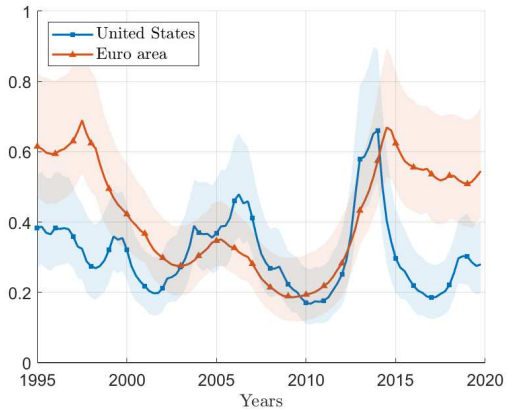

(c) Monetary policy shock volatility

Note: Contemporaneous coefficients on inflation and output gap are respectively given by $c_{r\pi,t}$ and $c_{rg,t}$, and the volatility of monetary policy shocks is captured by $\delta_{r,t}$ in equation (3). Median (solid lines) and 68% credible interval (shaded areas) of the posterior distribution of coefficients are plotted for each indicated variable.

Figure I.F.26 – Interest rate smoothing and long-run coefficients from the estimated monetary policy rule (calibration of priors)

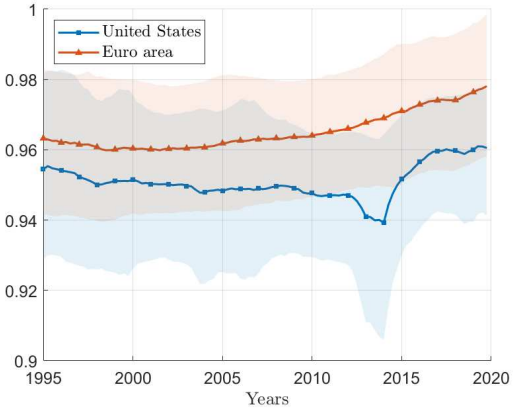

(a) Interest rate smoothing

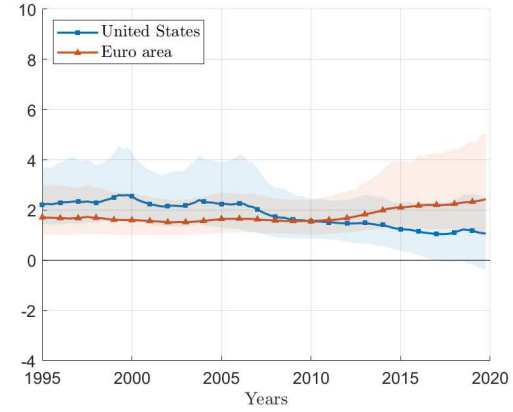

(b) Long-run coefficient on inflation

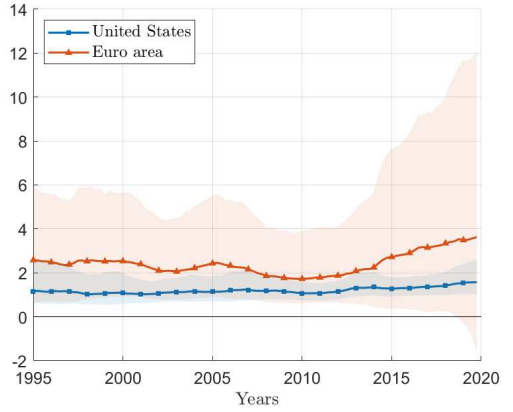

(c) Long-run coefficient on output gap

Note: Interest rate smoothing is given by the sum $\gamma_{1,rr,t}+\gamma_{2,rr,t}$, and long-run coefficients on inflation and output gap are respectively given by $(c_{r\pi,t}+\gamma_{1,r\pi,t}+\gamma_{2,r\pi,t})/(1-\gamma_{1,rr,t}-\gamma_{2,rr,t})$ and $(c_{rg,t}+\gamma_{1,rg,t}+\gamma_{2,rg,t})/(1-\gamma_{1,rr,t}-\gamma_{2,rr,t})$ in equation (3). Median (solid lines) and 68% credible interval (shaded areas) of the posterior distribution of coefficients are plotted for each indicated variable.

Figure I.F.27 – TVP-VAR long-run coefficients (Prüser, 2021)

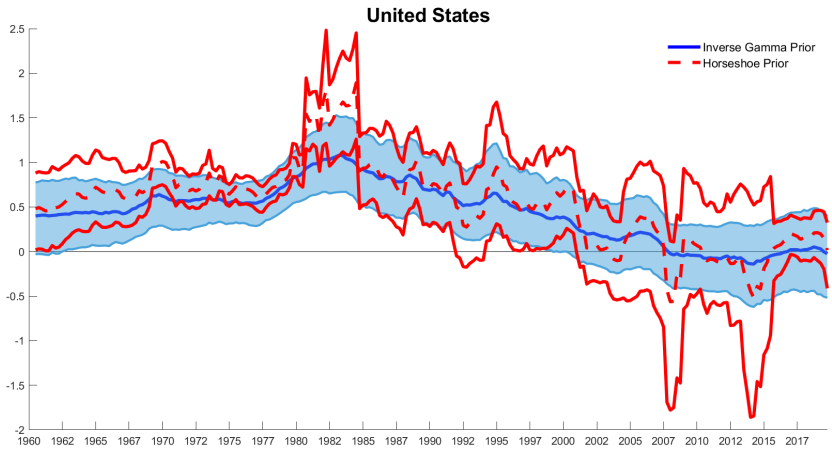

(a) Long-run response of R^s to a permanent increase in inflation

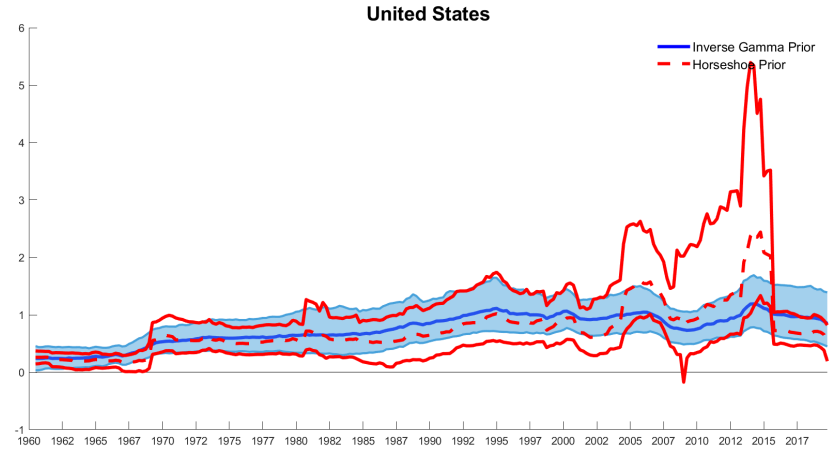

(b) Long-run response of R^s to a permanent increase in output gap

Note: Median long-run coeffficients on inflation and output gap with 68% credible bands.

Figure I.F.28 – Monetary policy shock volatility (Prüser, 2021)

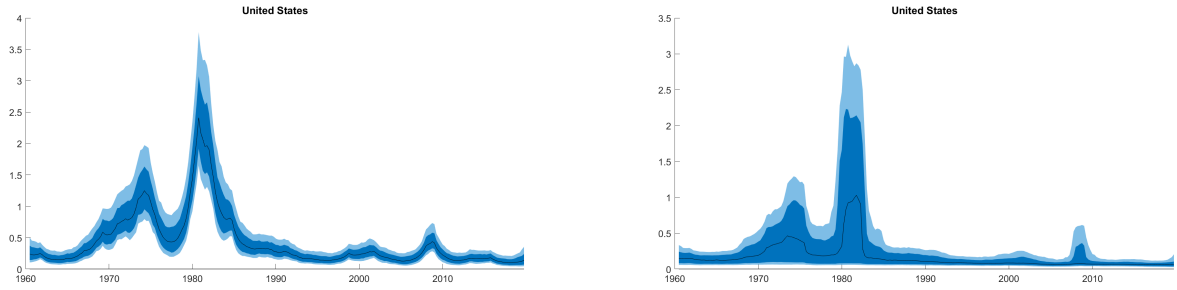

(a) Inverse Gamma prior

(b) Horseshoe prior

Note: Median monetary policy shock volatility with 68% and 90% credible bands.

Figure I.F.29 – TVP-VAR long-run coefficients (Prüser, 2021)

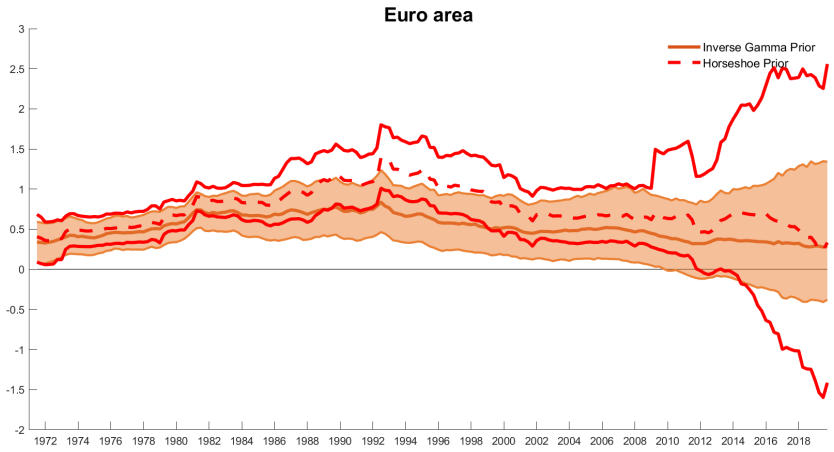

(a) Long-run response of R^s to a permanent increase in inflation

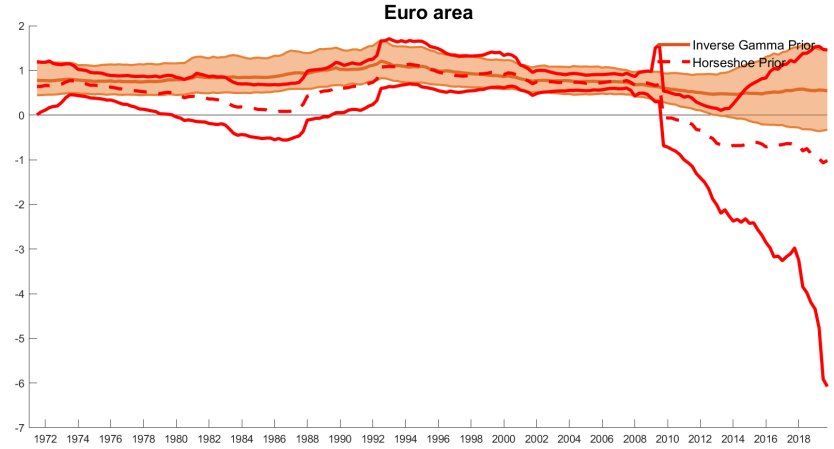

(b) Long-run response of R^s to a permanent increase in output gap

Note: Median long-run coeffficients on inflation and output gap with 68% credible bands.

Figure I.F.30 – Monetary policy shock volatility (Prüser, 2021)

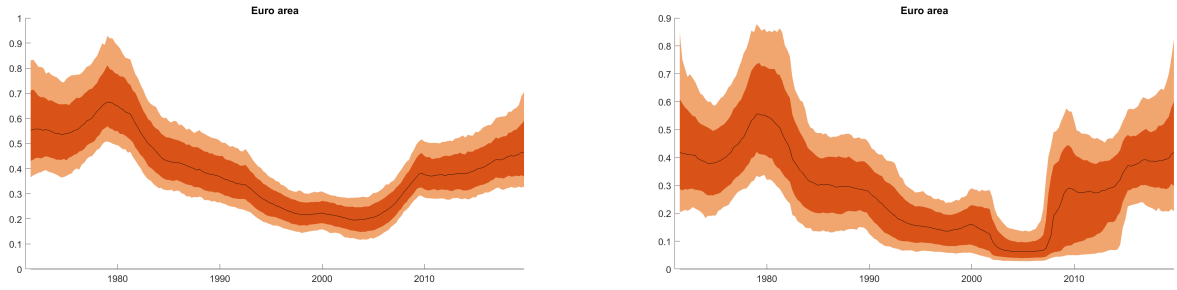

(a) Inverse Gamma prior

(b) Horseshoe prior

Note: Median monetary policy shock volatility with 68% and 90% credible bands.

Figure I.F.31 – Contemporaneous coefficients from the estimated monetary policy rule and monetary policy shock volatility (Cholesky factorization)

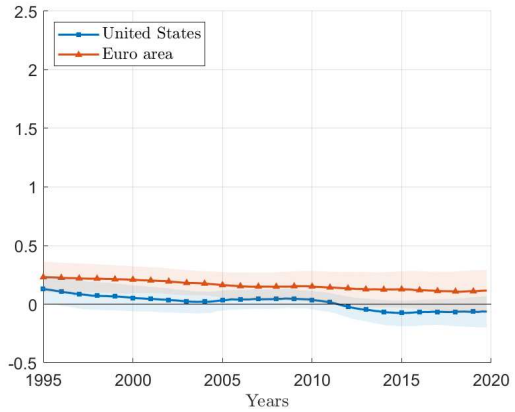

(a) Contemporaneous coefficient on inflation

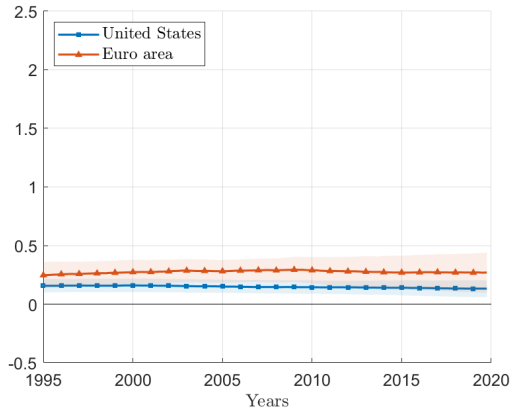

(b) Contemporaneous coefficient on output gap

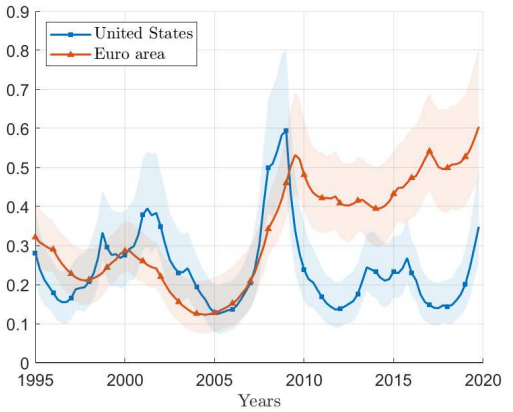

(c) Monetary policy shock volatility

Note: Contemporaneous coefficients on inflation and output gap are respectively given by $c_{r\pi,t}$ and $c_{rg,t}$, and the volatility of monetary policy shocks is captured by $\delta_{r,t}$ in equation (3). Median (solid lines) and 68% credible interval (shaded areas) of the posterior distribution of coefficients are plotted for each indicated variable.

Figure I.F.32 – Interest rate smoothing and long-run coefficients from the estimated monetary policy rule (Cholesky factorization)

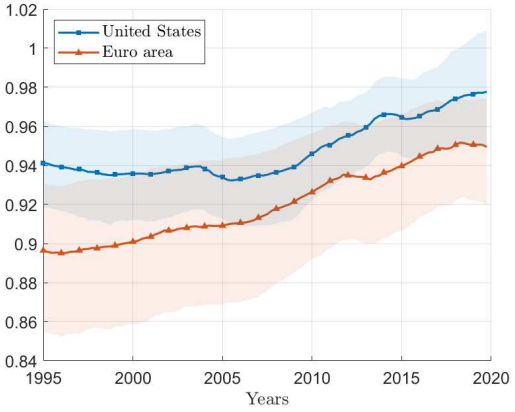

(a) Interest rate smoothing

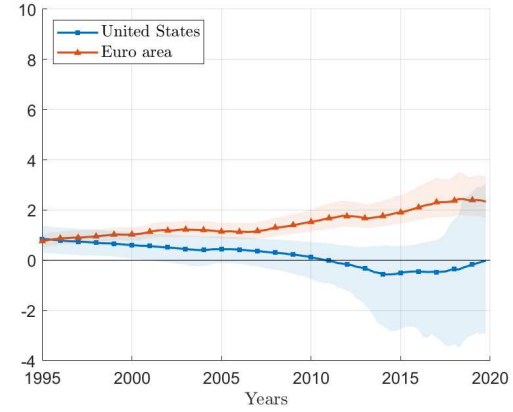

(b) Long-run coefficient on inflation

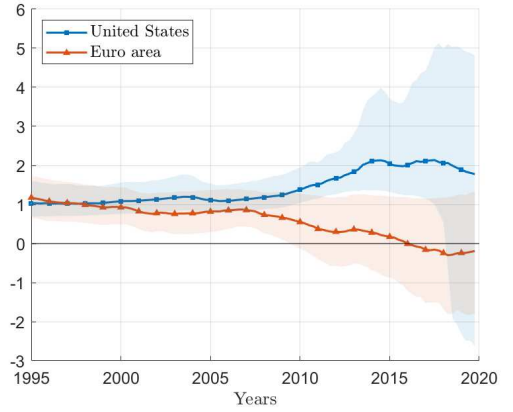

(c) Long-run coefficient on output gap

Note: Interest rate smoothing is given by the sum $\gamma_{1,rr,t}+\gamma_{2,rr,t}$, and long-run coefficients on inflation and output gap are respectively given by $(c_{r\pi,t}+\gamma_{1,r\pi,t}+\gamma_{2,r\pi,t})/(1-\gamma_{1,rr,t}-\gamma_{2,rr,t})$ and $(c_{rg,t}+\gamma_{1,rg,t}+\gamma_{2,rg,t})/(1-\gamma_{1,rr,t}-\gamma_{2,rr,t})$ in equation (3). Median (solid lines) and 68% credible interval (shaded areas) of the posterior distribution of coefficients are plotted for each indicated variable.

Figure I.F.33 – Contemporaneous coefficients from the estimated monetary policy rule and monetary policy shock volatility (unrestricted response to output)

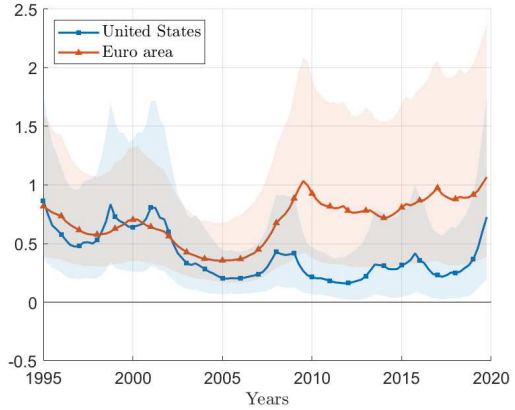

(a) Contemporaneous coefficient on inflation

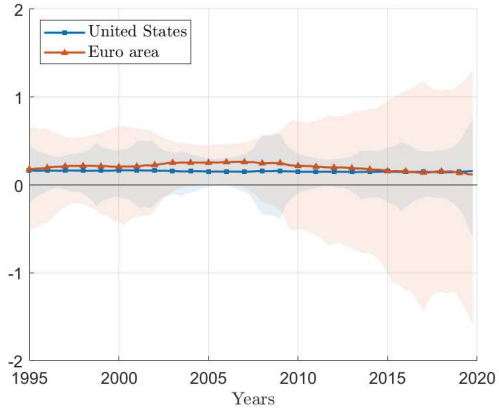

(b) Contemporaneous coefficient on output gap

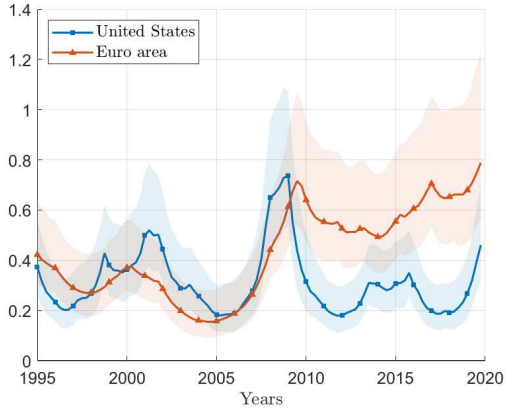

(c) Monetary policy shock volatility

Note: Contemporaneous coefficients on inflation and output gap are respectively given by $c_{r\pi,t}$ and $c_{rg,t}$, and the volatility of monetary policy shocks is captured by $\delta_{r,t}$ in equation (3). Median (solid lines) and 68% credible interval (shaded areas) of the posterior distribution of coefficients are plotted for each indicated variable.

Figure I.F.34 – Interest rate smoothing and long-run coefficients from the estimated monetary policy rule (unrestricted response to output)

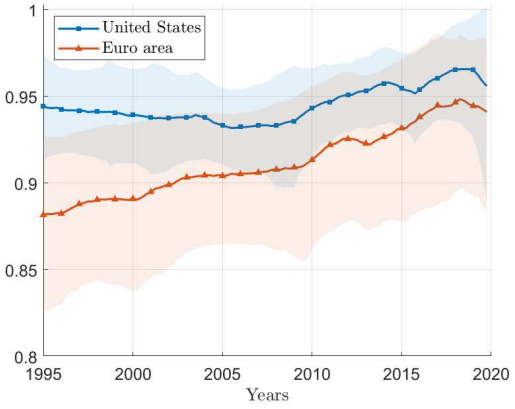

(a) Interest rate smoothing

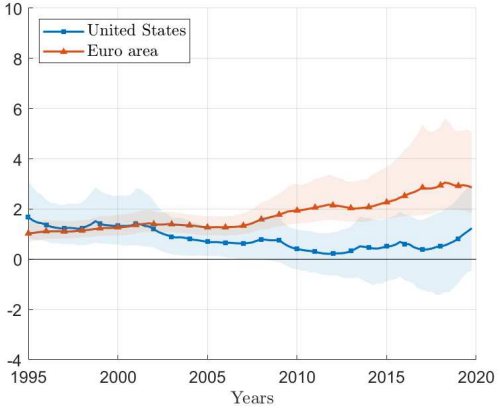

(b) Long-run coefficient on inflation

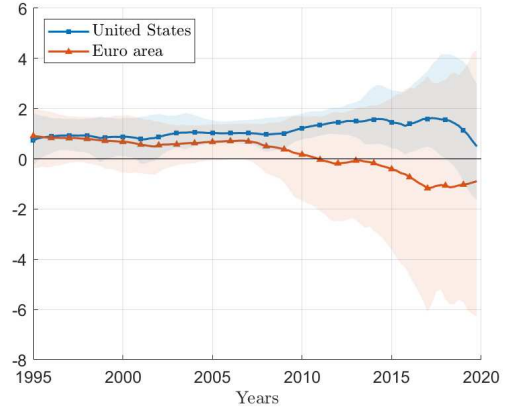

(c) Long-run coefficient on output gap

Note: Interest rate smoothing is given by the sum $\gamma_{1,rr,t}+\gamma_{2,rr,t}$, and long-run coefficients on inflation and output gap are respectively given by $(c_{r\pi,t}+\gamma_{1,r\pi,t}+\gamma_{2,r\pi,t})/(1-\gamma_{1,rr,t}-\gamma_{2,rr,t})$ and $(c_{rg,t}+\gamma_{1,rg,t}+\gamma_{2,rg,t})/(1-\gamma_{1,rr,t}-\gamma_{2,rr,t})$ in equation (3). Median (solid lines) and 68% credible interval (shaded areas) of the posterior distribution of coefficients are plotted for each indicated variable.

Figure I.F.35 – Counterfactual simulations (U.S., unrestricted response to output)

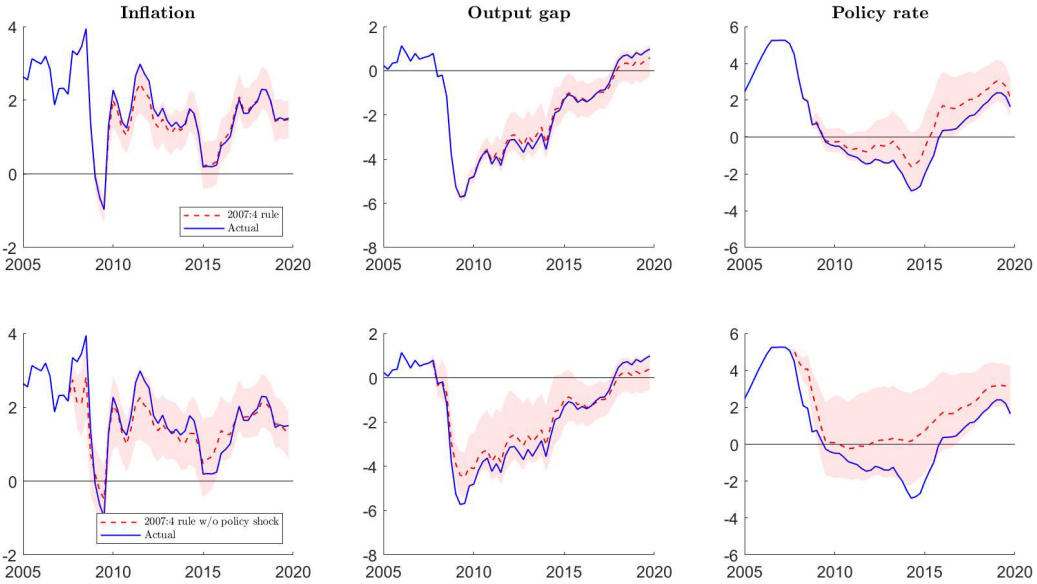

Note: Median counterfactual path (red dashed lines) and 68% credible interval (red shaded areas) are plotted for each indicated variable.

Figure I.F.36 – Counterfactual simulations (Euro area, unrestricted response to output)

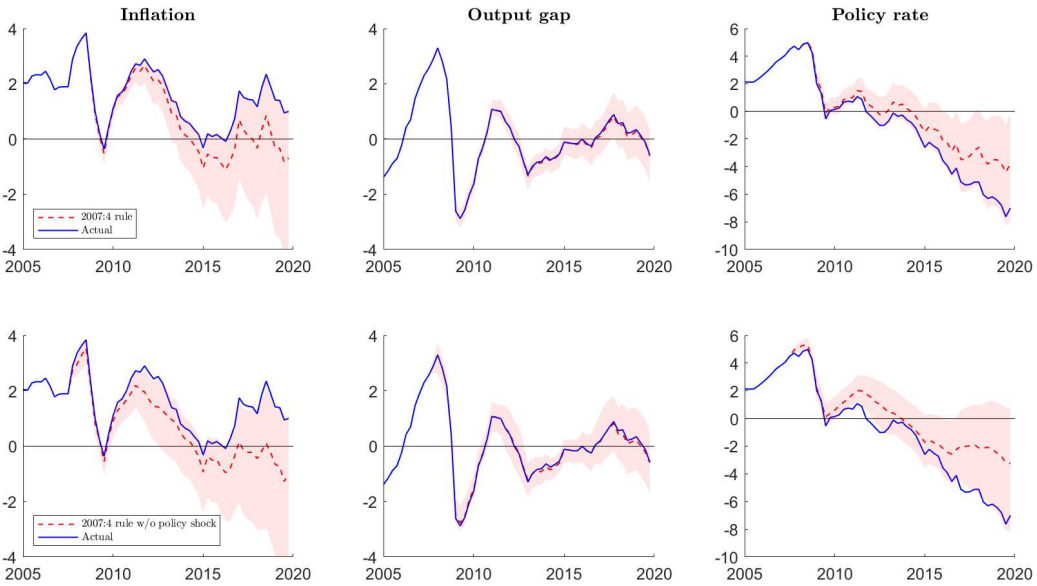

Note: Median counterfactual path (red dashed lines) and 68% credible interval (red shaded areas) are plotted for each indicated variable.

Chapter II

COVID-induced sovereign risk in the euro area: When did the ECB stop the spread?

Abstract. *This paper studies how the announcement of the ECB's monetary policies stopped the spread of the COVID-19 pandemic to the European sovereign debt market. We show that up to March 9, the occurrence of new cases in euro area countries had a sizeable and persistent effect on 10-year sovereign bond spreads relative to Germany: 10 new confirmed cases per million people were accompanied by an immediate spread increase of* 0.03 *percentage points (ppt) that lasted* 5 *days, for a total increase of* 0.35 *ppt. For periods afterwards, the effect falls to near zero and is not significant. We interpret this change as an indicator of the success of the ECB's March 12 press conference, despite the "we are not here to close spreads" controversy. Our results hold for the stock market, providing further evidence of the effectiveness of the ECB's March 12 announcements in stopping the financial turmoil. A counterfactual analysis shows that without the shift in the sensitivity of sovereign bond markets to COVID-19, spreads would have surged to* 4.2% *in France,* 12.5% *in Spain, and* 19.5% *in Italy by March 18, when the ECB's Pandemic Emergency Purchase Programme was finally announced.*

> *"I can assure you on that page that first of all we will make use of all the flexibilities that are embedded in the framework of the asset purchase programme, (...) but we*

are not here to close spreads." Christine Lagarde, president of the ECB, press conference, 12 March 2020.

"*The ECB will ensure that all sectors of the economy can benefit from supportive financing conditions that enable them to absorb this shock. This applies equally to families, firms, banks and governments.*" ECB Governing Council press release, 18 March 2020.

II.1 Introduction

The COVID-19 virus pandemic started on December 31, 2019, in China and reached Europe almost one month later, according to the World Health Organization (WHO).[1] As a serious threat to the economy, the rapid spread of the virus led to sizeable financial turmoil in Europe. The downturn was particularly strong in Italy, the most affected country in Europe, where the interest rate spread *vis-à-vis* Germany rose sharply from 1.4% to 2.5% and the stock market fell by 40% between February 19 and March 12 (Figure II.1.1). On March 12, the European Central Bank (ECB) announced a set of monetary policy measures to support the economy in the face of the pandemic. The announcement of these measures gave rise to controversy over ECB president Christine Lagarde's announcement that the ECB would certainly use "all the flexibilities that are embedded in the framework of the asset purchase programme" but also that the central bank was "not here to close spreads." This last sentence has been widely cited as a communication failure, contrasting with the famous "whatever it takes" of her predecessor Mario Draghi.[2] After a crash on March 12, the stock index plateaued, while the interest rate spread kept soaring to reach more than 2.8% on March 17. On March 18, the ECB conducted an exceptional longer-term refinancing operation (LTRO) to provide liquidity and announced the launch of a massive intervention program known as the Pandemic Emergency Purchase Programme (PEPP), which led to a turnaround in sovereign rates and a reboot in stock prices (Figure II.1.1). While the COVID-19 pandemic continued to spread in Europe, its transmission to financial markets stopped in Italy and the rest of the euro area. What was the role of these successive ECB interventions in stopping the spread of the pandemic to financial markets? What would have happened without these interventions?

[1] The WHO offers regular rolling updates on the coronavirus disease. See also its daily situation reports.

[2] The Bloomberg article "Christine Lagarde Does Whatever It Doesn't Take" illustrates the reaction in the press and social media to Christine Lagarde's press conference.

Figure II.1.1 – COVID-19 pandemic outbreak, government bond spread and stock market in Italy

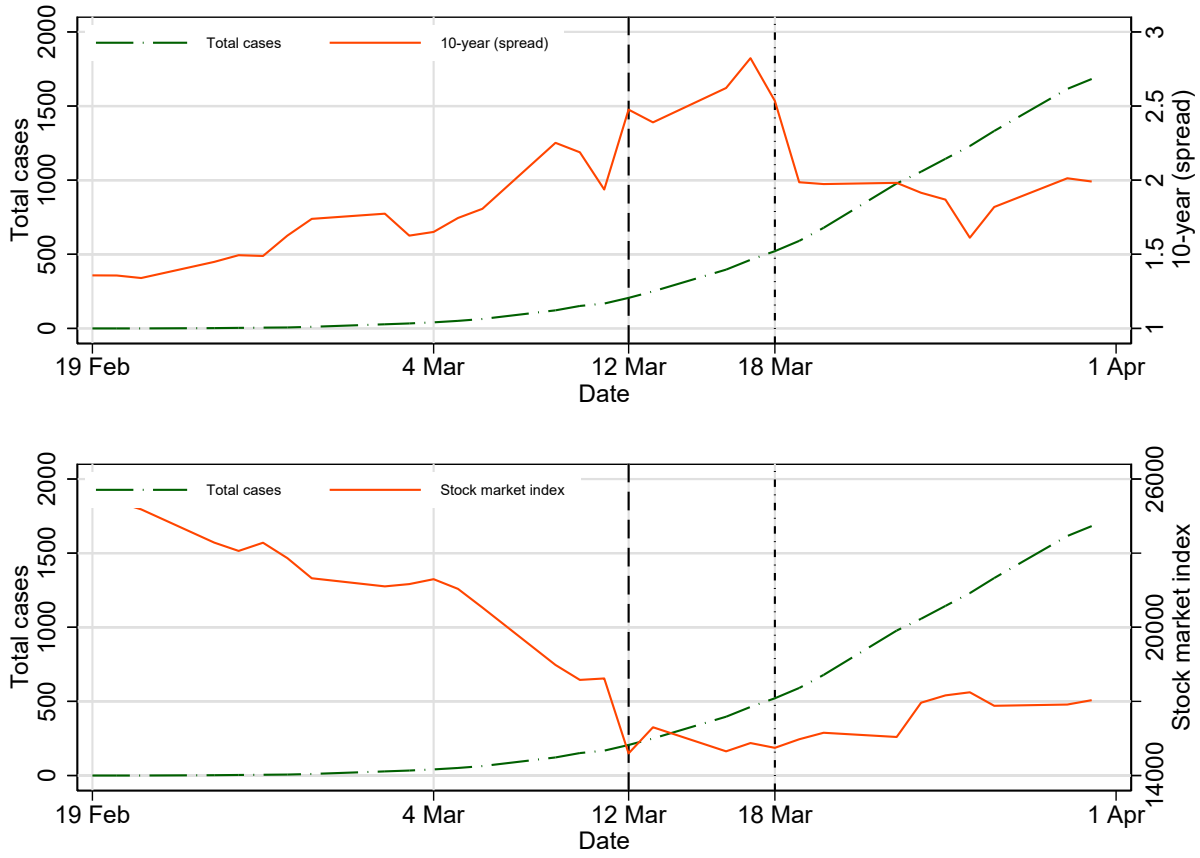

Note: Vertical lines correspond to ECB announcement dates: March 12, 2020 (dashed), and March 18, 2020 (dot-dashed). LHS: Total COVID-19 confirmed cases are reported as the number of cases per million people. RHS: 10-year government spread (in %) is computed relative to the yield on 10-year German bonds; the stock market index is the FTSE MIB index.

To answer these questions, we measure the reaction of sovereign spreads to new COVID-19 cases and examine how it evolved around the time of the ECB interventions. Using local projection methods developed by Jordà (2005), we measure the reaction at the time of impact, that is, on the day of the occurrence of COVID-19 cases, and in dynamics, that is, up to 5 days after the release of data on new confirmed COVID cases. We provide state-dependent estimates of the sovereign spread reaction to COVID-19 by splitting our full sample (from January 2, 2020, to May 29, 2020) into two subsamples divided at a reference date falling between March 5 and March 25. We include national stock markets and both country and time fixed effects to capture an unbiased measure of the time-varying impact of COVID-19 severity on euro area sovereign risk.

We show that despite the controversy generated by the "we are not here to close spreads"

declaration of Christine Lagarde (March 12),[3] the ECB actually stopped the spread of the pandemic-sparked crisis to the euro area sovereign debt markets on March 12, before the announcement of the PEPP and the conduct of market operations that occurred on March 18, leading to the reversal of sovereign spreads (Figure II.1.1). Unfortunately, it should be stressed that the methodology and the data used in this paper do not allow us to dissociate the effects of ECB monetary policy announcements from those of Christine Lagarde's statements at the press conference. Indeed, these two events took place simultaneously on March 12, and it is quite possible that Christine Lagarde's statement substantially canceled out the effects of the ECB announcements.[4] Nevertheless, our study allows us to identify the effectiveness of ECB communication since the announcements on March 12 were not accompanied by any major market operations.[5] In fact, the ECB's balance sheet expansion in reaction to the COVID-19 pandemic outbreak started the week after, on March 18, through substantial LTROs of €109.1305 billion, while the PEPP actually began on March 24.

At the start of the pandemic outbreak, the sovereign spread reaction to COVID-19 was increasing in the time horizon: the occurrence of 10 new cases per million people was accompanied by an immediate spread increase of 0.03 percentage points (ppt), which lasted 5 days for a total increase of almost 0.35 ppt. This explosive pattern is a hallmark of financial market turmoil in times of sovereign debt crises. Thus, we support the view that the ECB's unprecedented monetary policy responses to the COVID-19 pandemic were very effective in disrupting the explosive path of sovereign default risk within eurozone countries.[6] Indeed, our estimates indicate that without these interventions, sovereign debt rates would have risen to 4.2% in France, 12.5% in Spain, and 19.5% in Italy by March 18, which would have undoubtedly raised the question of debt sustainability in these countries and potentially led to a sovereign debt

[3]Christine Lagarde walked back this spreads comment by stating in a CNBC interview after the press conference, "I am fully committed to avoid any fragmentation in a difficult moment for the euro area. High spreads due to the coronavirus impair the transmission of monetary policy. We will use the flexibility embedded in the asset purchase programme, including within the public sector purchase programme. The package approved today can be used flexibly to avoid dislocations in bond markets, and we are ready to use the necessary determination and strength."

[4]Our daily data do not allow us to identify the specific effects of each event, and our conclusions should be interpreted as the global effect of all March 12 announcements. Further work should be carried out in the future using intradaily data to dissociate the effects of the different announcements on the markets, taking into account the television interview of Ms. Lagarde on CNBC.

[5]We are conscious of the above-described dramatic consequences of the March 12 statement on that day, in particular for Italian financial markets. We consider that despite this crash, this ECB intervention could have stopped the transmission of the pandemic outbreak to sovereign spreads and stock indices.

[6]The ECB was not the only European institution involved in the management of the crisis. However, as explained in Section II.2, its interventions were earlier than those of other bodies such as the European Commission and the European Council.

crisis.

Our study provides empirical evidence for the theoretical framework developed in Arellano et al. (2020) that clarifies the link between the ongoing COVID-19 pandemic and the increasing probability of sovereign debt default in emerging economies. Introducing a standard epidemiological methodology into a sovereign default model, the authors argue that lockdowns imposed by governments in reaction to the pandemic-induced health crisis save lives but are costly in terms of output and unemployment. They show how fiscal transfers engaged by governments to smooth consumption are constrained by borrowing capacity and default risk, which, in turn, increases the cost of lockdown. Hence, according to their model, the more severe the pandemic, the higher the risk of default on sovereign debt. This argument holds for the euro area as well. Indeed, ECB (2020a) indicates that the outbreak of the crisis led to an immediate increase in direct costs, mainly to address the public health consequences, but that from a macroeconomic perspective, much of the impact relates to the containment measures, which place a severe economic burden on firms, workers and households, and the packages of fiscal measures implemented in all euro area countries. As a result, the general government budget deficit in the euro area was projected to increase significantly in 2020 to 8% of GDP, compared with 0.6% in 2019. The risk of transmission to the banking sector through a worsening of bank balance sheets was emphasized early by Schularick and Steffen (2020) and analyzed in Couppey-Soubeyran et al. (2020), among others. In a recent publication, ECB (2020b) warns that banks in some countries have indeed increased their domestic sovereign debt holdings, triggering concerns that the sovereign-bank nexus could re-emerge in the euro area.

Our paper also supplements recent empirical works on the drivers of euro area sovereign risk during the COVID-19 crisis. Among them, Delatte and Guillaume (2020) highlight the heterogeneous effects of European policies on sovereign spreads: while the announcement of the PEPP reduced spreads in the euro area, the contrary was true for the financial assistance announced by the European Council. In regard to the direct impact of the COVID-19 crisis, they report a nonlinear relationship between spreads and the logarithm of the number of deaths per 100,000 people but do not consider the variation in the number of cases and deaths, as we do. Augustin et al. (2020) and Klose and Tillmann (2021) are closer to our setup since they consider the daily percentage change in COVID-19 cases. Augustin et al. (2020) use a large international panel of developed countries (including European countries) and also report results for a set of U.S. states. They show that countries' sovereign risk reacts positively and significantly to

the pandemic outbreak and that the strength of this reaction is conditional on initial fiscal conditions. Klose and Tillmann (2021) consider both sovereign and equity markets in Europe and conclude that monetary policy has been more effective in closing spreads. Finally, Andries et al. (2020) measure the intensity of the pandemic as the day when the number of cases and deaths reaches a threshold and do not consider the daily change, as we do. They study how the intensity of the pandemic and policy measures explain the cumulative abnormal returns of sovereign Credit Default Swap (CDS) spreads.

Our contribution with respect to these references is as follows. First, we go further by dealing with the dynamic response of sovereign bond spreads to the COVID-19 pandemic outbreak in the euro area. Our results demonstrate that these dynamics are a key feature of COVID-induced sovereign risk, which is cumulative over days. Focusing on the sensitivity of spreads to COVID-19 news at the time of impact leads to a sharp underestimation of the severity of the issue. Second, by running a split sample analysis, we can identify when this sensitivity was broken and interpret the results as being in line with the calendar of policy announcements. Third, we apply our empirical procedure to the stock market to provide additional evidence on the evolution of the nexus between the ongoing pandemic and financial markets. Fourth, we assess possible spillovers from the spread of the pandemic in Italy that may have been at work during the COVID crisis. Fifth, we provide a counterfactual analysis by simulating the path of sovereign bond spreads that would have occurred without this change in the sensitivity of bond spreads to the COVID-19 crisis.

Related literature. This paper is part of the burgeoning literature on the macroeconomic effects of the COVID-19 crisis and policy responses to the pandemic outbreak, as studied in Guerrieri et al. (2020), for instance. Atkeson (2020) and Eichenbaum et al. (2020) investigate the economic impact of the spread of the pandemic using a simple SIR model.[7] In the latter, the severity of the pandemic is measured by the number of new deaths. This proxy has been found to strongly affect macroeconomic aggregates such as GDP or consumption and rates of return on stocks and government bills (Barro et al., 2020, Jordà et al., 2020b).

This paper also contributes to the extensive strand of literature using panel regression to estimate the determinants of long-term government yields and sovereign bond spreads in

[7]SIR models are widely used in epidemiology and consist of studying the transmission of infectious diseases through a population (SIR stands for three population categories: S=number of susceptible, I=number of infectious and R=number of recovered–or deceased–individuals).

European Monetary Union (EMU) countries, including Manganelli and Wolswijk (2009), Favero and Missale (2012), Aizenman et al. (2013), Georgoutsos and Migiakis (2013), Costantini et al. (2014), and Afonso et al. (2015b). Furthermore, Delatte et al. (2017) use a panel smooth threshold regression model and show that EMU sovereign risk pricing is state dependent. Other papers assess a time-varying relationship between EMU sovereign spreads and their fundamental determinants such as liquidity or risk factors, as in Afonso et al. (2015a), Afonso et al. (2018) or Afonso and Jalles (2019). The latter papers also highlight the role of ECB monetary policies as an important driver of sovereign bond spreads.[8]

The methodology used in this paper is based on the growing literature employing local projection methods developed by Jordà (2005). Local projection methods have been employed to conduct inference on dynamic impulse responses to address several issues in applied macroeconomics.[9] For instance, Ramey and Zubairy (2018), Auerbach and Gorodnichenko (2013), Born et al. (2019) and Cloyne et al. (2020) use state-dependent local projections to examine fiscal policy issues. Meanwhile, state-dependent aspects of monetary policy transmission are also studied in Tenreyro and Thwaites (2016).[10]

Structure of the paper. The rest of the paper is organized as follows. Section II.2 presents the data and the chronology of events related to COVID-induced sovereign risk in the euro area. Section II.3 explains the methodology used in this paper. Section II.4 is devoted to the results. Section II.5 is dedicated to several robustness checks. Section II.6 proposes an extension of our baseline model, including an application to the stock market in the euro area, a cross-country analysis, and a counterfactual exercise. Section II.7 concludes.

[8] Asset purchase and especially bond-buying programs have directly contributed to lowering bond spreads within the euro area, as discussed by Falagiarda and Reitz (2015), Kilponen et al. (2015), Szczerbowicz (2015), Eser and Schwaab (2016), Fratzscher et al. (2016), Gibson et al. (2016), Ghysels et al. (2017), Jäger and Grigoriadis (2017), De Pooter et al. (2018), Krishnamurthy et al. (2018), and Pacicco et al. (2019). Casiraghi et al. (2016) focus on the impact of the ECB's unconventional monetary policy on Italian government bond yields, Trebesch and Zettelmeyer (2018) emphasize the Greek case, and Lhuissier and Nguyen (2021) uses an external instrument to estimate the impact of ECB's APP on intra-euro area sovereign spreads.

[9] See the series of papers using local projections to assess the impact of credit expansion on business cycle fluctuations (Jordà et al., 2013), equity and housing price bubbles on financial crisis risks (Jordà et al., 2015, Jordà et al., 2016), austerity on macroeconomic performance (Jordà and Taylor, 2016), and monetary interventions on exchange rates and capital flows (Jordà et al., 2020a). Recently, local projections have been introduced for micro data as an alternative to vector autoregressive (VAR) models to avoid any distortion in impulse responses in nonlinear frameworks (see Favara and Imbs, 2015, Crouzet and Mehrotra, 2020 and Cezar et al., 2020).

[10] Similarly, local projection methods have been applied in other monetary analyses to investigate the yield impact of unconventional monetary policy (Swanson, 2021) or uncertainty (Castelnuovo, 2019, Tillmann, 2020).

II.2 Data sources and chronology

This section presents the sources of data and summarizes the main events of the COVID-19 outbreak in Europe. The data are given at a business daily frequency (5 days per week) and run from January 2, 2020, to May 29, 2020. They come from different sources.

European sovereign debt and stock markets. Long-term interest rates and stock indices are from Datastream via Thomson Reuters Eikon.[11] Sovereign bond spreads are constructed as the yield differentials between bonds issued by each euro area government and German bonds at a given maturity. The 10-year spread is our benchmark, and we consider the 2-year spread for robustness analysis. We restrict the sample to 15 euro area countries for which 10-year spreads and stock market indices are available on a daily basis for this period: Austria, Belgium, Cyprus, Finland, France, Greece, Ireland, Italy, Lithuania, Malta, Netherlands, Portugal, Slovakia, Slovenia, and Spain.

Spreads are plotted for each country in Appendix II.B. The pattern highlighted above for Italy in Figure II.1.1 is representative of most European countries, which experienced a sharp increase in their government spreads when the pandemic spread to Europe.

Stock market indices are also plotted in Appendix II.B. The figures show that all the countries in our sample experienced an enormous drop in their main national stock market index. This crash occurred at the same time that euro area government spreads started to skyrocket, stressing how severe financial markets in the euro area interpreted the economic impact of the pandemic to be.

Health statistics on the COVID-19 pandemic in Europe. COVID-19 data are extracted from the European Centre for Disease Prevention and Control (ECDC), an agency of the European Union aimed at strengthening defenses against infectious diseases.[12] Since the beginning of the pandemic, the ECDC has been collecting the number of COVID-19 cases and deaths on a daily basis based on reports from health authorities worldwide. To be consistent

[11] The Reuters identification codes (RICs) used to construct the dataset are listed in Appendix II.A.

[12] The complete COVID-19 dataset is updated daily by "Our World in Data" and is available in a CSV file on the OWID webpage. We downloaded the dataset on May 30, 2020, and do not consider updated versions since we are interested in the market reaction to the numbers of cases and deaths publicly available in real time during the pandemic outbreak and not in the revised data reported afterwards. We have checked with the ECDC Epidemic Intelligence team and the Head of Data of OWID that no major data retro-correction has been recorded from January to May 2020 to make sure that our results are not affected by any COVID data revision.

with our financial series database, we discard observations for weekends to obtain a business week database of COVID-19 cases and deaths. The main implication of this transformation is that (business) daily variations in the number of cases and deaths on Monday are computed with respect to the previous Friday and not to Saturday or Sunday, when financial markets are closed. Total cases and deaths are plotted for each country of our sample in Appendix II.B.

Our database starts just after the report by the Wuhan Municipal Health Commission in Wuhan City of a cluster of 27 pneumonia cases (December 31).[13] The pandemic then spread to Europe. The first European case was reported in France on January 24, but Italy was the most heavily affected country in Europe. The Italian authorities reported clusters in Lombardy on February 22 and implemented lockdown measures on March 8 at the regional level, which were rapidly extended to the national level on March 11. The Director General of the WHO declared COVID-19 a global pandemic on March 11 and said that Europe had become the epicenter of the pandemic on March 13. All countries of the European Union were affected by March 25, according to the ECDC.

ECB interventions. Central banks' response to the COVID-19 crisis was quick and massive, as documented by Cavallino et al. (2020) and Delatte and Guillaume (2020). Major central banks across advanced economies launched new asset purchases and lending operations to face the pandemic outbreak. Among them, the ECB reacted strongly to the COVID-induced economic downturn by making substantial decisions during March 2020.[14] On March 12, the Governing Council decided on a package of policy measures providing *(i)* additional longer-term refinancing operations (LTROs) to provide liquidity for the euro area financial system until June 2020, *(ii)* more favorable terms for the third series of targeted longer-term refinancing operations (TLTRO III) from June 2020 to June 2021 to support bank lending to small and medium-sized enterprises affected by the spread of the virus, and *(iii)* a temporary envelope of additional net asset purchases of €120 billion until the end of 2020 to support financing conditions under the existing Asset Purchase Programme (APP). On March 18, the ECB announced the launch of a new temporary asset purchase program called the Pandemic Emergency Purchase Programme (PEPP) consisting of assets purchases of €750 billion, including assets eligible for the APP, until the end of 2020.[15]

[13] For additional information, see the ECDC timeline and WHO timeline.

[14] https://www.ecb.europa.eu/press/pr/html/index.en.html.

[15] Simultaneously, the ECB stated on March 18, " The Governing Council was unanimous in its analysis that in addition to the measures it decided on 12 March 2020, the ECB will continue to monitor closely the

Figure II.2.2 shows the growth rate of ECB total assets (in percentage, at weekly frequency) and the respective contribution of the two main open market operations: "LTROs" and "Securities held for monetary policy purposes". The category "Others" includes all other assets on the ECB balance sheet. Unfortunately, these series are not available on a daily basis and cannot be decomposed into national shares.[16] However, they provide several helpful insights for interpreting our results.

ECB interventions can be classified as only communication on March 12 and as a mix of communication and market operations on March 18. Indeed, the ECB balance sheet expansion started the week that ended on March 20 and not on March 13. Thus, the ECB intervention on March 12 can be considered a communication policy only, without significant market operations. This is not the case for the ECB press conference on March 18. On this date, the ECB provided exceptional LTROs of €109.1305 billion for 98 days,[17] which implies an enormous increase of 17.73% for LTROs in comparison with their level in the previous week. Considering the full balance sheet, this increase explains half of the 4.74% increase in total assets on March 20–with increases of 2.31% from LTROs, 0.36% from securities held for monetary policy purposes, and 2.05% from other assets.[18] Actually, the new PEPP was announced on March 18 by Christine Lagarde but was only effective from March 24.[19] As shown in Figure II.2.2, the rise in debt securities held for monetary policy purposes (which include the PEPP) was gradual and became predominant in the expansion of the ECB balance sheet only from April 2020. Thus, the ECB intervention on March 18 was a mix of communication (mainly on the PEPP) and market operations (through LTROs).

Additionally, it is important to mention that all European institutions were involved in managing the crisis.[20] On March 10, the members of the European Council and heads of European institutions, including the ECB's Christine Lagarde, held a video conference on COVID-19. They discussed how to coordinate European Union efforts to respond to the pandemic out-

consequences for the economy of the spreading coronavirus and that the ECB stands ready to adjust all of its measures, as appropriate, should this be needed to safeguard liquidity conditions in the banking system and to ensure the smooth transmission of its monetary policy in all jurisdictions."

[16]The ECB publishes a bimonthly breakdown of public sector securities under the PEPP.

[17]There was also an MRO of €1.4699 billion for 7 days this day; see the calendar of open market operations.

[18]This was mainly due to the change in the net position of the Eurosystem in foreign currency, as explained by the ECB (link).

[19]See the Q&A on PEPP. March 24 is the date of the publication of the ECB decision. In June 2020, monthly net purchases under the PEPP reached a maximum with an amount of €120,321 million, in comparison with €15,444 million in March 2020.

[20]See the "Timeline of EU action".

Figure II.2.2 – Growth of ECB balance sheet

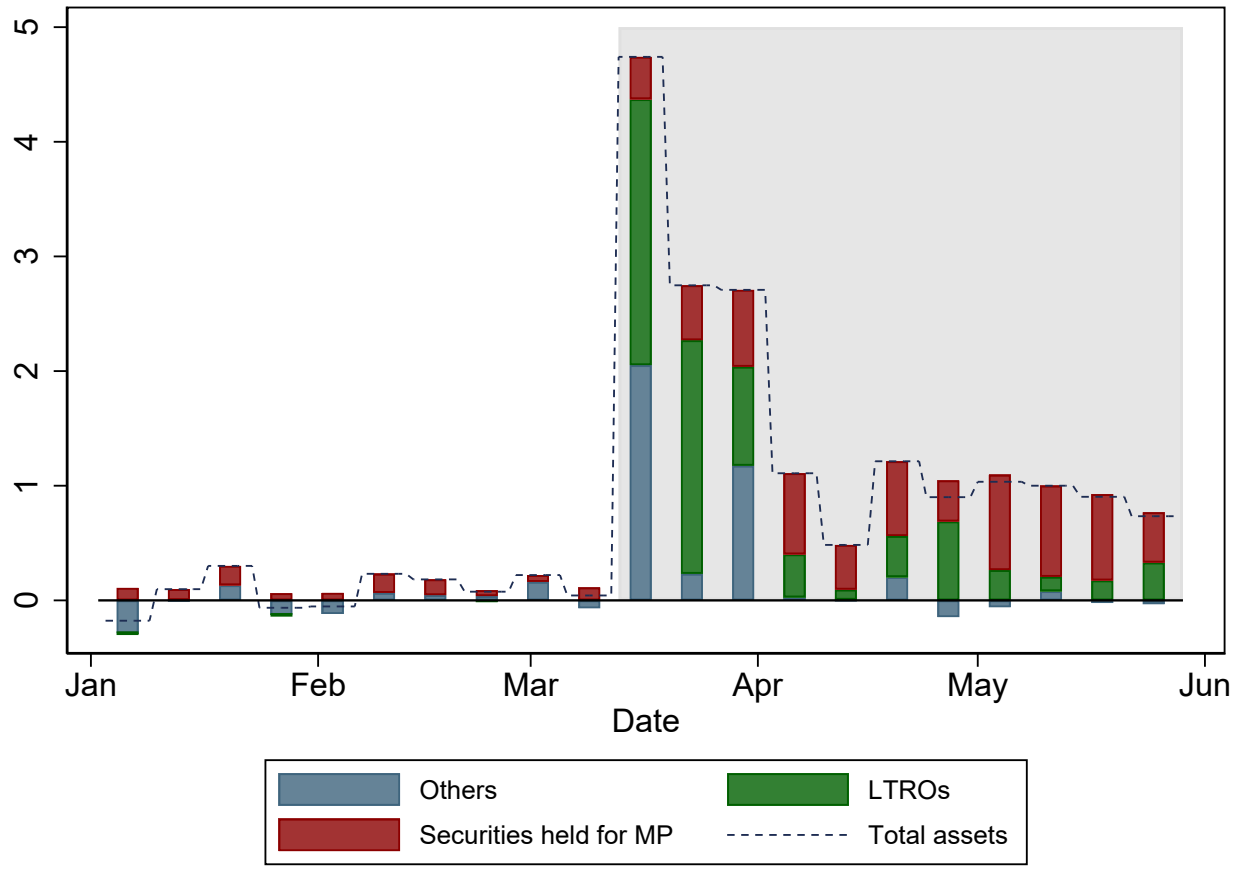

Note: The dashed line represents the growth of total assets/liabilities in percent. The bar chart depicts the contribution of "LTROs" (green bars), "Securities held for monetary policy purposes" (red bars) and "Others" (blue bars) to the growth of total assets in ppt. The category "Others" is computed as $Others = Total\ assets - (LTROs + Securities\ held\ for\ monetary\ policy\ purposes)$. The gray shaded area covers the period from March 16, 2020, onward. Source: ECB.

break.[21] We focus on the ECB interventions, which came earlier and were more commented on in terms of their effects on sovereign debt markets. For example, the activation of the general escape clause of the Stability and Growth Pact was proposed by the European Commission on March 20 and agreed upon by the ministers of finance of the member states of the EU on March 23, after the main ECB interventions.

The March 5-25 window. Based on the data and on the abovementioned events, we focus on the March 5-25 period to identify when and how the sovereign interest rate response to the spread of the COVID-19 pandemic changed. This choice is motivated by two considerations.

[21] Four priorities were identified at the end of the meeting: limiting the spread of the virus, providing medical equipment, promoting research (including vaccine research), and dealing with the socioeconomic consequences. For more details, see the dedicated meeting webpage.

First, March 5 fell one business week before the first ECB intervention (March 12), and March 25 fell one week after the ECB decision of March 18. Thus, the window is large enough to ensure that we do not miss any monetary policy effects in our analysis. Second, by March 5, only a few European countries had reported deaths (France, Italy, and Spain), while by March 25, only Latvia, Malta and Slovakia had not reported deaths from COVID-19. Thus, the window corresponds to the period of the generalization of the pandemic in Europe. In the remainder of this paper, we take as our benchmark the series of COVID-19 cases and not that of deaths. Since the number of confirmed cases leads the number of reported deaths, the series of COVID-19 cases provides more data for the estimation at the beginning of the sample–by March 5, only six countries had not reported cases, against fourteen that had not reported deaths.

II.3 Methodology

Our primary interest is in the dynamic response of government spreads to the outbreak of the COVID-19 pandemic. To obtain an estimate of the response, we rely on the local projection method following Jordà (2005). Considering the whole sample period, we estimate:

$$\Delta s_{i,t+h} = \alpha_{i,h} + \eta_{t,h} + \beta_h \Delta x_{i,t} + \mathbf{\Gamma}_h(L) s_{i,t-1} + \mathbf{\Theta}_h(L) z_{i,t} + \varepsilon_{i,t+h} \tag{II.1}$$

for country i and horizon $h = 0, 1, \ldots, H$ as of time t, where $\varepsilon_{i,t+h}$ is the error term. $\Delta s_{i,t+h} = s_{i,t+h} - s_{i,t-1}$ is the variation in the 10-year government bond spread at horizon h. $\Delta x_{i,t} = x_{i,t} - x_{i,t-1}$ is the daily change in the number of total COVID-19 cases in country i as of time t. We consider the change in the number of cases per 100,000 people. The main motivation for this choice is that the attention of observers has been focused on the number of daily new cases by population since the beginning of the pandemic, sometimes in absolute terms but never as a percentage of the number of total cases already reported, as illustrated by the very popular figures published and massively distributed by the *Financial Times*. However, we check the robustness of our results by considering the daily change in the number of deaths per million people due to COVID-19, the 3-day rolling average of new cases, new cases in absolute terms, the lagged values of new cases, and the growth rate of total cases as the independent variable. Additionally, other robustness checks involve separately adding the growth rate of total cases, the logarithm of the total number of cases, the first difference of new cases, or the lagged values

of new cases as control variables in the baseline specification. Tables and figures containing the results are given in Appendices II.D and II.E. The coefficient of interest β_h measures the variation in government spreads h days after the release of data on new COVID-19 cases. A series of regressions are estimated for each horizon h. Since the model is estimated on a business daily basis, we assume that a one-week horizon is sufficiently long to capture the path of the response coefficients β_h. Then, we set $H = 5$.

To obtain an accurate estimate of these coefficients, we use a two-way fixed effects framework and add a set of control variables as recommended by Herbst and Johannsen (2020).[22] First, country fixed effects $\alpha_{i,h}$ take into account the structural differences between countries. Second, time fixed effects $\eta_{t,h}$ absorb features that are common across all countries but change over time, including the global evolution of the COVID-19 pandemic. Third, the current value and the first four lags of the log of the stock index $z_{i,t}$ control for the state of the economy and the effects of other news that could have an impact on government spreads. $\mathbf{\Theta}_h(L)$ is a polynomial in the lag operator associated with the domestic stock markets, with $\mathbf{\Theta}_h(L) = \sum_{n=0}^{N} \theta_{h,n} L^n$, where N stands for the number of lags. Finally, it also includes the first four lags of the dependent variable to control for any serial correlation in the error term through the polynomial in the lag operator $\mathbf{\Gamma}_h(L)$, defined by $\mathbf{\Gamma}_h(L) = \sum_{n=0}^{N-1} \gamma_{h,n+1} L^n$. We set $N = 4$ as the number of lags.

The linear local projection method described above can be transformed into a state-dependent model. State-dependent local projection methods have been mainly applied to fiscal policy issues by Auerbach and Gorodnichenko (2013) and Ramey and Zubairy (2018). For the linear model, we estimate a series of regressions at each horizon h:

$$\begin{aligned} \Delta s_{i,t+h} = \alpha_{i,h} + \eta_{t,h} + D_{t,\bar{t}}\Big[\beta_{a,h}\Delta x_{i,t} + \mathbf{\Gamma}_{a,h}(L)s_{i,t-1} + \mathbf{\Theta}_{a,h}(L)z_{i,t}\Big] \\ +(1 - D_{t,\bar{t}})\Big[\beta_{b,h}\Delta x_{i,t} + \mathbf{\Gamma}_{b,h}(L)s_{i,t-1} + \mathbf{\Theta}_{b,h}(L)z_{i,t}\Big] + \varepsilon_{i,t+h} \end{aligned} \tag{II.2}$$

where $D_{t,\bar{t}}$ is a dummy variable that takes 0 before a given date $\bar{t}$, that is, when $t < \bar{t}$, and 1 thereafter, when $t \geq \bar{t}$. Equation (II.2) captures the dynamic response of government bond spreads to new COVID-19 cases conditional on the ECB intervention through the coefficients $\beta_{a,h}$ and $\beta_{b,h}$. It is worth emphasizing that this response is different from the direct effect of a policy intervention on sovereign rates, which is gauged by the time fixed effect $\eta_{t,h}$. Since we are

[22] Moreover, Herbst and Johannsen (2020) also suggest using large sample sizes to avoid bias in impulse responses estimated by local projections. Our setup is in line with this recommendation since the size of our subsample exceeds 500 observations.

mostly interested in the $\beta_{a,h}$ and $\beta_{b,h}$ coefficients, responses in period $t+h$ to new information on the severity of the COVID-19 situation at time t, conditional on the state of the economy, are computed as in Born et al. (2019) by the following expression:

$$\left.\frac{\partial \Delta s_{i,t+h}}{\partial \Delta x_{i,t}}\right|_{D_{t,\bar{t}}} = D_{t,\bar{t}} \times \beta_{a,h} + (1 - D_{t,\bar{t}}) \times \beta_{b,h} \tag{II.3}$$

which is a linear combination of impulse response coefficients. As our aim is to investigate possible nonlinearities in the response coefficient β_h according to the state of the economy during the March 5-25 window (see Section II.2), event dummies are constructed according to $\bar{t} \in \{3/5, ..., 3/25\}$.

II.4 Results

This section presents our main results to identify when the COVID-induced rise in sovereign spreads was halted.

Results for the full sample. Let us start with equation (II.1) for the full sample of observations. Figure II.4.3 shows the path of the estimated coefficient β_h and the 95% confidence interval, and Table II.C.1 contains the estimation results. The response coefficient is slightly negative at all horizons. However, the magnitude of the effect is very small: the change in the interest rate spread is very close to zero at all horizons and reaches -0.002 ppt at horizon $h = 3$ for 10 new cases per million people. As shown by the confidence interval, the impact of new cases is not significantly different from zero when we consider the full sample. As explained above, this does not mean that policy interventions have no direct effects on sovereign interest rates[23] but that these rates do not react significantly to the occurrence of new COVID-19 cases. What happens, however, when the sample is split? In particular, we draw attention to the period before ECB interventions.

The difference between the beginning and the end of the March 5-25 window. Figure II.4.4 compares the response coefficients $\beta_{b,h}$ and $\beta_{a,h}$ of 10-year government spreads to new COVID-19 cases before and after March 5 ($\bar{t} = 3/5$, the first date of our window). For the period before March 5, without the ECB intervention, the response coefficient $\beta_{b,h}$ follows

[23] Indeed, as indicated in Figure II.C.1, the time fixed effects $\eta_{t,h}$ are significantly negative around key ECB intervention dates, namely, on March 12 and March 18.

Figure II.4.3 – Impulse responses of 10-year government bond spreads to new COVID-19 cases in the euro area

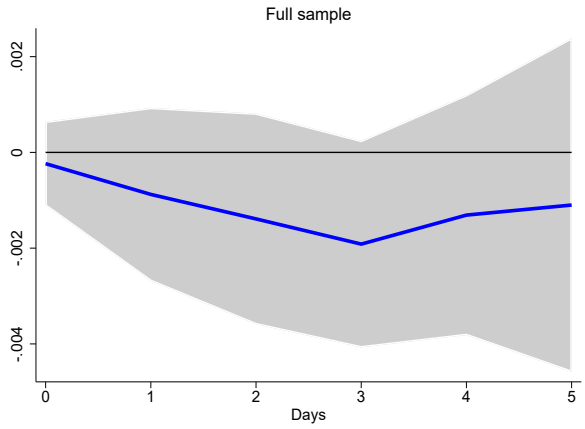

Note: Impulse responses represent the β_h coefficient from equation (II.1), and the gray shaded area represents the 95% confidence interval.

an explosive path. Spreads on 10-year government bonds increase by more than 0.021 ppt for 10 new cases per million people on impact. This rise significantly accelerates to reach 0.240 ppt up to 5 business days. This explosive path severely threatened debt sustainability in the euro area as the pandemic spread. On March 12, Italy reported 38.256 new cases per million residents and Spain 24.66 and France 7.614 new cases. This $\beta_{b,5}$ estimate considering only this date would imply a cumulative increase in the spread over 5 days of 0.92 ppt in Italy, 0.59 ppt in Spain and 0.18 ppt in France for 10 new cases per million people. After March 5, the estimates for this sample including the ECB interventions show a response coefficient $\beta_{a,h}$ that is very close to zero and not significant.

Figure II.4.5 also compares the response coefficients $\beta_{b,h}$ and $\beta_{a,h}$ of bond spreads to new COVID confirmed cases before and after March 25 ($\bar{t} = 3/25$, the last date of our window). The response coefficient $\beta_{b,h}$ on impact ($h = 0$) is smaller (0.001 ppt against 0.021 for $\bar{t} = 3/5$) and still not significantly different from zero. However, in this case, the coefficient no longer follows an explosive path: the response of the interest rate spreads to new cases is even below zero at a 3-day horizon and becomes slightly positive up to a 5-day horizon (reaching 0.002 instead of 0.240 for $\bar{t} = 3/5$). Note that the $\beta_{b,h}$ coefficient is not significant at any horizon. Similarly, the response coefficient $\beta_{a,h}$ is muted when we consider the subsample after March 25. In the latter case, government bond spreads do not react to new cases at all. These results indicate that a major change took place in the euro area sovereign debt market between March 5 and March 25. To identify when it occurred, we now consider various split dates $\bar{t}$ falling

Figure II.4.4 – Impulse responses of 10-year government bond spreads to new COVID-19 cases in the euro area

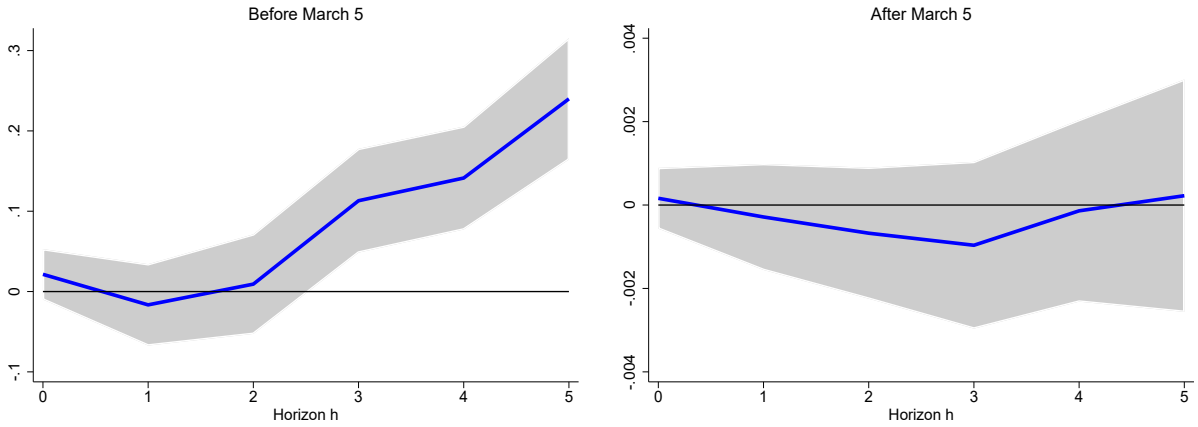

Note: Impulse responses are computed following equation (II.2). The left panel shows the coefficient $\beta_{b,h}$ (before the split date), whereas the right panel shows the coefficient $\beta_{a,h}$ (after the split date). The gray shaded area represents the 95% confidence interval.

within this time interval.

Time-varying split dates for the March 5-25 window. Figure II.4.6 depicts estimated values of the coefficient $\beta_{b,h}$ at each horizon h based on various split dates $\bar{t} \in \{3/5, ..., 3/25\}$. At horizon $h = 0$, the coefficient is positive and significantly different from zero up to March 9. After this date, $\beta_{b,0}$ is not significantly different from zero when the estimation sample includes the announcement of the ECB on March 12 and then decreases continuously with $\bar{t}$. This pattern is even more striking at horizons between $h = 2$ and $h = 5$, with $\beta_{b,h}$ first sharply falling around $\bar{t} = 3/9$ and remaining positive afterwards but not significantly different from zero and falling again around $\bar{t} = 3/18$, after which the coefficients are very close to zero.

Figure II.4.7 summarizes the three regimes of the response coefficients: highly significant and explosive (in red, for $\bar{t} = 3/5, ..., 3/9$), low and not strongly significant (in blue, for $\bar{t} = 3/10, ..., 3/16$), and close to zero and not significant at all (in green, for $\bar{t} = 3/17, ..., 3/25$). When we look at the calendar of (monetary) policy interventions in March 2020 in the euro area, these coefficient regimes are identified according to break dates that coincide with dates around the first ECB announcements. Moreover, it seems that the ECB intervention on March 12 (prior to March 18) strongly contributed to lower COVID-induced sovereign risk in EMU countries and broke the sovereign risk-pandemic outbreak dynamics within the euro area. To identify more precisely when the ECB closed spreads, we implement a statistical test for structural breaks.

Figure II.4.5 – Impulse responses of 10-year government bond spreads to new COVID-19 cases in the euro area

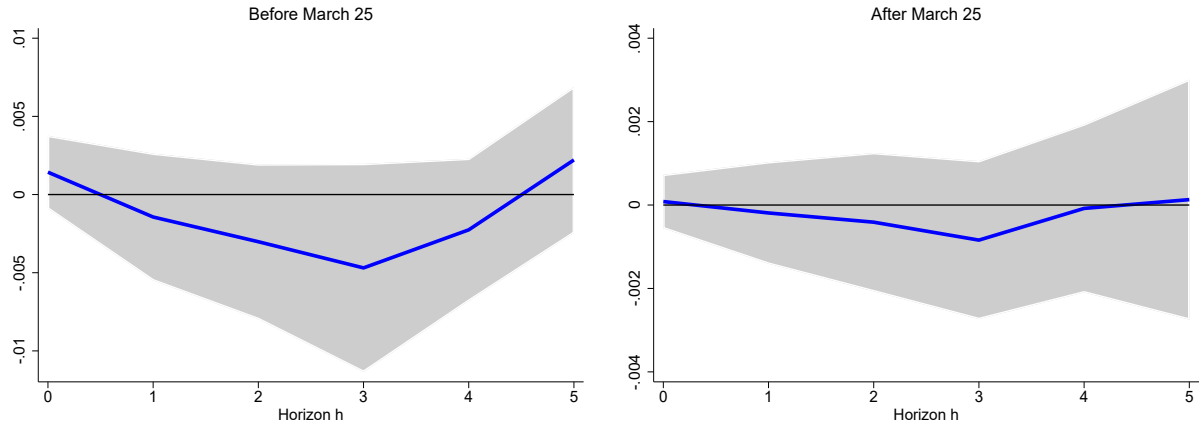

Note: Impulse responses are computed following equation (II.2). The left panel shows the coefficient $\beta_{b,h}$ (before the split date), whereas the right panel shows the coefficient $\beta_{a,h}$ (after the split date). The gray shaded area represents the 95% confidence interval.

Testing for structural breaks in response coefficients. Table II.4.1 shows the results of a Chow test (Chow, 1960) to confirm the existence of structural breaks in the estimated response coefficients. It presents p-values from the Chow test at horizons ranging from $h = 0$ to $h = 5$ and for break dates $\bar{t}$ between March 5 and March 25. We select March 9 as the structural break date on which the $\beta_{a,h}$ and $\beta_{b,h}$ coefficients are no longer statistically equal at each horizon simultaneously. Indeed, the p-value of the test implemented on the coefficients $\beta_{a,h}$ and $\beta_{b,h}$ is lower than 5% at all horizons on March 9 only, which is not the case for any other dates. In other words, the results suggest rejecting the null hypothesis that the $\beta_{b,h}$ and $\beta_{a,h}$ coefficients are equivalent at the 5% level of significance after March 9. Figure II.4.8 shows the path of the response coefficients associated with this reference date, and Table II.C.2 contains the estimation results.

The Chow test results confirm the existence of a highly significant break in the dynamic response of sovereign risk to the COVID-19 outbreak around the date of the first ECB intervention on March 12. To link this date with the timeline of political events, it should be emphasized that an impact response at a 3-day horizon on March 9 measures the effect of new cases reported on March 9 on spreads 3 days later (i.e., March 12). Moreover, the March 10 video conference between the members of the European Council and heads of European institutions, including the ECB (see Section II.2), may have been perceived by financial markets as a positive signal of future ECB decisions scheduled on March 12. Hence, it could explain our

Figure II.4.6 – Evolution of impulse response coefficients by horizon

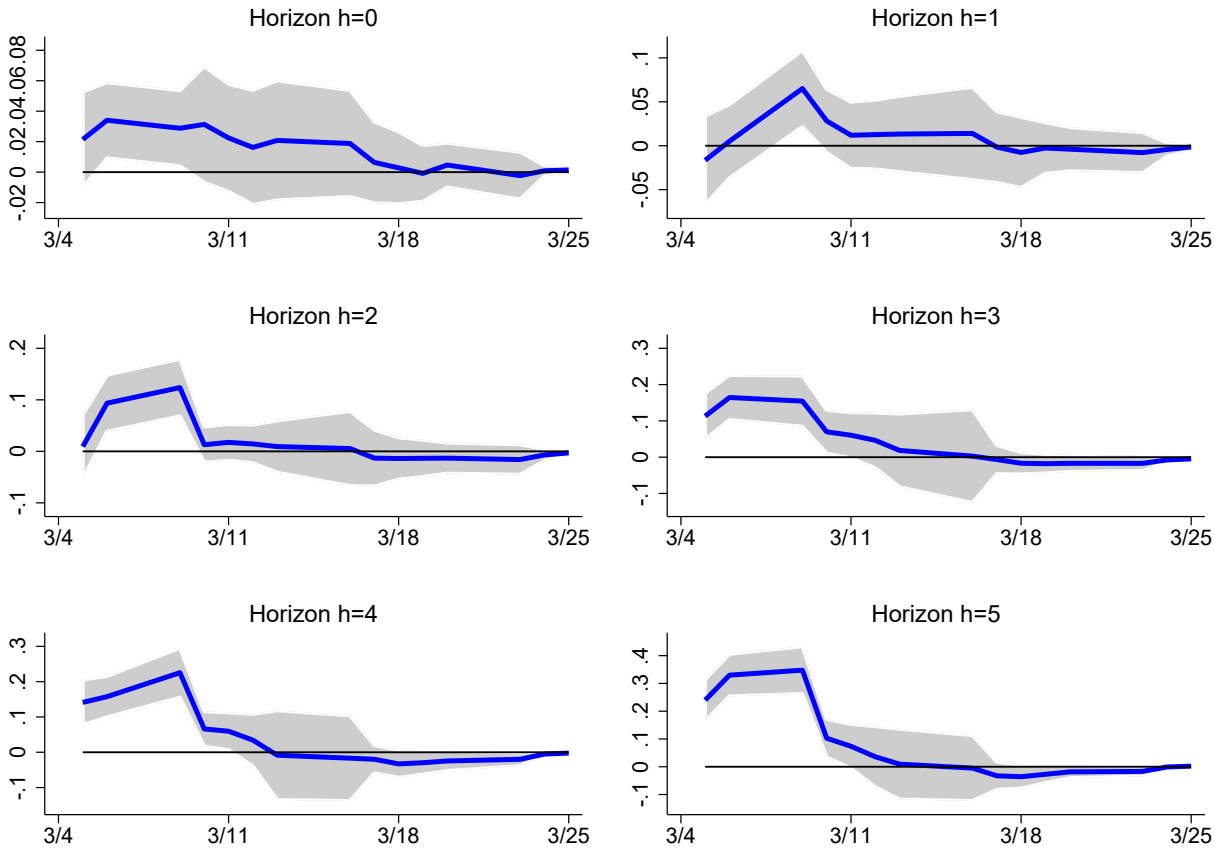

Note: Impulse responses are computed following equation (II.2). Each panel shows the impulse response coefficients $\beta_{b,h}$ estimated before split dates $\bar{t} \in \{3/5, ..., 3/25\}$ at different horizons. The gray shaded area represents the 95% confidence interval.

key finding of a break date on March 9 through market expectations.[24] Overall, our results indicate that the decision made by the ECB on March 12 was decisive in closing the spread of the COVID-19-induced financial crisis to euro area sovereign bonds.

Although we believe that ECB interventions–particularly those on March 12–were effective in controlling the COVID-induced sovereign risk in the euro area, we are fully aware that the break around March 12 may be the consequence of the generalization of the pandemic and not of ECB announcements. From this point of view, the strong relationship identified between COVID-19 cases and sovereign spreads may have been relevant only at the beginning of the pandemic, allowing financial markets to integrate the risk associated with the occurrence of a pandemic before losing their sensitivity to the severity of the health crisis. Thus, it is crucial

[24]This point is discussed in detail in Section II.6.1. Note also that the meeting held on March 12 was scheduled, which was not the case for the meeting of March 18 (see ECB's March 2020 calendar).

Figure II.4.7 – Impulse responses of 10-year government bond spreads to new COVID-19 cases in the euro area

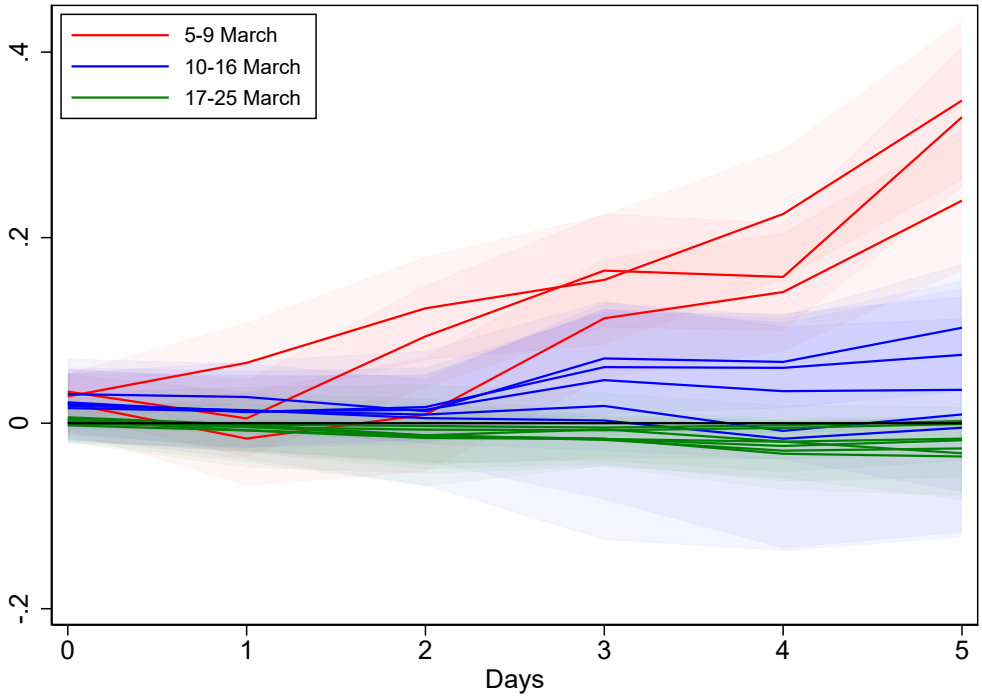

Note: Impulse responses are computed following equation (II.2). The impulse response coefficients $\beta_{b,h}$ are estimated before the following split dates: $\bar{t} \in \{3/5, ..., 3/9\}$ in red, $\bar{t} \in \{3/10, ..., 3/16\}$ in blue, and $\bar{t} \in \{3/17, ..., 3/25\}$ in green. The shaded area represents the 95% confidence interval for each coefficient.

to check the robustness of our results to the modeling of the pandemic outbreak.

II.5 Robustness

This section is dedicated to alternative specifications of our model to test the robustness of our results. First, alternative measures of pandemic dynamics are introduced as controls in the specification to differently capture the evolution of the pandemic. Then, the sample countries are divided into two subgroups according to their debt-to-GDP level to assess the role of initial fiscal conditions in COVID-induced sovereign risk in the euro area. Additional robustness tests are provided in Appendix II.D, where our baseline model is specified with alternative dependent and independent variables.

Figure II.4.8 – Impulse responses of 10-year government bond spreads to new COVID-19 cases in the euro area

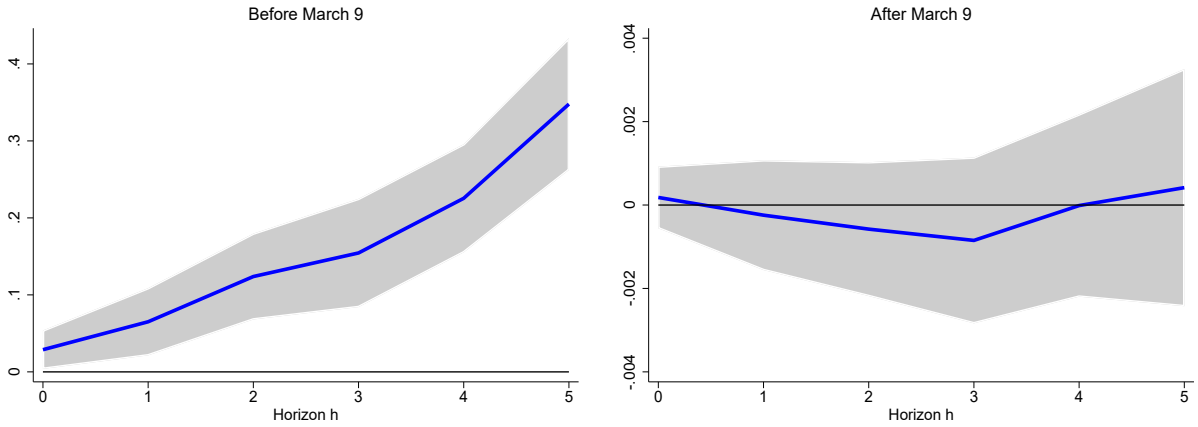

Note: Impulse responses are computed following equation (II.2). The left panel shows the coefficient $\beta_{b,h}$ (before the split date), whereas the right panel shows the coefficient $\beta_{a,h}$ (after the split date). The gray shaded area represents the 95% confidence interval.

II.5.1 Controlling for the shape of the pandemic

Our baseline regression (II.2) is extended to include additional controls. Using the reference date, we investigate whether these controls may alter our estimate of $\beta_{a,h}$ and $\beta_{b,h}$ for the reference date $\bar{t}$. The specification now takes the following form:

$$\begin{aligned}\Delta s_{i,t+h} = \alpha_{i,h} + \eta_{t,h} + D_{t,\bar{t}}\Big[\beta_{a,h}\Delta x_{i,t} + \mathbf{\Psi}_{a,h}(L)X_{i,t} + \mathbf{\Gamma}_{a,h}(L)s_{i,t-1} + \mathbf{\Theta}_{a,h}(L)z_{i,t}\Big] \\ +(1 - D_{t,\bar{t}})\Big[\beta_{b,h}\Delta x_{i,t} + \mathbf{\Psi}_{b,h}(L)X_{i,t} + \mathbf{\Gamma}_{b,h}(L)s_{i,t-1} + \mathbf{\Theta}_{b,h}(L)z_{i,t}\Big] + \varepsilon_{i,t+h}\end{aligned} \tag{II.4}$$

where $\mathbf{\Psi}_{\bullet,h}(L)$ is a polynomial in the lag operator associated with the control variable $X_{i,t}$ defined hereafter. The results are reported in regression tables in Appendix II.E.[25] The symbol $\bullet$ indicates both before (b) and after (a) for estimated coefficients.

Growth rate of total cases. First, we control for the growth rate of the number of total cases. The growth rate of total cases is measured as the first difference (daily change) of the logarithm of the number of total cases. Hence, $X_{i,t} = \Delta \log x_{i,t}$. Moreover, since no lagged value of controls is included in the estimate, we set $\mathbf{\Psi}_{\bullet,h}(L) = \sum_{n=0}^{N} \psi_{\bullet,h,n} L^n$, with $N = 0$. Table II.E.1 shows that including the growth rate of the number of total cases in the model does not alter our baseline results. The $\psi_{b,h,0}$ coefficient is close to zero and not significant at all over

[25] March 9 is chosen as the break date in all the regression tables to allow for comparison with our baseline results. Figures depicting the impulse response functions and Chow test tables are available upon request.

Table II.4.1 – Chow test (p-values)

	Horizon					
	h=0	h=1	h=2	h=3	h=4	h=5
March 5	0.17	0.50	0.74	0.00	0.00	0.00
March 6	0.01	0.79	0.00	0.00	0.00	0.00
March 9	0.03	0.01	0.00	0.00	0.00	0.00
March 10	0.10	0.11	0.42	0.03	0.01	0.01
March 11	0.20	0.50	0.30	0.06	0.03	0.07
March 12	0.37	0.49	0.40	0.21	0.34	0.49
March 13	0.28	0.51	0.68	0.68	0.90	0.87
March 16	0.27	0.56	0.84	0.94	0.78	0.94
March 17	0.61	0.97	0.65	0.79	0.31	0.19
March 18	0.77	0.73	0.51	0.29	0.09	0.09
March 19	0.99	0.90	0.45	0.18	0.08	0.08
March 20	0.50	0.75	0.36	0.15	0.08	0.09
March 23	0.75	0.48	0.26	0.10	0.04	0.06
March 24	0.62	0.28	0.22	0.06	0.10	0.72
March 25	0.22	0.53	0.30	0.29	0.41	0.44

Note: The table displays p-values of Chow statistics from the test.

the horizon.

Logarithm of total cases. We also control for the logarithm of the number of total cases to take into account the state of the ongoing pandemic in its effect on sovereign bond spreads. Hence, $X_{i,t} = \log x_{i,t}$. As in the previous case, we set $\mathbf{\Psi}_{\bullet,h}(L) = \sum_{n=0}^{N} \psi_{\bullet,h,n} L^n$, with $N = 0$. Table II.E.2 shows that including the log of total cases by population in the model does not alter our baseline results, even if the $\psi_{b,h,0}$ coefficient is significantly positive up to horizon $h = 4$.

Lagged values of new cases. Next, we control for lagged values of new COVID cases, and we estimate equation (II.4) setting $\mathbf{\Psi}_{\bullet,h}(L) = \sum_{n=0}^{N-1} \psi_{\bullet,h,n+1} L^n$, with $N = 2$. The control variable is expressed as $X_{i,t} = \Delta x_{i,t-1}$, where $\Delta x_{i,t-1} = x_{i,t-1} - x_{i,t-2}$. The lagged values of new cases are measured as the first and second lags of new cases per 100,000 people. Table II.E.3 reports the results. The $\beta_{b,h}$ coefficient is not as strong and statistically significant as in our baseline estimates. Note that both coefficients on the first and second lagged values of new cases, $\psi_{b,h,1}$ and $\psi_{b,h,2}$, respectively, are often significant over the horizon. This is especially true for the $\psi_{b,h,2}$ coefficient. Thus, we capture the persistent effect of new confirmed COVID cases on government bond spreads.

First difference of new cases. Finally, we use the "variation of the variation" of new COVID-19 cases to account for the stretched S-shaped dynamics of the pandemic. In this case, $X_{i,t} = \Delta x_{i,t} - \Delta x_{i,t-1}$, which is positive in the first phase of the pandemic outbreak and negative at the end. The new cases variable (in its first difference) is now measured as the daily change in the number of new cases per 100,000 people. Also, we set $\mathbf{\Psi}_{\bullet,h}(L) = \sum_{n=0}^{N} \psi_{\bullet,h,n} L^n$, with $N = 0$. We then estimate equation (II.4). The results in Table II.E.4 show that including the first difference of new cases as a control variable does not change our baseline results much. Note, however, that the $\psi_{b,h,0}$ coefficient is significantly positive on impact and turns out to be negative over the horizon but is always lower than the estimated $\beta_{b,h}$.

II.5.2 Public debt-to-GDP

Delatte and Guillaume (2020) and Augustin et al. (2020), among others, highlight the key role of initial fiscal conditions in the sovereign debt market reaction to the pandemic outbreak. To investigate the role of country fiscal conditions, we run the regressions defined by equation (II.2) for two subsamples of countries. The first subsample refers to high debt-to-GDP countries and consists of states for which the debt-to-GDP ratio is above the median calculated for the full sample at the end of 2019: Belgium, Cyprus, Spain, France, Greece, Italy, and Portugal. The second subsample refers to low debt-to-GDP states and includes countries with a ratio below the median: Austria, Finland, Ireland, Lithuania, Malta, the Netherlands, Slovenia, and Slovakia.

Estimation results are shown in Appendix II.F. Figure II.F.1 reports the results for our benchmark split date, that is, March 9. Like Delatte and Guillaume (2020) and Augustin et al. (2020), we observe substantial heterogeneity in the response of bond spreads to new COVID-19 cases, which are positive and significant in the high debt-to-GDP subsample but not significantly different from zero in the low debt-to-GDP subsample of countries. We then investigate whether this heterogeneity alters our narrative of the crisis. To do so, we conduct a Chow test to identify structural breaks between the coefficients $\beta_{a,h}$ and $\beta_{b,h}$ in high debt-to-GDP countries only. The results are reported in Table II.F.1. The test results indicate that the null hypothesis is now rejected at the 10% level of significance for the period after March 9. For the full sample, March 9 turns out to be the key reference date after which the sovereign debt markets no longer reacted to the development of the pandemic.

II.6 Extensions

This section extends the analysis to three issues. First, we assess whether the ECB stopped the euro area stock market crash. Second, we assess the existence of spillovers from the Italian pandemic outbreak to other European sovereign markets. Third, and finally, we investigate what would have happened without the structural break identified in the sovereign market reaction to the occurrence of new COVID cases.

II.6.1 Did the ECB stop the euro area stock market crash?

In this section, we extend our empirical strategy to assess the dynamic effect of the COVID-19 outbreak on stock markets in the euro area. Thus far, we have included equity market data as a control variable in our regressions for sovereign spreads to measure their reaction to the occurrence of new COVID-19 cases given all the information already anticipated by the markets.[26] Cox et al. (2020) find evidence that Federal Reserve announcements were decisive in the reversal of the U.S. equity markets in March and April after the market crash in February. At that time, only a tiny fraction of the credit announced had been distributed, leading the authors to conclude that market movements were the outcome of a shift in investors' risk aversion.

To investigate the response of the stock market to new cases in the euro area, the model defined by equation (II.1) now takes the form:

$$\Delta z_{i,t+h} = \alpha_{i,h} + \eta_{t,h} + \beta_h \Delta x_{i,t} + \mathbf{\Gamma}_h(L) z_{i,t-1} + \mathbf{\Theta}_h(L) s_{i,t} + \varepsilon_{i,t+h} \tag{II.5}$$

with the notation described in Section II.3. The dependent variable is written $\Delta z_{i,t+h} = z_{i,t+h} - z_{i,t-1}$ and is the variation of the log of the stock index (i.e., the cumulative logarithmic return) at horizon h. The coefficient of interest β_h is the response of the national stock index to the pandemic outbreak. The model is still specified with country and time fixed effects and a set of control variables including the first four lags of the dependent variable and the current and four past values of 10-year sovereign bond spreads. The horizon is still 5 days, $H = 5$.

In the spirit of equation (II.2), the state-dependent local projection framework is now ex-

[26] Davis et al. (2021) shows that the stock market foreshadows workplace mobility.

Figure II.6.9 – Impulse responses of stock market indices (in logs) to new COVID-19 cases in the euro area

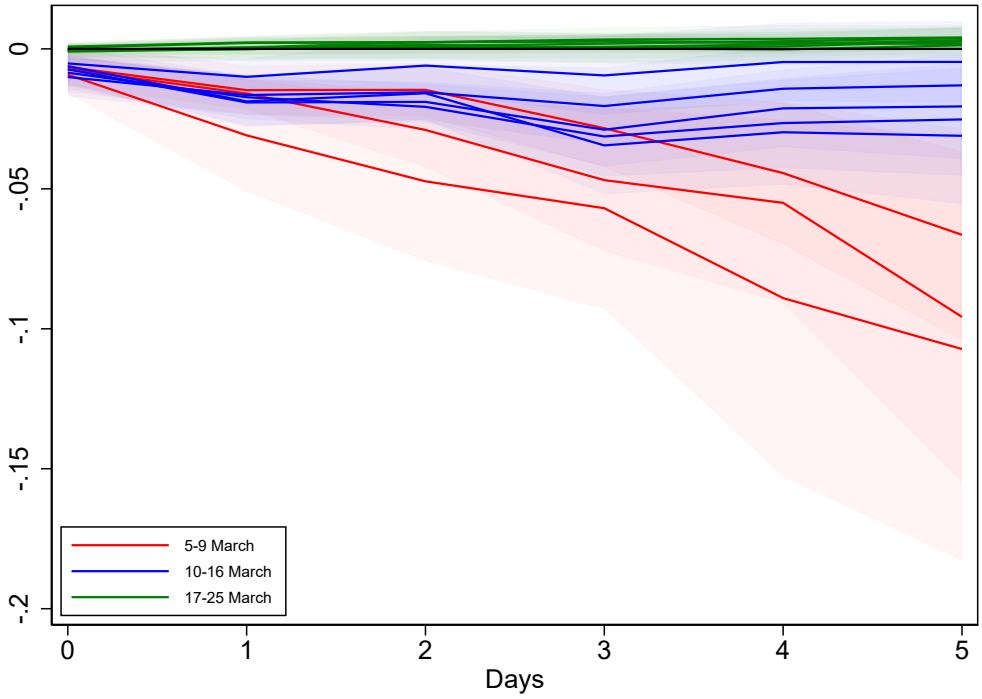

Note: Impulse responses represent the $\beta_{b,h}$ coefficient from equation (II.6). The impulse response coefficients $\beta_{b,h}$ are estimated before split dates: $\bar{t} \in \{3/5, ..., 3/9\}$ in red, $\bar{t} \in \{3/10, ..., 3/16\}$ in blue, and $\bar{t} \in \{3/17, ..., 3/25\}$ in green. The shaded area represents the 95% confidence interval for each coefficient.

pressed as follows:

$$\begin{aligned}\Delta z_{i,t+h} = \alpha_{i,h} + \eta_{t,h} + D_{t,\bar{t}}\Big[\beta_{a,h}\Delta x_{i,t} + \mathbf{\Gamma}_{a,h}(L)z_{i,t-1} + \mathbf{\Theta}_{a,h}(L)s_{i,t}\Big] \\ +(1 - D_{t,\bar{t}})\Big[\beta_{b,h}\Delta x_{i,t} + \mathbf{\Gamma}_{b,h}(L)z_{i,t-1} + \mathbf{\Theta}_{b,h}(L)s_{i,t}\Big] + \varepsilon_{i,t+h}\end{aligned} \tag{II.6}$$

where $D_{t,\bar{t}}$ is a dummy variable that takes 0 before a given date $\bar{t}$, that is, when $t < \bar{t}$, and 1 thereafter, that is, when $t \geq \bar{t}$. Here, again, these event dummies are constructed according to $\bar{t} \in \{3/5, ..., 3/25\}$. We employ exactly the same procedure as that developed in Section II.4: comparing the impulse response coefficients $\beta_{a,h}$ and $\beta_{b,h}$ with the split dates set on March 5 ($\bar{t} = 3/5$) and March 25 ($\bar{t} = 3/25$), focusing on the path of $\beta_{b,h}$ when the model runs over various split dates $\bar{t} \in \{3/5, ..., 3/25\}$, and testing for structural changes in the response coefficients over time.

The results are presented in Appendix II.G and summarized in Figure II.6.9, which replicates Figure II.4.7 for the cumulated stock market return instead of the sovereign spread. For the

period up to March 9, the stock market response to new COVID-19 cases is explosive, with a cumulative fall of 11% in the stock market index 5 days after the occurrence of new cases.[27] The response is no longer explosive thereafter (blue lines) and is completely muted when the last dates of the window are considered (green lines). Hence, ECB interventions not only closed spreads in the euro area but also prevented an even more dramatic stock market crash. Given the timing of balance sheet expansion, these results also support the existence of the communication channel linking the ECB intervention to stock markets–as reported in Cox et al. (2020) for the U.S. economy–since there was no significant balance sheet expansion before March 18.

II.6.2 Are there spillovers from the Italian pandemic outbreak?

As recalled in Section II.2, Italy was the first country in Europe to be severely affected by the COVID-19 pandemic. It is interesting to assess the extent to which both sovereign debt and stock markets in other European countries reacted to the health crisis in Italy, which may indicate how the markets anticipated the spread of the pandemic and the economic crisis in the rest of Europe. In this regard, we investigate potential spillovers from the Italian pandemic outbreak on financial markets across the euro area. For the sake of clarity, it is noteworthy that the notion of spillovers that is used hereafter refers to the effect of new COVID cases reported in Italy on sovereign spreads and stock indices in the other countries of our sample. This definition differs from the one employed in the literature on financial markets' interdependence following Diebold and Yilmaz (2009), which measures spillovers from one financial market to others.[28]

To examine this issue, we adapt our empirical framework as follows. Instead of using panel data regressions defined by equation (II.2), we estimate country by country[29] the following

[27] Lucca and Moench (2015) and Cieslak et al. (2019) show that asset prices could be affected by central banks outside of the public communication events. Interestingly, and as a possible explanation of our main results, the former paper documents high stock excess returns in anticipation of monetary policy decisions made at scheduled meetings of the Federal Open Market Committee (FOMC) in the U.S.

[28] Bostanci and Yilmaz (2020) recently applied this methodology to sovereign debt markets.

[29] Canova (2020) discusses the reliability of cross-sectional estimates and shows how their results could be biased due to heterogeneity.

series of regressions at each horizon h:

$$\begin{aligned}\Delta s_{i,t+h} = \alpha_{i,h} &+ D_{t,\bar{t}}\Big[\beta_{a,h,i}\Delta x_{i,t} + \beta^{\texttt{IT}}_{a,h,i}\Delta x_{\texttt{IT},t} + \mathbf{\Gamma}_{a,h,i}(L)s_{i,t-1} + \mathbf{\Theta}_{a,h,i}(L)z_{i,t}\Big] \\ &+(1-D_{t,\bar{t}})\Big[\beta_{b,h,i}\Delta x_{i,t} + \beta^{\texttt{IT}}_{b,h,i}\Delta x_{\texttt{IT},t} + \mathbf{\Gamma}_{b,h,i}(L)s_{i,t-1} + \mathbf{\Theta}_{b,h,i}(L)z_{i,t}\Big] + \varepsilon_{i,t+h}\end{aligned} \tag{II.7}$$

with the notation described in Section II.3. There are a couple of differences with respect to equation (II.2). First, we consider the occurrence of new COVID cases per 100,000 people as explanatory variables both in country i ($\Delta x_{i,t}$) and in Italy ($\Delta x_{\texttt{IT},t}$) simultaneously, $\beta^{\texttt{IT}}_{\bullet,h,i}$ being the response of sovereign spreads in country i to new COVID cases in Italy. Second, all other estimated coefficients $\beta_{\bullet,h,i}$, $\mathbf{\Gamma}_{\bullet,h,i}$, and $\mathbf{\Theta}_{\bullet,h,i}$ are also now specific to country i. Third, there are no longer time fixed effects, and $\alpha_{i,h}$ denotes an intercept. Fourth, we drop Italy from the sample of countries.

The aim of this estimation is to compare the distribution of $\beta_{b,h,i}$, that is, the sensitivity of sovereign spreads to domestic COVID cases, with $\beta^{\texttt{IT}}_{b,h,i}$, that is, the sensitivity of sovereign spreads to COVID cases in Italy, before the reference date $\bar{t}$. A high value of $\beta^{\texttt{IT}}_{b,h,i}$ would suggest strong spillovers from the pandemic outbreak in Italy to other European countries. Figure II.6.10 shows the distribution of the estimated coefficients (the median and the interquartile range) before $\bar{t}$ using March 9 as the reference date.

Our main results are as follows. First, it can be seen that the median of the coefficients $\beta_{b,h,i}$ estimated using the country-by-country regressions defined by equation (II.7) is not too far from the average estimate $\beta_{b,h}$ using panel regressions. Interestingly, even if the interquartile range is quite large, it does not include the zero value, which reinforces the robustness of our main results described in Section II.4. Second, the median of the coefficients $\beta^{\texttt{IT}}_{b,h,i}$ is much lower than $\beta_{b,h,i}$ at all horizons h, and the interquartile range of $\beta^{\texttt{IT}}_{b,h,i}$ includes the zero value at horizon $h \leq 2$. We thus conclude that national sovereign spreads are much more sensitive to the COVID cases that occur domestically than to those in Italy. Considering that the health crisis in Italy preceded those in other European countries, we conclude that the spillover effects of the Italian crisis were fairly weak and did not lead to significant anticipation in other European sovereign debt markets.

We replicate this country-by-country analysis for the stock markets by estimating the fol-

Figure II.6.10 – Impulse responses of 10-year government bond spreads to new COVID-19 cases in the euro area

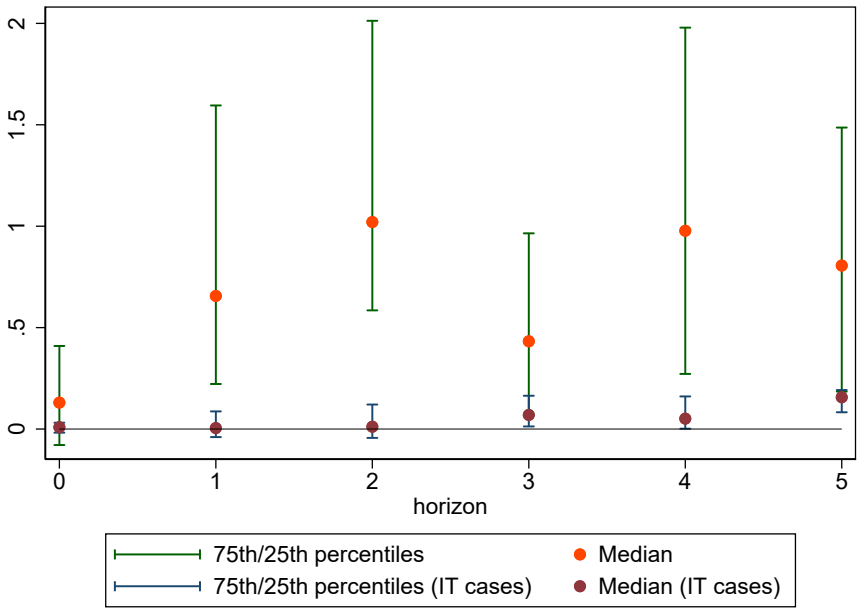

Note: Distribution of $\beta_{b,h,i}$ and $\beta^{\text{IT}}_{b,h,i}$ for COVID cases in Italy (IT). Impulse responses are computed following equation (II.7) before the split date (March 9).

lowing regressions:

$$\begin{aligned}\Delta z_{i,t+h} = \alpha_{i,h} + D_{t,\bar{t}}\Big[\beta_{a,h,i}\Delta x_{i,t} + \beta^{\text{IT}}_{a,h,i}\Delta x_{\text{IT},t} + \mathbf{\Gamma}_{a,h,i}(L)s_{i,t-1} + \mathbf{\Theta}_{a,h,i}(L)z_{i,t}\Big] \\ +(1 - D_{t,\bar{t}})\Big[\beta_{b,h,i}\Delta x_{i,t} + +\beta^{\text{IT}}_{b,h,i}\Delta x_{\text{IT},t} + \mathbf{\Gamma}_{b,h,i}(L)s_{i,t-1} + \mathbf{\Theta}_{b,h,i}(L)z_{i,t}\Big] + \varepsilon_{i,t+h}\end{aligned} \tag{II.8}$$

where the dependent variable $\Delta z_{i,t+h}$ is the variation of the log of the stock index (i.e., the cumulative logarithmic return) at horizon h and the notation used is that described in Section II.3 and Section II.6.1. Figure II.6.11 reports the results. They confirm the robustness of our conclusions based on panel data regressions and show weak spillover effects from new COVID cases reported in Italy to other European stock markets.

II.6.3 What would have happened without the structural breaks?

This section proposes a counterfactual analysis. We simulate the path of the spread between March 9 and March 18 given the number of cases reported during this period using the estimated coefficient $\beta_{b,h}$ for $\bar{t} = \{3/9\}$ depicted in Figure II.4.8.[30] We interpret this path as the spread

[30]The regression results are reported in Appendix II.C.

Figure II.6.11 – Impulse responses of the stock market (in logs) to new COVID-19 cases in the euro area

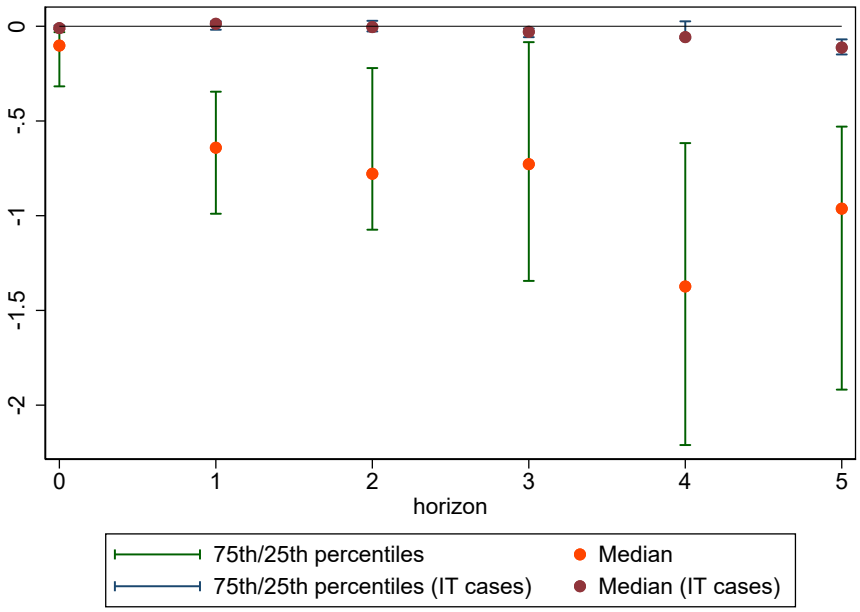

Note: Distribution of $\beta_{b,h,i}$ and $\beta^{\text{IT}}_{b,h,i}$ for COVID cases in Italy (IT). Impulse responses are computed following equation (II.8) before the split date (March 9).

induced by the COVID crisis that would have occurred without the break in the relationship between the pandemic outbreak and sovereign risk that we attribute to policy interventions during this period. New cases $\Delta x_{i,t}$ in country i at time t induce a spread variation for the h period ahead denoted $\Delta s^x_{i,t+h}$ that is defined as follows:

$$\Delta s^x_{i,t+h} = \beta_{b,h} \Delta x_{i,t} \tag{II.9}$$

for $h = 0, 1, ., H$. The COVID-induced spread deviation as of time t is then the sum of the values of new cases reported H periods before weighted by the coefficient $\beta_{b,h}$:

$$\Delta s^x_{i,t} = \sum_{h=0}^{H} \beta_{b,h} \Delta x_{i,t-h} \tag{II.10}$$

By definition, the spread at K periods ahead is equal to the initial value of the spread plus the cumulative sum of spread variations. Then, the spread induced by the COVID crisis is given by:

$$s^x_{i,t+K} = s_{i,t-1} + \sum_{h=0}^{H} \sum_{k=h}^{K} \beta_{b,h} \Delta x_{i,t+k-h} \tag{II.11}$$

where $K = 0$ on March 9. Also, we assume that new cases reported up to March 9 have no impact on the predicted spreads series.

Figure II.6.12 shows the evolution of $s^x_{i,t+K}$ between March 9 and March 18 for Italy, Spain, and France. On March 6, the Italian government bond spread, denoted by $s_{i,t-1}$ in equation (II.11), was at 1.807%, and the number of total confirmed cases per million people rose from 121.978 to 521.089 between March 9 and March 18 in Italy. Given the value of $\beta_{b,h}$ estimated before March 9, the spread induced by the COVID crisis in Italy would have surged during this week to reach 19.5% on March 18. We can then conclude that without any change in the effect of new COVID cases on sovereign yields in Italy, a sovereign debt crisis may have occurred in the middle of March. The pattern for Spain and France would have been less dramatic but still dangerous with spreads of approximately 13% and 4%, respectively. Hence, this counterfactual analysis shows that the earlier policy intervention of the ECB on March 12 seriously restrained the spread of pandemic-induced crisis to sovereign debt markets.

II.7 Conclusion

The COVID-19 health crisis has revived fears of a sovereign debt crisis in Europe. The results presented in this paper indicate that the first confirmed COVID-19 cases were at the origin of an explosive increase in interest rate spreads on sovereign debt. The results also show that this explosive dynamic broke around the time of the ECB's intervention on March 12 and that otherwise, there could have been a sudden surge in rates in the countries most affected by COVID-19 (Italy, Spain, and France), reaching spread values close to those observed during the 2010-2012 sovereign debt crisis in Europe within just a few days.

This conclusion rests on the study of sovereign debt markets during the first few months of the sanitary crisis and is corroborated by the extension of our analysis to stock markets. The duration of this health crisis is still uncertain given the state of medical knowledge. However, its economic consequences for public finances will certainly be longer lasting and raise additional challenges for public decision-makers in Europe and around the world in managing the public debt induced by the COVID crisis.

Figure II.6.12 – Counterfactual sovereign spreads

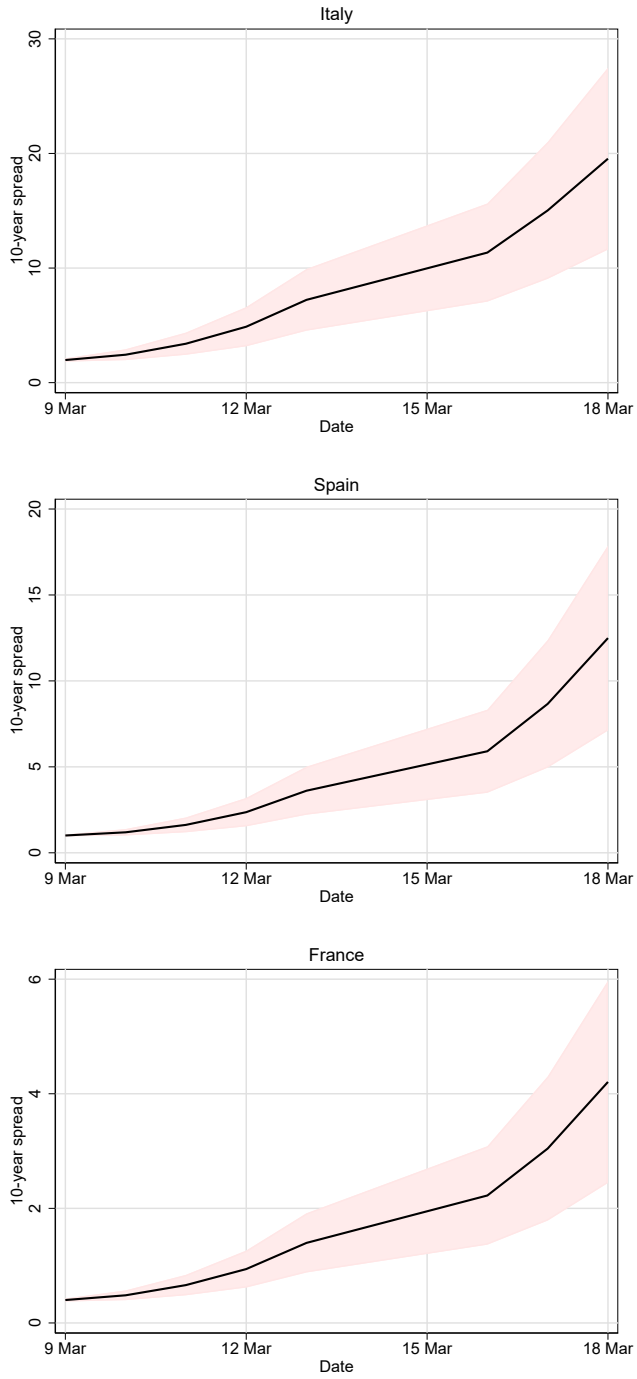

Note: Counterfactual sovereign bond spreads (in %) are computed following equation (II.11). The historical series are presented in Appendix II.B. The red shaded area represents the 95% confidence interval.

Appendix

COVID-induced sovereign risk in the euro area: When did the ECB stop the spread?

II.A Thomson Reuters Eikon - Datastream

Table II.A.1 – Government bond yields series in the euro area

Country (countrycode)	**Bond yield**	**Datastream**
Austria (AT)	2-year	AT2YT=RR
	10-year	AT10YT=RR
Belgium (BE)	2-year	BE2YT=RR
	10-year	BE10YT=RR
Cyprus (CY)	2-year	—
	10-year	CY10YT=RR
Finland (FI)	2-year	FI2YT=RR
	10-year	FI10YT=RR
France (FR)	2-year	FR2YT=RR
	10-year	FR10YT=RR
Germany (DE)	2-year	DE2YT=RR
	10-year	DE10YT=RR
Greece (GR)	2-year	—
	10-year	GR10YT=RR
Ireland (IE)	2-year	IE2YT=RR
	10-year	IE10YT=RR
Italy (IT)	2-year	IT2YT=RR
	10-year	IT10YT=RR
Latvia (LV)	2-year	LV2YT=RR
	10-year	—
Lithuania (LT)	2-year	—
	10-year	LT10YT=RR

Table II.A.2 – Government bond yields series in the euro area (cont'd)

Country (countrycode)	**Bond yield**	**Datastream**
Malta (MT)	2-year	—
	10-year	MT10YT=RR
Netherlands (NL)	2-year	NL2YT=RR
	10-year	NL10YT=RR
Portugal (PT)	2-year	PT2YT=RR
	10-year	PT10YT=RR
Slovakia (SK)	2-year	SK2YT=RR
	10-year	SK10YT=RR
Slovenia (SI)	2-year	SI2YT=RR
	10-year	SI10YT=RR
Spain (ES)	2-year	ES2YT=RR
	10-year	ES10YT=RR

Note: "—" means not reported. Estonia and Luxembourg are missing since neither 2-year nor 10-year government bond yields are reported.

Table II.A.3 – Stock index series in the euro area

Country (countrycode)	**Stock index**	**Datastream**
Austria (AT)	ATX	.ATX
Belgium (BE)	BEL 20	.BFX
Cyprus (CY)	Cyprus Main Market	.CYMAIN
Finland (FI)	OMX Helsinki 25	.OMXH25
France (FR)	CAC 40	.FCHI
Germany (DE)	DAX	.GDAXI
Greece (GR)	Athens General Composite	.ATG
Ireland (IE)	ISEQ	.ISEQ
Italy (IT)	FTSE MIB	.FTMIB
Latvia (LV)	Riga Stock Exchange	.OMXRGI
Lithuania (LT)	Vilnius Stock Exchange	.OMXVGI
Malta (MT)	Malta Stock Exchange	.MSE
Netherlands (NL)	AEX	.AEX
Portugal (PT)	PSI 20	.PSI20
Slovakia (SK)	SAX	.SAX
Slovenia (SI)	SBITOP	.SBITOP
Spain (ES)	IBEX 35	.IBEX

Note: Main national stock index for each euro area countries in the sample. Estonia and Luxembourg are missing since neither 2-year nor 10-year government bond yields are reported.

II.B Figures: Raw data

Figure II.B.1 – Total number of COVID-19 cases

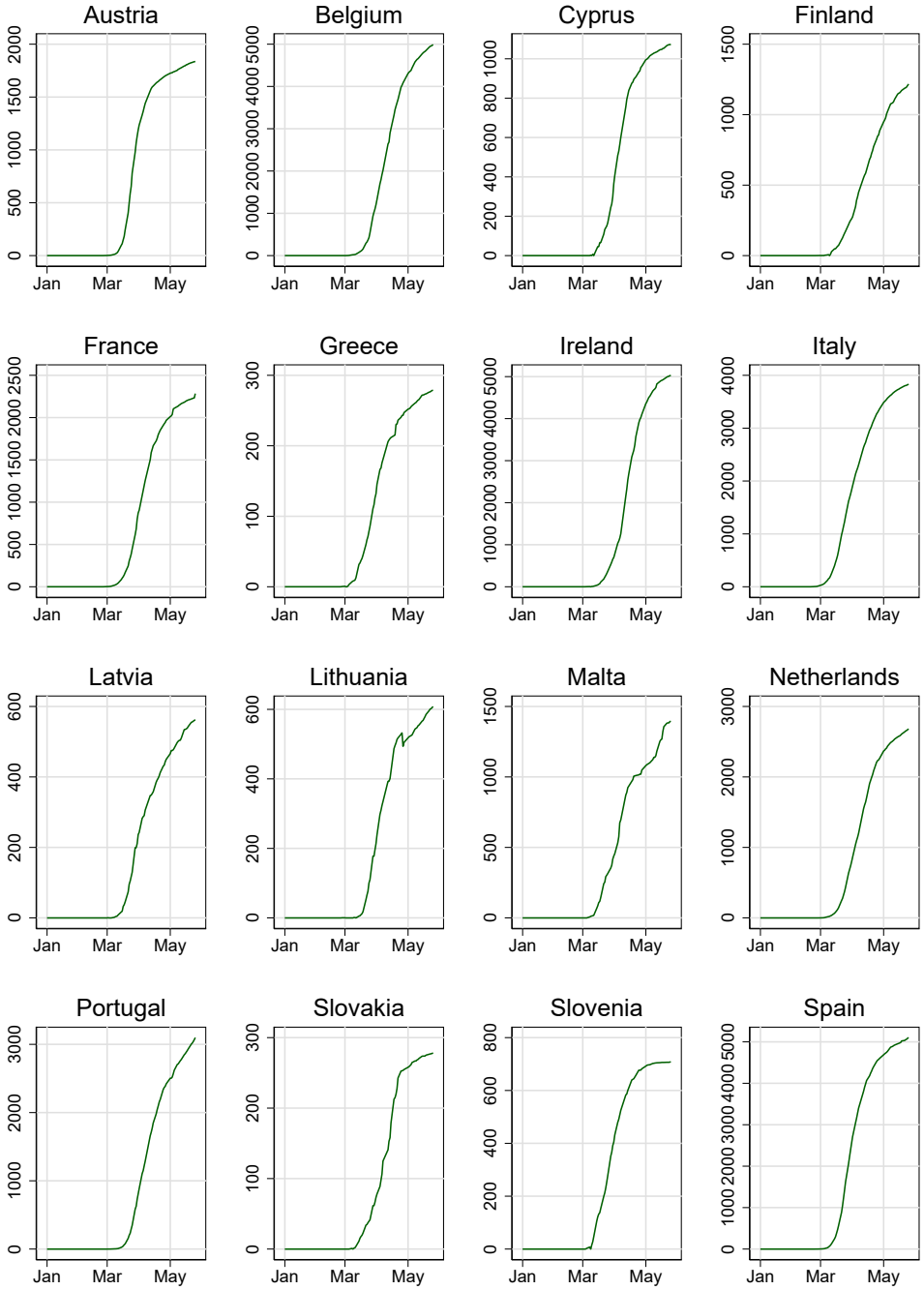

Note: Total COVID-19 confirmed cases are reported as the number of cases per million people. Sources: European Centre for Disease Prevention and Control (ECDC)

Figure II.B.2 – Total number of deaths due to COVID-19

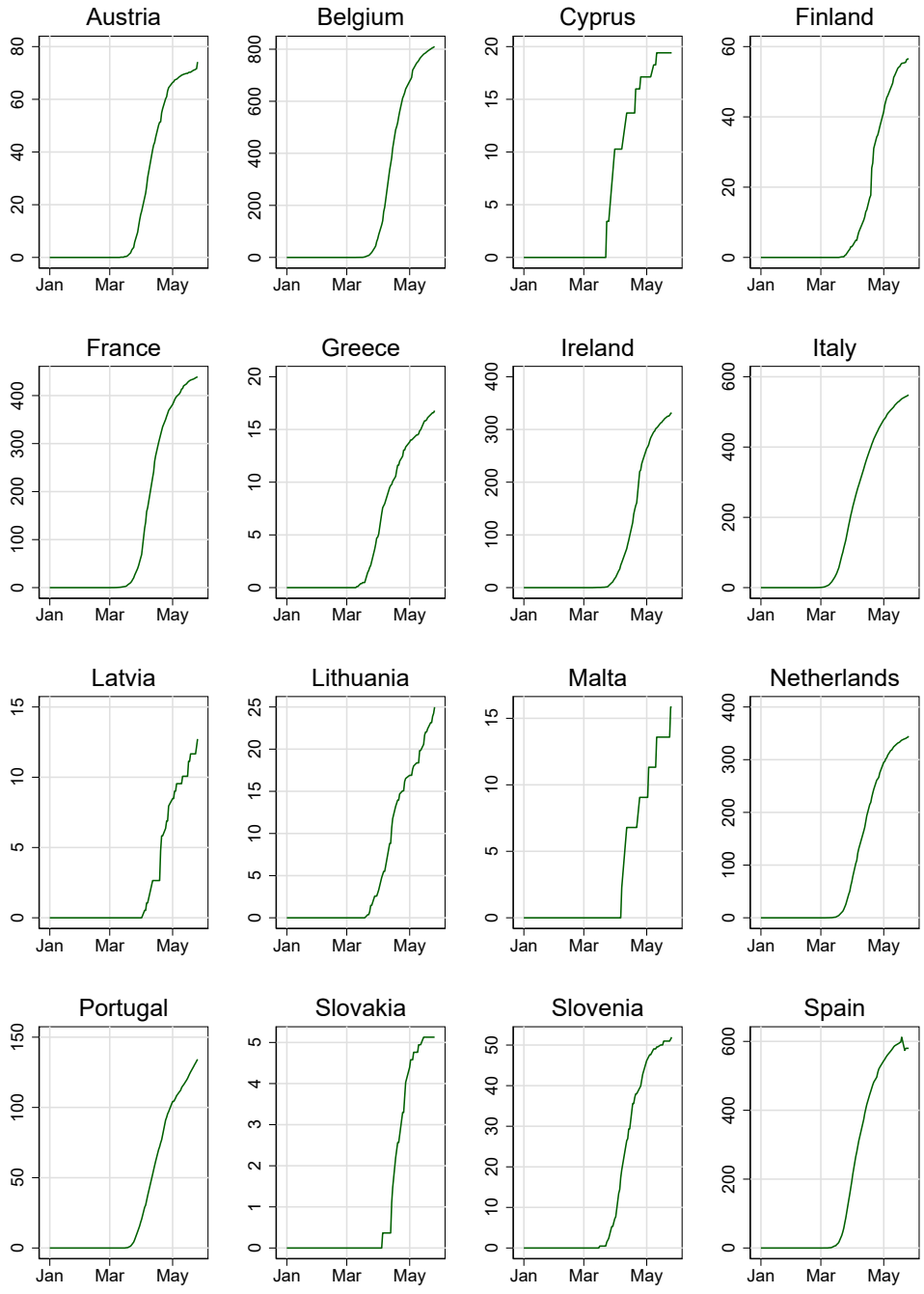

Note: Total deaths due to COVID-19 are reported as the number of deaths per million people. Sources: European Centre for Disease Prevention and Control (ECDC)

Figure II.B.3 – Government spreads (2- and 10-year maturity)

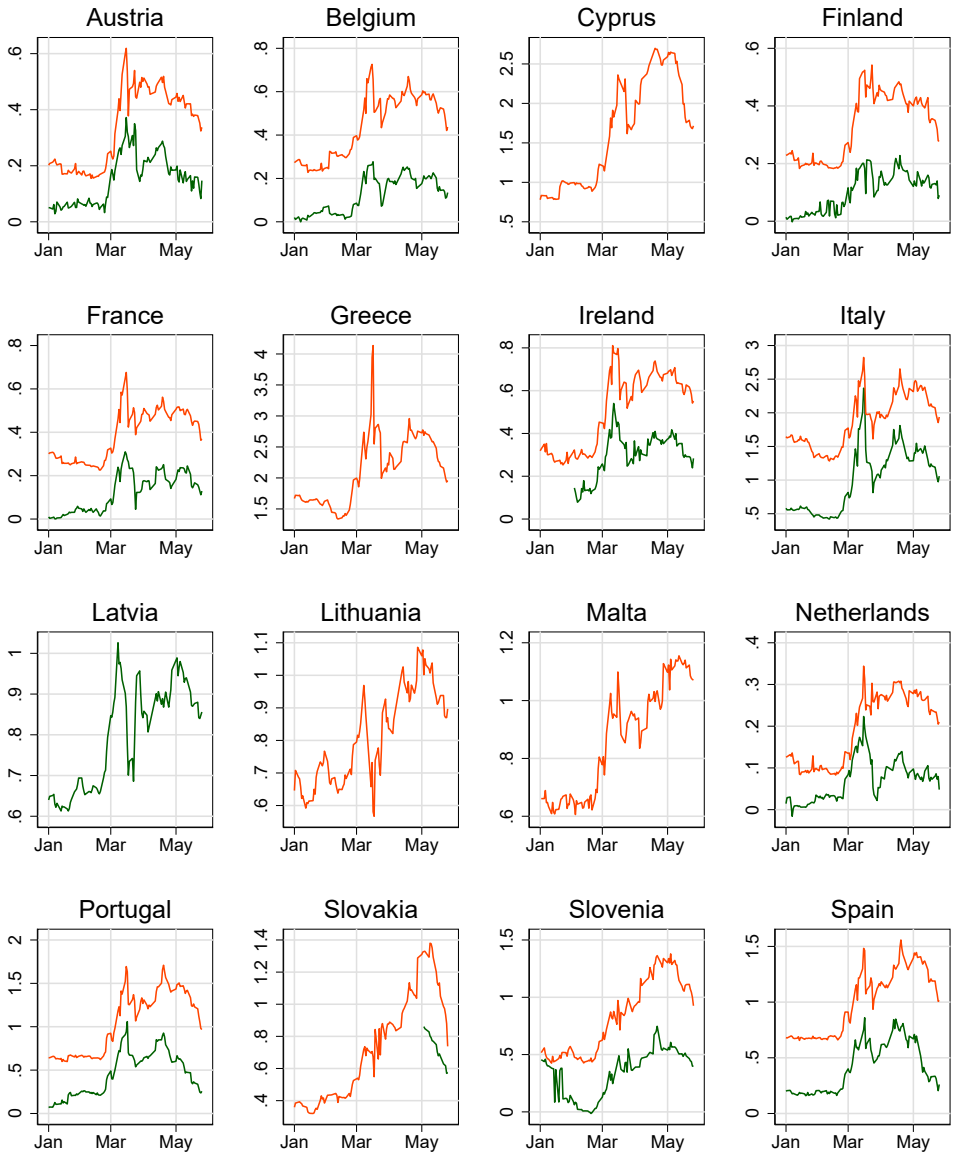

Note: 2- and 10-year government spread are computed relatively to the yield on 2- and 10-year German bunds, respectively. Green line: 2-year government spread. Orange line: 10-year governmend spread.

Figure II.B.4 – Stock market indices

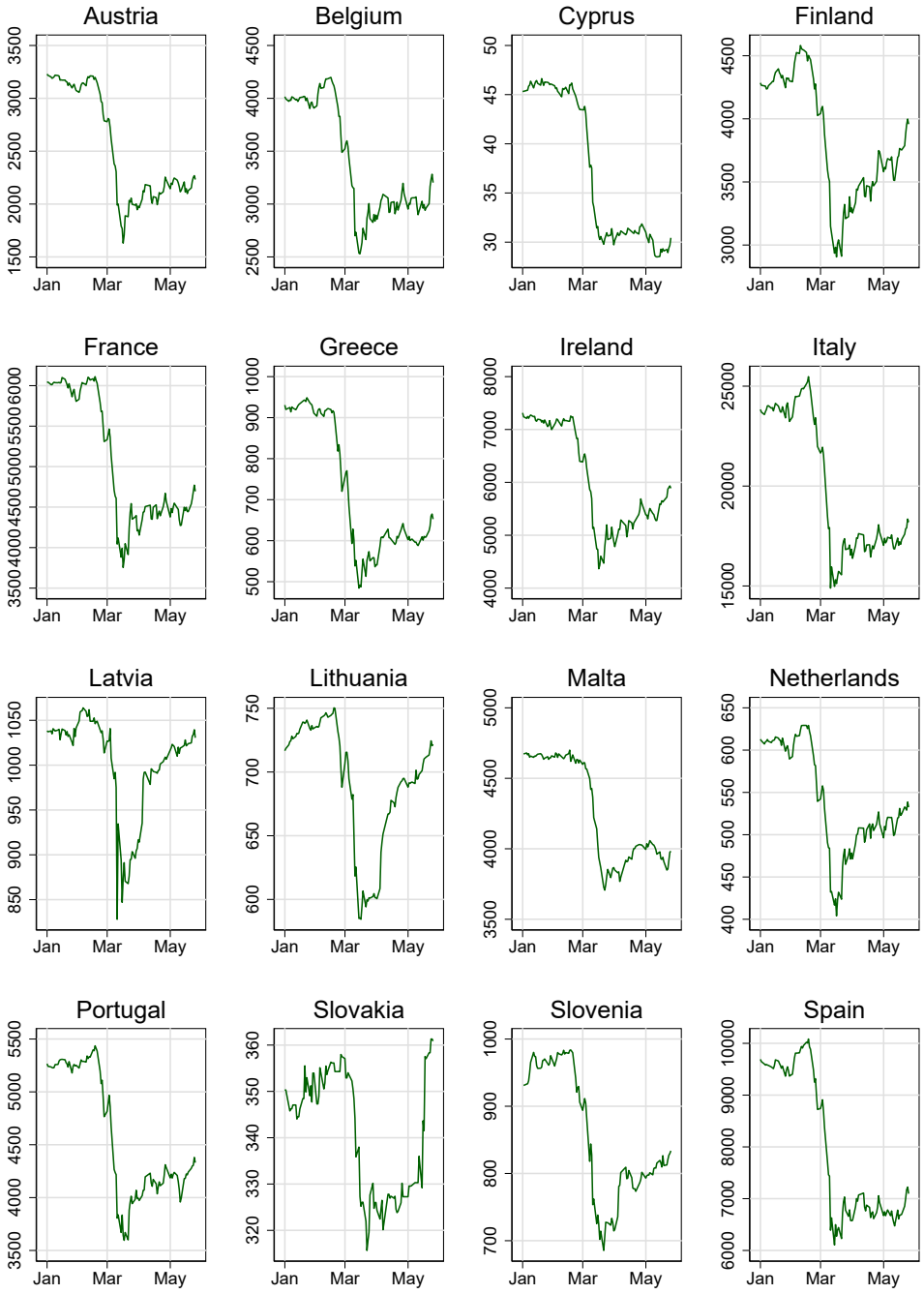

Note: Main national stock index for each euro area countries in the sample.

II.C Baseline results

Figure II.C.1 – Time-fixed effects

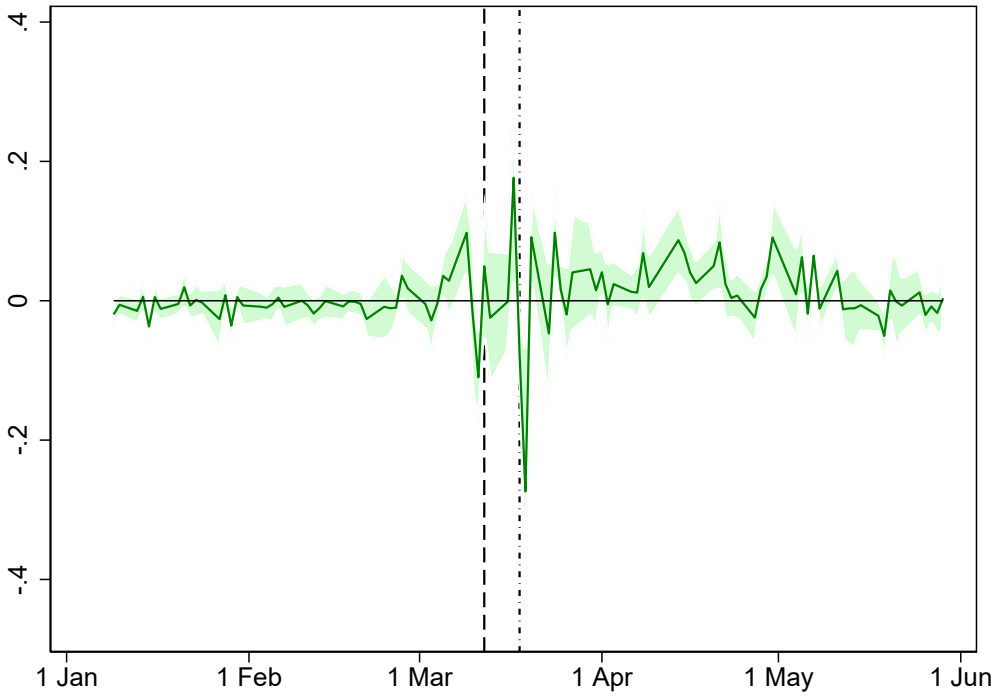

Note: Time-fixed effects $\eta_{t,h}$ estimated using equation (II.1). Vertical lines correspond to ECB's announcement dates: March 12, 2020 (dashed) and March 18, 2020 (dashed-dot). Shaded area represents the 95% confidence interval.

Table II.C.1 – Dependent variable 10-year spread (full sample period)

	Day 0	Day 1	Day 2	Day 3	Day 4	Day 5
new cases	-0.000	-0.001	-0.001	-0.002*	-0.001	-0.001
	(0.00)	(0.00)	(0.00)	(0.00)	(0.00)	(0.00)
R^2	0.477	0.516	0.545	0.558	0.562	0.577
Observations	1374	1349	1331	1316	1304	1291

Note: * $p < 0.10$, ** $p < 0.05$, *** $p < 0.01$. Clustered standard errors by country in parentheses. This table reports the coefficient β_h introduced in the regression equation (II.1). The new cases variable is measured as the daily change in the number of total cases per 100,000 people.

Table II.C.2 – Dependent variable 10-year spread (before and after March 9)

	Day 0	Day 1	Day 2	Day 3	Day 4	Day 5
new cases – *before*	0.029**	0.065***	0.124***	0.154***	0.225***	0.348***
	(0.01)	(0.02)	(0.03)	(0.03)	(0.03)	(0.04)
new cases – *after*	0.000	-0.000	-0.001	-0.001	-0.000	0.000
	(0.00)	(0.00)	(0.00)	(0.00)	(0.00)	(0.00)
R^2	0.498	0.540	0.574	0.593	0.606	0.633
Observations	1374	1349	1331	1316	1304	1291

Note: * $p < 0.10$, ** $p < 0.05$, *** $p < 0.01$. Clustered standard errors by country in parentheses. This table reports the $\beta_{b,h}$ and $\beta_{a,h}$ coefficients introduced in the regression equation (II.2) for $\bar{t} = \{3/9\}$. The new cases variable is measured as the daily change in the number of total cases per 100,000 people.

II.D Robustness: Alternative variables

This section replicates our baseline estimation for six alternative dependent and independent variables. For each of them, it provides the equivalent of Figure II.4.7 for the impulse response functions and of Table II.4.1 for the Chow test outcome.

Two-year government bond spreads. First, we run the model using 2-year government bond spreads instead of the 10-year maturity for the dependent variable $\Delta s_{i,t+h}$ in equation (II.2). Given the availability of the data presented in Appendices II.A and II.B, the list of euro area countries in our sample is restricted to Austria, Belgium, Finland, France, Ireland, Italy, Latvia, Netherlands, Portugal, Slovakia, Slovenia, and Spain. Moreover, some 2-year government bond yield data are missing for Ireland and Slovakia at the beginning of the sample period. However, those changes in the composition of our sample do not invalidate our main results: the response coefficient of sovereign spreads to the pandemic outbreak is explosive for the period before March 9, small between March 10 and March 16, and almost muted thereafter, as shown in Figure II.D.1. According to the Chow test results in Table II.D.1, the regime switches one day later (on March 10) than in our benchmark results.

Figure II.D.1 – Impulse responses of 2-year government bond spreads to new COVID-19 cases in the euro area

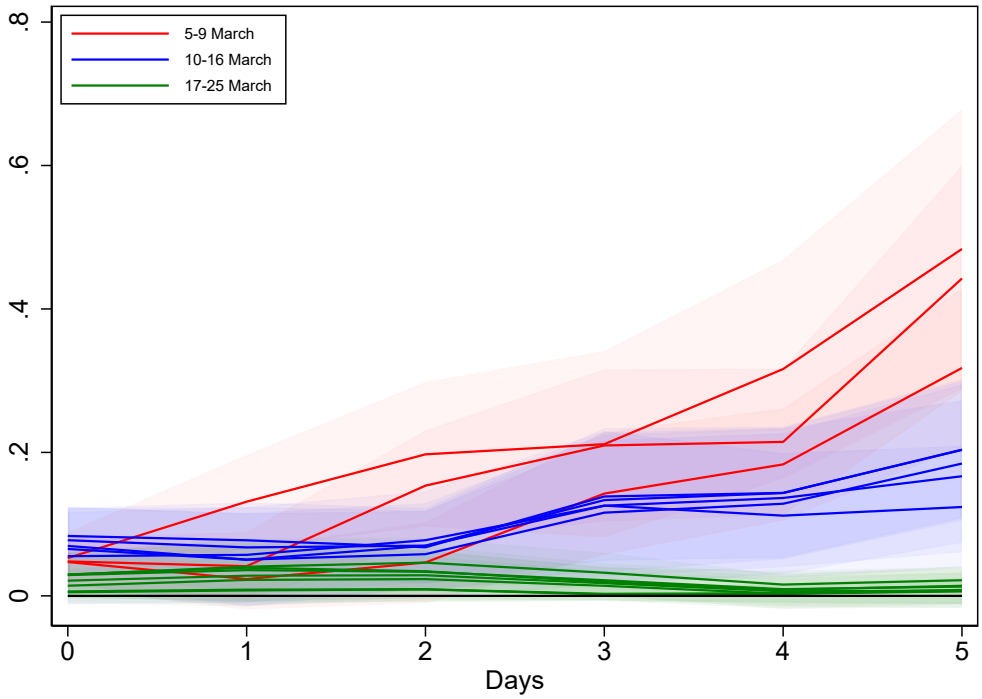

Note: Impulse responses are computed following equation (II.2). Impulse response coefficients $\beta_{b,h}$ are estimated before splitting dates: $\bar{t} \in \{3/5, ..., 3/9\}$ in red, $\bar{t} \in \{3/10, ..., 3/16\}$ in blue, and $\bar{t} \in \{3/17, ..., 3/25\}$ in green. Shaded area represents the 95% confidence interval for each coefficient.

Table II.D.1 – Chow test (p-values, using 2-year maturity)

	Horizon					
	h=0	h=1	h=2	h=3	h=4	h=5
March 5	0.02	0.26	0.10	0.00	0.00	0.00
March 6	0.01	0.08	0.00	0.00	0.00	0.00
March 9	0.01	0.00	0.00	0.00	0.00	0.00
March 10	0.00	0.00	0.01	0.01	0.01	0.00
March 11	0.00	0.04	0.01	0.01	0.01	0.00
March 12	0.02	0.11	0.06	0.03	0.02	0.00
March 13	0.03	0.12	0.03	0.02	0.01	0.01
March 16	0.10	0.09	0.03	0.02	0.02	0.01
March 17	0.07	0.05	0.02	0.03	0.01	0.02
March 18	0.07	0.04	0.03	0.05	0.45	0.24
March 19	0.07	0.11	0.07	0.07	0.37	0.27
March 20	0.18	0.18	0.10	0.12	0.54	0.56
March 23	0.21	0.18	0.14	0.17	0.78	0.51
March 24	0.19	0.28	0.19	0.49	0.64	0.51
March 25	0.28	0.36	0.30	0.66	0.70	0.53

Note: p-values of Chow statistics from the test.

New deaths. Next, we replace the number of new confirmed cases with the number of new deaths due to COVID-19 as a relevant measure of the pandemic severity to be in line with Eichenbaum et al. (2020) for the independent variable $\Delta x_{i,t}$ in equation (II.2). The variable is now constructed as the total number of new deaths per million inhabitants. Figure II.D.2 shows that for the period before March 9, the response coefficient of sovereign spreads to new deaths due to COVID-19 is steeper than that considering new cases in the baseline regression. The value of $\beta_{b,h}$ with new deaths up to a 5-day horizon reaches 0.916. This is almost three times the value of the response coefficient to new cases shown previously. After March 9, the $\beta_{a,h}$ response coefficient is quite similar to that estimated in the baseline specification. However, it is significantly different from zero at horizon 3 in the case where we consider new deaths instead of new cases in the estimates. The results of the Chow test in Table II.D.2 suggest significant differences in the response coefficients up to March 11.

Figure II.D.2 – Impulse responses of 10-year government bond spreads to new deaths due to COVID-19 in the euro area

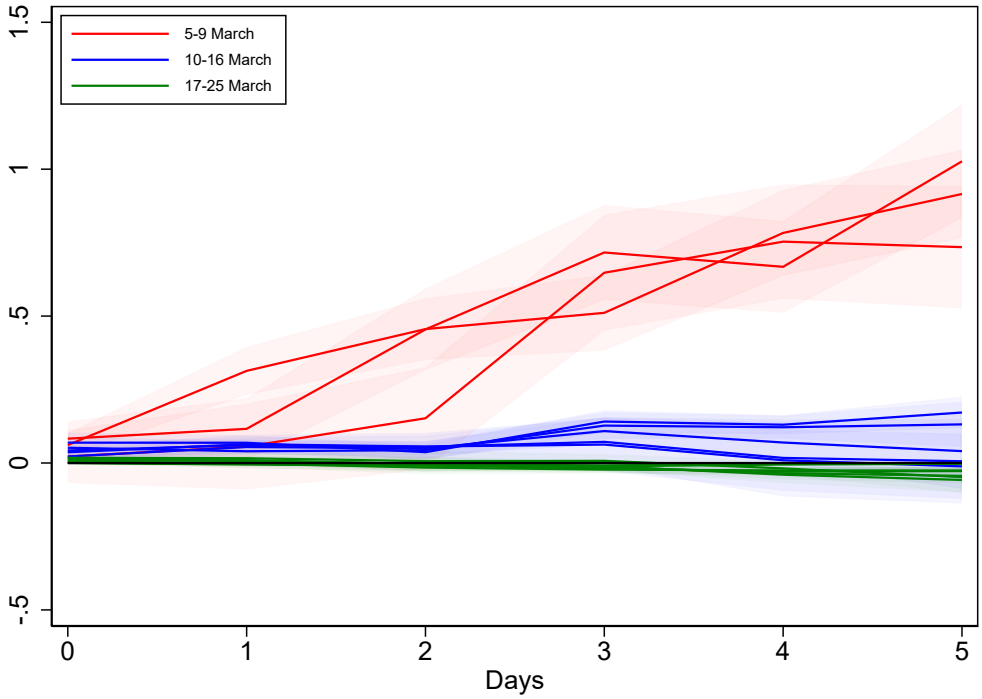

Note: Impulse responses are computed following equation (II.2). Impulse response coefficients $\beta_{b,h}$ are estimated before splitting dates: $\bar{t} \in \{3/5, ..., 3/9\}$ in red, $\bar{t} \in \{3/10, ..., 3/16\}$ in blue, and $\bar{t} \in \{3/17, ..., 3/25\}$ in green. Shaded area represents the 95% confidence interval for each coefficient.

Table II.D.2 – Chow test (p-values, using new deaths)

	Horizon					
	h=0	h=1	h=2	h=3	h=4	h=5
March 5	0.61	0.42	0.08	0.00	0.00	0.00
March 6	0.01	0.03	0.00	0.00	0.00	0.00
March 9	0.01	0.00	0.00	0.00	0.00	0.00
March 10	0.00	0.00	0.01	0.00	0.00	0.00
March 11	0.01	0.03	0.01	0.00	0.00	0.00
March 12	0.13	0.00	0.00	0.00	0.05	0.50
March 13	0.00	0.00	0.01	0.08	0.77	0.92
March 16	0.00	0.00	0.02	0.15	0.83	0.84
March 17	0.03	0.16	0.66	0.39	0.15	0.07
March 18	0.06	0.51	0.90	0.22	0.01	0.01
March 19	0.22	0.11	0.76	0.09	0.00	0.00
March 20	0.00	0.12	0.44	0.02	0.00	0.00
March 23	0.38	0.88	0.16	0.00	0.00	0.00
March 24	0.83	0.09	0.04	0.00	0.04	0.44
March 25	0.52	0.06	0.01	0.00	0.23	0.72

Note: p-values of Chow statistics from the test.

Rolling average of new cases. We also consider the 3-day rolling average[31] of new COVID-19 cases as the independent variable $\Delta x_{i,t}$ in equation (II.2). When the COVID-19 pandemic is measured as the rolling average of new cases, the response coefficient $\beta_{b,h}$ rises from 0.051 on impact to 0.248 at $h = 5$. Figure II.D.3 plots the $\beta_{b,h}$ response coefficients associated with the rolling average of new confirmed cases at each split date. Note that the regime of explosive coefficients seems to include March 10 rather than March 9 as a break date in that specification. According to the Chow test results in Table II.D.3, March 10 is the key date for the break in response coefficients. The p-values are considerably higher than in our benchmark but still below 10 percent, which can be explained by the smoothing effects of the rolling average.

Figure II.D.3 – Impulse responses of 10-year government bond spreads to new COVID-19 cases (3-day rolling average) in the euro area

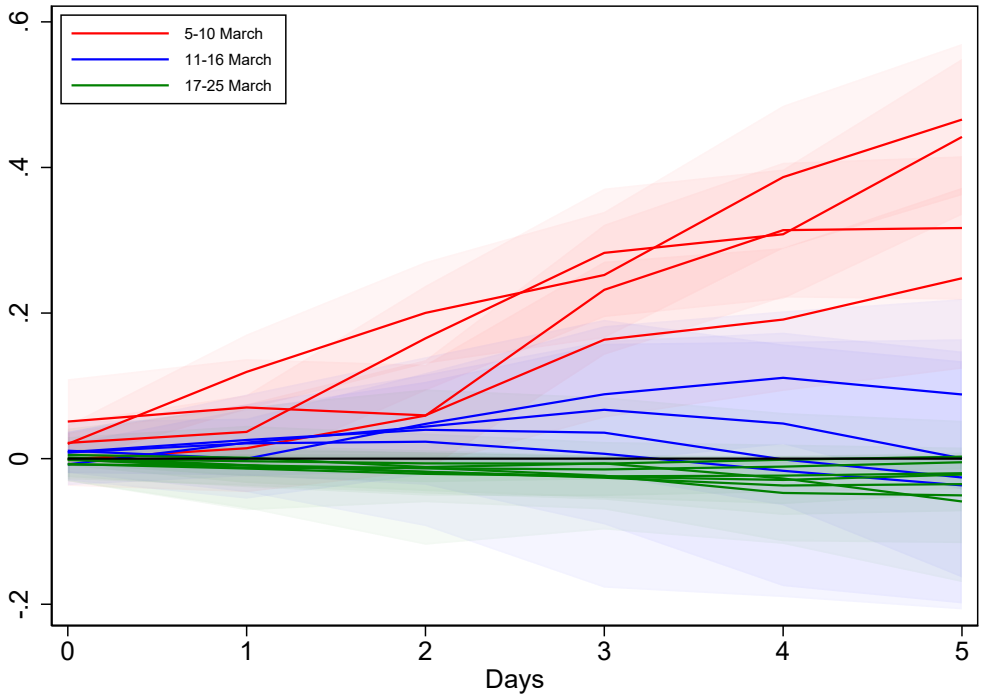

Note: Impulse responses are computed following equation (II.2). Impulse response coefficients $\beta_{b,h}$ are estimated before splitting dates: $\bar{t} \in \{3/5, ..., 3/10\}$ in red, $\bar{t} \in \{3/11, ..., 3/16\}$ in blue, and $\bar{t} \in \{3/17, ..., 3/25\}$ in green. Shaded area represents the 95% confidence interval for each coefficient.

[31] The 3-day rolling average is computed as a right-aligned moving average in the form $\frac{1}{N}\sum_{n=0}^{N-1} x_{i,t-n}$, with $N = 3$.

Table II.D.3 – Chow test (p-values, using new cases (3-day rolling average)

	Horizon					
	h=0	h=1	h=2	h=3	h=4	h=5
March 5	0.97	0.58	0.11	0.00	0.00	0.00
March 6	0.12	0.13	0.00	0.00	0.00	0.00
March 9	0.11	0.00	0.00	0.00	0.00	0.00
March 10	0.08	0.04	0.09	0.01	0.00	0.00
March 11	0.56	0.95	0.16	0.06	0.02	0.17
March 12	0.58	0.30	0.14	0.14	0.37	0.98
March 13	0.50	0.26	0.27	0.54	1.00	0.77
March 16	0.50	0.48	0.64	0.92	0.86	0.67
March 17	0.73	0.91	0.86	0.92	0.54	0.28
March 18	0.98	0.71	0.64	0.31	0.15	0.12
March 19	0.45	0.56	0.23	0.08	0.06	0.06
March 20	0.70	0.50	0.17	0.08	0.07	0.10
March 23	0.41	0.30	0.16	0.07	0.04	0.07
March 24	0.60	0.26	0.18	0.05	0.07	0.34
March 25	0.98	0.59	0.33	0.25	0.75	0.37

Note: p-values of Chow statistics from the test.

New cases in absolute terms. We use the number of new cases in absolute terms as a proxy for pandemic severity. Figure II.D.4 shows that the evolution of the $\beta_{b,h}$ coefficient over each indicated split date is very close to that observed in our baseline results, and March 9 is the significant break date according to the Chow test results (see Table II.D.4).

Figure II.D.4 – Impulse responses of 10-year government bond spreads to new COVID-19 cases (in absolute terms) in the euro area

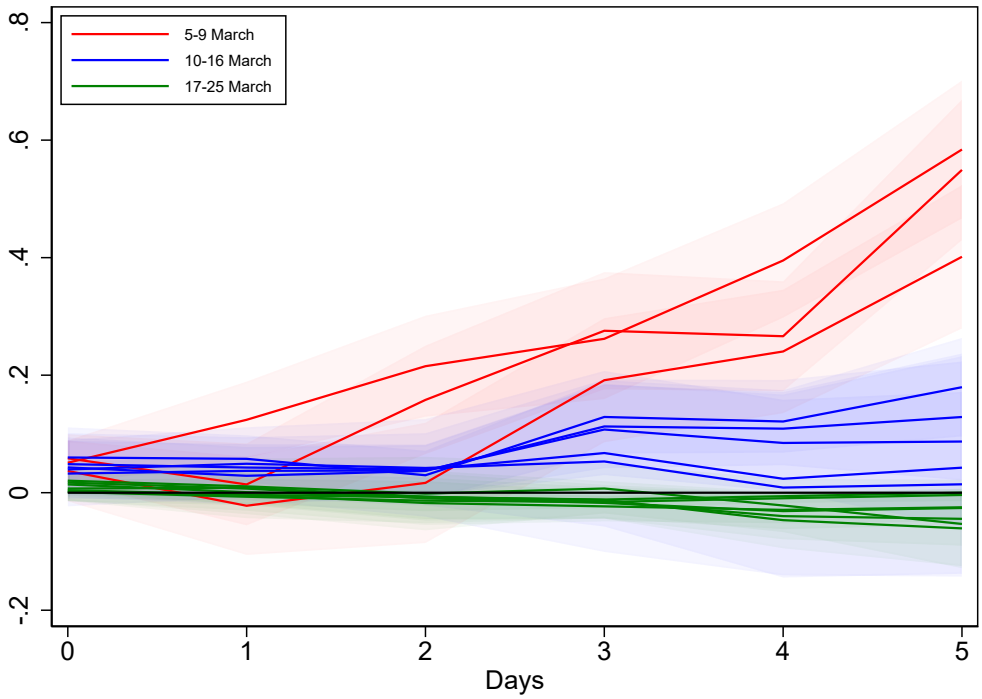

Note: Impulse responses are computed following equation (II.2). Impulse response coefficients $\beta_{b,h}$ are estimated before splitting dates: $\bar{t} \in \{3/5, ..., 3/9\}$ in red, $\bar{t} \in \{3/10, ..., 3/16\}$ in blue, and $\bar{t} \in \{3/17, ..., 3/25\}$ in green. Shaded area represents the 95% confidence interval for each coefficient.

Table II.D.4 – Chow test (p-values, using new cases in absolute terms)

	Horizon					
	h=0	h=1	h=2	h=3	h=4	h=5
March 5	0.16	0.57	0.71	0.00	0.00	0.00
March 6	0.01	0.69	0.00	0.00	0.00	0.00
March 9	0.01	0.00	0.00	0.00	0.00	0.00
March 10	0.02	0.01	0.13	0.00	0.00	0.00
March 11	0.09	0.22	0.08	0.00	0.00	0.02
March 12	0.23	0.09	0.07	0.01	0.05	0.24
March 13	0.06	0.08	0.17	0.26	0.79	0.66
March 16	0.11	0.10	0.28	0.47	0.94	0.90
March 17	0.21	0.64	0.93	0.73	0.26	0.11
March 18	0.29	0.99	0.69	0.40	0.04	0.04
March 19	0.45	0.59	0.64	0.23	0.04	0.04
March 20	0.05	0.71	0.44	0.14	0.03	0.03
March 23	0.74	0.59	0.26	0.06	0.01	0.02
March 24	0.83	0.15	0.11	0.01	0.02	0.08
March 25	0.89	0.17	0.07	0.02	0.04	0.18

Note: p-values of Chow statistics from the test.

Lagged new cases. We consider here the lags of the number of cases. Our reference variable used in the baseline specification is measured by the number of COVID-19 cases published by public health offices at time t. However, it is possible that these data are only available at the end of the day, after the markets close, or even on the day after. In that case, it is the values recorded on the day before that matters for the financial markets. To take into account these delays, the first and second lagged values of new cases are used as independent variables $\Delta x_{i,t-1}$ or $\Delta x_{i,t-2}$ in equation (II.2). The results are reported only for the second lag of new cases in Figure II.D.5–the $\beta_{b,h}$ coefficient is now the response of sovereign spreads to the second lag of new COVID cases–and confirms our narrative of the crisis. In this context, we assume that at time t, financial markets have information on COVID cases published the day before $(t-1)$ containing the number of new COVID cases reported the day before that $(t-2)$. The structural break occurred later than March 9, our reference break date, which is consistent with the two lags introduced in the independent variable and in line with the Chow test results reported in Table II.D.5.

Figure II.D.5 – Impulse responses of 10-year government bond spreads to the second lagged value of new COVID-19 cases in the euro area

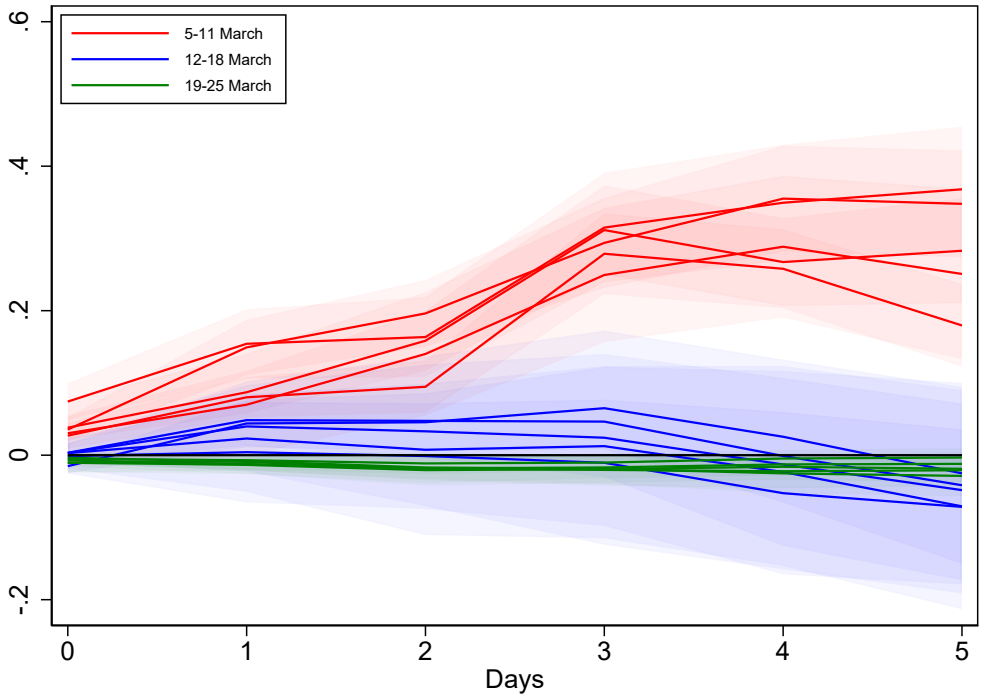

Note: Impulse responses are computed following equation (II.2). Impulse response coefficients $\beta_{b,h}$ are estimated before splitting dates: $\bar{t} \in \{3/5, ..., 3/11\}$ in red, $\bar{t} \in \{3/12, ..., 3/18\}$ in blue, and $\bar{t} \in \{3/19, ..., 3/25\}$ in green. Shaded area represents the 95% confidence interval for each coefficient.

Table II.D.5 – Chow test (p-values, second lagged value of new cases)

	Horizon					
	h=0	h=1	h=2	h=3	h=4	h=5
March 5	0.01	0.00	0.00	0.00	0.00	0.00
March 6	0.00	0.00	0.00	0.00	0.00	0.00
March 9	0.00	0.00	0.00	0.00	0.00	0.00
March 10	0.00	0.00	0.00	0.00	0.00	0.00
March 11	0.17	0.05	0.00	0.00	0.00	0.00
March 12	0.01	0.01	0.03	0.03	0.55	0.69
March 13	0.54	0.01	0.07	0.21	1.00	0.52
March 16	0.55	0.18	0.49	0.72	0.87	0.49
March 17	0.73	0.48	0.87	0.82	0.72	0.31
March 18	0.98	0.84	0.99	0.82	0.34	0.18
March 19	0.11	0.34	0.04	0.07	0.07	0.05
March 20	0.46	0.22	0.03	0.06	0.07	0.07
March 23	0.13	0.06	0.06	0.05	0.10	0.07
March 24	0.12	0.12	0.08	0.03	0.13	0.17
March 25	0.19	0.41	0.16	0.11	0.53	0.75

Note: p-values of Chow statistics from the test.

Growth rate of total cases. In our baseline estimation, we consider $\Delta x_{i,t}$ as the daily change in the number of total cases per million people between t and $t-1$, denoted $x_{i,t}$. Here, we take the daily change in the logarithm of the number of cases per million people as an alternative variable, that is, $\Delta \log x_{i,t}$. This specification takes into account the shape of the pandemic by considering the relative instead of absolute change in $x_{i,t}$. The results reported in Figure II.D.6 and Table II.D.6 indicate that when we consider the log difference, the occurrence of COVID-19 cases has no significant effects on the sovereign spreads, regardless of the break date considered. Our model indicates that $\Delta x_{i,t}$ has a strong and significant effect on sovereign spreads, while $\Delta \log x_{i,t}$ has no effect. Considering that the growth rate is the typical measure used for economic variables with a trend (such as output or prices), it may not be relevant for measuring the outbreak of a pandemic, which has a stretched S-shaped (or sigmoid) growth curve. Indeed, at the start of the pandemic, the very small number of total cases made the growth rate extremely high with each new confirmed case. Then, the growth rate sharply decreased with the development of the pandemic. This may explain why sovereign markets did not react to the growth rate of COVID-19 cases. Moreover, sovereign markets (and financial markets in general) are well known to be highly sensitive to news published in the press and social media. As mentioned before, the very popular figures published and massively distributed by the *Financial Times* (among others) show the path of the number of total or new cases in absolute terms but never in terms of the growth rate (as a percentage of the number of total cases already reported). Since we focus on the first few weeks of the pandemic in Europe, we keep the variation in the total number of cases as our benchmark. Moreover, we consider this series in extra specifications to test whether the impact of new cases on sovereign spreads is robust to the inclusion of various controls for the shape of the pandemic.

Figure II.D.6 – Impulse responses of 10-year government bond spreads to the growth rate of total COVID-19 cases in the euro area

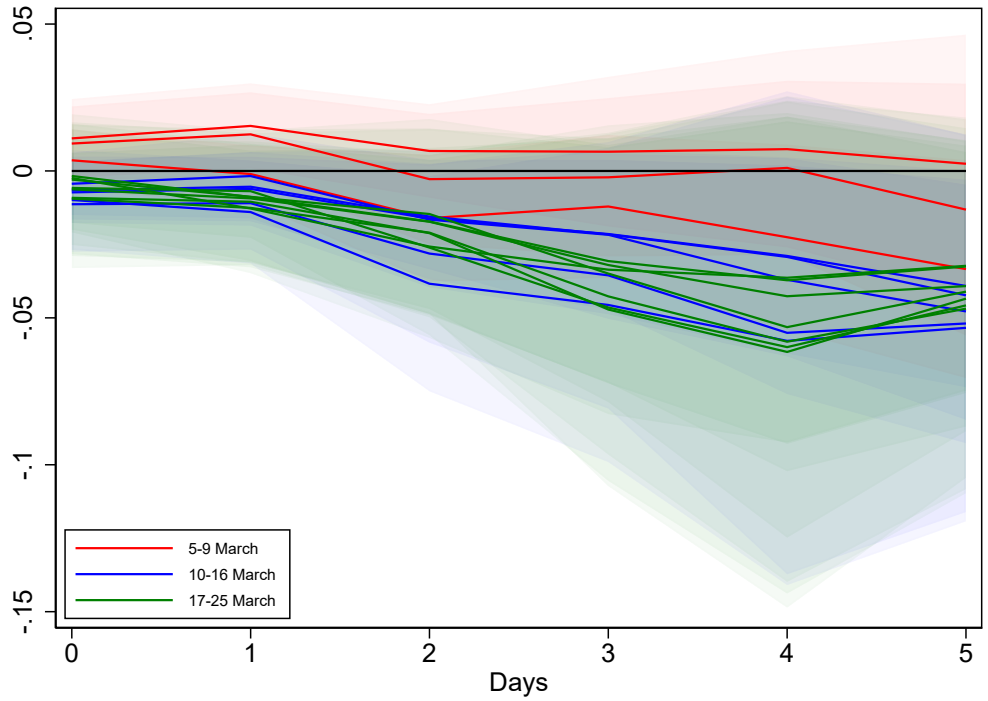

Note: Impulse responses are computed following equation (II.2). Impulse response coefficients $\beta_{b,h}$ are estimated before splitting dates: $\bar{t} \in \{3/5, ..., 3/9\}$ in red, $\bar{t} \in \{3/10, ..., 3/16\}$ in blue, and $\bar{t} \in \{3/17, ..., 3/25\}$ in green. Shaded area represents the 95% confidence interval for each coefficient.

Table II.D.6 – Chow test (p-values, new cases growth rate)

	Horizon					
	h=0	h=1	h=2	h=3	h=4	h=5
March 5	0.33	0.15	0.12	0.09	0.12	0.12
March 6	0.33	0.13	0.12	0.09	0.08	0.10
March 9	0.48	0.32	0.37	0.14	0.42	0.69
March 10	0.93	0.48	0.33	0.25	0.60	0.88
March 11	0.96	0.38	0.35	0.27	0.70	0.62
March 12	0.89	0.44	0.40	0.33	0.99	0.18
March 13	0.89	0.61	0.78	0.74	0.12	0.10
March 16	0.76	0.95	0.45	0.48	0.19	0.28
March 17	0.68	0.56	0.89	0.54	0.26	0.27
March 18	0.80	0.86	0.84	0.44	0.23	0.28
March 19	0.59	0.73	0.89	0.48	0.23	0.35
March 20	0.57	0.37	0.36	0.90	0.20	0.23
March 23	0.72	0.25	0.29	0.87	0.40	0.54
March 24	0.13	0.13	0.37	0.43	0.99	0.84
March 25	0.16	0.17	0.54	0.53	0.90	0.76

Note: p-values of Chow statistics from the test.

II.E Robustness: Controlling for the shape of the pandemic

Table II.E.1 – Dependent variable 10-year spread controlling for the growth rate of total cases (before and after March 9)

	Day 0	Day 1	Day 2	Day 3	Day 4	Day 5
new cases – *before*	0.057***	0.101***	0.164***	0.236***	0.268***	0.407***
	(0.02)	(0.03)	(0.04)	(0.05)	(0.06)	(0.08)
new cases – *after*	0.000	-0.000	-0.001	-0.001	0.000	0.001
	(0.00)	(0.00)	(0.00)	(0.00)	(0.00)	(0.00)
growth of total cases – *before*	0.006	0.002	-0.011	-0.004	-0.014	-0.020
	(0.01)	(0.01)	(0.01)	(0.01)	(0.02)	(0.02)
growth of total cases – *after*	-0.042	-0.070	-0.089	-0.176	-0.115	-0.080
	(0.06)	(0.07)	(0.08)	(0.11)	(0.11)	(0.08)
R^2	0.508	0.547	0.589	0.617	0.645	0.678
Observations	893	870	853	840	828	815

Note: * $p < 0.10$, ** $p < 0.05$, *** $p < 0.01$. Clustered standard errors by country in parentheses. This table reports the $\beta_{b,h}$ and $\beta_{a,h}$ coefficients introduced in the regression equation (II.4) for $\bar{t} = \{3/9\}$. The new cases variable is measured as the daily change in the number of total cases per 100,000 people. The growth rate of total cases is measured as the first-difference (daily change) of the logarithm of the number of total cases.

Table II.E.2 – Dependent variable 10-year spread controlling for the log of total cases (before and after March 9)

	Day 0	Day 1	Day 2	Day 3	Day 4	Day 5
new cases – *before*	0.019	0.023	0.092**	0.136***	0.180***	0.355***
	(0.01)	(0.02)	(0.04)	(0.05)	(0.05)	(0.07)
new cases – *after*	-0.000	-0.001	-0.001	-0.002**	-0.001	-0.001
	(0.00)	(0.00)	(0.00)	(0.00)	(0.00)	(0.00)
total cases (log) – *before*	0.011***	0.020**	0.021**	0.026**	0.027*	0.016
	(0.00)	(0.01)	(0.01)	(0.01)	(0.01)	(0.01)
total cases (log) – *after*	0.005	0.011	0.019	0.029	0.026	0.027
	(0.01)	(0.02)	(0.03)	(0.03)	(0.03)	(0.04)
R^2	0.511	0.555	0.598	0.621	0.643	0.677
Observations	917	894	877	863	851	838

Note: * $p < 0.10$, ** $p < 0.05$, *** $p < 0.01$. Clustered standard errors by country in parentheses. This table reports the $\beta_{b,h}$ and $\beta_{a,h}$ coefficients introduced in the regression equation (II.4) for $\bar{t} = \{3/9\}$. The new cases variable is measured as the daily change in the number of total cases per 100,000 people. The log of total cases is measured as the logarithm of the number of total cases per 100,000 people.

Table II.E.3 – Dependent variable 10-year spread controlling for lagged values of new cases (before and after March 9)

	Day 0	Day 1	Day 2	Day 3	Day 4	Day 5
new cases – *before*	0.057***	-0.014	0.019	0.022	-0.018	0.225***
	(0.01)	(0.02)	(0.02)	(0.03)	(0.02)	(0.04)
new cases – *after*	0.000	0.000	-0.000	-0.001	0.000	0.001
	(0.00)	(0.00)	(0.00)	(0.00)	(0.00)	(0.00)
L1.new cases – *before*	-0.097***	-0.015	0.046**	-0.042*	0.217***	0.139***
	(0.01)	(0.02)	(0.02)	(0.02)	(0.02)	(0.02)
L2.new cases – *before*	0.059***	0.172***	0.153***	0.308***	0.222***	0.083**
	(0.01)	(0.02)	(0.03)	(0.03)	(0.03)	(0.03)
L1.new cases – *after*	-0.000	-0.000	-0.001	0.000	0.001	-0.000
	(0.00)	(0.00)	(0.00)	(0.00)	(0.00)	(0.00)
L2.new cases – *after*	-0.001	-0.001	-0.000	0.000	-0.001	-0.001
	(0.00)	(0.00)	(0.00)	(0.00)	(0.00)	(0.00)
R^2	0.497	0.540	0.577	0.607	0.627	0.644
Observations	1354	1329	1312	1298	1285	1273

Note: * $p < 0.10$, ** $p < 0.05$, *** $p < 0.01$. Clustered standard errors by country in parentheses. This table reports the $\beta_{b,h}$ and $\beta_{a,h}$ coefficients introduced in the regression equation (II.4) for $\bar{t} = \{3/9\}$. The new cases variable is measured as the daily change in the number of total cases per 100,000 people. The lagged values of new cases are measured as the first and second lags of new cases per 100,000 people.

Table II.E.4 – Dependent variable 10-year spread controlling for new cases in first-difference (before and after March 9)

	Day 0	Day 1	Day 2	Day 3	Day 4	Day 5
new cases – *before*	-0.001	0.086***	0.166***	0.184***	0.352***	0.417***
	(0.01)	(0.02)	(0.03)	(0.03)	(0.04)	(0.04)
new cases – *after*	-0.000	-0.001	-0.001	-0.001	0.000	-0.000
	(0.00)	(0.00)	(0.00)	(0.00)	(0.00)	(0.00)
D.new cases – *before*	0.073***	-0.053***	-0.104***	-0.074**	-0.311***	-0.171***
	(0.01)	(0.02)	(0.02)	(0.02)	(0.03)	(0.02)
D.new cases – *after*	0.000	0.001	0.001	-0.000	-0.000	0.001
	(0.00)	(0.00)	(0.00)	(0.00)	(0.00)	(0.00)
R^2	0.499	0.541	0.576	0.593	0.612	0.634
Observations	1374	1349	1331	1316	1304	1291

Note: * $p < 0.10$, ** $p < 0.05$, *** $p < 0.01$. Clustered standard errors by country in parentheses. This table reports the $\beta_{b,h}$ and $\beta_{a,h}$ coefficients introduced in the regression equation (II.4) for $\bar{t} = \{3/10\}$. The new cases variable is measured as the daily change in the number of total cases per 100,000 people. The new cases variable (in first-difference) is measured as the daily change in the number of new cases per 100,000 people.

II.F Robustness: Public debt-to-GDP

Figure II.F.1 – Impulse responses of 10-year government bond spreads to new COVID-19 cases in the euro area

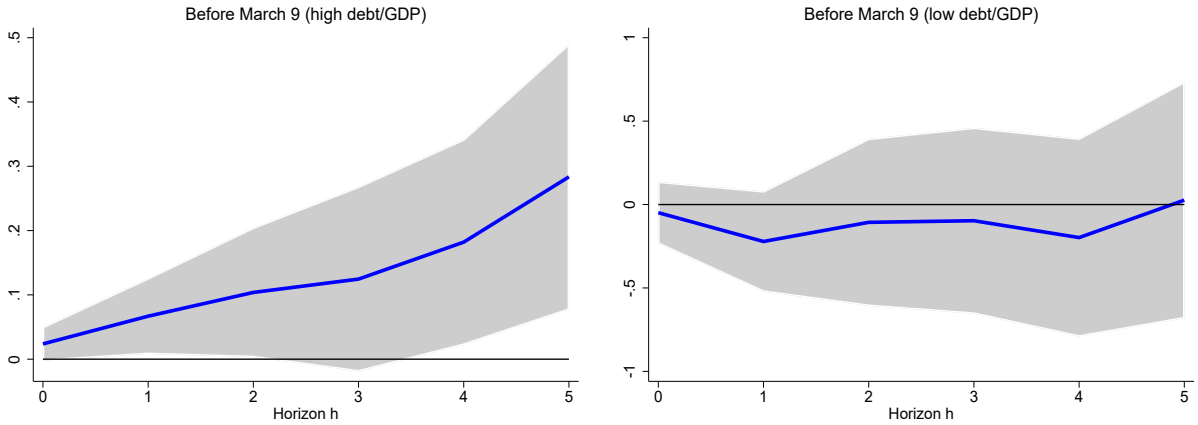

Note: Impulse responses are computed following equation (II.2). Left panel shows coefficient $\beta_{b,h}$ for countries with a high debt/GDP ratio, whereas right panel shows coefficient $\beta_{b,h}$ for countries with a low debt/GDP ratio. Both panels show response coefficients estimated before the splitting date. Grey shaded area represents the 95% confidence interval.

Table II.F.1 – Chow test (p-values) for high debt/GDP subsample of countries

	Horizon					
	h=0	h=1	h=2	h=3	h=4	h=5
March 5	0.17	0.55	0.89	0.11	0.05	0.02
March 6	0.08	0.83	0.11	0.06	0.05	0.01
March 9	0.06	0.03	0.04	0.08	0.03	0.02
March 10	0.13	0.38	0.89	0.22	0.18	0.19
March 11	0.46	0.87	0.96	0.39	0.39	0.56
March 12	0.68	0.81	0.95	0.54	0.73	1.00
March 13	0.51	0.84	0.78	0.86	0.55	0.66
March 16	0.46	0.74	0.99	0.88	0.58	0.63
March 17	0.88	0.63	0.39	0.63	0.31	0.14
March 18	0.93	0.40	0.28	0.33	0.13	0.09
March 19	0.57	0.46	0.26	0.18	0.13	0.11
March 20	0.50	0.42	0.19	0.20	0.17	0.17
March 23	0.54	0.27	0.18	0.18	0.21	0.20
March 24	0.98	0.28	0.38	0.72	0.94	0.94
March 25	0.80	0.48	0.79	0.93	0.84	0.69

Note: p-values of Chow statistics from the test.

II.G COVID-induced stock market crash in the euro area

Figure II.G.1 – Impulse responses of stock market indices (in log) to new COVID-19 cases in the euro area

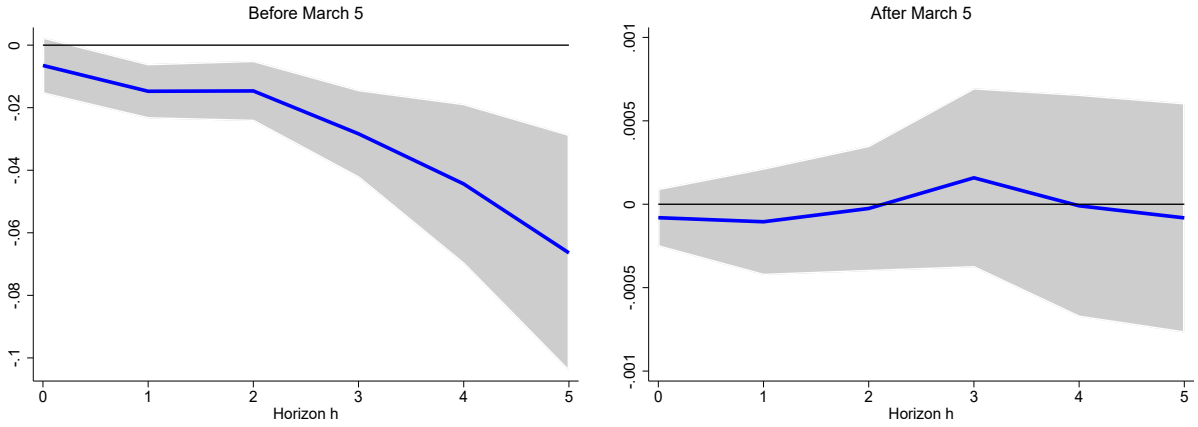

Note: Impulse responses represent $\beta_{b,h}$ and $\beta_{a,h}$ coefficients from equation (II.6). Left panel shows coefficient $\beta_{b,h}$ (before the splitting date), whereas right panel shows coefficient $\beta_{a,h}$ (after the splitting date). Grey shaded area represents the 95% confidence interval.

Figure II.G.2 – Impulse responses of stock market indices (in log) to new COVID-19 cases in the euro area

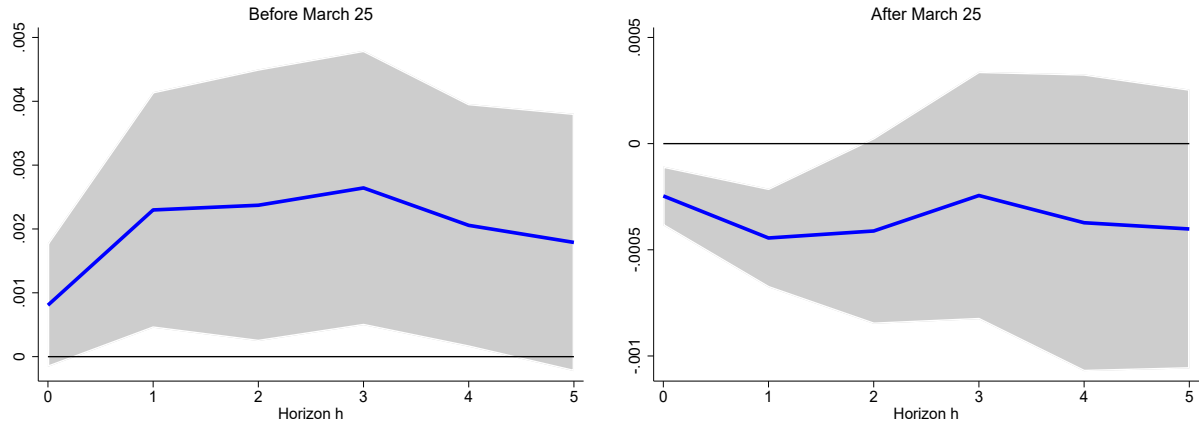

Note: Impulse responses represent $\beta_{b,h}$ and $\beta_{a,h}$ coefficients from equation (II.6). Left panel shows coefficient $\beta_{b,h}$ (before the splitting date), whereas right panel shows coefficient $\beta_{a,h}$ (after the splitting date). Grey shaded area represents the 95% confidence interval.

Figure II.G.3 – Evolution of impulse response coefficients by horizon

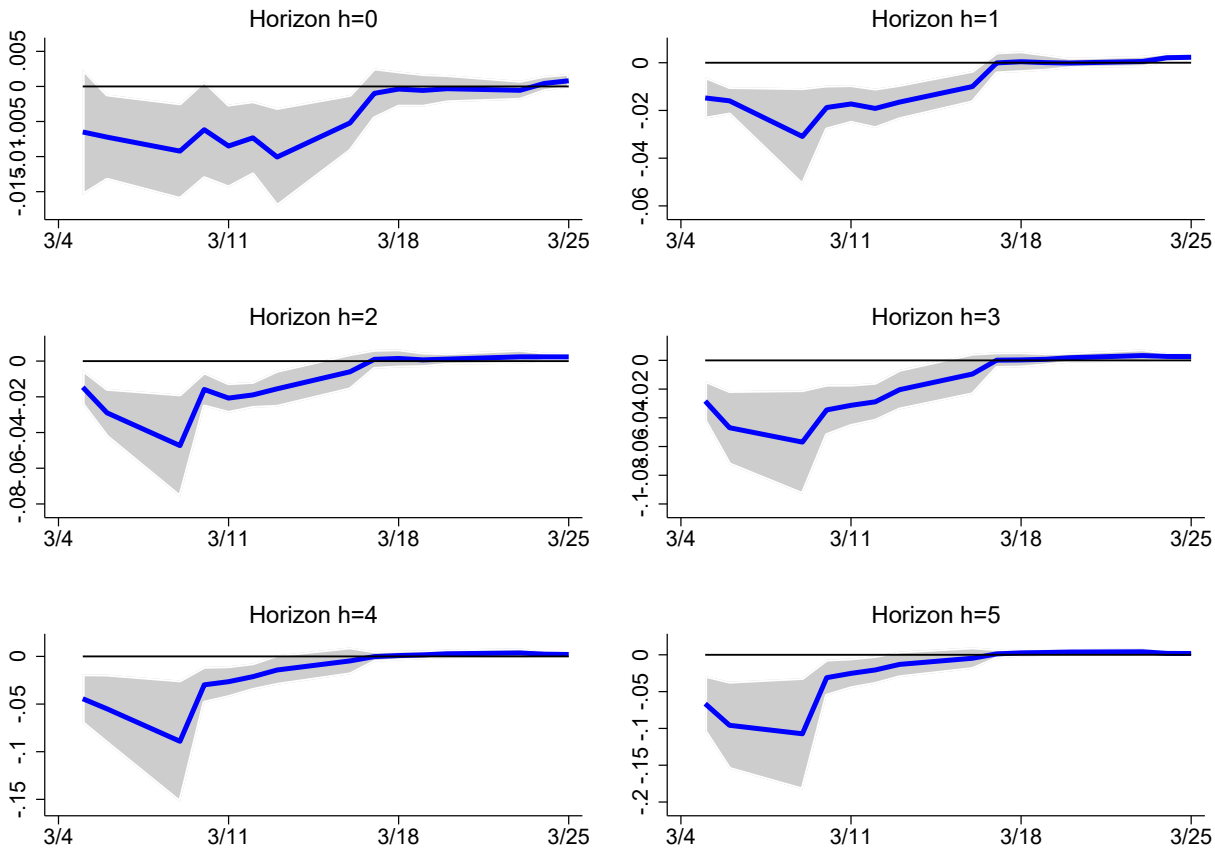

Note: Impulse responses represent $\beta_{b,h}$ coefficients from equation (II.6). Each panel shows impulse response coefficients $\beta_{b,h}$ estimated before splitting dates $\bar{t} \in \{3/5, ..., 3/25\}$ at different horizon. Grey shaded area represents the 95% confidence interval.

Table II.G.1 – Dependent variable log of stock market indices (before and after March 9)

	Day 0	Day 1	Day 2	Day 3	Day 4	Day 5
new cases – *before*	-0.009**	-0.031***	-0.047***	-0.057***	-0.089***	-0.107***
	(0.00)	(0.01)	(0.01)	(0.02)	(0.03)	(0.04)
new cases – *after*	-0.000	-0.000	-0.000	0.000	-0.000	-0.000
	(0.00)	(0.00)	(0.00)	(0.00)	(0.00)	(0.00)
R^2	0.719	0.732	0.764	0.794	0.816	0.831
Observations	1374	1350	1334	1320	1308	1294

Note: * $p < 0.10$, ** $p < 0.05$, *** $p < 0.01$. Clustered standard errors by country in parentheses. This table reports the $\beta_{b,h}$ and $\beta_{a,h}$ coefficients introduced in the regression equation (II.6) for $t < \{3/9\}$. The new cases variable is measured as the daily change in the number of total cases per 100,000 people.

Chapter III

The Risk of Inflation Dispersion in the Euro Area

Abstract. *We document the time-varying divergence of predictive inflation distributions across euro area countries and explore their macroeconomic origins. While the dispersion of inflation rates mainly concerns upside inflation risks during the first decade of the euro area, it shifted to downside inflation risks during the second decade. The dispersion of downside and upside risks to inflation reaches record levels in the wake of the COVID crisis. The main determinant of the dispersion at the bottom of the distribution is the development of financial stress. In the wake of the COVID crisis, value chain pressures drove the dispersion of upside inflation risks. Overall, the dispersion of inflation rates is largely caused by heterogeneous Phillips curves between countries rather than by different national economic contexts.*

III.1 Introduction

Our objective in this paper is to document the time-varying divergence in the predictive inflation distributions across euro area countries and explore their macroeconomic origins. Fluctuations in the dispersion of the *conditional mean* of inflation between countries over time are a well-known phenomenon. Average inflation differentials between countries show a clear cyclical pattern, rising sharply in economic downturns and falling in booms, as shown in Figure III.1.1. The literature has been widely devoted to studying the key drivers behind these cross-country

differences. By contrast, the study of the divergences in the *tails* of the inflation distribution remains completely unexplored. Yet, the dispersion of inflation in the euro area (both headline and core) appears to be more pronounced in the tails of the distribution than in the middle, as shown in Table III.1.1. The (unconditional) standard deviation across countries of inflation (both headline and core) tends to be two to three times higher in the 10^{th} and 90^{th} quantiles than that in the median. In this paper, we aim at providing a more complete picture of inflation differentials across euro area countries by delivering measures of inflation dispersion over time associated to the different quantiles of the predictive inflation distributions, and at identifying their main drivers.

Our approach builds on the concept of inflation-at-risk developed by Andrade et al. (2014), Banerjee et al. (2020), and López-Salido and Loria (2022), which is itself highly related to that of Growth-at-Risk developed by Adrian et al. (2019).[1] Inflation-at-risk approach aims at forecasting shifts in the tails of inflation distribution. López-Salido and Loria (2022) provide an in-depth analysis of inflation-at-risk in the euro area and the U.S. grounded on a quantile Phillips curve. Here, we are not interested in the inflation risk for one country *per see*, but in the dispersion of these inflation risks between euro area countries.

The literature on inflation-at-risk is relatively silent when it comes to the analysis of this risk of inflation dispersion. However, as for inflation itself, it is critical for the policy maker to know what type of tail risks (upside or downside) are causing the dispersion of inflation especially in a monetary union. The conduct of a single monetary policy, with a common inflation target, is indeed more difficult if countries have diverging inflation rates. Countries with high inflation differentials will suffer from inappropriate monetary policy decisions with respect to their specific economic context. Inflation dispersion at the bottom of the inflation distribution exposes diverging economies to the risk of costly deflation due to nominal downward rigidity while at the top of the distribution, diverging economies are exposed to the risk of inflationary spirals.

To elaborate our measure of risk of inflation dispersion, we proceed as follows. Firstly, we estimate a quantile Phillips curve based on López-Salido and Loria (2022) for each euro area country and not for the euro area as a whole as done by these authors. We can then compute the predictive inflation distributions by country. Conditional quantiles vary over time according to the evolution of key economic and financial variables included in the Phillips curve (namely, past

[1] See also Plagborg-Møller et al. (2020) and Figueres and Jarociński (2020) for an application to the euro area.

Figure III.1.1 – Cross-sectional standard deviation of inflation rates in the euro area

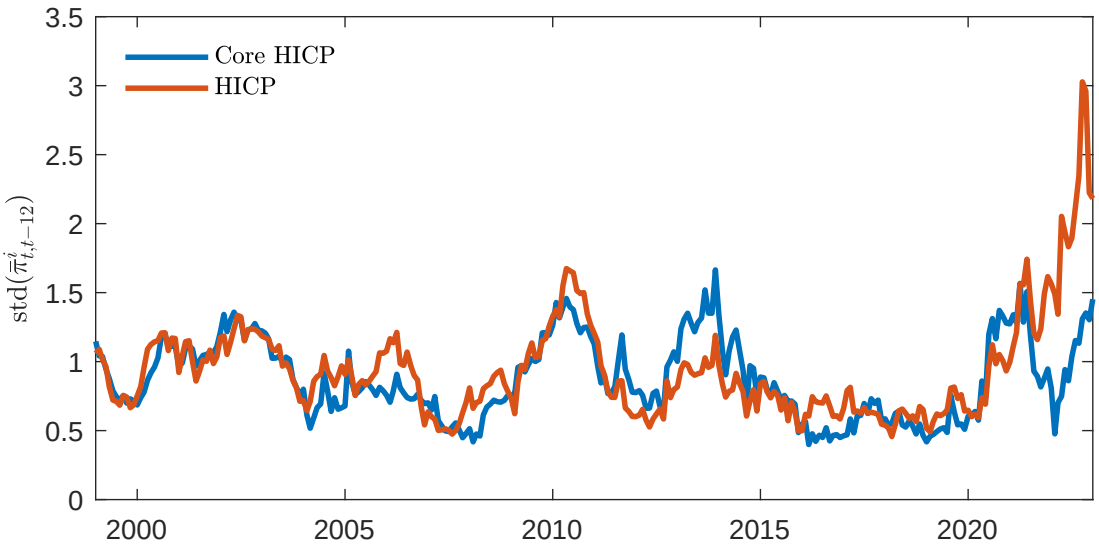

Note: $\bar{\pi}^i_{t,t-12}$ denotes the average over the last 12 months of the monthly inflation rate (core and headline inflation rates, annualized) for the country i of the euro area (12 countries, fixed composition, Austria, Belgium, Finland, France, Germany, Greece, Ireland, Italy, Luxembourg, Netherlands, Portugal, Spain). The sample is January 1999 to January 2023. The figure shows the cross-country unweighted standard deviation of annual inflation rates in the euro area. See Section III.A in the online appendix for data description.

and expected inflation rates, unemployment gap, financial stress, oil inflation, and supply chain pressures). Secondly, for each date, we compute the standard deviation across these national quantiles of inflation. By looking at the different quantiles of the inflation distribution, we can evaluate the cross-country dispersion of the inflation-at-risk at the bottom of the distribution (i.e. the risk of low inflation or deflation) and at the top of the distribution (i.e. the risk of excessive inflation). Third, we investigate the drivers of inflation dispersion by considering various scenarios regarding the national economic series and the structure of the Phillips curve.

Table III.1.1 – Moments of inflation by country

	Core HICP				HICP			
	Mean	Median	10^{th}	90^{th}	Mean	Median	10^{th}	90^{th}
Germany	1.25	1.12	0.42	2.24	1.78	1.48	0.31	3.58
France	1.19	1.15	0.53	1.90	1.70	1.52	0.67	2.94
Italy	1.76	1.78	0.75	2.76	1.77	1.69	0.22	3.43
Spain	1.71	1.68	0.27	3.20	2.28	2.06	-0.12	4.98
Netherlands	1.72	1.43	0.60	3.14	2.23	1.78	0.43	4.50
Finland	1.44	1.30	0.48	2.57	1.81	1.50	0.28	3.68
Ireland	1.52	1.50	-0.88	3.98	1.88	1.66	-0.87	4.92
Austria	1.85	1.70	1.06	2.82	2.09	1.81	0.70	3.79
Portugal	1.66	1.47	-0.03	3.61	2.03	1.75	-0.13	4.55
Belgium	1.75	1.63	1.16	2.49	2.13	2.00	0.62	3.82
Luxembourg	1.80	1.70	1.13	2.58	2.55	2.33	0.49	4.88
Greece	1.44	1.48	-1.23	4.08	2.10	1.86	-0.87	5.42
Mean	1.59	1.50	0.36	2.95	2.03	1.79	0.14	4.21
Std. Dev.	0.22	0.22	0.75	0.68	0.25	0.25	0.55	0.77

Note: Mean, median, 10^{th} and 90^{th} quantiles for each country of the euro area (12 countries, fixed composition: Austria, Belgium, Finland, France, Germany, Greece, Ireland, Italy, Luxembourg, Netherlands, Portugal, Spain). The sample is January 1999 to January 2023. The last two rows are the unweighted means and the standard deviations of moments across countries. See Section III.A in the online appendix for data description.

We apply this framework to a euro area made from its first 12 member countries (Austria, Belgium, Finland, France, Germany, Greece[2], Ireland, Italy, Luxembourg, Netherlands, Portugal, Spain). We restrict ourselves to this euro area with fixed composition to avoid the dispersion of inflation rates that would result from changes in the composition of the euro area due to the more recent entry of countries. The analysis is done for the period starting in January 1999, at the creation of the euro, to January 2023. Our main results are as follows.

1. There has been a shift in the nature of inflation dispersion in the euro area. While the dispersion of inflation rates mainly concerns the top of the distribution during the first decade of the euro area, it shifted to the bottom of the distribution during the second decade of the euro area.

2. The dispersion of inflation-at-risk reaches record levels in the wake of the COVID crisis, a period marked by international tensions on energy prices and supply chains.

3. The main determinant of this dispersion at the bottom of the distribution was the evolution of financial stress associated with the financial and sovereign debt crisis.

[2]We include Greece in our sample even though it officially adopted the euro in 2001, two years after its creation.

4. In the wake of the COVID crisis, value chain pressures drove the dispersion of inflation at the top of the distribution.

5. Overall, the dispersion of inflation rates is largely caused by heterogeneous Phillips curves between countries rather than by different national economic contexts.

Relation to other studies. Our paper contributes to the literature on inflation dynamics in the euro area context. We contribute to the literature on inflation dispersion, which has been a long-standing issue in the European Monetary Union. Inflation dispersion was an important issue in defining the ECB's strategy at its inception, see Issing et al. (2003), as well as in its recent strategy review in 2021 as discussed in depth by Consolo et al. (2021) and Reichlin et al. (2021). Recent papers show the renewed interest in inflation differentials in the euro area. Among them, Checherita-Westphal et al. (2023) empirically study the role of fiscal policy on inflation differentials in the EMU. It is also worth mentioning that inflation differentials per see may not be detrimental to the monetary union if they reflect the process of nominal convergence and economic development catch up. That being said, as highlighted by the ECB (2005), it is necessary to assess the underlying causes of inflation differentials observed at the early stage of the euro area to formulate the most appropriate monetary policy response.[3] Inflation differentials in the euro area has also been discussed in the academic literature. Angeloni and Ehrmann (2007) investigate the sources of euro area inflation differentials from 1998 to 2003. As a result, they identify that demand shocks have been the main source of inflation differentials in the early years of the EMU, followed by cost-push shocks and exchange rate shocks. Beck et al. (2009) decompose regional inflation rates into a common area-wide, a country-specific and an idiosyncratic regional component. They warn of the potential high welfare costs that may represents inflation differentials fueled by national economic distortions. Estrada et al. (2013) explore the role of EMU in inflation convergence/divergence among euro area countries. Despite persistent inflation differentials in the euro area, they do find any critical role for the EMU in inflation convergence in the euro area. Haan (2010) offers a survey of this abundant literature subsequent to the creation of the euro area. We revisit this literature by providing a more complete picture of inflation differentials across euro area countries through measures of inflation dispersion associated to the different quantiles of the predictive inflation distributions.

We also contribute to the literature on the estimation of the Phillips curve. Since recent

[3] Cœuré (2019) underlines how the ECB has always found a way to deal with the heterogeneity that could have impaired the transmission of monetary policy across euro area countries.

debates have focused on the death (and the revival) of the Phillips curve, and especially in the U.S. (see Blanchard et al. (2015), Coibion and Gorodnichenko (2015), Coibion et al. (2019), Del Negro et al. (2020) and Hazell et al. (2022), among others), little recent evidence have been put forward regarding the Phillips curve in the euro area. Importantly, and in line with our paper, Ball and Mazumder (2021) focus on an estimated Phillips curve using euro area core inflation. Their results suggest a non-negligible role of inflation expectations and output gap in driving core inflation fluctuations in the euro area. Eser et al. (2020) give a broad picture of the implication of the Phillips curve analysis in the euro area for the conduct of ECB's monetary policy. The article of this literature that is closest to ours is López-Salido and Loria (2022) who bring to this Phillips curve literature the quantile analysis to highlight the role of financial conditions in the downside risk to inflation. Our contribution to this literature is to elaborate cross-country measures of risk dispersion. Using national data of euro area members, we show that there are contrasting responses to economic and financial variables between the inflation tails and median.

The rest of the paper is organized as follows. Section III.2 describes the empirical strategy to estimate the inflation-at-risk by country and then compute measures of inflation-at-risk dispersion. Section III.3 examines the evolution of the risk of inflation dispersion in the euro area. Section III.4 discusses the drivers of inflation dispersion. Section III.5 conducts robustness checks by performing a Markov-switching approach. Section III.6 concludes.

III.2 Empirical Strategy

In the existing literature, the study of the determinants of cross-country dispersion of the conditional mean of inflation has been an important step to assess the relevance of regional divergence within the euro area for economic policies and the single monetary policy. To provide a more complete picture, we examine the entire inflation distribution, with a particular focus on the response of the tails of the predictive inflation distribution to economic and financial developments.

This section presents the general methodology employed in this paper. Section III.2.1 discusses the baseline statistical model in which conditional inflation quantiles are expressed as a function of economic and financial conditions for each country. By doing so, we are able to study the reaction of each quantile of the distribution of future inflation as a function

of the state of the economy, with a particular focus on lower and higher quantiles. Section III.2.2 shows how to use the quantiles to approximate the entire inflation distribution using a flexible yet parametric specification. This allows us to capture the first four moments and to show probability density functions. Finally, Section III.2.3 describes our different measures of cross-country dispersion of inflation risks.

We use augmented quantile Phillips curve models along the lines of López-Salido and Loria (2022) to examine the effects of different factors on inflation differentials across euro area countries. That is, we extend the model by incorporating a measure of global supply chain pressure to take into account supply chain disruptions that have harmed the global economy since the start of the COVID-19 pandemic. Many commentators have perceived such disruptions as having been a key driver of the rise and fall of inflation over the recent period. Once our augmented model is estimated for each country, we are able to deliver measures of cross-country inflation dispersion over time associated to the different quantiles of inflation distribution. By doing so, we test the role of different risk factors on the inflation differentials of mean versus the tail risks of the inflation distributions.

III.2.1 Phillips Curve Quantile Regressions

We rely on quantile regression models for studying the determinants of cross-country dispersion of the entire distribution of inflation. Let us denote by $\bar{\pi}^i_{t+1,t+h}$ the annualized average growth rate of core Harmonized Index of Consumer Prices (HICP) between $t+1$ and $t+h$ for country i, and by x^i_t a $1 \times k$-dimensional vector containing the conditioning variables for country i, including a constant. Our benchmark for the the horizon is $h = 12$, that is the average inflation over the next year.

Following López-Salido and Loria (2022), we consider a linear model for the conditional inflation quantiles whose predicted value:

$$\hat{Q}_\tau(\bar{\pi}^i_{t+1,t+h}|x^i_t) = x^i_t \hat{\beta}^i_\tau, \tag{III.1}$$

is a consistent linear estimator of the quantile function of $\bar{\pi}^i_{t+1,t+h}$ conditional on x^i_t; where $\tau \in (0,1)$, $\hat{\beta}^i_\tau$ is a $k \times 1$-dimensional vector of estimated quantile-specific parameters.

Our model for conditional inflation quantile augments the Phillips curve model used in the

literature as follows:

$$\hat{Q}_\tau(\bar{\pi}^i_{t+1,t+h}|x^i_t) = \hat{\mu}^i_\tau + \left(1-\hat{\lambda}^i_\tau\right)\pi^{*,i}_{t-1} + \hat{\lambda}^i_\tau \pi^{LTE,i}_t + \hat{\theta}^i_\tau\left(u^i_t - u^{*,i}_t\right) + \hat{\gamma}^i_\tau\left(\pi^{o,*}_t - \pi^{*,i}_t\right) + \hat{\delta}^i_\tau f^i_t + \hat{\phi}^i_\tau sc_t, \tag{III.2}$$

where all variables are monthly time series covering January 1999 through January 2023. Data sources are presented in Appendix III.A.

The variables $\pi^{*,i}_{t-1}$ and $\pi^{LTE,i}_t$ represent average inflation over the previous twelve months and a measure of long-term inflation expectations, respectively. The relative importance of both variables is determined by the parameter λ^i_τ. We impose $(1-\lambda^i_\tau)+\lambda^i_\tau = 1, 0 \leq (1-\lambda^i_\tau) \leq 1$ and $0 \leq \lambda^i_\tau \leq 1$, as in Blanchard et al. (2015) and López-Salido and Loria (2022)[4], using the inequality constrained quantile regression method developed by Koenker and Ng (2005). We use six- to ten-year-ahead inflation expectations from Consensus Economics as long-term inflation expectation series.

Our second risk factor is the unemployment gap measured as the difference between the unemployment rate u^i_t and the natural rate of unemployment $u^{*,i}_t$, which is obtained by applying the HP filter to the unemployment rate with the smoothing parameter equal to 14,400. The parameter θ^i_τ captures the slope of the Phillips curve at various inflation quantiles. Following Blanchard et al. (2015), we impose $\theta^i_\tau \leq 0$.

The third risk factor $\pi^{o,*}_t - \pi^{*,i}_t$ represents variations in relative oil price, where $\pi^{o,*}_t$ is the average inflation over the previous twelve months of crude oil price. This allows to capture the pass-through of oil prices into core inflation measures.[5] The literature provides mixed evidence of the role of energy price and import prices as a key inflation determinant. For instance, Kilian and Zhou (2021) find that gasoline prices do not explain the improved fit of the Phillips curve augmented by household inflation expectations during the years that followed the Great Recession. On the other hand, Matheson and Stavrev (2013) find an increasing importance of import-price in explaining inflation fluctuations, while Salisu et al. (2018) point a better forecast performance when including oil prices into the Phillips curve. Based on an open-economy New Keynesian framework applied to U.K. data, Batini et al. (2005) provide further evidence of the benefits of augmenting the Phillips curve with oil price to fit the data. Our

[4] Hazell et al. (2022) impose $\lambda = 1$ to estimate U.S. regional Phillips curve.

[5] We also consider commodity and energy prices instead of oil price using the above-described specification of the augmented quantile Phillips curve. The results are robust to the choice of the series and are not reported here.

approach captures the effects of oil prices not only on the conditional mean of inflation, but on the entire inflation distribution. Cross-quantile and cross-country variations in the parameters γ_τ^i in Equation (III.2) capture its effects. Here again, we follow Blanchard et al. (2015) and impose $\gamma_\tau^i \geq 0$.[6]

The fourth risk factor f_t^i represents financial conditions. The literature has documented firms financing conditions also helps to explain inflation dynamics. Notable examples include Del Negro et al. (2015), Christiano et al. (2015) and Gilchrist et al. (2017). More importantly, López-Salido and Loria (2022) extend the analysis to consider the effect of financial conditions on the inflation distribution, with a particular focus on downside risks to inflation. Following these authors, we approximate f_t^i by the Composite Indicator of Systemic Stress (CISS) developed by Kremer et al. (2012), except for Luxembourg for which we use the Country-Level Index of Financial Stress (CLIFS) proposed by Peltonen et al. (2015). The CISS is a weekly index maintained by the ECB. It includes 15 raw series, mainly market-based financial stress measures that are split equally into five categories: financial intermediaries, money markets, equity markets, bond markets and foreign exchange markets. The CLIFS follows the approach of the CISS, but with slightly different market segments. The parameter associated with financial conditions in our empirical specification of the Phillips curve is δ_τ^i. This coefficient is left unconstrained in that case, since no consensus has been reached in the literature regarding the effect of financial conditions on the overall inflation distribution.

Finally, the last risk factor we consider is related to global supply chain pressures. Since the beginning of the COVID-19 pandemic, supply chain disruptions have become a major challenge for the global economy. Moreover, recent research by Peersman (2022) suggests that international food commodity prices explain a large part of variations in retail prices of food in the euro area through the food supply chain. We thus allow for supply chain conditions in Equation (III.2) to affect differently the conditional inflation quantiles. The variable sc_t is the global supply chain pressure index proposed by Benigno et al. (2022) and updated on a regular basis by the Federal Reserve Bank of New York. This series is built on variables that are meant to capture factors that put pressure on the global supply chain, both domestically and internationally. Its effects on the entire distribution of inflation is captured by the cross-quantile and cross-country parameters ϕ_τ^i. Following recent studies exploring the role of supply chain pressures in large post-COVID inflation fluctuations (see for instance Amiti et al., 2021

[6] Blanchard et al. (2015) consider import-price inflation in their estimated Phillips curve, that is proxied by oil price inflation at a monthly frequency in López-Salido and Loria (2022).

and Di Giovanni et al., 2022), we impose $\phi_\tau^i \geq 0$.

III.2.2 The Conditional Inflation Distribution

We generally report the direct estimates from the quantile regressions for the 10^{th}, the 50^{th}, and the 90^{th} percentiles. We also map the quantile regression estimates into a skewed t-distribution along the lines of Adrian et al. (2019) to recover and show a probability density function. The skewed t-distribution was developed by Azzalini and Capitanio (2003) and has the following form:

$$f(\bar{\pi}^i_{t+1,t+h}|x^i_t, \mu^i_t, \sigma^i_t, \eta^i_t, \kappa^i_t) = \frac{2}{\sigma^i_t} t(z^i_{t,t+h}; \kappa^i_t) T\left(\eta^i_t z^i_{t,t+h} \sqrt{\frac{\kappa^i_t + 1}{\kappa^i_t + (z^i_{t,t+h})^2}}; \kappa^i_t + 1\right) \tag{III.3}$$

where $z^i_{t,t+h} = \frac{\bar{\pi}^i_{t+1,t+h}(x_t) - \mu^i_t}{\sigma^i_t}$, and t and T represent the density and cumulative distribution function of the student t-distribution, respectively. The four time-varying parameters of the distribution pin down the location μ^i_t, scale σ^i_t, shape η^i_t, and fatness κ^i_t for each country i, where η^i_t and κ^i_t parameters control the skewness and the kurtosis of the distribution, respectively.

For each month and each country, we choose the four parameters (μ_t, σ_t, η_t, κ_t) of the skewed t-distribution to minimize the squared distance between our estimated quantile function $\hat{Q}_\tau(\bar{\pi}^i_{t+1,t+h}|x^i_t)$ obtained from the quantile Phillips curve model in Equation (III.2) and the quantile function of the skew t-distribution to match the 5^{th}, 25^{th}, 75^{th} and 95^{th} quantiles.

III.2.3 Measuring Dispersion in Tail Risks

Using our estimated predictive densities, we can construct informative measures of downside and upside risks. For each county, we define the concept of Inflation-at-Risk (IaR), the value at risk of future inflation. As made clear in López-Salido and Loria (2022), estimating the x^{th} quantile of the predictive inflation distribution is similar to constructing IaR measures at $x\%$. Hence, we refer to IaR to measure the probability that inflation falls below or above a given value in each country of our sample. IaR is defined by the quantiles of inflation rates for a given probability α between periods t and $t+h$ given x^i_t (the information set available at time t for country i). To distinguish downside and upside risks, we define the downside IaR as

$$\Pr\left(\bar{\pi}^i_{t+1,t+h} \leq {}^{-}\text{IaR}^i_{t+h}\left(\alpha|x^i_t\right)\right) = \alpha, \tag{III.4}$$

where ${}^{-}\text{IaR}^{i}_{t+h}(\alpha|x^{i}_{t})$ is the downside IaR for country i in h months in the future at α probability, typically equal to 10% in our empirical application. The upside IaR is defined as follows

$$\Pr\left(\bar{\pi}^{i}_{t+1,t+h} \geq {}^{+}\text{IaR}^{i}_{t+h}\left(\alpha|x^{i}_{t}\right)\right) = \alpha, \tag{III.5}$$

where ${}^{+}\text{IaR}^{i}_{t+h}(\alpha|x^{i}_{t})$ is the upside IaR for country i in h months in the future at α probability.

Alternatively, we also rely on expected shortfall and longrise measures, which capture the severity of an event that occurs in either the left tail (for expected shortfall) or right tail (for expected longrise) of the predictive distribution. These two measures can be written as follows:

$$\text{SF}^{i}_{t+h} = \frac{1}{p}\int_{0}^{p} \hat{F}^{-1}_{\bar{\pi}^{i}_{t+1,t+h}|x^{i}_{t}}(\tau|x^{i}_{t})\,\mathrm{d}\tau, \qquad \text{LR}^{i}_{t+h} = \frac{1}{p}\int_{1-p}^{1} \hat{F}^{-1}_{\bar{\pi}^{i}_{t+1,t+h}|x^{i}_{t}}(\tau|x^{i}_{t})\,\mathrm{d}\tau, \tag{III.6}$$

for a chosen target probability p, and where $\hat{F}^{-1}(\bullet)$ is the conditional inverse cumulative distribution of average future inflation over horizon h in country i. To be consistent with our choice for $\alpha = 0.10$, we set $p = 0.10$ in our empirical application.

Once we have calculated risk measures, it is straightfward to obtain a measure of inflation dispersion across countries. Our preferred measure of dispersion is the cross-country standard deviation of risks at horizon h, according to:

$$\sigma_{\text{RISK}^{i}_{t+h}} = \sqrt{\left[\frac{1}{N}\sum_{i=1}^{N}\left(\text{RISK}^{i}_{t+h} - \overline{\text{RISK}}_{t+h}\right)^{2}\right]} \tag{III.7}$$

where $\text{RISK}^{i}_{t+h} = [{}^{-}\text{IaR}^{i}_{t+h}, {}^{+}\text{IaR}^{i}_{t+h}, \text{SF}^{i}_{t+h}, \text{LR}^{i}_{t+h}]$, and $\overline{\text{RISK}}_{t+h}$ is the mean of our risk measures across countries.

III.3 The Dispersion of Inflation-at-Risk

This section describes the dispersion of inflation-at-risk for the euro area using the different metrics defined in Section III.2. Before focusing on the dispersion across countries, we discuss some results of Phillips curve estimates for each country of the sample.

III.3.1 National Phillips Curve Estimates

This section presents the results of the quantile Phillips curve estimates by country. The results are displayed in Tables III.B.1 to III.B.3 in Appendix III.B. Each table reports the estimated

coefficients of the equation (III.2) for each country for quantiles $\tau = \{0.1, 0.5, 0.9\}$, respectively. The last two rows of the tables report the unweighted means and the standard deviations of coefficients across countries.

First of all, the mean and the standard deviation of coefficient λ_τ^i associated to long-term inflation expectations across countries remain stable over the quantiles. Overall, the weight of inflation expectations is greater than that of past inflation for all three quantiles. However, the anchoring is not the same when looking at the weight of inflation expectations country-by-country. For instance, the coefficient is equal to 1 in Germany in the middle or at the top of the distribution (50^{th} and 90^{th} quantiles), whereas it is equal to 0.56 at the bottom of the distribution (10^{th} quantile). Inversely, the coefficient is equal to 1 in France at the bottom of the distribution but decreases to 0.69 and 0.74 in the middle and at the top of the distribution, respectively. Globally, inflation is weakly anchored in periphery countries (Italy, Spain, Ireland, Portugal and Greece), regardless of the quantile.

Focusing on the θ_τ^i coefficient (i.e. the slope of the Phillips curve), the magnitude of the cross-sectional mean is twice higher for the 50^{th} and 90^{th} quantiles than for the 10^{th} quantile, though the coefficient is generally not significant from zero. Unemployment seems to affect inflation much more at the top of the distribution than at the bottom in the euro area, on average. This result suggests that labor market conditions matter more for upside risks to inflation than for downside inflation risks. Such nonlinearities in the relationship between slack and inflation corroborate those from Gagnon and Collins (2019) in which the Phillips curve is normally steep but becomes nonlinear only when inflation is low. Once again, even if the cross-sectional standard deviation does not change significantly from a quantile to another, the estimated slope of the Phillips curve shows important disparities across countries within and between quantiles. For instance, the coefficient is strongly negative in the Netherlands for the 10^{th} as for the 50^{th} quantile, but is null at the top of the distribution. This highlights important disparities across countries for each quantile.

The cross-sectional mean of the coefficient associated with financial stress, δ_τ^i, is still negative with a magnitude almost seven times larger for the 10^{th} quantile than in the 90^{th} quantile (-1.29 against -0.19). This is consistent with the role of tighter financial conditions in the occurrence of low inflation episodes in the euro area. Our results corroborate a vast literature maintaining that there is a nonlinear relationship between financial sector and macroeconomy depending on the state of the economy. Notable examples include He and Krishnamurthy (2012, 2013)

and Brunnermeier and Sannikov (2014) for the theory, and Hubrich and Tetlow (2015) and Lhuissier (2017) for the empirics. Since this coefficient is the only to be left unconstrained in the benchmark specification of the augmented Phillips curve model, it shows important disparities between euro area countries. The cross-sectional standard deviation is indeed very high for the three quantiles (1.33 for the 90^{th} quantile, 1.63 for the 50^{th} quantile, and 2.34 for the 10^{th} quantile). However, as for the other estimated coefficients of the model, the effect of financial stress on inflation varies across countries and over the quantiles. For instance, the coefficient is positive at the top but negative at the bottom of the distribution in Austria (0.85 for the 90^{th} quantile and -0.17 for the 10^{th} quantile), whereas it is much higher (but always negative) in Greece at the bottom of the distribution (-5.84 for the 10^{th} quantile, -5.48 for the 50^{th} quantile, and -0.04 for the 90^{th} quantile).

Capturing the effect of supply chain pressures on inflation, the ϕ_τ^i coefficient is similar from the 10^{th} to the 50^{th} quantile, but the mean and the standard deviation across countries is interestingly and considerably larger for at the top of the distribution. In line with the recent period, this suggests that tensions on global supply chain is a key feature of upside inflation risks across euro area countries.

Finally, the cross-sectional mean of the γ_τ^i coefficient is slightly higher for the 90^{th} quantile, suggesting that oil price affects upside risks to inflation more than downside inflation risks.

As a whole, and despite constrained coefficients (except on financial conditions), estimated national Phillips curve results show important non-linearities across quantiles. Moreover, it is worth noting that the non-linearities across quantiles are not the same for all countries, providing grounds for looking at the dispersion of conditional quantiles across euro area countries.

III.3.2 Conditional Quantiles

Figure III.3.2 depicts the standard deviation of inflation quantiles across countries for the one-year forecast horizon. Panel A shows the evolution of the cross-sectional standard deviation of the 50^{th} quantile over time, i.e. the median of the predictive inflation distribution. The figure indicates no clear pattern of the dispersion of the 50^{th} quantile over the entire sample period. Except for slight increases in troubled times — especially after the 2008 and the COVID crises, inflation dispersion in the middle of the distribution across countries displays a relatively stable evolution over time.

This is however not the case when looking at the tails of the dispersion of predictive inflation

Figure III.3.2 – Dispersion of conditional quantiles

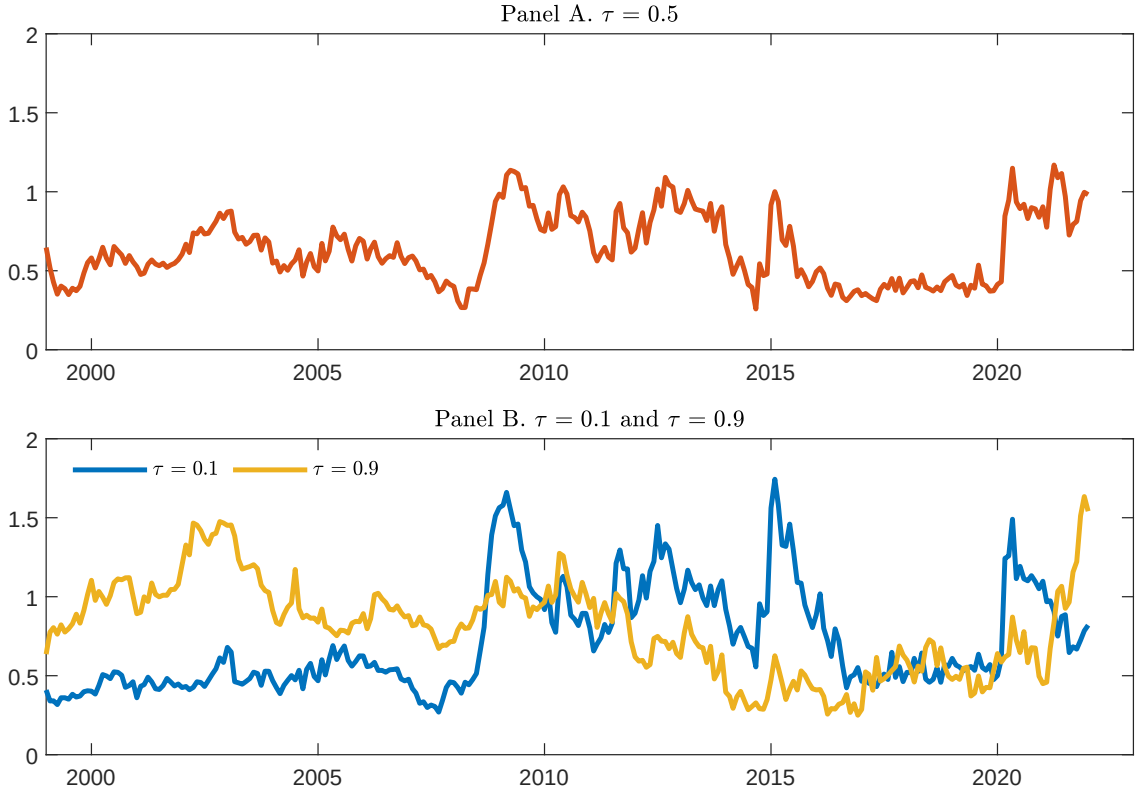

Note: Standard deviation of conditional inflation quantiles $\hat{Q}_\tau(\bar{\pi}^i_{t+1,t+h}|x^i_t)$ across country i, for quantiles $\tau = \{0.1; 0.5; 0.9\}$ and forecast horizon $h = 12$. Panel A shows the standard deviation of the conditional quantile $\tau = 0.5$. Panel B shows the standard deviation of conditional quantiles $\tau = 0.1$ and $\tau = 0.9$. Conditional quantiles $\hat{Q}_\tau(\bar{\pi}^i_{t+1,t+h}|x^i_t)$ are simulated using the estimates of equation (III.2). Figures III.D.1 and III.D.2 in Appendix III.D report the conditional quantiles by country.

distribution across countries. Panel B plots the time-varying evolution of the standard deviation of the 10$^{\text{th}}$ and 90$^{\text{th}}$ quantiles of inflation distribution across countries. During the first decade of the euro area, inflation dispersion is clearly higher for the 90$^{\text{th}}$ quantile associated with risk of high inflation. Until the end of 2008, the standard deviation of the 90$^{\text{th}}$ quantile is always higher than the standard deviations of the 10$^{\text{th}}$ quantile; its highest point is reached in 2003 during this period. Thereafter, until the Great Recession of 2008-2009, inflation dispersion is relatively low regardless of the quantile considered. These findings are consistent with the fact that the first decade of the euro area is still marked by the process of nominal convergence of countries that entered the euro area with different initial conditions in terms of inflation. In particular, some countries, such as Spain or Ireland, had inflation rates above the other countries.

From the Great Recession (2008-09) to the COVID crisis, the situation is reversed. Highest inflation dispersions concern the 10$^{\text{th}}$ quantile associated with low inflation risk. The dispersion

Figure III.3.3 – Dispersion of conditional quantiles for out-of-sample forecasts

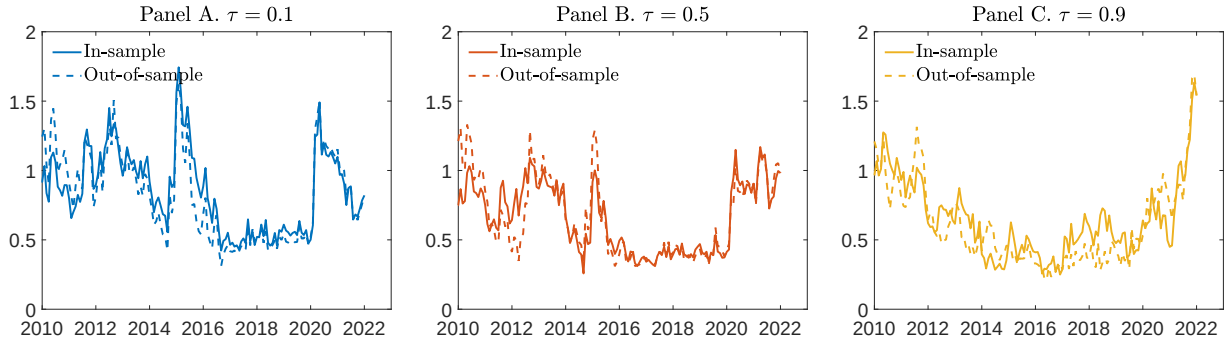

Note: Standard deviation of conditional inflation quantiles $\hat{Q}_\tau(\bar{\pi}^i_{t+1,t+h}|x^i_t)$ across country i, for quantiles $\tau = \{0.1; 0.5; 0.9\}$ and forecast horizon $h = 12$. Solid lines are for the in-sample estimates: conditional quantiles $\hat{Q}_\tau(\bar{\pi}^i_{t+1,t+h}|x^i_t)$ are simulated using the estimates of equation (III.2) using all the sample of data. Dotted lines are for the out-of-sample estimates: conditional quantiles $\hat{Q}_\tau(\bar{\pi}^i_{t+1,t+h}|x^i_t)$ are simulated using a new estimate of equation (III.2) for each new date t which is sequentially includes in the sample of data.

of the 90$^{\text{th}}$ quantile is overall lower than that of the 10$^{\text{th}}$ quantile, except in 2010 when all dispersion measures are high and in the years before the COVID crisis characterized by low dispersion both at the bottom and at the top of the distribution. The key highlight of the post-crisis period is the spikes reached by the dispersion of the 10$^{\text{th}}$ quantile between 2008 and 2015. They largely exceed the dispersion levels observed during the first decade of the euro area. The succession of financial and sovereign debt crises during this period has clearly fueled the dispersion of inflation in the euro area through strong differentials in the risk of low inflation between these countries. In Appendix III.C, we illustrate this fact by comparing the full predictive inflation distribution of two polar economies of the euro area (Germany and Greece) before and during the financial crisis.

In the recent period, the evolution of inflation dispersion shows a sharp increase in the dispersion of the 90$^{\text{th}}$ quantile of the distribution, reaching an all-time high. This spike in the dispersion of inflation at the top of the distribution is accompanied by a decrease in the dispersion of the 10$^{\text{th}}$ quantile after the peak observed during the COVID crisis.

III.3.3 Out-of-Sample Analysis

In this section, we provide out-of-sample evidence of the results based on the quantile regression. Following Adrian et al. (2019), we use data from January 1999 to December 2009, and we estimate the predictive distribution of inflation for December 2010 (one-year-ahead). Then, the procedure is repeated for each month until the end of the sample (i.e. January 2023). At each iteration, the sample is expanded through the estimation steps described earlier in Section

Figure III.3.4 – Dispersion of inflation expected shortfall and longrise

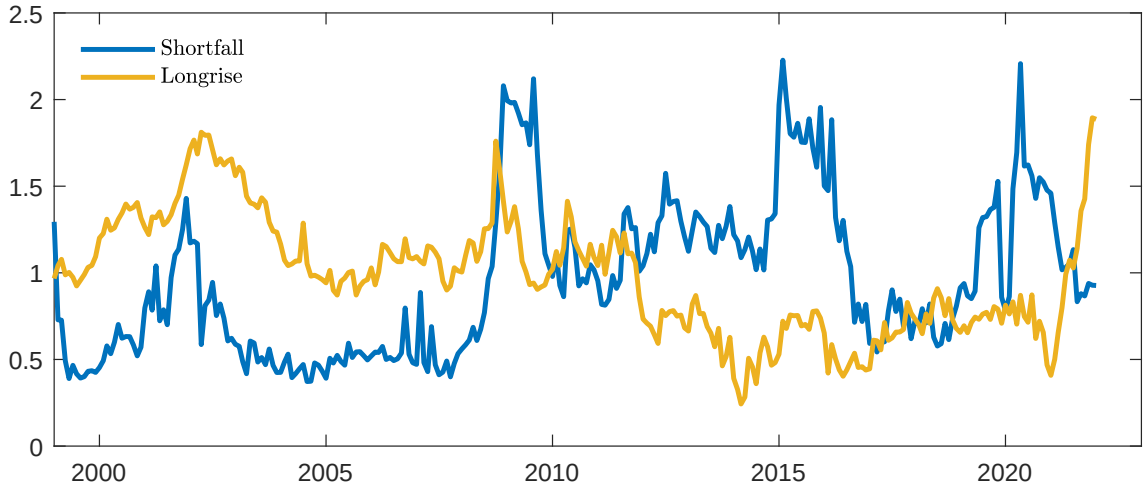

Note: Standard deviation of expected shortfall and longrise SF^i_{t+h} and LR^i_{t+h} across country i, for $p = 0.10$ and forecast horizon $h = 12$. SF^i_{t+h} and LR^i_{t+h} are defined by equation (III.6). Figures III.D.3 and III.D.4 in Appendix III.D report the expected shortfall and longrise by country.

III.2.

Results for the out-of-sample forecasting exercise are depicted in Figure III.3.3. The figure shows that the in-sample and out-of-sample estimates of the quantiles are quite similar, except during the post-2010 euro area sovereign debt crisis regarding the 90^{th} quantile (Panel C). Out-of-sample predictions also constantly overestimate the peak of the dispersion in the middle (50^{th} quantile) and the bottom (10^{th} quantile) of the distribution of inflation during the COVID crisis (Panels A and B). Otherwise, out-of-sample predictions for the selected quantiles of inflation dispersion are shown to perform well in tracking the evolution of the full sample estimation of this dispersion. Importantly, they exhibit good performance in predicting the recent increase in the dispersion of the risk of high inflation driven by spikes in 50^{th} and 90^{th} conditional quantiles (Panels B and C).

III.3.4 Expected Shortfall and Longrise

The dispersion of inflation quantiles is an interesting measure but it does not exploit all the information of the predictive inflation distribution. Indeed, as explained earlier, the x^{th} quantile gives the value of inflation such that there is $x\%$ chance that inflation is below this value, but it does not depend on the exact distribution of inflation below this threshold. The interest of expected shortfall and longrise metrics developed by Adrian et al. (2019) for economic growth is to exploit all this information. Following these authors, we apply these metrics to inflation

Figure III.4.5 – Dispersion of conditional quantiles without financial stress

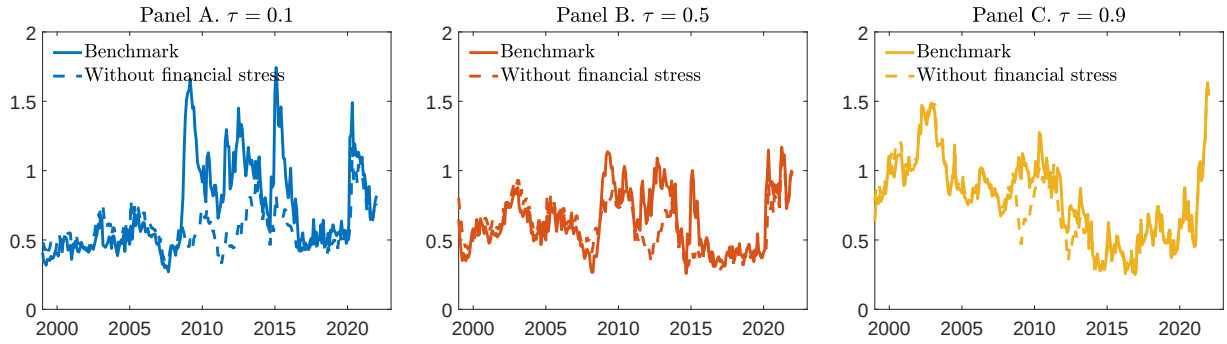

Note: The case without financial stress corresponds to the standard deviation of conditional quantiles predicted for $f_t^i = 0$ in the quantile Phillips curve (III.2) for quantiles $\tau = \{0.1; 0.5; 0.9\}$ and forecast horizon $h = 12$.

differentials.

Figure III.3.4 depicts the standard deviations of the longrises and shortfalls associated with the 10% risk level for the one-year ahead horizon. These figures confirm the pattern previously described using the dispersion of inflation quantiles. During the first decade of the euro area, the longrise outweighs the shortfall, while afterwards the shortfall is a more pronounced source of inflation dispersion.

III.4 The Drivers of Inflation Dispersion

Having described the nature of the dispersion of the inflation in the euro area according to the nature of the extreme risk, either upside or downside, we investigate in this section the drivers of inflation dispersion. For this purpose, we elaborate counterfactual scenarios by muting selected explanatory variables in the right-hand side of the estimated quantile Phillips curve.

III.4.1 Financial Stress

The first scenario assesses the role of financial conditions in the dynamics of inflation dispersion. We predict for each country the conditional quantiles of inflation under the assumption that the financial stress variable is set to zero for all countries at each date ($f_t^i = 0$) in equation (III.2). In this prediction, we keep the estimated values of the Phillips curve for each country and the realizations of the other economic variables unchanged. Figure III.4.5 shows the results for the forecast horizon $h = 12$, and the three quantiles of interest, $\tau = \{0.1, 0.5, 0.9\}$. Each panel compares the benchmark inflation dispersion (solid lines) and the dispersion without financial stress (dashed lines).

Up to the Great Recession of 2008-2009, the euro area was immune to financial stress and therefore the predicted dispersion without this stress is very close to the benchmark. The role of financial stress then takes on great importance. This is especially the case for the 10^{th} quantile. Looking at Panel A, the dispersion would have remained stable throughout the financial crisis period between 2008 and 2015 at a level three times smaller than the observed peaks. It is interesting to note that the absence of financial stress would also have led to less dispersion in inflation for the 50^{th} quantile (Panel B). The results are however less striking for the 90^{th} quantile, even if tighter financial conditions have still affected inflation dispersion.

These results are consistent with the common analysis of the role of financial crises in the extreme risk of deflation that weighed on the euro area. Since then, the situation has changed. International tensions in value chains and energy prices following the end of the COVID crisis and the war in Ukraine have raised the specter of a return to the extreme inflation of the 1970s.

III.4.2 Pressures on Supply Chains and Energy Prices

To analyze this recent period, we develop two scenarios: the scenario without oil price for $\pi_t^{o,i} = \pi_t^{*,i}$ and the scenario without supply chain pressures for $sc_t = 0$. As before, for these predictions, we keep the estimated values of the Phillips curve for each country and the realizations of the other economic variables unchanged. Figure III.4.6 shows the results for the three quantiles, $\tau = \{0.1, 0.5, 0.9\}$ using core inflation. Each panel compares the benchmark inflation dispersion (solid lines), the dispersion without oil price (dotted lines), and the dispersion without supply chain pressures (dashed lines). We report results only for the period after 2018 to facilitate the interpretation of the figure.

The results are reported for two forecast horizons, one year and one quarter (i.e. $h = 12$ and $h = 3$, respectively). The one-year forecast is more informative of trends than the one-quarter forecast. On the other hand, the advantage of the one-quarter forecast is that it provides information at a higher frequency. For instance, the abruptness of the COVID crisis is more accurately measured with the one-quarter forecast than with the one-year forecast, because inflation series are averaged over a shorter period. The interest of the latter is also to be able to include in the analysis the last nine months of observation during the recent period marked by strong changes in the dynamics of inflation. More precisely, the one-quarter forecast has the ability to portray the dispersion of inflation until October 2022 (in the case where $h = 3$, the last point in October 2022 is the average of expected inflation between November 2022 and January

Figure III.4.6 – Dispersion of conditional quantiles without oil price and supply chain pressures

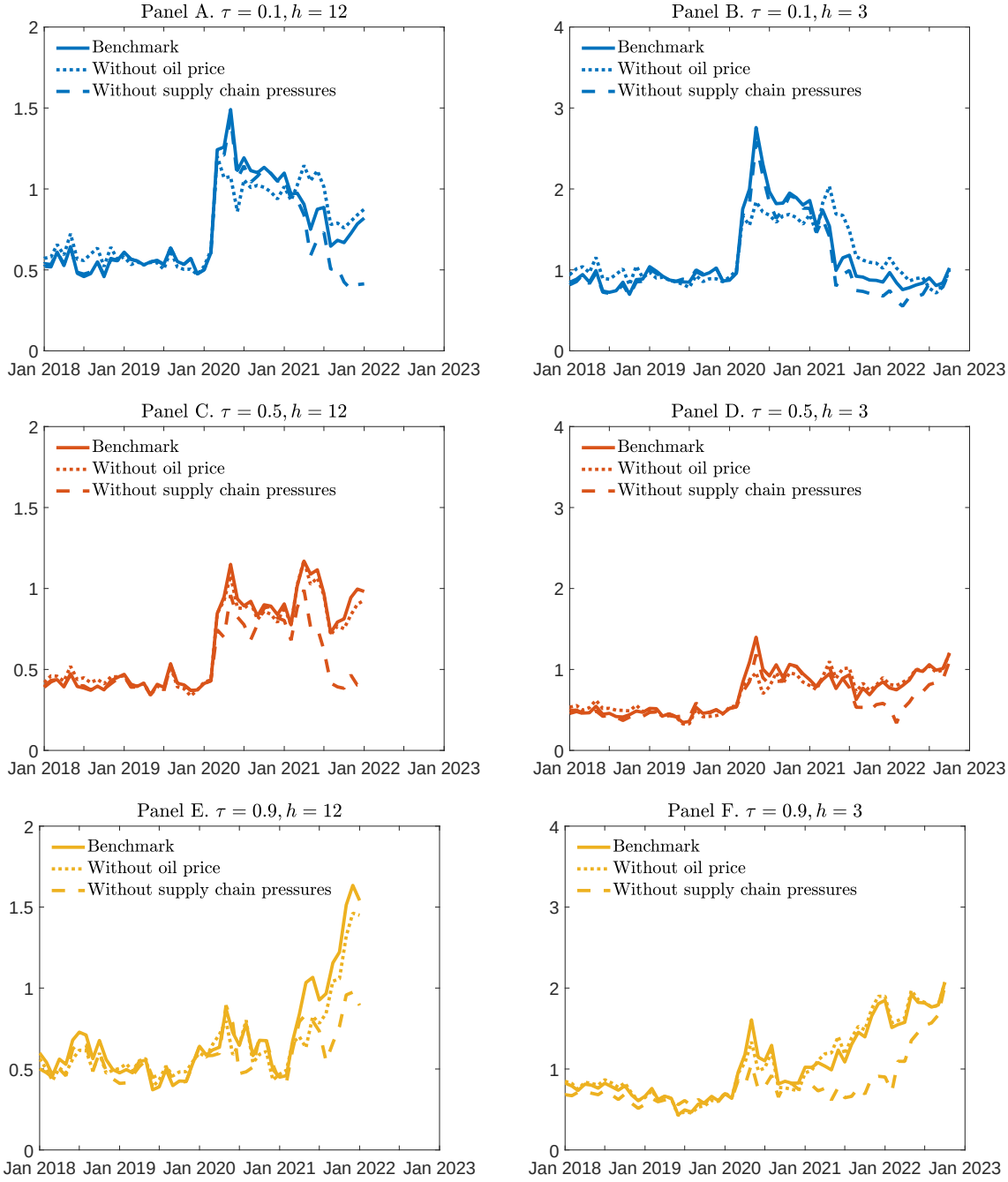

Note: The case without oil price corresponds to the standard deviation of conditional quantiles predicted for $\pi_t^{o,*} = \pi_t^{*,i}$ in the quantile Phillips curve (III.2). The case without supply chain pressures corresponds to the standard deviation of conditional quantiles predicted for $sc_t = 0$ in the quantile Phillips curve (III.2). The first column of panels is for the one-year forecast ($h = 12$) and the second one is for the one-quarter forecast ($h = 3$). The first row of panels is for the 10^{th} quantile, the second one for the 50^{th} quantile, and the third one for the 90^{th} quantile.

2023, the last observation of our sample, given the data observed in October 2022), whereas the one-year forecast computes the dispersion of inflation based on data until January 2022 (recall that in the case where $h = 12$, the last point in January 2022 is the average of expected inflation between February 2022 and January 2023, given the data observed in January 2022). Therefore, looking at recent increase in oil price and supply chain pressures index over the last months, we expect that estimating the model with $h = 3$ will allow to give new evidence on the effects of the recent evolution of oil price and supply chain pressures on the dispersion of inflation across euro area countries.

Supply chain tensions play a more prominent role than oil price in the dynamics of inflation dispersion. It is noteworthy that value chain pressures play a major role in the two extreme quantiles of inflation (10^{th} and 90^{th}). For both quantiles, inflation dispersion would have returned to pre-COVID values without the pressures on value chains.[7]

As a robustness check, we have also conducted those counterfactual exerises using HICP instead of core HICP. Considering headline inflation in the analysis confirm the previous results of the role of global supply chain in the evolution of inflation distribution. See Appendix III.E for further details.

III.4.3 Structural Heterogeneity

We propose a last exercise of counterfactual scenarios to assess the role of economic structure heterogeneity in inflation dispersion. Inflation may diverge between countries, either because they are exposed to different economic events or because their different economic structures lead them to react differently to these events. To assess the respective role of structures and the economic context, we proceed as follows. We take France as a reference country. Then, we simulate the conditional quantiles of inflation under two assumptions: (i) all countries share the same Phillips curve coefficients as France, but are exposed to the economic variables actually observed in their own country; (ii) all countries are exposed to the same economic variables as France, but retain the estimated Phillips curve coefficients for each of them. Figure III.4.7 shows the predicted inflation dispersion by quantiles under the two assumptions (we only consider in this case the one-year forecast). The dispersion of inflation is clearly higher when common

[7] To check the robustness of our results, we also run the benchmark model considering energy price rather than oil price. Despite differences in the two series over the last few months due to a record-high increase in natural gas prices in Europe, the results are robust to the choice of the series (the correlation between energy and oil prices is 0.96 from January 1999 to January 2023).

Figure III.4.7 – Dispersion of inflation quantiles for common structure or common economic series

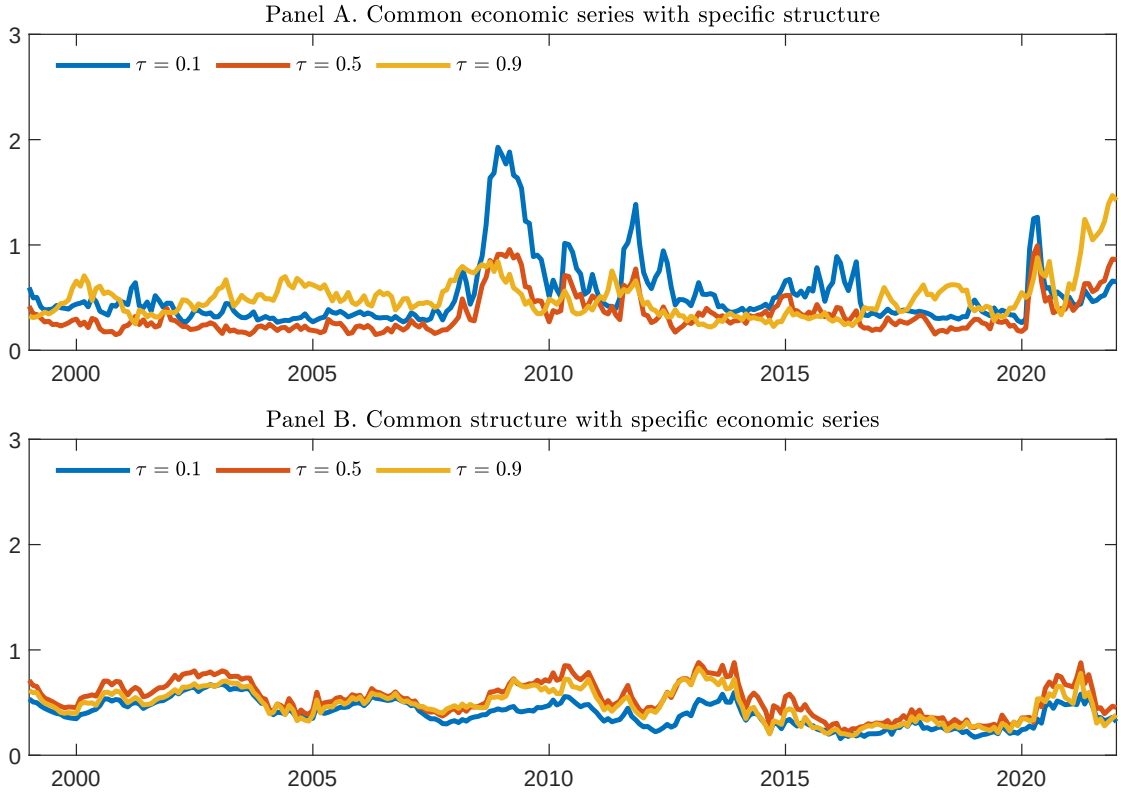

Note: Standard deviation of conditional inflation quantiles $\hat{Q}_\tau(\bar{\pi}^i_{t+1,t+h}|x^i_t)$ across country i, for quantiles $\tau = \{0.1; 0.5; 0.9\}$ and forecast horizon $h = 12$. Panel A shows the standard deviation of the conditional quantiles assuming that all countries experienced the French economic series while preserving their own estimated coefficients for the Phillips curve. Panel B shows the standard deviation of the conditional quantiles assuming that all countries share the estimated coefficients for the French Phillips curve while preserving their own national economic series.

economic series is considered (Panel A) than when we consider common structure (Panel B). This result indicates that the great heterogeneity in the national Phillips curves is the main driver of inflation dispersion in the euro area.

III.5 Robustness Analysis: a Markov-switching Approach

In the existing literature, Markov-switching models have been proposed as an alternative method over quantile regressions to characterize business cycle variation in the probability distribution and time-varying risks around GDP growth. Using a semi-structural model subject to Markov mean and variance shifts, Caldara et al. (2021) investigate the role of the financial and real conditions to predict tail risks in the U.S. economy. Lhuissier (2022) proposes a regime-switching skew-normal model to examine time variation in the third moment of

the predictive distribution of euro area economic growth. López-Salido and Loria (2022) also propose a Markov-switching framework as an alternative method to study time variation in the predictive distribution of inflation in the U.S. This section follows this recent literature and adopts a Markov-switching framework as a robustness analysis.

III.5.1 The Framework

We employ a statistical model in which the observation $\bar{\pi}^i_{t+1,t+h}$ is generated as follows:

$$\bar{\pi}^i_{t+1,t+h} = \mu^i(s^i_t) + \left(1 - \lambda^i(s^i_t)\right)\pi^{*,i}_{t-1} + \lambda^i(s^i_t)\pi^{LTE,i}_t + \theta^i(s^i_t)\left(u^i_t - u^{*,i}_t\right) + \gamma^i(s^i_t)\left(\pi^{o,*}_t - \pi^{*,i}_t\right) + \delta^i(s^i_t)f^i_t + \phi^i(s^i_t)sc_t + \sigma^i(s^i_t)\varepsilon^i_t, \tag{III.8}$$

where ε^i_t follows a standard normal distribution, and s^i_t is an exogenous three-states first-order Markov process with the following transition matrix Q^i

$$Q^i = \begin{bmatrix} q^i_{1,1} & q^i_{1,2} & q^i_{1,3} \\ q^i_{2,1} & q^i_{2,2} & q^i_{2,3} \\ q^i_{3,1} & q^i_{3,2} & q^i_{3,3} \end{bmatrix}, \tag{III.9}$$

where $q^i_{u,v} = \Pr(s^i_t = u | s^i_{t-1} = v)$ denote the transition probabilities that s^i_t is equal to u given that s^i_{t-1} is equal to v, with $u, v \in \{1, 2, 3\}$, $q^k_{u,v} \geq 0$ and $\sum_{v=1}^3 q^i_{u,v} = 1$.

Our framework is subject to Markov mean and variance shifts over time. In particular, we impose three regimes of inflation, which can be considered as regimes of low (Regime 1), medium (Regime 2) and high (Regime 3) inflation. Both coefficients and standard deviations can change over time according to the same Markov process, meaning that the time of changes for coefficients is stochastically dependent of the times of changes for standard deviations.

We rely on Bayesian methods to estimate our Markov-switching model. When dealing with a Markov-switching model, the likelihood can be evaluated according to the Hamilton (1989)'s filter, and then combined with a prior distribution for the parameters. We use the idea of Gibbs sampling to obtain the empirical joint posterior density by sampling alternately from the following conditional posterior distribution. Our Gibbs sampler procedure begins with setting parameters at the peak of the posterior density function. The Monte Carlo Markov Chains (MCMC) sampling sequence involves a 4-block Gibbs sampler, in which we can generate in a flexible and straightforward manner alternatively draws from full conditional posterior

distributions. Overall, our procedure follows the MCMC approach proposed by Albert and Chib (1993).

Regarding our prior, they are very dispersed and cover a large parameter space so that so that the data, through the likelihood, dominate the posterior distribution. It may be worth noting that we impose the exact same prior across regimes, so that the differences in parameters between regimes result more from data (i.e., the likelihood) rather than priors. Moreover, we impose the same restrictions on the coefficients as those imposed in the estimation of quantile regressions.

The online appendix provides the computational details for our maximization and MCMC procedures, as well as for the choice of the prior.

III.5.2 Empirical Results

Since we are studying whether a Markov-switching framework is able to produce quantitatively similar dispersion measures as those from a quantile regressions approach, we put in the appendix the estimates of Markov-switching Phillips curves by country — see Tables III.F.1, III.F.2, III.F.3 and III.F.4. However, it may worth saying that, in spite of differences in coefficients estimated at the country level, the results of cross-sectional mean and standard deviation give similar interpretation than those from the quantile regression model: high and stable anchoring of inflation expectations across inflation regimes (low, medium and high), steeper slope of the Phillips curve in medium and high than in low inflation regimes, key role of financial stress in low inflation regime with high dispersion across countries, and important role of global supply chain in high inflation regime.

Figure III.5.8 reports the regime probabilities — evaluated at the mode — for each country. We report the smoothed probabilities in the sense of Kim (1994); i.e., full sample information is used in getting the regime probabilities at each date. One can see from the figure that each euro area country has been characterized by numerous switches between regimes over time. The times of changes are most of the time unsynchronized across countries, suggesting that the dispersion across countries is very much in evidence. For example, during the sovereign debt crisis in 2010-2012, countries most hit by the crisis like Portugal, Greece, Spain and Ireland, experienced a regime of low inflation, while others like Germany, Finland, and Austria were in a high or medium inflation regime. One exception regarding the divergence across countries is during the recent period where the high inflation regime has been the predominant regime for

Figure III.5.8 – Regime Probabilities

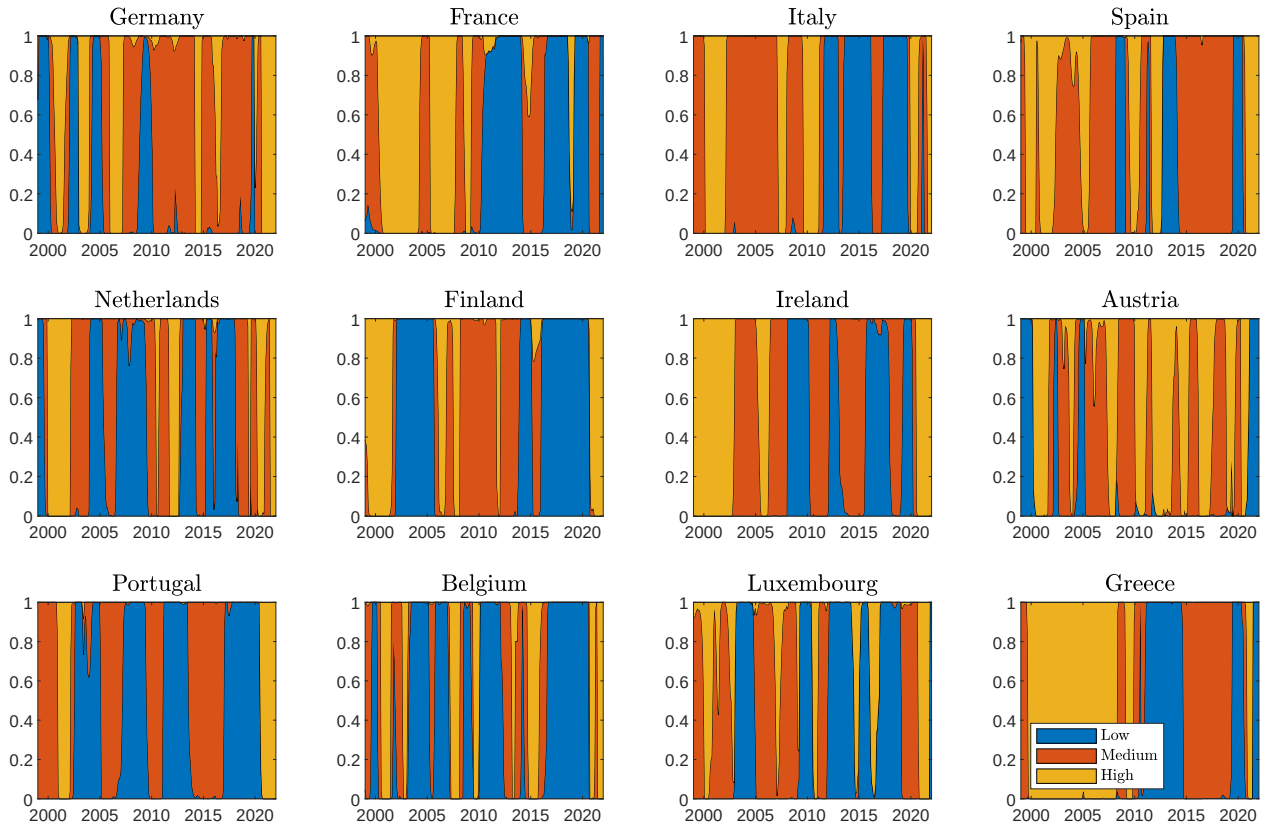

Note: Probabilities are smoothed in the sense of Kim (1994), i.e., full sample information is used in getting the regime probabilities at each date. The color code is as follows: blue (Regime 1, low inflation), red (Regime 2, medium inflation), yellow (Regime 3, high inflation).

most of countries.

To provide a more formal analysis of inflation dispersion and, to be more in line with the results of our quantile regressions, we also produce the cross-country dispersion of the expected shortfall and longrise measures produced from our Markov-switching model, as shown in Figure III.5.9. Following Lhuissier (2022), the calculation of these measures follows a simulation procedure. First, we recover the smoothed regime probabilities for each date. Second, we generate our predictive distribution from the mixture of normal distributions using those probabilities as weights. Third, we compute the individual metrics using the empirical distribution, and then compute the dispersion measures. As shown by the figure, inflation dispersion is clearly higher for upside risks (expected longrise) than for downside risks (expected shortfall) during the first decade of the euro area. Thereafter, the pattern is reversed. The dispersion of downside risks prevails over upside risks since the Great Recession of 2008-2009. These findings are thus consistent with the stylized facts produced from quantile regressions as shown in Figure III.4.5.

Figure III.5.9 – Dispersion of inflation expected shortfall and longrise from Markov-switching model

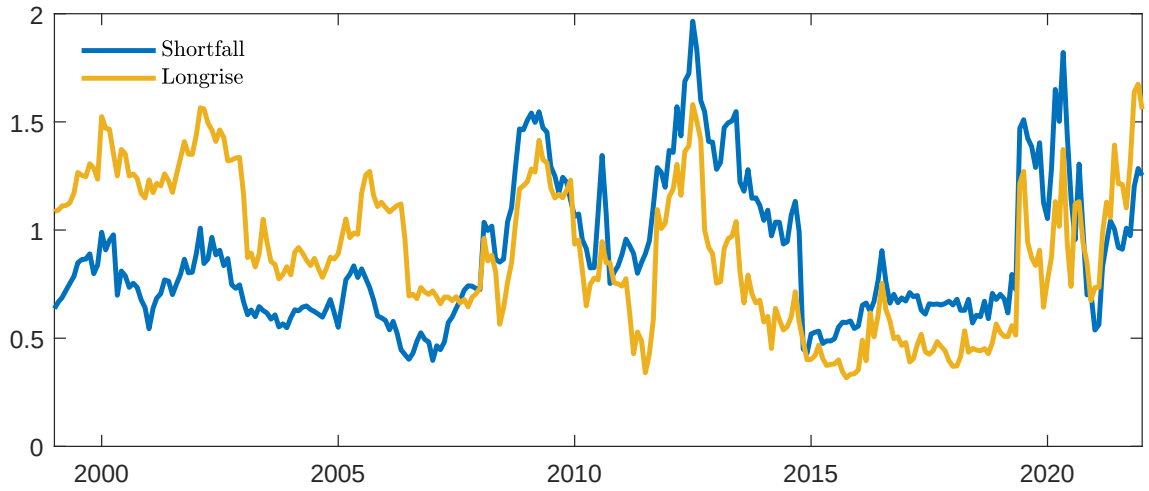

Note: Standard deviation of expected shortfall and longrise SF^i_{t+h} and LR^i_{t+h} across country i and for forecast horizon $h = 12$. SF^i_{t+h} and LR^i_{t+h} are computed using the Markov-switching model.

Overall, our parametric Markov-switching framework is able to produce quantitatively similar results to the more flexible approach of Quantile Regressions of Adrian et al. (2019). We thus confirm the results of Caldara et al. (2021), that is, "*the estimates of tail risk have robust features that can be captured with multiple models*".

III.6 Conclusion

To study inflation differentials in the euro area, we have adopted a "beyond the mean" approach by considering downside and upside inflation risks. This approach enabled us to identify three phases in the euro area. The first decade of the euro area where the risk of inflation dispersion in the euro area is associated with still significant upside risks despite the ongoing convergence process. The second decade of the euro area during which the risk of dispersion comes from downside risks to inflation or even deflation risks in a context of financial crises. The present period, in the wake of the COVID crisis with pressures on oil price and value chains, where the two risks, downside and upside, co-exist and feed the dispersion of inflation in the euro area.

Our results show that the high dispersion of extreme inflation risks described in this article is more the consequence of heterogeneous economic structures than of exposure to different national shocks. In this context, it is well known, at least since Benigno (2004), that targeting an average inflation rate of the monetary union, weighted by the size of the economies, may not be optimal when union's members are heterogeneous. Instead, Benigno (2004) suggested

targeting an average inflation rate using a weighting scheme that gives more weight to economies with the highest degree nominal rigidities–recently, Kekre (2022) proposes a similar analysis leading to giving greater weights to economies with more sclerotic labor markets. Future research would be of interest in investigating optimal monetary policy rules in the context of dispersed inflation tail risks.

Appendix

The Risk of Inflation Dispersion in the Euro Area

III.A Data

All variables are monthly time series covering January 1999 through January 2023. The following variables use data obtained directly from different sources:

- Harmonized Index of Consumer Prices
  - Source: ECB - ICP (Indices of Consumer prices)
  - Details: Monthly – Neither seasonally nor working day adjusted – HICP - All-items excluding energy and food – Eurostat – Index
  - Data transformation: Authors' calculations using the x13 toolbox to get seasonally adjusted series for each euro area member countries.
- Unemployment rate
  - Source: Eurostat - Unemployment by sex and age – monthly data
  - Details: Monthly – Seasonally adjusted data, not calendar adjusted data – Total – Percentage of population in the labor force
- Natural Rate of Unemployment
  - Source: Authors' calculations

  - Details: HP-filtered trend (with smoothing parameter $\lambda = 14,400$ of unemployment rate).

- Oil Prices
  - Source: U.S. Energy Information Administration - Spot Prices
  - Details: Crude Oil Prices: Brent - Europe - Dollars per Barrel, Not Seasonally Adjusted

- Supply Chain index
  - Source: New York Fed's website
  - Details: Global Supply Chain Pressure Index (GSCPI)

- Financial conditions (CISS)
  - Source: ECB - CISS
  - Details: Daily – ECB – Economic indicator – New Composite Indicator of Systemic Stress (CISS) – Index
  - Data transformation: Authors' calculations to get monthly average of the series.

- Financial conditions (CLIFS)
  - Source: ECB - CLIFS
  - Details: Monthly – ECB – Economic indicator – Country-Level Index of Financial Stress (CLIFS) Composite Indicator – Index

- Long-Term Inflation Expectations
  - Source: Consensus Economics
  - Details: Six-to-ten-year-ahead mean CPI inflation forecasts.
  - Data transformation: Euro area forecasts for Luxembourg (no forecast available), spline interpolation for all missing data in April 1999.

III.B National Phillips Curve Estimates (tables)

Table III.B.1 – Phillips curve estimates for the 10^{th} quantile

	$\hat{\mu}^i_\tau$	$\hat{\lambda}^i_\tau$	$\hat{\theta}^i_\tau$	$\hat{\gamma}^i_\tau$	$\hat{\delta}^i_\tau$	$\hat{\phi}^i_\tau$
Germany	−1.02 [−1.17;−0.88]	0.55 [0.30;0.81]	−0.00 [−0.13;0.13]	0.35 [0.15;0.54]	0.72 [0.29;1.15]	0.24 [0.09;0.38]
France	−0.88 [−1.11;−0.66]	0.65 [0.42;0.88]	−0.00 [−0.16;0.16]	0.41 [0.19;0.64]	−0.72 [−1.34;−0.10]	0.21 [0.11;0.31]
Italy	−0.95 [−1.16;−0.74]	0.56 [0.40;0.72]	−0.00 [−0.13;0.13]	0.00 [−0.22;0.22]	−0.70 [−1.70;0.29]	0.00 [−0.06;0.06]
Spain	−0.94 [−1.36;−0.52]	0.49 [0.22;0.76]	−0.00 [−0.14;0.14]	0.68 [0.18;1.19]	−4.19 [−5.85;−2.53]	0.32 [0.13;0.51]
Netherlands	−1.12 [−1.21;−1.03]	0.86 [0.77;0.94]	−0.74 [−0.94;−0.54]	0.36 [0.16;0.56]	0.36 [−0.16;0.87]	0.28 [0.15;0.40]
Finland	−0.86 [−1.00;−0.72]	0.30 [0.15;0.45]	−0.17 [−0.28;−0.06]	0.45 [0.14;0.77]	0.67 [−0.04;1.38]	0.44 [0.30;0.58]
Ireland	−1.29 [−1.56;−1.02]	0.79 [0.58;1.01]	0.00 [−0.05;0.05]	0.23 [−0.36;0.82]	−4.59 [−6.81;−2.36]	0.33 [0.11;0.56]
Austria	−0.57 [−0.68;−0.47]	0.75 [0.62;0.89]	−0.01 [−0.05;0.04]	−0.00 [−0.06;0.06]	−0.15 [−0.59;0.30]	0.15 [0.06;0.25]
Portugal	−1.24 [−1.47;−1.00]	0.51 [0.37;0.64]	−0.00 [−0.04;0.04]	0.40 [−0.03;0.83]	−0.67 [−1.49;0.15]	0.00 [−0.04;0.04]
Belgium	−0.68 [−0.75;−0.62]	1.00 [0.90;1.10]	−0.01 [−0.11;0.08]	0.07 [−0.04;0.18]	0.43 [0.13;0.73]	0.07 [0.01;0.14]
Luxembourg	−0.43 [−0.56;−0.31]	0.71 [0.49;0.92]	−0.00 [−0.17;0.16]	0.60 [0.42;0.78]	−0.34 [−1.05;0.37]	0.15 [0.05;0.25]
Greece	−0.96 [−1.72;−0.20]	0.46 [0.30;0.61]	−0.14 [−0.33;0.05]	1.53 [0.27;2.80]	−6.03 [−7.92;−4.14]	0.04 [−0.15;0.24]
Mean	-0.91	0.64	-0.09	0.42	-1.27	0.19
Std. Dev.	0.25	0.20	0.21	0.41	2.31	0.14

Note: Table III.B.1 displays the coefficients of the quantile Phillips curve defined by equation (III.2): $\hat{Q}_\tau(\bar{\pi}^i_{t+1,t+h}|x^i_t) = \hat{\mu}^i_\tau + \left(1-\hat{\lambda}^i_\tau\right)\pi^{*,i}_{t-1} + \hat{\lambda}^i_\tau \pi^{LTE,i}_t + \hat{\theta}^i_\tau\left(u^i_t - u^{*,i}_t\right) + \hat{\gamma}^i_\tau\left(\pi^{o,*}_t - \pi^{*,i}_t\right) + \hat{\delta}^i_\tau f^i_t + \hat{\phi}^i_\tau sc_t$ estimated by country for the 10^{th} quantile. The last two rows show the unweighted means and the standard deviations of coefficients across countries.

Table III.B.2 – Phillips curve estimates for the 50$^{\text{th}}$ quantile

	$\hat{\mu}^i_\tau$	$\hat{\lambda}^i_\tau$	$\hat{\theta}^i_\tau$	$\hat{\gamma}^i_\tau$	$\hat{\delta}^i_\tau$	$\hat{\phi}^i_\tau$
Germany	−0.41 [−0.51;−0.32]	0.95 [0.88;1.02]	−0.17 [−0.33;−0.00]	0.15 [0.02;0.28]	−0.22 [−0.50;0.05]	0.40 [0.25;0.54]
France	−0.06 [−0.23;0.11]	0.50 [0.34;0.66]	−0.21 [−0.41;−0.00]	0.34 [0.16;0.52]	−1.60 [−2.16;−1.05]	0.12 [0.02;0.22]
Italy	0.05 [−0.13;0.23]	0.34 [0.14;0.55]	−0.00 [−0.22;0.22]	0.10 [−0.17;0.37]	−0.97 [−2.03;0.10]	0.19 [0.06;0.32]
Spain	−0.15 [−0.28;−0.03]	0.53 [0.39;0.67]	−0.00 [−0.06;0.06]	0.40 [0.14;0.66]	−1.10 [−2.13;−0.07]	0.00 [−0.17;0.17]
Netherlands	−0.33 [−0.51;−0.15]	0.68 [0.53;0.83]	−0.77 [−1.08;−0.45]	0.62 [0.35;0.89]	0.62 [−0.64;1.88]	0.62 [0.38;0.86]
Finland	0.00 [−0.12;0.13]	0.10 [−0.05;0.24]	−0.00 [−0.07;0.07]	0.66 [0.33;0.99]	0.66 [−0.17;1.50]	0.55 [0.40;0.70]
Ireland	−0.22 [−0.48;0.03]	0.49 [0.31;0.66]	−0.00 [−0.12;0.12]	1.15 [0.62;1.68]	−2.30 [−4.36;−0.23]	0.26 [0.02;0.50]
Austria	−0.03 [−0.15;0.09]	0.97 [0.87;1.08]	−0.00 [−0.04;0.04]	0.19 [0.06;0.33]	0.02 [−0.59;0.64]	0.36 [0.16;0.56]
Portugal	−0.18 [−0.42;0.05]	0.53 [0.34;0.71]	−0.07 [−0.23;0.09]	0.43 [−0.05;0.91]	−1.54 [−2.76;−0.31]	0.11 [−0.17;0.40]
Belgium	−0.30 [−0.42;−0.17]	0.92 [0.78;1.07]	−0.04 [−0.15;0.08]	0.13 [0.01;0.26]	0.31 [−0.19;0.81]	0.10 [−0.06;0.25]
Luxembourg	0.01 [−0.10;0.12]	0.81 [0.66;0.95]	−0.38 [−0.56;−0.21]	0.49 [0.34;0.64]	−0.37 [−1.01;0.27]	0.25 [0.11;0.40]
Greece	0.34 [0.01;0.66]	0.47 [0.36;0.57]	−0.45 [−0.73;−0.17]	0.28 [−0.24;0.80]	−4.68 [−7.38;−1.99]	0.16 [−0.14;0.46]
Mean	-0.11	0.61	-0.17	0.41	-0.93	0.26
Std. Dev.	0.20	0.27	0.24	0.30	1.51	0.19

Note: Table III.B.2 displays the coefficients of the quantile Phillips curve defined by equation (III.2): $\hat{Q}_\tau(\bar{\pi}^i_{t+1,t+h}|x^i_t) = \hat{\mu}^i_\tau + \left(1-\hat{\lambda}^i_\tau\right)\pi^{*,i}_{t-1} + \hat{\lambda}^i_\tau \pi^{LTE,i}_t + \hat{\theta}^i_\tau\left(u^i_t - u^{*,i}_t\right) + \hat{\gamma}^i_\tau\left(\pi^{o,*}_t - \pi^{*,i}_t\right) + \hat{\delta}^i_\tau f^i_t + \hat{\phi}^i_\tau sc_t$ estimated by country for the 50$^{\text{th}}$ quantile. The last two rows show the unweighted means and the standard deviations of coefficients across countries.

Table III.B.3 – Phillips curve estimates for the 90$^{\text{th}}$ quantile

	$\hat{\mu}^i_\tau$	$\hat{\lambda}^i_\tau$	$\hat{\theta}^i_\tau$	$\hat{\gamma}^i_\tau$	$\hat{\delta}^i_\tau$	$\hat{\phi}^i_\tau$
Germany	0.55 [0.37;0.74]	1.00 [0.93;1.07]	−0.07 [−0.20;0.07]	−0.00 [−0.13;0.13]	−0.98 [−1.47;−0.49]	0.65 [0.43;0.86]
France	0.41 [0.29;0.53]	0.62 [0.52;0.72]	−0.39 [−0.59;−0.18]	0.04 [−0.06;0.15]	−1.54 [−1.96;−1.12]	0.33 [0.20;0.46]
Italy	0.91 [0.71;1.11]	0.50 [0.30;0.71]	−0.24 [−0.53;0.05]	0.42 [0.09;0.75]	1.14 [−0.27;2.56]	0.11 [−0.04;0.25]
Spain	1.01 [0.66;1.36]	0.58 [0.39;0.77]	−0.22 [−0.49;0.04]	0.28 [−0.11;0.68]	−0.93 [−2.15;0.28]	0.49 [0.22;0.75]
Netherlands	1.14 [0.73;1.56]	0.49 [0.25;0.74]	−0.99 [−1.76;−0.23]	1.80 [1.17;2.43]	0.57 [−2.52;3.66]	0.60 [0.29;0.90]
Finland	0.48 [0.31;0.65]	0.59 [0.43;0.76]	−0.00 [−0.08;0.08]	0.83 [0.62;1.03]	1.52 [0.25;2.79]	0.48 [0.31;0.66]
Ireland	1.87 [1.40;2.34]	0.25 [0.06;0.44]	−0.00 [−0.22;0.22]	0.91 [0.31;1.50]	−2.44 [−4.69;−0.19]	0.64 [0.35;0.93]
Austria	0.80 [0.60;1.00]	0.82 [0.68;0.97]	−0.33 [−0.47;−0.19]	0.29 [0.08;0.50]	0.68 [−0.04;1.40]	0.88 [0.61;1.14]
Portugal	1.94 [1.37;2.52]	0.18 [−0.05;0.40]	−0.33 [−0.72;0.05]	0.92 [0.48;1.35]	−1.80 [−3.79;0.18]	0.89 [0.49;1.29]
Belgium	0.71 [0.52;0.91]	0.78 [0.65;0.91]	−0.53 [−0.74;−0.32]	0.30 [0.11;0.49]	0.13 [−0.84;1.10]	0.59 [0.38;0.80]
Luxembourg	0.54 [0.38;0.70]	0.74 [0.61;0.86]	−0.37 [−0.64;−0.10]	0.35 [0.18;0.52]	0.50 [−0.20;1.21]	0.57 [0.37;0.77]
Greece	1.60 [1.14;2.05]	0.60 [0.43;0.77]	−0.61 [−0.96;−0.26]	1.00 [0.54;1.47]	−1.69 [−4.01;0.64]	0.84 [0.41;1.27]
Mean	1.00	0.60	-0.34	0.60	-0.40	0.59
Std. Dev.	0.54	0.23	0.28	0.51	1.31	0.23

Note: Table III.B.3 displays the coefficients of the quantile Phillips curve defined by equation (III.2): $\hat{Q}_\tau(\bar{\pi}^i_{t+1,t+h}|x^i_t) = \hat{\mu}^i_\tau + \left(1-\hat{\lambda}^i_\tau\right)\pi^{*,i}_{t-1} + \hat{\lambda}^i_\tau \pi^{LTE,i}_t + \hat{\theta}^i_\tau\left(u^i_t - u^{*,i}_t\right) + \hat{\gamma}^i_\tau\left(\pi^{o,*}_t - \pi^{*,i}_t\right) + \hat{\delta}^i_\tau f^i_t + \hat{\phi}^i_\tau sc_t$ estimated by country for the 90$^{\text{th}}$ quantile. The last two rows show the unweighted means and the standard deviations of coefficients across countries.

III.C Case study: Germany and Greece during the Financial Crisis

In this section, we propose a case study to illustrate the situation of increasing dispersion of downside inflation risks. We compare the conditional distributions of predicted inflation for two polar countries of the euro area, Germany and Greece, for two specific dates. The first one, January 2006, reflects the quiet period of the euro area. The second, May 2012, is instead in the period of financial turmoil. Figure III.C.1 shows the conditional distribution of inflation forecast one year ahead ($h = 12$) using the estimated skewed t-density functions defined by equation (III.3) for each country at these two dates.

In January 2006, predicted inflation is higher in Greece than in Germany. The distribution for Greece is shifted to the right compared to Germany. For this date, the dispersion is homogeneous for the whole distribution (the differences between the quantiles are between 1.34 and 2.21 percentage points of inflation).

The situation is radically different in May 2012, mainly due to the change in the distribution of inflation in Greece. Greece is then subject to a severe risk of deflation. The distribution of inflation has shifted to the left but it has also flattened considerably giving rise to a high level of downside inflation risk. There is then a 10% chance that inflation will be below -2.38% in the coming year. In terms of dispersion, this is no longer homogeneous for the entire distribution in May 2012, unlike January 2006. The 10^{th} quantile for Greece is 3.17 percentage points lower than that of Germany. This is almost twice as much as the gap in the 50^{th}. Interestingly, the gap in the 90^{th} quantile is now very close to zero, meaning that the dispersion of inflation rates between Germany and Greece in May 2012 has not been associated with the dispersion of quantiles at the top of the distribution. May 2012 is thus a typical example of high risk of inflation dispersion from the bottom of the distribution, i.e. associated with an extreme risk of low inflation.

Figure III.C.1 – Probability densities

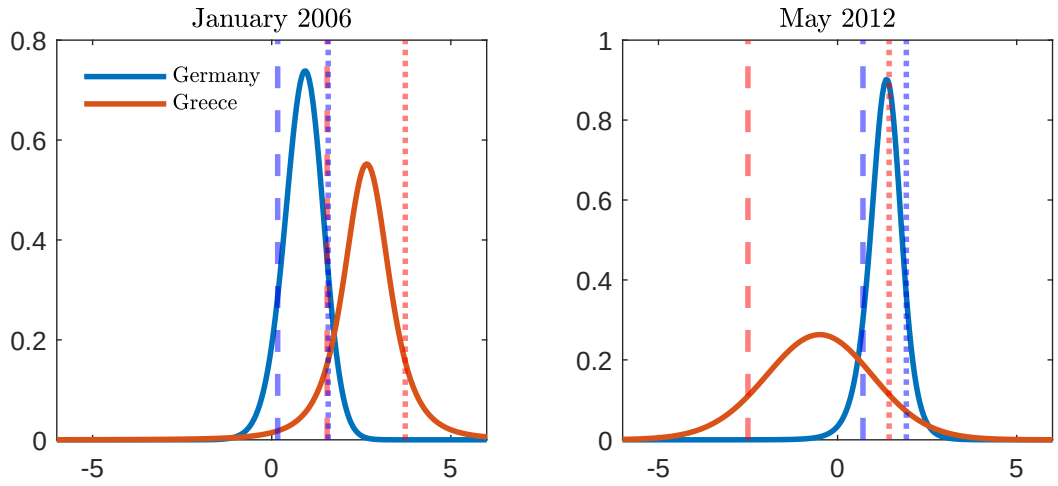

Note: Estimated skewed t-density functions defined by equation (III.3) for one-year-ahead ($h = 12$) inflation rates for Germany and Greece in January 2006 (left panel) and May 2012 (right panel). Vertical lines represent the respective quantiles extracted from the estimated distribution: dashed blue (red) lines represent quantile $\tau = 0.1$ for Germany (Greece), and dotted blue (red) lines represent quantile $\tau = 0.9$ for Germany (Greece).

III.D Conditional Quantiles, Expected Shortfall and Longrise

Figure III.D.1 – Conditional quantiles by country

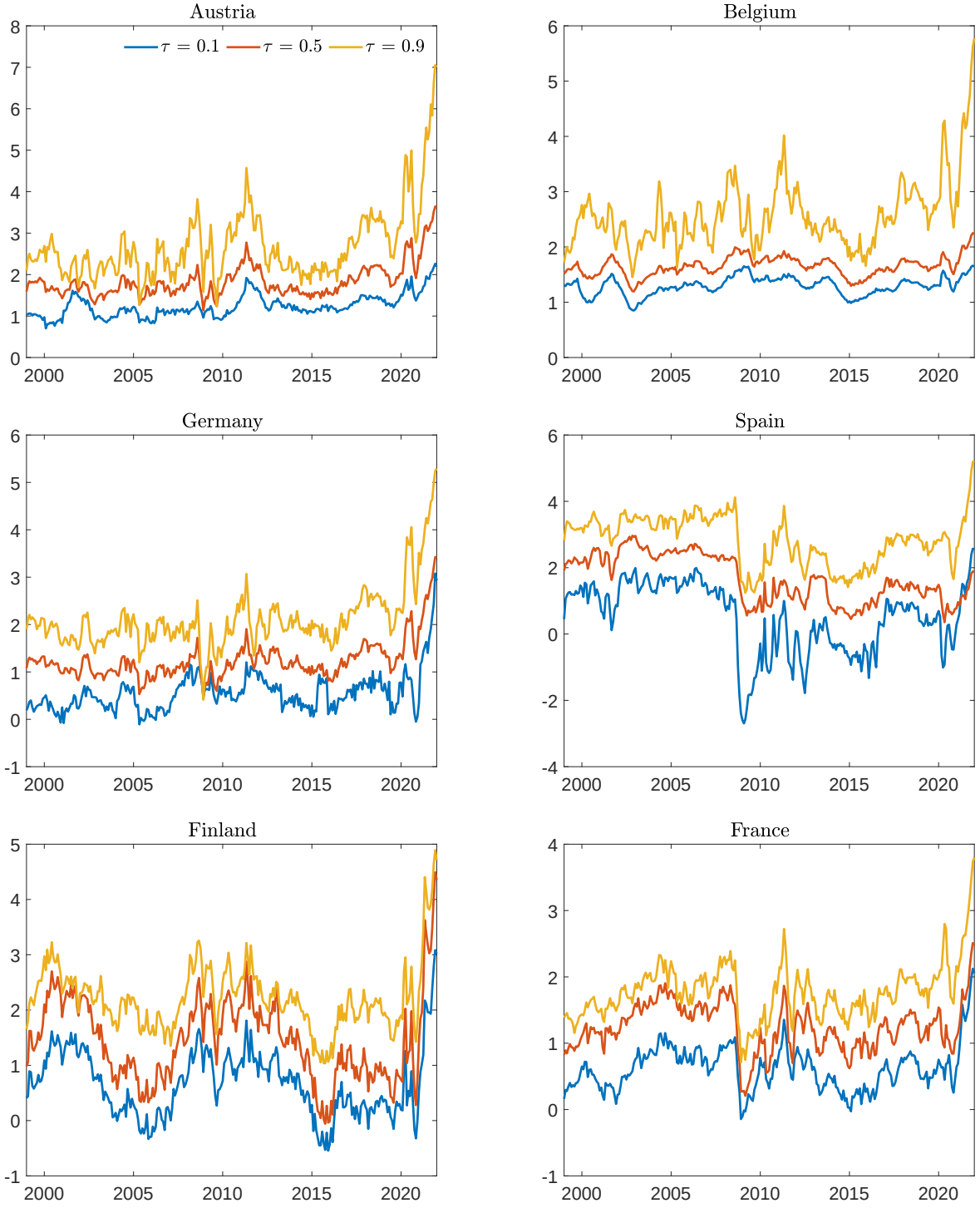

Note: Conditional inflation quantiles $\hat{Q}_\tau(\bar{\pi}^i_{t+1,t+h}|x^i_t)$ for country i, quantiles $\tau = \{0.1; 0.5; 0.9\}$ and forecast horizon $h = 12$. Conditional quantiles $\hat{Q}_\tau(\bar{\pi}^i_{t+1,t+h}|x^i_t)$ are simulated using the estimates of equation (III.2).

Figure III.D.2 – Conditional quantiles by country

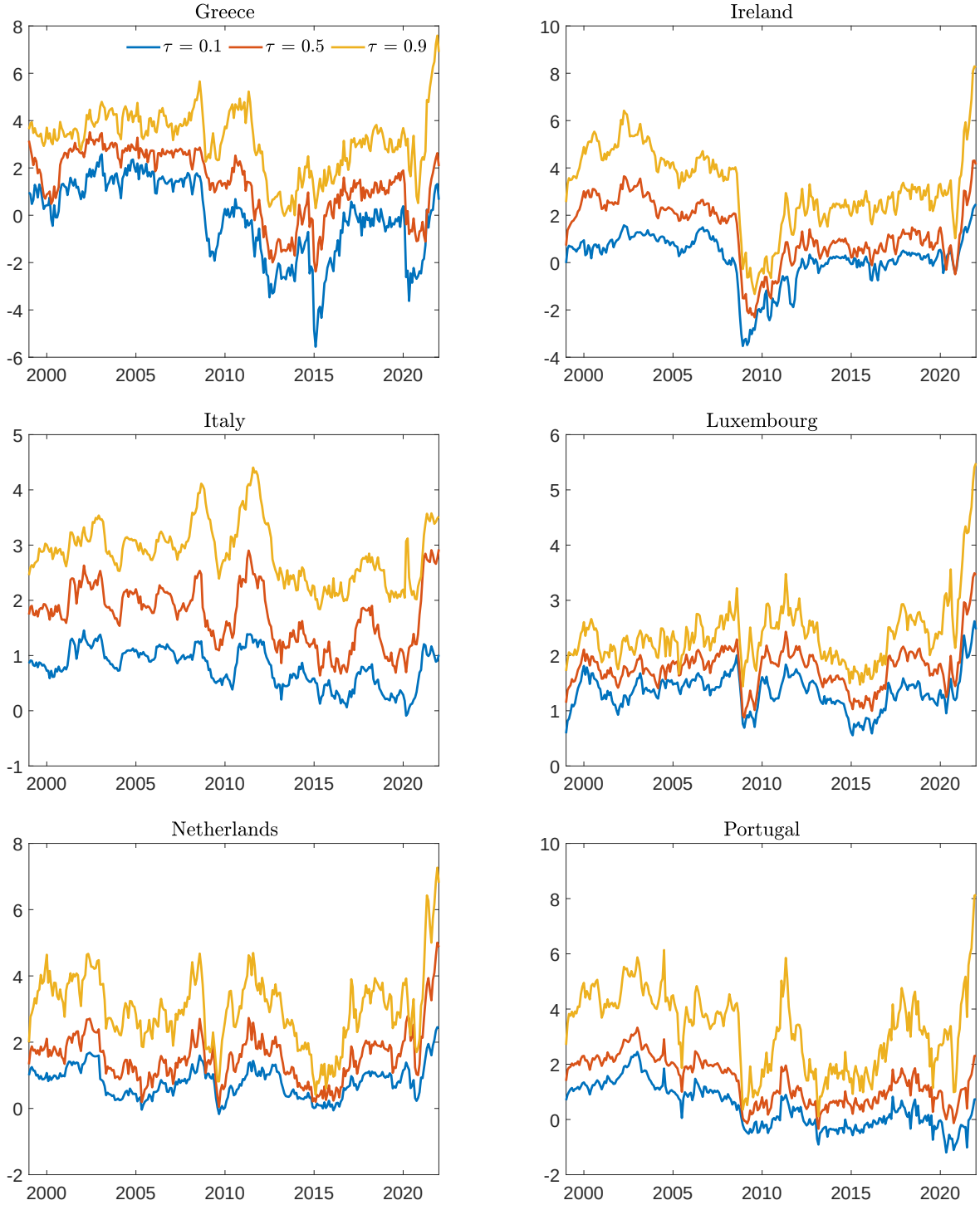

Note: Conditional inflation quantiles $\hat{Q}_\tau(\bar{\pi}^i_{t+1,t+h}|x^i_t)$ for country i, quantiles $\tau = \{0.1; 0.5; 0.9\}$ and forecast horizon $h = 12$. Conditional quantiles $\hat{Q}_\tau(\bar{\pi}^i_{t+1,t+h}|x^i_t)$ are simulated using the estimates of equation (III.2).

Figure III.D.3 – Expected shortfall and longrise by country

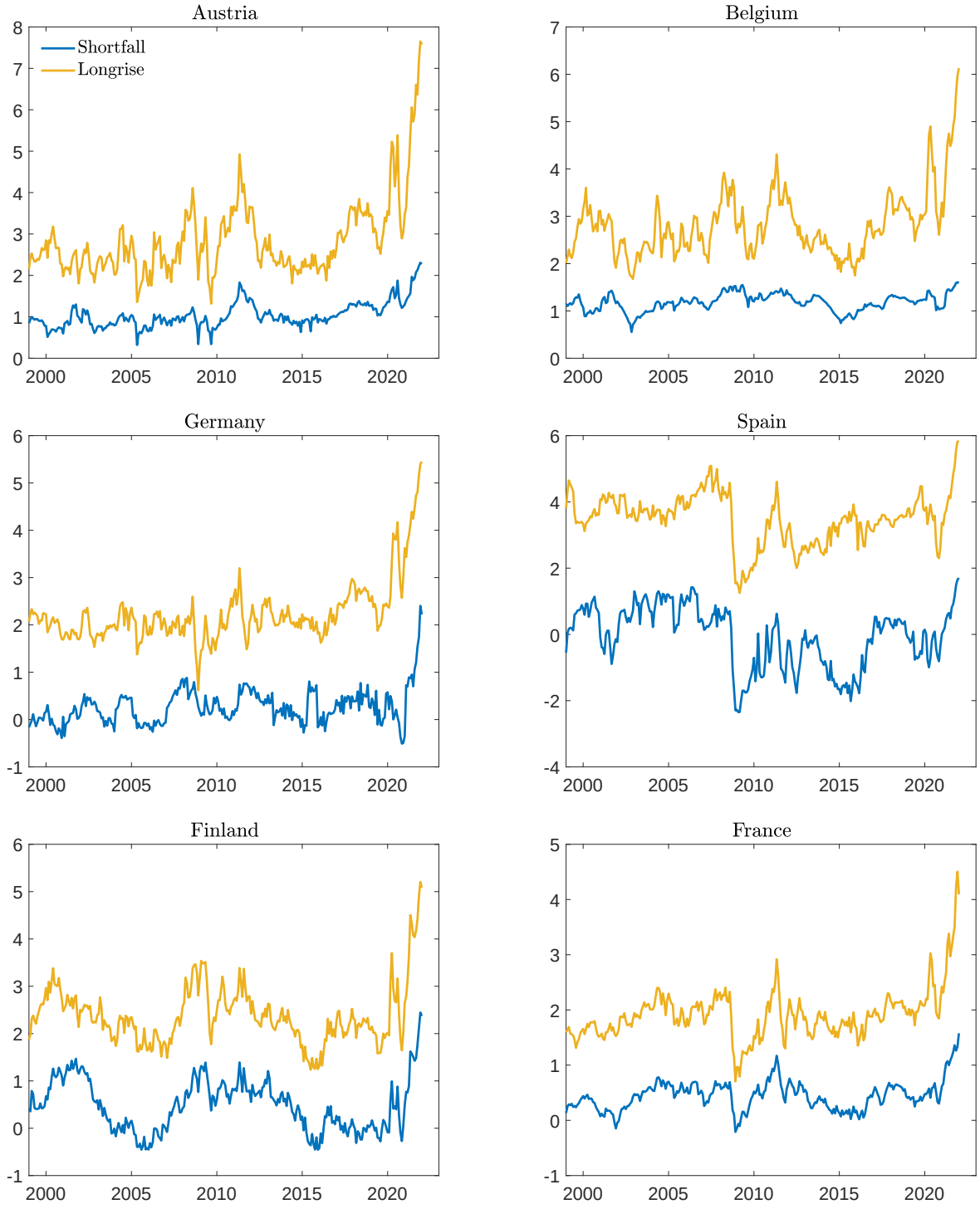

Note: Expected shortfall and longrise SF^i_{t+h} and LR^i_{t+h} for country i, $p = 0.10$ and forecast horizon $h = 12$. SF^i_{t+h} and LR^i_{t+h} are defined by equation (III.6).

Figure III.D.4 – Expected shortfall and longrise by country

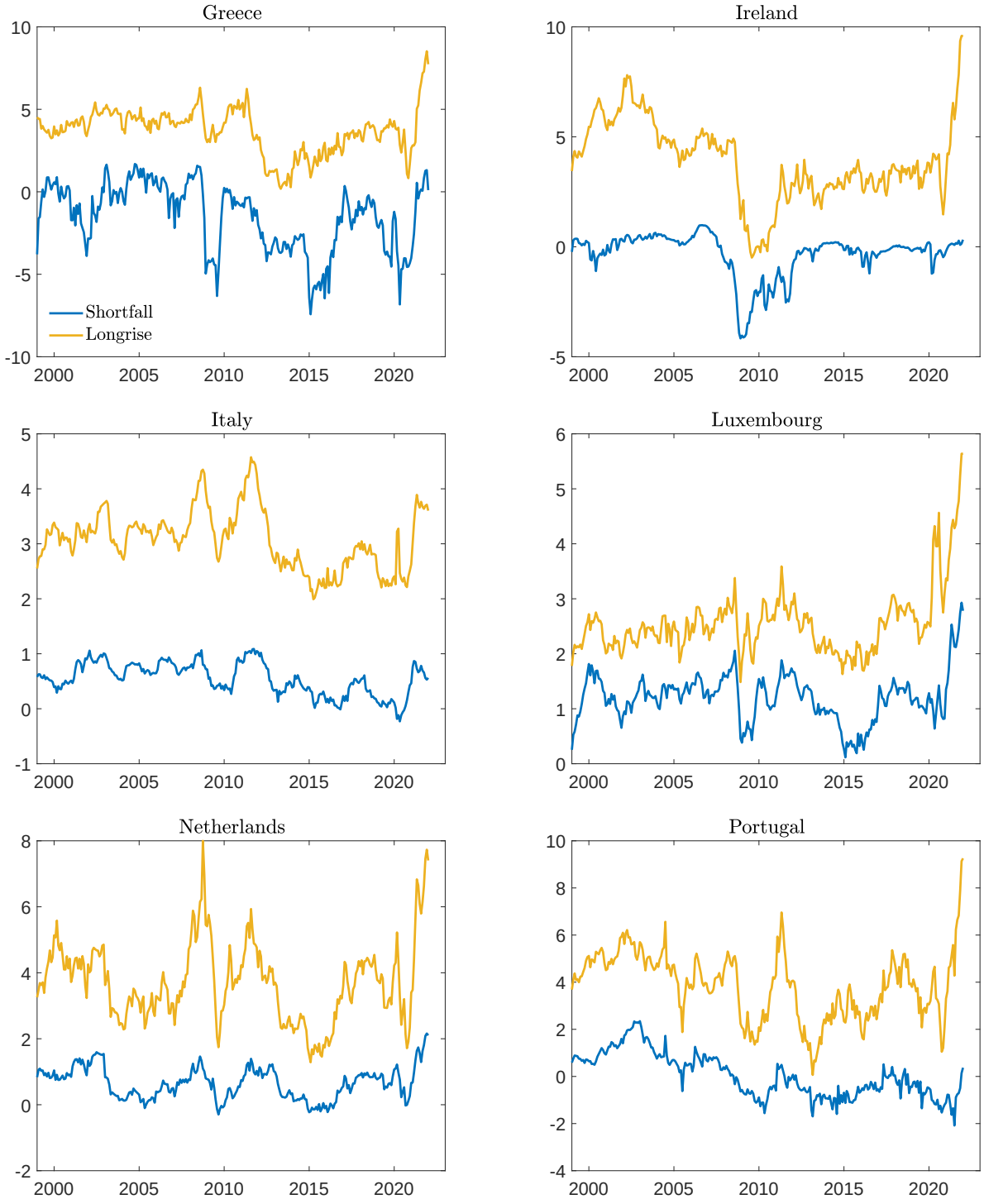

Note: Expected shortfall and longrise SF^i_{t+h} and LR^i_{t+h} for country i, $p = 0.10$ and forecast horizon $h = 12$. SF^i_{t+h} and LR^i_{t+h} are defined by equation (III.6).

III.E Counterfactual Exercises using HICP

Figure III.E.5 depicts the results using HICP instead of core HICP used in the benchmark model. Considering headline inflation in the analysis confirms previous results of the role of global supply chain in the evolution of inflation distribution. However, the results are even more striking than in the case where core inflation is used, especially regarding the results for $h = 12$ and the 90^{th} quantile (Panel E). The dispersion peaks around March 2020 and at the end of the sample period of estimation to reach levels almost thrice the one observed during the COVID crisis. However, without supply chain pressures, the dispersion of inflation at the top of the distribution would have been muted, or at least similar to the level observed before the pandemic outbreak. From this point of view, tensions on global supply chain is a more important feature of HICP dispersion than core inflation dispersion across euro area countries.

On the other hand, the results for $h = 3$ and the 90^{th} quantile (Panel F) contrast a little with the previous ones, at least regarding the last months of the estimation period. They suggest that supply chain pressures have played a less prominent role in inflation dispersion during the COVID crisis, and that this effect has been particularly decreasing over the last few months of the sample period. Simulated series without supply chain seems to catch up the dispersion series estimated with the benchmark model.

Figure III.E.5 – Dispersion of conditional quantiles without oil price and supply chain pressures (HICP inflation)

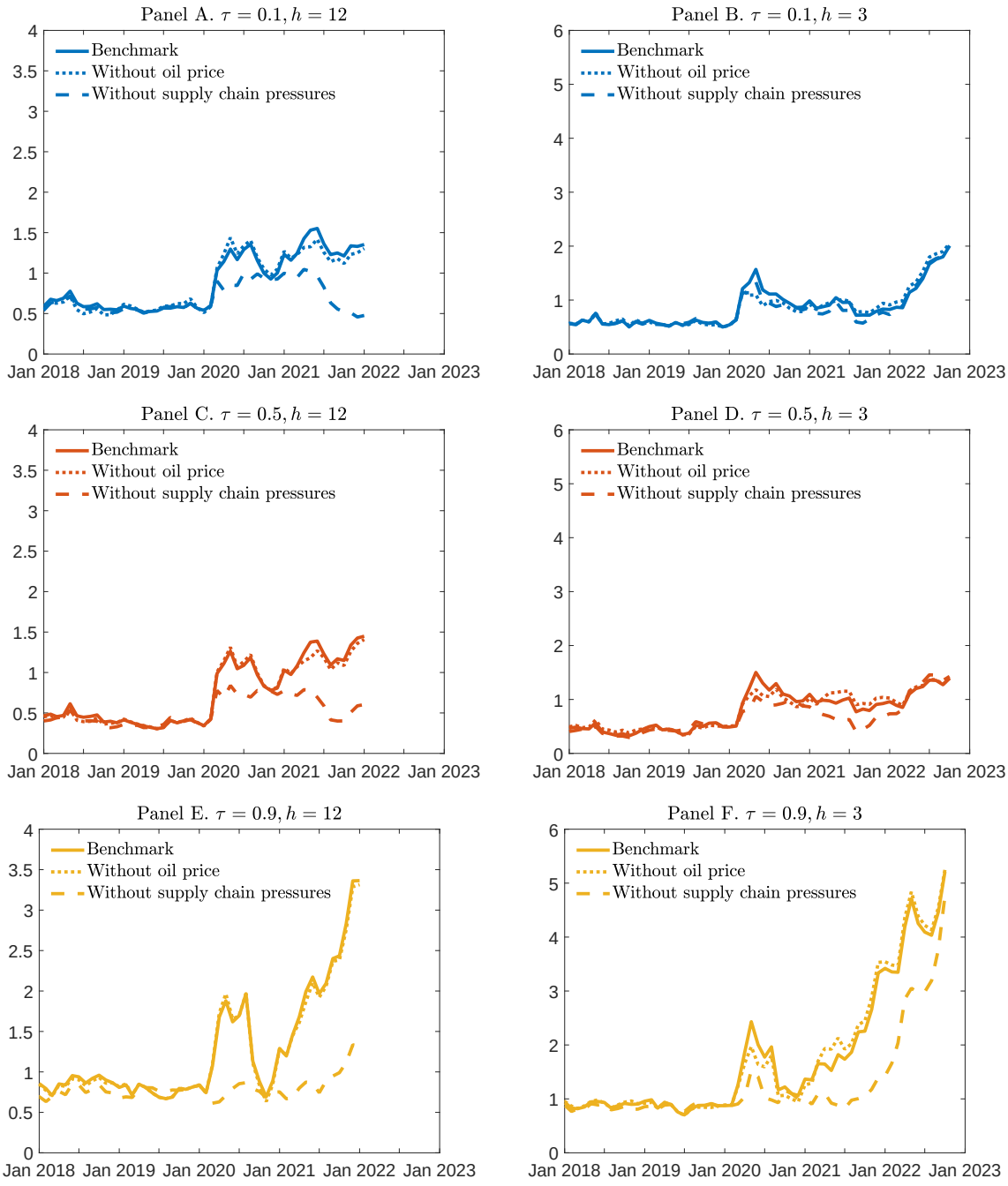

Note: The case without oil price corresponds to the standard deviation of conditional quantiles predicted for $\pi_t^{o,*} = \pi_t^{*,i}$ in the quantile Phillips curve (III.2) estimated with HICP. The case without supply chain pressures corresponds to the standard deviation of conditional quantiles predicted for $sc_t = 0$ in the quantile Phillips curve (III.2). The first column of panels is for the one-year forecast ($h = 12$) and the second one is for the one-quarter forecast ($h = 3$). The first row of panels is for the 10^{th} quantile, the second one for the 50^{th} quantile, and the third one for the 90^{th} quantile.

III.F Markov-switching Procedure

III.F.1 The Posterior Density

Since the posterior density function of Markov-switching models is very non-Gaussian, it is essential to find the posterior mode via an optimization routine prior to sample from the posterior density. The estimate of the mode not only represents the most likely value, but also serves as a crucial starting point for initializing different chains of Monte Carlo Markov Chains (MCMC) draws.

The strategy to find the posterior mode is to generate a sufficient number of draws from the prior distribution of each parameter. Each set of points is then used as starting points to the `CSMINWEL` program, the optimization routine developed by Christopher A. Sims. Starting the optimization process at different values allows us to correctly cover the parameter space and avoid getting stuck in a "local" peak. Note, however, that we do not need to use a more complicated method for finding the mode like the blockwise optimization method developed by Sims et al. (2008). The authors employ a class of richly parameterized multivariate Markov-switching models in which the parameters are break into several subblocks, and then apply a standard hill-climbing quasi-Newton optimization routine to each block, while keeping the other subblocks constant, in order to maximize the posterior density. The size of Markov-switching univariate models remains relatively small and allows us to employ a more standard technique.

The posterior density is not of standard form, making it impossible to sample directly from this probability distribution. One can, however, use the idea of Gibbs sampling to obtain the empirical joint posterior density by sampling alternately from the following conditional posterior distribution. Our Gibbs sampler procedure begins with setting parameters at the peak of the posterior density function. The MCMC sampling sequence involves a 4-block Gibbs sampler, in which we can generate in a flexible and straightforward manner alternatively draws from full conditional posterior distributions. Overall, our procedure follows the MCMC approach proposed by Albert and Chib (1993).

In the remainder of this section, we simplify the notation by suppressing the superscript i denoting the country of interest. For $1 \leq k \leq H$, let $\theta(k) = [\mu(k), \lambda(k), \theta(k), \gamma(k), \delta(k), \phi(k)]'$, $S_t = [s_1, \ldots, s_t]$, and q_k be the k-th column of Q. The objets $\theta(k)$ and q_k are vectors of

parameters. The prior on the set of parameters is given by:

$$p(\theta(k)) = \text{normal}(\theta(k)|\bar{\theta}_1, \bar{\theta}_2), \tag{III.10}$$

$$p(\sigma(k)) = \text{inv-gamma}(\sigma(k)|\bar{\sigma}_1, \bar{\sigma}_2), \tag{III.11}$$

$$p(q_k) = \text{dirichlet}(q_k|\bar{q}_{1,k}, \bar{q}_{2,k}, \bar{q}_{3,k}), \tag{III.12}$$

where $\bar{\theta}_1$, $\bar{\theta}_2$, $\bar{q}_{1,j}$, $\bar{q}_{2,j}$, and $\bar{q}_{3,j}$ are the hyperparameters; normal$(x|.)$ denotes the multivariate normal distribution; inv-gamma$(x|.)$ denotes the inverse gamma distribution; and dirichlet$(x|.)$ denotes the dirichlet distribution.

In our empirical setting, our normal prior for $\theta(k)$ is very dispersed and cover a large parameter space. We choose a prior with the mean 0.00 and the standard deviation 5.00, except for the prior of $\lambda(k)$, of which the mean 0.50 and the standard deviation 0.20, and truncated to values between zero and one. The inverse-gamma prior for the scale parameter, $\sigma(k)$, are set as $\bar{\sigma}_1 = 0.1938$ and $\bar{\sigma}_2 = 2.1551$. It may be worth noting that we impose the exact same prior across regimes and across countries, so that the differences in parameters between regimes and countries result more from data (i.e., the likelihood) rather than priors. We imply a prior belief that the average duration of staying in the same regime is about eleven months. This means that, for example, the hyperparameters are $\bar{q}_{1,j} = 20$, $\bar{q}_{2,j} = \bar{q}_{3,j} = 1$ for the first regime. See Sims et al. (2008) for further details on how to define prior beliefs about the persistence of the regimes.

The MCMC sampling scheme at the (n)st iteration, for $n = 1, \ldots, N_1 + N_2$, consists of sampling from the following conditional posterior distributions

1. $p\left(S_T^{(n)}|Y_T, \theta^{(n-1)}, Q^{(n-1)}\right)$,
2. $p\left(Q^{(n)}|S_T\right)$,
3. $p\left(\theta^{(n)}(k)|Y_T, S_T^{(n)}, \sigma^{(n-1)}\right)$,
4. $p\left(\sigma(k)^{(n)}|Y_T, S_T^{(n)}, \theta^{(n)}\right)$,

where Y_t are observed data, $\theta = \theta(k)_{k\in H}$, and $\sigma = \sigma(k)_{k\in H}$. Simulation from the conditional posterior density $p\left(S_T^{(n)}|Y_T, \theta^{(n-1)}\right)$, given θ and Q, is standard and in closed form. Simulation from the conditional posterior density $p\left(Q^{(n)}|S_T\right)$ is of the dirichlet form. Simulations from the conditional posterior densities $p\left(\theta^{(n)}(k)|Y_T, S_T^{(n)}, \sigma^{(n-1)}\right)$ and $p\left(\sigma(k)^{(n)}|Y_T, S_T^{(n)}, \theta^{(n)}\right)$ reduces to Bayesian inference for Markov-switching models with known allocations, S_T.

The sampler begins with setting parameters at the peak of the posterior density function. We generate $N_1 + N_2 = 11,000$ draws, the first $N_1 = 1{,}000$ are discarded as burn-in and of the remaining $N2 = 10,000$ draws, one of every 10 draws is retained to get $1,000$ draws of parameters and sequences of regimes.

We now provide further details on each of these conditional density functions. In the remainder of this section, we simplify the notation by suppressing the superscript n denoting the n-th draws of the simulation.

Conditional posterior densities, $p\left(S_T|Y_T,\theta,Q\right)$

Following the Carter and Kohn (1994b)'s multi-move Gibbs-sampling procedure, one can stimulate S_T as a block. We begin with a draw from $p(s_T|Y_T,\theta,Q)$ obtained with the Hamilton (1989) basic filter, and then iterate recursively backward to draw $s_{T-1}, s_{T-2}, \ldots, 1$ according to

$$p(s_t|Y_T,\theta,Q) = \sum_{s_{t+1}\in H} p(s_t|Y_t,\theta,Q,s_{t+1})p(s_{t+1}|Y_T,\theta,Q), \tag{III.13}$$

where

$$p(s_t|Y_t,\theta,Q,s_{t+1}) = \frac{q_{s_{t+1},s_t}p(s_t|Y_t,\theta,Q)}{p(s_{t+1}|Y_t,\theta,Q)} \tag{III.14}$$

Conditional posterior densities, $p\left(Q|S_T\right)$

Given the historical path of regimes, the transition matrix can be directly simulate from the Dirichlet distribution. For each column k of Q, denoted q_k, the conditional posterior distribution is given by

$$p(q_k|S_T) = \text{dirichet}(q_k|\bar{q}_{1,k}+\eta_{1,k}, \bar{q}_{2,k}+\eta_{2,k}, \bar{q}_{3,k}+\eta_{3,k}), \tag{III.15}$$

where $\bar{q}_{1,k}, \bar{q}_{2,k}$ and $\bar{q}_{3,k}$ are the parameters describing the prior, and $\eta_{i,k}$ denotes the numbers of transitions from state k to state i.

Conditional posterior densities, $p\left(\theta(k)|Y_T,S_T,\sigma\right)$

Geweke (1996) implements a Gibbs sampling procedure for the problem of multiple linear regression with a set of independent inequality linear constraints. We follow a similar procedure for our Markov-switching model with known allocations S_T.

The Markov-switching model in (III.8) can be rewritten in a compact as $y_t = \theta(s_t)'x_t + \sigma(s_t)\varepsilon_t$, where y_t is our variable of interest, and x_t contains the vectors of observed data at date

t. Let $y_t^* = \frac{y_t}{\sigma_{s_t}}$, and $x_t^* = \frac{x_t}{\sigma_{s_t}}$, we obtain an homoskedastic model as follows

$$y_t^* = \theta(s_t)' x_t^* + \nu_t, \tag{III.16}$$

where ν_t follows a standard normal distribution. Then, simulation from the full conditional distribution of Ψ, given Y_T, S_T, and σ, becomes straightforward, given a conjugate prior distribution. For $1 \leq k \leq H$, the posterior is defined as

$$p\left(\theta(k)|Y_T, S_T\right) = \text{truncated-normal}\left(\theta(k)|m_{\mu,k}, M_{\mu,k}\right)_{a \leq \theta(k) \leq b}, \tag{III.17}$$

where truncated-normal$(x|\bar{x}_1, \bar{x}_2)_{a \leq x \leq b}$ is the truncated multivariate normal distribution with mean $\bar{x}_1$, variance-covariance $\bar{x}_2$, and inequality constraints $a \leq x \leq b$. The vector $m_{\mu,k}$ and matrix $M_{\mu,k}$ are defined as follows

$$m_{\mu,k} = \left(\bar{\theta}_2^{-1} + \Sigma_{xx,k}\right)^{-1} \left(\bar{\theta}_2^{-1}\bar{\theta}_1 + \Sigma_{xy,k}\right), \tag{III.18}$$

$$M_{\mu,k} = \left(\bar{\theta}_2^{-1} + \Sigma_{xx,k}\right)^{-1}, \tag{III.19}$$

with $\bar{\theta}_1$ and $\bar{\theta}_2$ are known hyperparameters of the prior distribution, and

$$\Sigma_{xx,k} = \sum_{t \in \{t:s_t=k\}} x_t^* x_t^{*'},$$

$$\Sigma_{xy,k} = \sum_{t \in \{t:s_t=k\}} x_t^* y_t^*.$$

This step implies a computational complication that requires the simulation from a truncated multivariate normal distribution. We use the minimax tilting method proposed by Botev (2017) for exact independently and identically distributed data simulation from the truncated multivariate normal distribution.[8] The method is an excellent algorithm designed for extremely fast simulation.

[8]The Matlab function is available at https://fr.mathworks.com/matlabcentral/fileexchange/53792-truncated-multivariate-normal-generator.

Conditional posterior densities, $p\left(\sigma(k)|Y_T, S_T, \theta\right)$

Given Y_t, S_T, and θ, the scale parameter $\sigma(k)$ can be drawn using the following inverse-gamma distribution

$$p\left(\sigma(k)|Y_T, S_T, \theta\right) = \text{inv-gamma}(\sigma(k)|\tilde{\alpha}, \tilde{\beta}), \tag{III.20}$$

where

$$\begin{aligned}
\tilde{\alpha} &= \bar{\sigma}_1 + \sum_{t\in\{t:s_t=k\}} \left(y_t - \theta'_{s_t} x_t\right)^2, \\
\tilde{\beta} &= \bar{\sigma}_2 + T_k,
\end{aligned}$$

with $\sum_{t\in\{t:s_t=k\}} \left(y_t - \theta'_{s_t} x_t\right)^2$ is the sum of squared residual, T_k is the number of elements of t's such that $s_t = k$ for $k = 1, 2, 3$, and $\bar{\sigma}_1$ and $\bar{\sigma}_2$ are the hyperparameters.

III.F.2 Additional Results

Tables III.F.1, III.F.2, III.F.3 and III.F.4 reports the posterior distribution of parameters for each country.

Table III.F.1 – Posterior Distributions - Markov-switching framework

	$\mu^i(s_t=1)$	$\lambda^i(s_t=1)$	$\theta^i(s_t=1)$	$\gamma^i(s_t=1)$	$\delta^i(s_t=1)$	$\phi^i(s_t=1)$	$\sigma^i(s_t=1)$
Germany	−1.09 [−1.35;−0.81]	0.46 [0.20;0.75]	−0.50 [−1.52;−0.05]	0.46 [0.10;0.84]	1.29 [−0.21;3.83]	0.16 [0.02;0.53]	0.33 [0.26;0.44]
France	−1.05 [−1.18;−0.90]	0.93 [0.78;0.99]	−0.07 [−0.22;−0.00]	0.15 [0.01;0.42]	−0.65 [−1.33;0.06]	0.11 [0.02;0.22]	0.21 [0.18;0.27]
Italy	−0.81 [−1.15;−0.43]	0.66 [0.33;0.94]	−0.11 [−0.31;−0.01]	0.13 [0.01;0.36]	0.29 [−1.17;1.38]	0.07 [0.01;0.24]	0.28 [0.22;0.33]
Spain	−1.78 [−2.05;−1.21]	0.90 [0.63;0.99]	−0.13 [−0.29;−0.01]	0.31 [0.03;0.86]	−0.56 [−2.38;0.32]	0.20 [0.04;0.40]	0.35 [0.26;0.50]
Netherlands	−0.93 [−1.07;−0.79]	0.89 [0.77;0.98]	−0.69 [−1.02;−0.30]	0.32 [0.07;0.62]	0.31 [−0.34;0.92]	0.18 [0.03;0.37]	0.30 [0.25;0.36]
Finland	−0.93 [−1.14;−0.70]	0.70 [0.49;0.89]	−0.12 [−0.27;−0.01]	0.12 [0.01;0.41]	0.56 [−1.23;2.00]	0.20 [0.03;0.38]	0.27 [0.23;0.32]
Ireland	−1.55 [−1.95;−1.28]	0.96 [0.87;1.00]	−0.04 [−0.14;−0.00]	0.09 [0.01;0.32]	−4.30 [−5.09;−3.38]	0.24 [0.02;0.55]	0.56 [0.47;0.68]
Austria	−0.62 [−0.82;−0.44]	0.81 [0.59;0.96]	−0.14 [−0.42;−0.01]	0.18 [0.02;0.55]	0.32 [−0.49;1.67]	0.25 [0.05;0.86]	0.27 [0.22;0.37]
Portugal	−0.79 [−1.01;−0.61]	0.48 [0.36;0.59]	−0.04 [−0.16;−0.00]	0.30 [0.05;0.69]	−1.01 [−1.64;−0.30]	0.04 [0.00;0.14]	0.54 [0.48;0.60]
Belgium	−0.54 [−8.36;−0.40]	0.81 [0.14;0.97]	−0.24 [−7.66;−0.03]	0.22 [0.02;801.67]	0.48 [−5.56;5.23]	0.14 [0.01;8.22]	0.21 [0.17;0.94]
Luxembourg	−0.47 [−0.65;−0.29]	0.86 [0.56;0.99]	−0.12 [−0.40;−0.01]	0.28 [0.05;0.56]	0.03 [−0.92;0.96]	0.16 [0.02;0.35]	0.24 [0.20;0.29]
Greece	−2.79 [−3.69;−1.96]	0.43 [0.04;0.99]	−0.10 [−0.38;−0.01]	1.99 [0.70;3.71]	0.17 [−5.26;3.82]	0.52 [0.08;1.10]	0.71 [0.51;1.03]
Mean	−1.11	0.74	−0.19	0.38	−0.26	0.19	0.36
Std. Dev.	0.65	0.19	0.20	0.52	1.41	0.12	0.16

Note: Posterior median of Phillips curve's parameters based on equation (III.8): $\bar{\pi}^i_{t+1,t+h} = \mu^i(s^i_t) + \left(1-\lambda^i(s^i_t)\right)\pi^{*,i}_{t-1} + \lambda^i(s^i_t)\pi^{LTE,i}_t + \theta^i(s^i_t)\left(u^i_t - u^{*,i}_t\right) + \gamma^i(s^i_t)\left(\pi^{o,*}_t - \pi^{*,i}_t\right) + \delta^i(s^i_t)f^i_t + \phi^i(s^i_t)sc_t + \sigma^i(s^i_t)\varepsilon^i_t$. The 90% probability interval is indicated in brackets.

Table III.F.2 – Posterior Distributions - Markov-switching framework

	$\mu^i(s_t=2)$	$\lambda^i(s_t=2)$	$\theta^i(s_t=2)$	$\gamma^i(s_t=2)$	$\delta^i(s_t=2)$	$\phi^i(s_t=2)$	$\sigma^i(s_t=2)$
Germany	−0.45 [−0.57;−0.33]	0.92 [0.77;0.99]	−0.43 [−0.71;−0.13]	0.24 [0.04;0.47]	−0.26 [−0.66;0.26]	0.19 [0.06;0.31]	0.27 [0.23;0.31]
France	−0.43 [−0.55;−0.28]	0.89 [0.76;0.98]	−0.30 [−0.55;−0.08]	0.11 [0.01;0.25]	−0.78 [−1.18;−0.35]	0.05 [0.01;0.16]	0.18 [0.15;0.22]
Italy	0.07 [−0.12;0.27]	0.76 [0.32;0.98]	−0.11 [−0.33;−0.01]	0.22 [0.04;0.50]	−0.35 [−1.66;1.42]	0.09 [0.01;0.22]	0.26 [0.20;0.32]
Spain	−0.27 [−0.42;−0.08]	0.50 [0.38;0.66]	−0.06 [−0.18;−0.01]	0.11 [0.01;0.53]	−0.21 [−0.98;0.69]	0.04 [0.00;0.14]	0.30 [0.25;0.36]
Netherlands	−0.18 [−0.43;0.01]	0.81 [0.63;0.96]	−0.91 [−1.49;−0.29]	0.36 [0.06;0.72]	0.35 [−1.01;2.85]	0.19 [0.03;0.59]	0.33 [0.25;0.45]
Finland	−0.04 [−0.20;0.10]	0.73 [0.39;0.94]	−0.13 [−0.31;−0.01]	0.44 [0.12;0.88]	0.51 [−0.12;4.89]	0.24 [0.05;0.48]	0.25 [0.20;0.31]
Ireland	−0.62 [−0.79;−0.45]	0.77 [0.67;0.89]	−0.08 [−0.26;−0.01]	0.41 [0.08;0.88]	−1.16 [−2.55;0.08]	0.10 [0.01;0.28]	0.38 [0.32;0.44]
Austria	−0.07 [−0.21;0.06]	0.91 [0.74;0.99]	−0.10 [−0.32;−0.01]	0.23 [0.04;0.48]	0.32 [−0.51;1.97]	0.22 [0.06;0.37]	0.23 [0.19;0.27]
Portugal	0.04 [−0.20;0.38]	0.33 [0.21;0.46]	−0.30 [−0.65;−0.05]	1.13 [0.86;1.40]	2.03 [0.55;3.12]	0.16 [0.02;0.42]	0.39 [0.33;0.45]
Belgium	0.03 [−0.51;0.42]	0.89 [0.70;0.99]	−0.19 [−0.62;−0.02]	0.12 [0.01;0.41]	0.12 [−1.48;1.07]	0.12 [0.02;0.54]	0.22 [0.18;0.29]
Luxembourg	0.08 [−0.06;0.20]	0.85 [0.69;0.98]	−0.22 [−0.49;−0.04]	0.24 [0.05;0.49]	−0.20 [−0.93;0.62]	0.04 [0.00;0.14]	0.18 [0.15;0.21]
Greece	−1.08 [−1.30;−0.81]	0.72 [0.58;0.93]	−0.48 [−0.74;−0.08]	0.19 [0.02;0.51]	0.64 [−0.67;1.84]	0.29 [0.05;0.54]	0.48 [0.37;0.57]
Mean	−0.24	0.76	−0.28	0.32	0.08	0.14	0.29
Std. Dev.	0.35	0.18	0.24	0.28	0.81	0.08	0.09

Note: Posterior median of Phillips curve's parameters based on equation (III.8): $\bar{\pi}^i_{t+1,t+h} = \mu^i(s^i_t) + \left(1-\lambda^i(s^i_t)\right)\pi^{*,i}_{t-1} + \lambda^i(s^i_t)\pi^{LTE,i}_t + \theta^i(s^i_t)\left(u^i_t - u^{*,i}_t\right) + \gamma^i(s^i_t)\left(\pi^{o,*}_t - \pi^{*,i}_t\right) + \delta^i(s^i_t)f^i_t + \phi^i(s^i_t)sc_t + \sigma^i(s^i_t)\varepsilon^i_t$. The 90% probability interval is indicated in brackets.

Table III.F.3 – Posterior Distributions - Markov-switching framework

	$\mu^i(s_t=3)$	$\lambda^i(s_t=3)$	$\theta^i(s_t=3)$	$\gamma^i(s_t=3)$	$\delta^i(s_t=3)$	$\phi^i(s_t=3)$	$\sigma^i(s_t=3)$
Germany	0.65 [0.41;0.95]	0.91 [0.71;0.99]	−0.15 [−0.65;−0.01]	0.21 [0.02;0.69]	−2.67 [−4.17;−0.79]	0.37 [0.19;0.56]	0.48 [0.38;0.62]
France	0.17 [0.02;0.33]	0.84 [0.61;0.98]	−0.57 [−0.93;−0.20]	0.13 [0.01;0.36]	−0.87 [−3.02;1.43]	0.30 [0.19;0.42]	0.21 [0.18;0.26]
Italy	0.78 [0.53;1.07]	0.58 [0.25;0.87]	−0.22 [−0.75;−0.03]	0.21 [0.02;0.59]	0.75 [−0.93;2.78]	0.08 [0.00;0.30]	0.33 [0.25;0.41]
Spain	0.97 [0.73;1.23]	0.90 [0.69;0.99]	−0.73 [−1.06;−0.41]	0.11 [0.01;0.39]	−2.55 [−3.82;−1.15]	0.45 [0.25;0.70]	0.44 [0.35;0.53]
Netherlands	1.24 [0.82;1.92]	0.91 [0.68;0.99]	−1.16 [−2.29;−0.37]	1.11 [0.40;1.70]	−0.17 [−2.85;3.35]	0.08 [0.01;0.30]	0.57 [0.40;0.73]
Finland	0.31 [0.01;0.81]	0.56 [0.18;0.89]	−0.18 [−0.51;−0.02]	0.73 [0.21;1.13]	1.42 [−1.06;4.59]	0.39 [0.13;0.57]	0.27 [0.21;0.36]
Ireland	1.68 [1.21;2.18]	0.68 [0.52;0.86]	−0.65 [−1.21;−0.16]	0.16 [0.02;0.53]	0.67 [−4.09;5.03]	0.71 [0.41;1.02]	0.84 [0.73;0.98]
Austria	0.61 [0.28;0.92]	0.80 [0.34;0.98]	−0.20 [−0.58;−0.02]	0.47 [0.10;0.95]	0.39 [−0.92;1.96]	0.60 [0.32;0.81]	0.30 [0.23;0.38]
Portugal	2.06 [1.62;2.51]	0.72 [0.29;0.96]	−2.02 [−2.89;−1.00]	1.54 [0.70;2.26]	0.66 [−4.27;5.26]	0.43 [0.08;1.01]	0.52 [0.39;0.71]
Belgium	0.64 [0.40;1.26]	0.87 [0.28;0.99]	−0.49 [−0.84;−0.10]	0.37 [0.05;0.90]	−0.36 [−2.20;1.48]	0.31 [0.07;0.52]	0.33 [0.24;0.42]
Luxembourg	0.63 [0.29;1.00]	0.59 [0.26;0.89]	−0.32 [−0.87;−0.03]	0.26 [0.03;0.64]	−0.30 [−2.89;2.00]	0.40 [0.24;0.55]	0.28 [0.20;0.40]
Greece	0.48 [0.21;0.73]	0.87 [0.73;0.97]	−0.35 [−0.70;−0.06]	0.66 [0.27;1.03]	1.55 [−0.26;3.65]	0.33 [0.03;0.65]	0.58 [0.49;0.67]
Mean	0.85	0.77	−0.59	0.50	−0.12	0.37	0.43
Std. Dev.	0.56	0.14	0.54	0.45	1.36	0.18	0.18

Note: Posterior median of Phillips curve's parameters based on equation (III.8): $\bar{\pi}^i_{t+1,t+h} = \mu^i(s^i_t) + \left(1-\lambda^i(s^i_t)\right)\pi^{*,i}_{t-1} + \lambda^i(s^i_t)\pi^{LTE,i}_t + \theta^i(s^i_t)\left(u^i_t - u^{*,i}_t\right) + \gamma^i(s^i_t)\left(\pi^{o,*}_t - \pi^{*,i}_t\right) + \delta^i(s^i_t)f^i_t + \phi^i(s^i_t)sc_t + \sigma^i(s^i_t)\varepsilon^i_t$. The 90% probability interval is indicated in brackets.

Table III.F.4 – Posterior Distributions - Transition Matrices

	q^i_{11}	q^i_{21}	q^i_{31}	q^i_{12}	q^i_{22}	q^i_{32}	q^i_{13}	q^i_{23}	q^i_{33}
Germany	0.87 [0.80;0.93]	0.08 [0.03;0.15]	0.04 [0.01;0.10]	0.04 [0.02;0.07]	0.93 [0.88;0.96]	0.03 [0.01;0.07]	0.03 [0.01;0.07]	0.08 [0.04;0.15]	0.89 [0.82;0.94]
France	0.92 [0.85;0.96]	0.05 [0.01;0.11]	0.03 [0.01;0.08]	0.06 [0.02;0.13]	0.89 [0.80;0.94]	0.05 [0.02;0.12]	0.02 [0.00;0.07]	0.05 [0.01;0.10]	0.92 [0.87;0.96]
Italy	0.94 [0.89;0.98]	0.04 [0.01;0.09]	0.02 [0.00;0.04]	0.04 [0.02;0.10]	0.91 [0.84;0.95]	0.05 [0.02;0.09]	0.02 [0.00;0.06]	0.07 [0.03;0.13]	0.90 [0.84;0.95]
Spain	0.89 [0.82;0.94]	0.07 [0.03;0.14]	0.03 [0.01;0.09]	0.03 [0.01;0.06]	0.92 [0.88;0.96]	0.04 [0.02;0.08]	0.03 [0.01;0.07]	0.07 [0.03;0.13]	0.90 [0.84;0.95]
Netherlands	0.92 [0.87;0.95]	0.07 [0.03;0.11]	0.02 [0.00;0.04]	0.07 [0.03;0.12]	0.89 [0.83;0.94]	0.04 [0.01;0.09]	0.03 [0.01;0.09]	0.06 [0.02;0.12]	0.90 [0.83;0.96]
Finland	0.95 [0.91;0.98]	0.03 [0.01;0.06]	0.02 [0.00;0.05]	0.04 [0.01;0.08]	0.91 [0.84;0.95]	0.05 [0.02;0.11]	0.03 [0.01;0.08]	0.07 [0.03;0.13]	0.90 [0.82;0.95]
Ireland	0.91 [0.85;0.96]	0.06 [0.02;0.12]	0.02 [0.00;0.06]	0.04 [0.02;0.08]	0.93 [0.89;0.96]	0.02 [0.01;0.05]	0.02 [0.00;0.05]	0.04 [0.02;0.08]	0.94 [0.89;0.97]
Austria	0.88 [0.82;0.94]	0.09 [0.04;0.15]	0.03 [0.01;0.08]	0.05 [0.02;0.08]	0.90 [0.84;0.94]	0.05 [0.02;0.10]	0.02 [0.00;0.07]	0.09 [0.04;0.16]	0.88 [0.80;0.93]
Portugal	0.94 [0.90;0.97]	0.04 [0.01;0.07]	0.02 [0.00;0.04]	0.05 [0.02;0.09]	0.92 [0.88;0.96]	0.02 [0.01;0.05]	0.04 [0.01;0.10]	0.06 [0.02;0.13]	0.90 [0.81;0.96]
Belgium	0.91 [0.75;0.96]	0.06 [0.02;0.15]	0.03 [0.00;0.15]	0.06 [0.00;0.14]	0.89 [0.78;0.96]	0.06 [0.03;0.11]	0.02 [0.00;0.08]	0.08 [0.04;0.16]	0.89 [0.80;0.94]
Luxembourg	0.92 [0.88;0.96]	0.05 [0.02;0.10]	0.02 [0.00;0.06]	0.04 [0.02;0.08]	0.92 [0.88;0.96]	0.03 [0.01;0.07]	0.03 [0.01;0.09]	0.08 [0.03;0.16]	0.88 [0.79;0.94]
Greece	0.92 [0.86;0.96]	0.05 [0.02;0.11]	0.02 [0.01;0.07]	0.03 [0.01;0.07]	0.92 [0.88;0.96]	0.04 [0.02;0.08]	0.01 [0.00;0.04]	0.03 [0.01;0.06]	0.95 [0.92;0.98]

Note: Posterior median of transition matrices. The 90% probability interval is indicated in brackets.

Conclusion

In this thesis, I have studied three different issues related to the topic of monetary policy, inflation and financial markets in the euro area. Using empirical techniques, I tried to lay the emphasis on the role of ECB's monetary policy in stabilizing the economy and financial markets, especially during macroeconomic or financial downturns. I also attempted to shed light on how linkages between macroeconomic and financial risks matter for monetary policy.

This thesis is divided into three chapters. In the first chapter, I investigate possible changes in the reaction of monetary policy to inflation and real economic activity in the wake of the Great Recession, and how it may have affected macroeconomic performances. Using a time-varying parameters vector autoregressive model, the results show that the conduct of monetary policy in the euro area has evolved differently than in the U.S. after the 2008 crisis. Whereas the estimated U.S. policy rule does not suggest any significant change in the Fed's systematic reaction to macroeconomic fluctuations after 2008, euro area reaction function reveals important changes in ECB's monetary policy, which has considerably increased the weight it placed on stabilizing inflation. A counterfactual analysis shows that the shift in ECB monetary policy appears to be a key determinant of the level of inflation in the euro area at the ZLB, that would have suffered successive deflationary episodes from 2014 onward.

In the second part of the thesis, we study the role of the ECB during financial markets downturn in the early stage of the COVID pandemic outbreak. Using state-dependent local projections to measure the evolution of COVID-induced sovereign risk in the euro area around major ECB interventions, estimation results show that despite the controversy generated by the "we are not here to close spreads" declaration of Christine Lagarde, the ECB actually stopped the spread of the pandemic-sparked crisis to the euro area sovereign debt markets on March 12, before the announcement of the PEPP and the conduct of market operations that occurred on March 18, leading to the reversal of sovereign spreads. A counterfactual analysis indicates that without ECB's interventions, sovereign spreads in the euro area would have reached levels

comparable to those observed during the 2010-12 sovereign debt crisis.

In the last part of the thesis, we explore the topic of inflation differentials in the euro area, and focus especially on the dispersion of inflation risks among member countries. Constructing measures of risk of inflation dispersion based on the cross-country standard deviation of predictive inflation distribution, our results indicate that whereas the dispersion was concentrated on upside inflation risks until 2008, it has been stronger for the lower tail of the distribution after 2008. The results also show that inflation dispersion has been driven by successive episodes of downside and upside inflation risks over the post-COVID period. A counterfactual analysis highlights financial stress as being a key determinant of the dispersion of downside inflation risks, and supply chains disruptions a being an important driver of the dispersion of upside risk to inflation. Estimation results also reveal noticeable Phillips curves heterogeneity across countries, and underline the role of heterogeneous Phillips curve coefficients in the dispersion of inflation in the euro area.

The first two chapters of this thesis deal with the role of ECB monetary policy in a context of deflationary pressures, first during the Great Recession then in the early stage of the COVID crisis. On the other hand, the last chapter raises some policy implications of the current context marked by the return of high inflation. In this regard, the topic of the interplay between monetary policy, inflation and financial markets—the core topic of this thesis—is more relevant than ever since the ECB has recently entered a new phase of monetary policy. Figure 1 shows how the ECB has successively raised its key policy rate since July 2022 in reaction to the rapid surge in inflation of 2021. This increase in the main refinancing operations (MRO) rate contrasts with the relatively long period of ZLB and weak inflation in the euro area. Through these consecutive policy actions, the ECB has reaffirmed its determination to fight inflation and achieve its primary objective of price stability.

This topic is even more important in a context of unprecedented pace of rate hikes in the euro area. As depicted in Figure 2, the monetary tightening of 2022 has been stronger than previous interest rates hikes of 1999 or 2005. Regarding the magnitude of the cumulative increase since the first rate hike, the tightening cycle started in 2022 can be compared with the monetary easing of 2008, despite being more gradual than ECB interest rates reaction to the GFC.

Figure 1 – MRO rate, inflation, and the interest rate cycle

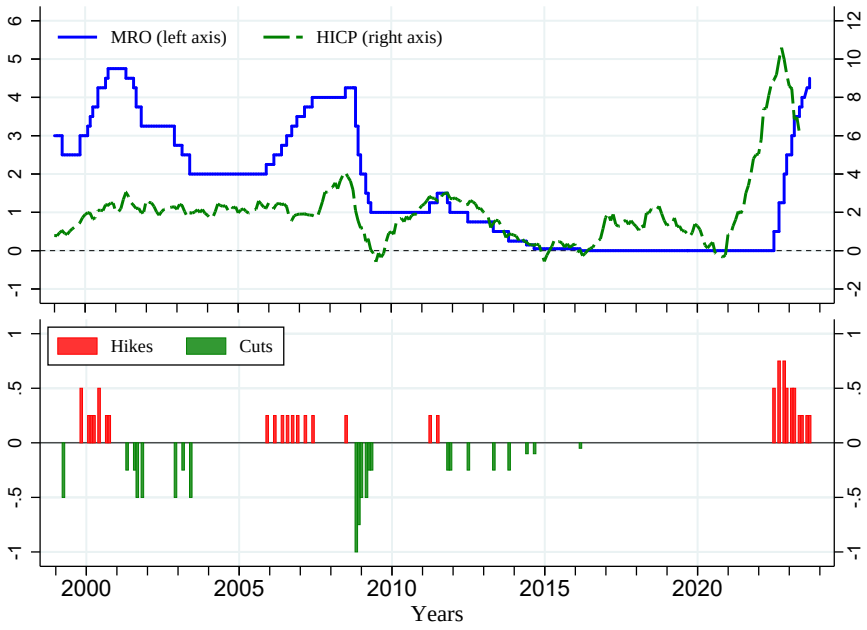

Note: The top panel shows the evolution of the main refinancing operations (MRO) rate and the annual growth rate of Harmonised Index of Consumer Prices (HICP) from January 1999 to September 2023. The bottom panel shows monthly changes in the MRO rate from January 1999 to September 2023.
Source: ECB and author's calculations.

Figure 2 – Pace of interest rate hikes and cuts

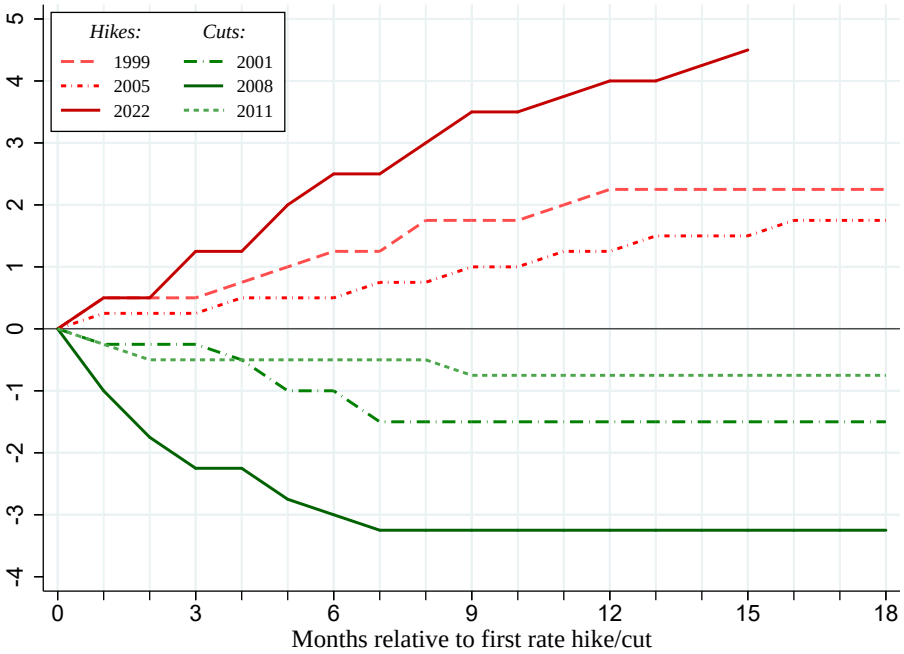

Note: The figure shows the evolution of the MRO rate since the first interest rate decision (interest rate hike or cut). On the x-axis, 0 denotes the month before the first rate hike/cut.
Source: ECB and author's calculations.

Overall, the ECB has proved to be equipped to meet big challenges in the euro area over the years. By using unconventional policies in reaction to the GFC and reviewing its strategy in 2021, it has shown its ability to adapt in a timely manner to manage economic fluctuations and provide financial assistance during downturns. Along with the current challenge posed by the trade-off between price and financial stability, a crucial question concerns ECB's ability to adapt its policy to address issues related to climate change.

Bibliography

Aastveit, K. A., Carriero, A., Clark, T. E., and Marcellino, M. (2017). Have standard vars remained stable since the crisis? *Journal of Applied Econometrics*, 32(5):931–951.

Aastveit, K. A., Furlanetto, F., and Loria, F. (2021). Has the fed responded to house and stock prices? a time-varying analysis. *The Review of Economics and Statistics*, pages 1–28.

Adrian, T., Boyarchenko, N., and Giannone, D. (2019). Vulnerable growth. *American Economic Review*, 109(4):1263–89.

Afonso, A., Arghyrou, M. G., Bagdatoglou, G., and Kontonikas, A. (2015a). On the time-varying relationship between emu sovereign spreads and their determinants. *Economic Modelling*, 44:363–371.

Afonso, A., Arghyrou, M. G., Gadea, M. D., and Kontonikas, A. (2018). "whatever it takes" to resolve the european sovereign debt crisis? bond pricing regime switches and monetary policy effects. *Journal of International Money and Finance*, 86:1–30.

Afonso, A., Arghyrou, M. G., and Kontonikas, A. (2015b). The determinants of sovereign bond yield spreads in the emu. *European Central Bank Working Paper Series No 1781*.

Afonso, A. and Jalles, J. T. (2019). Quantitative easing and sovereign yield spreads: Euro-area time-varying evidence. *Journal of International Financial Markets, Institutions and Money*, 58:208–224.

Ahmed, S., Levin, A., and Wilson, B. A. (2004). Recent us macroeconomic stability: good policies, good practices, or good luck? *Review of economics and statistics*, 86(3):824–832.

Aizenman, J., Hutchison, M., and Jinjarak, Y. (2013). What is the risk of european sovereign debt defaults? fiscal space, cds spreads and market pricing of risk. *Journal of International Money and Finance*, 34:37–59.

Albert, J. H. and Chib, S. (1993). Bayes inference via gibbs sampling of autoregressive time series subject to markov mean and variance shifts. *Journal of Business & Economic Statistics*,

11(1):1–15.

Altavilla, C., Brugnolini, L., Gürkaynak, R. S., Motto, R., and Ragusa, G. (2019). Measuring euro area monetary policy. *Journal of Monetary Economics*, 108:162–179.

Amir-Ahmadi, P., Matthes, C., and Wang, M.-C. (2016). Drifts and volatilities under measurement error: Assessing monetary policy shocks over the last century. *Quantitative Economics*, 7(2):591–611.

Amir-Ahmadi, P., Matthes, C., and Wang, M.-C. (2017). Measurement errors and monetary policy: Then and now. *Journal of Economic Dynamics and Control*, 79:66–78.

Amiti, M., Heise, S., and Wang, A. (2021). High import prices along the global supply chain feed through to us domestic prices. Technical report, Federal Reserve Bank of New York.

Andrade, P. and Ferroni, F. (2021). Delphic and odyssean monetary policy shocks: Evidence from the euro area. *Journal of Monetary Economics*, 117:816–832.

Andrade, P., Fourel, V., Ghysels, E., and Idier, J. (2014). The financial content of inflation risks in the euro area. *International Journal of Forecasting*, 30(3):648–659.

Andries, A. M., Ongena, S., and Sprincean, N. (2020). The covid-19 pandemic and sovereign bond risk. *Swiss Finance Institute Research Paper*, (20-42).

Angeloni, I. and Ehrmann, M. (2007). Euro area inflation differentials. *The BE Journal of Macroeconomics*, 7(1).

Arellano, C., Bai, Y., and Mihalache, G. (2023). Deadly debt crises: Covid-19 in emerging markets. *Review of Economic Studies*, forthcoming.

Arellano, C., Bai, Y., and Mihalache, G. P. (2020). Deadly debt crises: Covid-19 in emerging markets. Working Paper 27275, National Bureau of Economic Research.

Arias, J. E., Caldara, D., and Rubio-Ramirez, J. F. (2019). The systematic component of monetary policy in svars: An agnostic identification procedure. *Journal of Monetary Economics*, 101:1–13.

Arias, J. E., Rubio-Ramírez, J. F., and Waggoner, D. F. (2018). Inference based on structural vector autoregressions identified with sign and zero restrictions: Theory and applications. *Econometrica*, 86(2):685–720.

Aruoba, S. B., Mlikota, M., Schorfheide, F., and Villalvazo, S. (2022). Svars with occasionally-binding constraints. *Journal of Econometrics*, 231(2):477–499.

Atkeson, A. (2020). What will be the economic impact of covid-19 in the us? rough estimates

of disease scenarios. Working Paper 26867, National Bureau of Economic Research.

Auerbach, A. J. and Gorodnichenko, Y. (2013). Fiscal multipliers in recession and expansion. In Alesina, A. and Giavazzi, F., editors, *Fiscal Policy after the Financial Crisis*, pages 63–98. University of Chicago Press.

Augustin, P., Sokolovski, V., Subrahmanyam, M. G., and Tomio, D. (2020). In sickness and in debt: The covid-19 impact on sovereign credit risk. *Available at SSRN 3613432*.

Augustin, P., Sokolovski, V., Subrahmanyam, M. G., and Tomio, D. (2022). In sickness and in debt: The covid-19 impact on sovereign credit risk. *Journal of Financial Economics*, 143(3):1251–1274.

Azzalini, A. and Capitanio, A. (2003). Distributions generated by perturbation of symmetry with emphasis on a multivariate skew t-distribution. *Journal of the Royal Statistical Society: Series B (Statistical Methodology)*, 65:367–389.

Ball, L. and Mazumder, S. (2021). A phillips curve for the euro area. *International Finance*, 24(1):2–17.

Banerjee, R. N., Contreras, J., Mehrotra, A., and Zampolli, F. (2020). Inflation at risk in advanced and emerging market economies.

Barro, R. J., Ursúa, J. F., and Weng, J. (2020). The coronavirus and the great influenza pandemic: Lessons from the "spanish flu" for the coronavirus's potential effects on mortality and economic activity. Working Paper 26866, National Bureau of Economic Research.

Basu, S. and Bundick, B. (2017). Uncertainty shocks in a model of effective demand. *Econometrica*, 85(3):937–958.

Batini, N., Jackson, B., and Nickell, S. (2005). An open-economy new keynesian phillips curve for the uk. *Journal of Monetary Economics*, 52(6):1061–1071.

Bauer, M. D. and Rudebusch, G. D. (2014). The signaling channel for federal reserve bond purchases. *International Journal of Central Banking*, 10(3):233–289.

Bauer, M. D. and Rudebusch, G. D. (2016). Monetary policy expectations at the zero lower bound. *Journal of Money, Credit and Banking*, 48(7):1439–1465.

Baumeister, C. and Benati, L. (2013). Unconventional monetary policy and the great recession: Estimating the macroeconomic effects of a spread compression at the zero lower bound. *International Journal of Central Banking*, 9(2):165–212.

Baumeister, C. and Hamilton, J. D. (2015). Sign restrictions, structural vector autoregressions,

and useful prior information. *Econometrica*, 83(5):1963–1999.

Baumeister, C. and Hamilton, J. D. (2018). Inference in structural vector autoregressions when the identifying assumptions are not fully believed: Re-evaluating the role of monetary policy in economic fluctuations. *Journal of Monetary Economics*, 100:48–65.

Baxa, J., Horváth, R., and Vašíček, B. (2014). How does monetary policy change? evidence on inflation-targeting countries. *Macroeconomic Dynamics*, 18(3):593–630.

Baxter, M. and King, R. G. (1999). Measuring business cycles: approximate band-pass filters for economic time series. *Review of Economics and Statistics*, 81(4):575–593.

Beck, G. W., Hubrich, K., and Marcellino, M. (2009). Regional inflation dynamics within and across euro area countries and a comparison with the united states. *Economic Policy*, 24(57):142–184.

Belke, A. and Klose, J. (2013). Modifying taylor reaction functions in the presence of the zero-lower-bound—evidence for the ecb and the fed. *Economic Modelling*, 35:515–527.

Belke, A. and Polleit, T. (2007). How the ecb and the us fed set interest rates. *Applied Economics*, 39(17):2197–2209.

Belongia, M. T. and Ireland, P. N. (2016). The evolution of us monetary policy: 2000–2007. *Journal of Economic Dynamics and Control*, 73:78–93.

Benati, L. (2011). Would the bundesbank have prevented the great inflation in the united states? *Journal of Economic Dynamics and Control*, 35(7):1106–1125.

Benati, L. and Mumtaz, H. (2007). Us evolving macroeconomic dynamics: a structural investigation. *ECB Working Paper*, 746.

Benati, L. and Surico, P. (2008). Evolving us monetary policy and the decline of inflation predictability. *Journal of the European Economic Association*, 6(2-3):634–646.

Benigno, G., di Giovanni, J., Groen, J. J., and Noble, A. I. (2022). A new barometer of global supply chain pressures. Liberty street economics, Federal Reserve Bank of New York.

Benigno, P. (2004). Optimal monetary policy in a currency area. *Journal of international economics*, 63(2):293–320.

Bernanke, B. (2010). The economic outlook and monetary policy. In *Speech at the Federal Reserve Bank of Kansas City Economic Symposium, Jackson Hole, Wyoming*, volume 27.

Bernanke, B. S. (2003). Constrained discretion and monetary policy. *Remarks before the Money Marketeers of New York University, New York, New York*.

Bernanke, B. S. and Kuttner, K. N. (2005). What explains the stock market's reaction to federal reserve policy? *Journal of Finance*, 60(3):1221–1257.

Bernanke, B. S. and Mishkin, F. S. (1992). Central bank behavior and the strategy of monetary policy: observations from six industrialized countries. *NBER Macroeconomics Annual*, 7:183–228.

Blanchard, O., Cerutti, E., and Summers, L. (2015). Inflation and activity – two explorations and their monetary policy implications. Working Paper 21726, National Bureau of Economic Research.

Bognanni, M. (2018). A class of time-varying parameter structural vars for inference under exact or set identification. *Federal Reserve Bank of Cleveland Working Papers*, (18-11).

Boivin, J. (2006). Has u.s. monetary policy changed? evidence from drifting coefficients and real-time data. *Journal of Money, Credit and Banking*, 38(5):1149–1173.

Born, B., Müller, G. J., and Pfeifer, J. (2019). Does austerity pay off? *Review of Economics and Statistics*, pages 1–45.

Bostanci, G. and Yilmaz, K. (2020). How connected is the global sovereign credit risk network? *Journal of Banking & Finance*, 113:105761.

Botev, Z. I. (2017). The normal law under linear restrictions: simulation and estimation via minimax tilting. *Journal of the Royal Statistical Society Series B*, 79(1):125–148.

Brunnermeier, M. K. and Sannikov, Y. (2014). A macroeconomic model with a financial sector. *American Economic Review*, 104(2):379–421.

Caggiano, G., Castelnuovo, E., and Pellegrino, G. (2017). Estimating the real effects of uncertainty shocks at the zero lower bound. *European Economic Review*, 100:257–272.

Caldara, D., Cascaldi-Garcia, D., Cuba-Borda, P., and Loria, F. (2021). Understanding growth-at-risk: A markov-switching approach.

Caldara, D. and Herbst, E. (2019). Monetary policy, real activity, and credit spreads: Evidence from bayesian proxy svars. *American Economic Journal: Macroeconomics*, 11(1):157–92.

Campbell, J. R., Evans, C. L., Fisher, J. D., Justiniano, A., Calomiris, C. W., and Woodford, M. (2012). Macroeconomic effects of federal reserve forward guidance. *Brookings Papers on Economic Activity*, 42(1):1–80.

Canova, F. (2020). Should we trust cross sectional multiplier estimates? *CEPR Working Paper*, 15330.

Canova, F. and De Nicolo, G. (2002). Monetary disturbances matter for business fluctuations in the g-7. *Journal of Monetary Economics*, 49(6):1131–1159.

Canova, F. and Gambetti, L. (2009). Structural changes in the us economy: Is there a role for monetary policy? *Journal of Economic Dynamics and Control*, 33(2):477–490.

Canova, F. and Pérez Forero, F. J. (2015). Estimating overidentified, nonrecursive, time-varying coefficients structural vector autoregressions. *Quantitative Economics*, 6(2):359–384.

Caraiani, P. and Călin, A. C. (2018). The effects of monetary policy on stock market bubbles at zero lower bound: Revisiting the evidence. *Economics Letters*, 169:55–58.

Carriero, A., Clark, T. E., Marcellino, M., and Mertens, E. (2021). Forecasting with shadow-rate vars. *Federal Reserve Bank of Cleveland Working Papers*, (WP 21-09).

Carter, C. K. and Kohn, R. (1994a). On gibbs sampling for state space models. *Biometrika*, 81(3):541–553.

Carter, C. K. and Kohn, R. (1994b). On gibbs sampling for state space models. *Biometrika*, 81(3):541–553.

Casiraghi, M., Gaiotti, E., Rodano, L., and Secchi, A. (2016). Ecb unconventional monetary policy and the italian economy during the sovereign debt crisis. *International Journal of Central Banking*, 12(2):269–315.

Castelnuovo, E. (2006). The fed's preference for policy rate smoothing: overestimation due to misspecification? *Topics in Macroeconomics*, 6(2).

Castelnuovo, E. (2007). Taylor rules and interest rate smoothing in the euro area. *The Manchester School*, 75(1):1–16.

Castelnuovo, E. (2019). Yield curve and financial uncertainty: Evidence based on us data. *Australian Economic Review*, 52(3):323–335.

Castelnuovo, E. and Surico, P. (2004). Model uncertainty, optimal monetary policy and the preferences of the fed. *Scottish Journal of Political Economy*, 51(1):105–126.

Cavallino, P., De Fiore, F., et al. (2020). Central banks' response to covid-19 in advanced economies. *BIS Bulletin*, 21.

Cezar, R., Gigout, T., and Tripier, F. (2020). Cross-border investments and uncertainty: Firm-level evidence. *Journal of International Money and Finance*, page 102159.

Chan, J. C. and Eisenstat, E. (2018). Bayesian model comparison for time-varying parameter vars with stochastic volatility. *Journal of Applied Econometrics*, 33(4):509–532.

Checherita-Westphal, C. D., Leiner-Killinger, N., and Schildmann, T. (2023). Euro area inflation differentials: the role of fiscal policies revisited.

Chen, Q., Lombardi, M. J., Ross, A., and Zhu, F. (2017). Global impact of us and euro area unconventional monetary policies: a comparison. *BIS Working Papers*, 610.

Chow, G. C. (1960). Tests of equality between sets of coefficients in two linear regressions. *Econometrica: Journal of the Econometric Society*, pages 591–605.

Christensen, J. H. and Rudebusch, G. D. (2015). Estimating shadow-rate term structure models with near-zero yields. *Journal of Financial Econometrics*, 13(2):226–259.

Christiano, L., Motto, R., and Rostagno, M. (2008). Shocks, structures or monetary policies? the euro area and us after 2001. *Journal of Economic Dynamics and control*, 32(8):2476–2506.

Christiano, L. J., Eichenbaum, M. S., and Trabandt, M. (2015). Understanding the Great Recession. *American Economic Journal: Macroeconomics*, 7(1):110–167.

Christiano, L. J. and Fitzgerald, T. J. (2003). The band pass filter. *International Economic Review*, 44(2):435–465.

Cieslak, A., Morse, A., and Vissing-Jorgensen, A. (2019). Stock returns over the fomc cycle. *The Journal of Finance*, 74(5):2201–2248.

Clarida, R., Galí, J., and Gertler, M. (2000). Monetary policy rules and macroeconomic stability: evidence and some theory. *The Quarterly Journal of Economics*, 115(1):147–180.

Cloyne, J. S., Jordà, s., and Taylor, A. M. (2020). Decomposing the fiscal multiplier. Working Paper 26939, National Bureau of Economic Research.

Coenen, G., Montes-Galdon, C., and Schmidt, S. (2021). Macroeconomic stabilisation and monetary policy effectiveness in a low-interest-rate environment. *Journal of Economic Dynamics and Control*, page 104205.

Cœuré, B. (2014). Policy coordination in a multipolar world. In *5th annual Cusco conference, Central Reserve Bank of Peru and Reinventing Bretton Woods Committee, Cusco, July*, volume 22.

Cœuré, B. (2019). Heterogeneity and the ecb's monetary policy. In *Speech at the Banque de France Symposium & 34th SUERF Colloquium on the occasion of the 20th anniversary of the euro on "The Euro Area: Staying the Course through Uncertainties", Paris*, volume 29.

Cogley, T., Primiceri, G. E., and Sargent, T. J. (2010). Inflation-gap persistence in the us. *American Economic Journal: Macroeconomics*, 2(1):43–69.

Cogley, T. and Sargent, T. J. (2005). Drifts and volatilities: monetary policies and outcomes in the post wwii us. *Review of Economic Dynamics*, 8(2):262–302.

Coibion, O. (2012). Are the effects of monetary policy shocks big or small? *American Economic Journal: Macroeconomics*, 4(2):1–32.

Coibion, O. and Gorodnichenko, Y. (2015). Is the phillips curve alive and well after all? inflation expectations and the missing disinflation. *American Economic Journal: Macroeconomics*, 7(1):197–232.

Coibion, O., Gorodnichenko, Y., and Ulate, M. (2019). Is inflation just around the corner? the phillips curve and global inflationary pressures. In *AEA Papers and Proceedings*, volume 109, pages 465–69.

Consolo, A., Koester, G., Nickel, C., Porqueddu, M., and Smets, F. (2021). The need for an inflation buffer in the ecb's price stability objective: The role of nominal rigidities and inflation differentials. Technical report, ECB Occasional Paper.

Cook, T. and Hahn, T. (1989). The effect of changes in the federal funds rate target on market interest rates in the 1970s. *Journal of Monetary Economics*, 24(3):331–351.

Costantini, M., Fragetta, M., and Melina, G. (2014). Determinants of sovereign bond yield spreads in the emu: An optimal currency area perspective. *European Economic Review*, 70:337–349.

Couppey-Soubeyran, J., Perego, E., and Tripier, F. (2020). European banks and the covid-19 crash test. Technical report, CEPII Policy Brief 32.

Cox, J., Greenwald, D. L., and Ludvigson, S. C. (2020). What explains the covid-19 stock market? Working Paper 27784, National Bureau of Economic Research.

Creel, J. and Hubert, P. (2015). Has inflation targeting changed the conduct of monetary policy? *Macroeconomic Dynamics*, 19(1):1–21.

Crespo Cuaresma, J., Doppelhofer, G., Feldkircher, M., and Huber, F. (2019). Spillovers from us monetary policy: evidence from a time varying parameter global vector auto-regressive model. *Journal of the Royal Statistical Society: Series A (Statistics in Society)*.

Croushore, D. and Evans, C. L. (2006). Data revisions and the identification of monetary policy shocks. *Journal of Monetary Economics*, 53(6):1135–1160.

Crouzet, N. and Mehrotra, N. R. (2020). Small and large firms over the business cycle. *American Economic Review*, 110(11):3549–3601.

Davis, S. J., Liu, D., and Sheng, X. S. (2021). Stock prices, lockdowns, and economic activity in the time of coronavirus. Working Paper 28320, National Bureau of Economic Research.

De Pooter, M., Martin, R. F., and Pruitt, S. (2018). The liquidity effects of official bond market intervention. *Journal of Financial and Quantitative Analysis*, 53(1):243–268.

Debortoli, D., Galí, J., and Gambetti, L. (2019). On the empirical (ir) relevance ofthe zero lower bound constraint. *NBER Macroeconomics Annual 2019*, 34.

Debortoli, D., Galí, J., and Gambetti, L. (2020). On the empirical (ir) relevance of the zero lower bound constraint. *NBER Macroeconomics Annual*, 34(1):141–170.

Del Negro, M., Giannoni, M. P., and Schorfheide, F. (2015). Inflation in the Great Recession and New Keynesian Models. *American Economic Journal: Macroeconomics*, 7(1):168–196.

Del Negro, M., Lenza, M., Primiceri, G. E., and Tambalotti, A. (2020). What's up with the phillips curve? *Brookings Papers on Economic Activity*, pages 301–358.

Del Negro, M. and Primiceri, G. E. (2015). Time varying structural vector autoregressions and monetary policy: a corrigendum. *Review of Economic Studies*, 82(4):1342–1345.

Delatte, A.-L., Fouquau, J., and Portes, R. (2017). Regime-dependent sovereign risk pricing during the euro crisis. *Review of Finance*, 21(1):363–385.

Delatte, A.-L. and Guillaume, A. (2020). Covid 19: a new challenge for the emu. *CEPR Discussion Paper*, DP14848.

Dennis, R. (2006). The policy preferences of the us federal reserve. *Journal of Applied Econometrics*, 21(1):55–77.

Di Giovanni, J., Kalemli-Ozcan, S., Silva, A., and Yildirim, M. A. (2022). Global supply chain pressures, international trade, and inflation. Technical report, National Bureau of Economic Research.

Diebold, F. X. and Yilmaz, K. (2009). Measuring financial asset return and volatility spillovers, with application to global equity markets. *The Economic Journal*, 119(534):158–171.

Diegel, M. and Nautz, D. (2021). Long-term inflation expectations and the transmission of monetary policy shocks: Evidence from a svar analysis. *Journal of Economic Dynamics and Control*, 130:104192.

Doko Tchatoka, F., Groshenny, N., Haque, Q., and Weder, M. (2017). Monetary policy and indeterminacy after the 2001 slump. *Journal of Economic Dynamics and Control*, 82(C):83–95.

Draghi, M. (2019). Twenty years of the ecb's monetary policy. *Speech at ECB Forum on Central Banking, Sintra*, 18.

ECB (2005). Monetary policy and inflation differentials in a heterogeneous currency area. *Monthly Bulletin*, 5(2005):61–77.

ECB (2020a). The covid-19 crisis and its implications for fiscal policies. *ECB Monthly Bulletin June*.

ECB (2020b). Overview. *ECB Financial Stability Review, November*.

Eichenbaum, M. S., Rebelo, S., and Trabandt, M. (2020). The macroeconomics of epidemics. Working Paper 26882, National Bureau of Economic Research.

Ellington, M. (2022). The empirical relevance of the shadow rate and the zero lower bound. *Journal of Money, Credit and Banking*, 54(6):1605–1635.

Eo, Y. and Lie, D. (2020). The role of inflation target adjustment in stabilization policy. *Journal of Money, Credit and Banking*, 52(8):2007–2052.

Eser, F., Karadi, P., Lane, P. R., Moretti, L., and Osbat, C. (2020). The phillips curve at the ecb. *The Manchester School*, 88:50–85.

Eser, F. and Schwaab, B. (2016). Evaluating the impact of unconventional monetary policy measures: Empirical evidence from the ecb's securities markets programme. *Journal of Financial Economics*, 119(1):147–167.

Estrada, Á., Galí, J., and López-Salido, D. (2013). Patterns of convergence and divergence in the euro area. *IMF Economic Review*, 61(4):601–630.

Evans, C., Fisher, J., Gourio, F., and Krane, S. (2015). Risk management for monetary policy near the zero lower bound. *Brookings Papers on Economic Activity*, 2015(1):141–219.

Fagan, G., Henry, J., and Mestre, R. (2005). An area-wide model for the euro area. *Economic Modelling*, 22(1):39–59.

Falagiarda, M. and Reitz, S. (2015). Announcements of ecb unconventional programs: Implications for the sovereign spreads of stressed euro area countries. *Journal of International Money and Finance*, 53:276–295.

Faust, J. (1998). The robustness of identified var conclusions about money. *Carnegie-Rochester Conference Series on Public Policy*, 49:207–244.

Favara, G. and Imbs, J. (2015). Credit supply and the price of housing. *American Economic Review*, 105(3):958–92.

Favero, C. and Missale, A. (2012). Sovereign spreads in the eurozone: which prospects for a eurobond? *Economic Policy*, 27(70):231–273.

Favero, C. A. and Rovelli, R. (2003). Macroeconomic stability and the preferences of the fed: A formal analysis, 1961-98. *Journal of Money, Credit and Banking*, pages 545–556.

Ferrara, L., Mogliani, M., and Sahuc, J.-G. (2022). High-frequency monitoring of growth at risk. *International Journal of Forecasting*, 38(2):582–595.

Figueres, J. M. and Jarociński, M. (2020). Vulnerable growth in the euro area: Measuring the financial conditions. *Economics Letters*, 191:109126.

Forbes, K., Hjortsoe, I., and Nenova, T. (2018). The shocks matter: improving our estimates of exchange rate pass-through. *Journal of International Economics*, 114:255–275.

Fourçans, A. and Vranceanu, R. (2007). The ecb monetary policy: choices and challenges. *Journal of Policy Modeling*, 29(2):181–194.

Francis, N. R., Jackson, L. E., and Owyang, M. T. (2020). How has empirical monetary policy analysis in the us changed after the financial crisis? *Economic Modelling*, 84:309–321.

Fratzscher, M., Duca, M. L., and Straub, R. (2016). Ecb unconventional monetary policy: Market impact and international spillovers. *IMF Economic Review*, 64(1):36–74.

Frühwirth-Schnatter, S. (1994). Data augmentation and dynamic linear models. *Journal of time series analysis*, 15(2):183–202.

Gagnon, J. E. and Collins, C. G. (2019). Low Inflation Bends the Phillips Curve. Working Paper Series WP19-6, Peterson Institute for International Economics.

Galí, J., López-Salido, J. D., and Vallés, J. (2003). Technology shocks and monetary policy: assessing the fed's performance. *Journal of Monetary Economics*, 50(4):723–743.

Gambetti, L., Pappa, E., and Canova, F. (2008). The structural dynamics of us output and inflation: what explains the changes? *Journal of Money, Credit and Banking*, 40(2-3):369–388.

Garcia-Iglesias, J. M. (2007). How the european central bank decided its early monetary policy? *Applied Economics*, 39(7):927–936.

Garín, J., Lester, R., and Sims, E. (2019). Are supply shocks contractionary at the zlb? evidence from utilization-adjusted tfp data. *Review of Economics and Statistics*, 101(1):160–175.

Gavin, W. T., Keen, B. D., Richter, A. W., and Throckmorton, N. A. (2015). The zero lower bound, the dual mandate, and unconventional dynamics. *Journal of Economic Dynamics*

and Control, 55:14–38.

Georgiadis, G. (2016). Determinants of global spillovers from us monetary policy. *Journal of International Money and Finance*, 67:41–61.

Georgoutsos, D. A. and Migiakis, P. M. (2013). Heterogeneity of the determinants of euro-area sovereign bond spreads; what does it tell us about financial stability? *Journal of Banking & Finance*, 37(11):4650–4664.

Gerdesmeier, D. and Roffia, B. (2004). Empirical estimates of reaction functions for the euro area. *Swiss Society of Economics and Statistics*, 140(1):37–66.

Gerlach, S. (2011). Ecb repo rate setting during the financial crisis. *Economics Letters*, 112(2):186–188.

Gerlach, S. and Lewis, J. (2014a). Ecb reaction functions and the crisis of 2008. *International Journal of Central Banking*, 10(1):137–158.

Gerlach, S. and Lewis, J. (2014b). Zero lower bound, ecb interest rate policy and the financial crisis. *Empirical Economics*, 46(3):865–886.

Gerlach, S. and Schnabel, G. (2000). The taylor rule and interest rates in the emu area. *Economics Letters*, 67(2):165–171.

Geweke, J. (1992). Evaluating the accuracy of sampling-based approaches to the calculations of posterior moments. *Bayesian statistics*, 4:641–649.

Geweke, J. F. (1996). *Bayesian Inference for Linear Models Subject to Linear Inequality Constraints*, pages 248–263. Springer New York, New York, NY.

Ghysels, E., Idier, J., Manganelli, S., and Vergote, O. (2017). A high-frequency assessment of the ecb securities markets programme. *Journal of the European Economic Association*, 15(1):218–243.

Gibson, H. D., Hall, S. G., and Tavlas, G. S. (2016). The effectiveness of the ecb's asset purchase programs of 2009 to 2012. *Journal of Macroeconomics*, 47:45–57.

Gilchrist, S., Schoenle, R., Sim, J., and Zakrajšek, E. (2017). Inflation Dynamics during the Financial Crisis. *American Economic Review*, 107(3):785–823.

Giordani, P. (2004). An alternative explanation of the price puzzle. *Journal of Monetary Economics*, 51(6):1271–1296.

Givens, G. E. (2012). Estimating central bank preferences under commitment and discretion. *Journal of Money, Credit and Banking*, 44(6):1033–1061.

Gorter, J., Jacobs, J., and De Haan, J. (2008). Taylor rules for the ecb using expectations data. *Scandinavian Journal of Economics*, 110(3):473–488.

Gorter, J., Stolwijk, F., Jacobs, J. P., and de Haan, J. (2010). Ecb policy making and the financial crisis. *De Nederlandsche Bank Working Paper*, (272).

Greenspan, A. (2004). Risk and uncertainty in monetary policy. *American Economic Review*, 94(2):33–40.

Guerrieri, V., Lorenzoni, G., Straub, L., and Werning, I. (2020). Macroeconomic implications of covid-19: Can negative supply shocks cause demand shortages? Working Paper 26918, National Bureau of Economic Research.

Gürkaynak, R., Sack, B., and Swanson, E. (2005). Do actions speak louder than words? the response of asset prices to monetary policy actions and statements. *International Journal of Central Banking*, 1(1):55–93.

Haan, J. d. (2010). Inflation differentials in the euro area: a survey. In *The European Central Bank at Ten*, pages 11–32. Springer.

Halberstadt, A. and Krippner, L. (2016). The effect of conventional and unconventional euro area monetary policy on macroeconomic variables. *Bundesbank Discussion Paper*, 49.

Hamilton, J. D. (1989). A new approach to the economic analysis of nonstationary time series and the business cycle. *Econometrica*, 57:357–384.

Hamilton, J. D. (1994). *Time series analysis*. Princeton university press.

Hamilton, J. D. (2018). Why you should never use the hodrick-prescott filter. *Review of Economics and Statistics*, 100(5):831–843.

Hartmann, P. and Smets, F. (2018). The european central bank's monetary policy during its first 20 years. *Brookings Papers on Economic Activity*, 2018(2):1–146.

Hazell, J., Herreno, J., Nakamura, E., and Steinsson, J. (2022). The slope of the phillips curve: evidence from us states. *The Quarterly Journal of Economics*, 137(3):1299–1344.

He, Z. and Krishnamurthy, A. (2012). A model of capital and crises. *Review of Economic Studies*, 79(2):735–777.

He, Z. and Krishnamurthy, A. (2013). Intermediary asset prices. *American Economic Review*, 103(2):1–43.

Herbst, E. P. and Johannsen, B. K. (2020). Bias in local projections. *Finance and Economics Discussion Series*, 2020-010.

Hodrick, R. J. and Prescott, E. C. (1997). Postwar us business cycles: an empirical investigation. *Journal of Money, Credit and Banking*, pages 1–16.

Horvath, R. and Voslarova, K. (2016). International spillovers of ecb's unconventional monetary policy: the effect on central europe. *Applied Economics*, 49(24):2352–2364.

Hubrich, K. and Tetlow, R. J. (2015). Financial stress and economic dynamics: The transmission of crises. *Journal of Monetary Economics*, 70:100–115.

Hutchinson, J. and Smets, F. (2017). Monetary policy in uncertain times: Ecb monetary policy since june 2014. *The Manchester School*, 85:e1–e15.

Ikeda, D., Li, S., Mavroeidis, S., and Zanetti, F. (2020). Testing the effectiveness of unconventional monetary policy in japan and the united states. *arXiv preprint arXiv:2012.15158*.

Inoue, A. and Rossi, B. (2021). A new approach to measuring economic policy shocks, with an application to conventional and unconventional monetary policy. *Quantitative Economics*, 12(4):1085–1138.

Issing, O., Angeloni, I., Gaspar, V., Klöckers, H.-J., Masuch, K., Nicoletti-Altimari, S., Rostagno, M., and Smets, F. (2003). Background studies for the ecb's evaluation of its monetary policy strategy. *ECB*.

Iwata, S. and Wu, S. (2006). Estimating monetary policy effects when interest rates are close to zero. *Journal of Monetary Economics*, 53(7):1395–1408.

Jäger, J. and Grigoriadis, T. (2017). The effectiveness of the ecb's unconventional monetary policy: Comparative evidence from crisis and non-crisis euro-area countries. *Journal of International Money and Finance*, 78:21–43.

Johannsen, B. K. and Mertens, E. (2021). A time-series model of interest rates with the effective lower bound. *Journal of Money, Credit and Banking*, 53(5):1005–1046.

Jordà, Ò. (2005). Estimation and inference of impulse responses by local projections. *American Economic Review*, 95(1):161–182.

Jordà, Ò., Schularick, M., and Taylor, A. M. (2013). When credit bites back. *Journal of Money, Credit and Banking*, 45(s2):3–28.

Jordà, Ò., Schularick, M., and Taylor, A. M. (2015). Leveraged bubbles. *Journal of Monetary Economics*, 76:S1–S20.

Jordà, Ò., Schularick, M., and Taylor, A. M. (2016). The great mortgaging: housing finance, crises and business cycles. *Economic policy*, 31(85):107–152.

Jordà, Ò., Schularick, M., and Taylor, A. M. (2020a). The effects of quasi-random monetary experiments. *Journal of Monetary Economics*, 112:22–40.

Jordà, Ò., Singh, S. R., and Taylor, A. M. (2020b). Longer-run economic consequences of pandemics? *The Review of Economics and Statistics*, pages 1–29.

Jordà, Ò. and Taylor, A. M. (2016). The time for austerity: estimating the average treatment effect of fiscal policy. *The Economic Journal*, 126(590):219–255.

Keating, J. W., Kelly, L. J., Smith, A. L., and Valcarcel, V. J. (2019). A model of monetary policy shocks for financial crises and normal conditions. *Journal of Money, Credit and Banking*, 51(1):227–259.

Kekre, R. (2022). Optimal currency areas with labor market frictions. *American Economic Journal: Macroeconomics*, 14(2):44–95.

Kiley, M. T. and Roberts, J. M. (2017). Monetary policy in a low interest rate world. *Brookings Papers on Economic Activity*, 2017(1):317–396.

Kilian, L. and Zhou, X. (2021). Oil prices, gasoline prices and inflation expectations. *Journal of Applied Econometrics*.

Kilponen, J., Laakkonen, H., and Vilmunen, J. (2015). Sovereign risk, european crisis resolution policies and bond yields. *International Journal of Central Banking*, 11(2):285–323.

Kim, C.-J. (1994). Dynamic linear models with Markov-switching. *Journal of Econometrics*, 60(1-2):1–22.

Kim, C.-J. and Nelson, C. R. (2006). Estimation of a forward-looking monetary policy rule: A time-varying parameter model using ex post data. *Journal of Monetary Economics*, 53(8):1949–1966.

Kim, K., Laubach, T., and Wei, M. (2020). Macroeconomic effects of large-scale asset purchases: New evidence. Technical report, Board of Governors of the Federal Reserve System (US).

Kim, S., Shephard, N., and Chib, S. (1998). Stochastic volatility: likelihood inference and comparison with arch models. *The Review of Economic Studies*, 65(3):361–393.

Klose, J. and Tillmann, P. (2021). Covid-19 and financial markets: A panel analysis for european countries. *Jahrbücher für Nationalökonomie und Statistik*, forthcoming.

Koenker, R. and Ng, P. (2005). Inequality constrained quantile regression. *Sankhyā: The Indian Journal of Statistics (2003-2007)*, 67(2):418–440.

Koop, G., Leon-Gonzalez, R., and Strachan, R. W. (2009). On the evolution of the monetary

policy transmission mechanism. *Journal of Economic Dynamics and Control*, 33(4):997–1017.

Kortela, T. and Nelimarkka, J. (2020). The effects of conventional and unconventional monetary policy: identification through the yield curve. *Bank of Finland Research Discussion Paper*, (3).

Kremer, M., Lo Duca, M., and Holló, D. (2012). Ciss - a composite indicator of systemic stress in the financial system. Working Paper Series 1426, European Central Bank.

Krippner, L. (2013). Measuring the stance of monetary policy in zero lower bound environments. *Economics Letters*, 118(1):135–138.

Krippner, L. (2020). A note of caution on shadow rate estimates. *Journal of Money, Credit and Banking*, 52(4):951–962.

Krishnamurthy, A., Nagel, S., and Vissing-Jorgensen, A. (2018). Ecb policies involving government bond purchases: Impact and channels. *Review of Finance*, 22(1):1–44.

Kuttner, K. N. (2001). Monetary policy surprises and interest rates: Evidence from the fed funds futures market. *Journal of monetary economics*, 47(3):523–544.

Leombroni, M., Vedolin, A., Venter, G., and Whelan, P. (2021). Central bank communication and the yield curve. *Journal of Financial Economics*, 141(3):860–880.

Lhuissier, S. (2017). Financial intermediaries' instability and euro area macroeconomic dynamics. *European Economic Review*, 98:49–72.

Lhuissier, S. (2022). Financial conditions and macroeconomic downside risks in the euro area. *European Economic Review*, 143:104046.

Lhuissier, S., Mojon, B., and Rubio-Ramirez, J. F. (2020). Does the liquidity trap exist? *Banque de France Working Paper*, 762.

Lhuissier, S. and Nguyen, B. (2021). The dynamic effects of the ecb's asset purchases: a survey-based identification. Technical report, Banque de France WP 806.

Lombardi, M. and Zhu, F. (2018). A shadow policy rate to calibrate us monetary policy at the zero lower bound. *International Journal of Central Banking*, 14(5):305–346.

López-Salido, J. D. and Loria, F. (2022). Inflation at risk. Finance and Economics Discussion Series 2020-013, Board of Governors of the Federal Reserve System (U.S.).

Lubik, T. A. and Schorfheide, F. (2004). Testing for indeterminacy: an application to us monetary policy. *American Economic Review*, 94(1):190–217.

Lucas, R. E. (1976). Econometric policy evaluation: A critique. *Carnegie-Rochester Conference*

Series on Public Policy, 1:19–46.

Lucca, D. O. and Moench, E. (2015). The pre-fomc announcement drift. *The Journal of finance*, 70(1):329–371.

Lütkepohl, H. (2005). *New introduction to multiple time series analysis*. Springer Science & Business Media.

Manganelli, S. and Wolswijk, G. (2009). What drives spreads in the euro area government bond market? *Economic Policy*, 24(58):191–240.

Matheson, T. and Stavrev, E. (2013). The great recession and the inflation puzzle. *Economics Letters*, 120(3):468–472.

Mavroeidis, S. (2021). Identification at the zero lower bound. *Econometrica*, 89(6):2855–2885.

Mishkin, F. S. (2009). Is monetary policy effective during financial crises? *American Economic Review*, 99(2):573–77.

Mouabbi, S. and Sahuc, J.-g. (2019). Evaluating the macroeconomic effects of the ecb's unconventional monetary policies. *Journal of Money, Credit and Banking*, 51(4):831–858.

Mumtaz, H. and Surico, P. (2009). Time-varying yield curve dynamics and monetary policy. *Journal of Applied Econometrics*, 24(6):895–913.

Newey, W. K. and West, K. D. (1987). A simple, positive semi-definite, heteroskedasticity and autocorrelationconsistent covariance matrix. *Econometrica*, 55(3):703–708.

Nikolsko-Rzhevskyy, A., Papell, D. H., and Prodan, R. (2014). Deviations from rules-based policy and their effects. *Journal of Economic Dynamics and Control*, 49:4–17.

Okun, A. (1962). Potential gnp: its measurement and significance. In *American Statistical Association: Proceedings of the Business and Economics Statistics Section*, pages 98–104.

Orphanides, A. (2001). Monetary policy rules based on real-time data. *American Economic Review*, 91(4):964–985.

Orphanides, A. (2003). Historical monetary policy analysis and the taylor rule. *Journal of monetary economics*, 50(5):983–1022.

Orphanides, A. (2004). Monetary policy rules, macroeconomic stability, and inflation: A view from the trenches. *Journal of Money, Credit and Banking*, 36(2):151–175.

Ozlale, U. (2003). Price stability vs. output stability: tales of federal reserve administrations. *Journal of Economic Dynamics and Control*, 27(9):1595–1610.

Pacicco, F., Vena, L., and Venegoni, A. (2019). Market reactions to ecb policy innovations: A

cross-country analysis. *Journal of International Money and Finance*, 91:126–137.

Pasricha, G. K., Falagiarda, M., Bijsterbosch, M., and Aizenman, J. (2018). Domestic and multilateral effects of capital controls in emerging markets. *Journal of International Economics*, 115:48–58.

Peersman, G. (2022). International Food Commodity Prices and Missing (Dis)Inflation in the Euro Area. *The Review of Economics and Statistics*, 104(1):85–100.

Peersman, G. and Smets, F. (2003). The monetary transmission mechanism in the euro area: evidence from var analysis. In *Monetary policy transmission in the Euro area*, pages 36–55. Cambridge University Press.

Peltonen, T. A., Klaus, B., and Duprey, T. (2015). Dating systemic financial stress episodes in the EU countries. Working Paper Series 1873, European Central Bank.

Plagborg-Møller, M., Reichlin, L., Ricco, G., and Hasenzagl, T. (2020). When is growth at risk? *Brookings Papers on Economic Activity*, 2020(1):167–229.

Plante, M., Richter, A. W., and Throckmorton, N. A. (2017). The zero lower bound and endogenous uncertainty. *The Economic Journal*, 128(611):1730–1757.

Potjagailo, G. (2017). Spillover effects from euro area monetary policy across europe: A factor-augmented var approach. *Journal of International Money and Finance*, 72:127–147.

Primiceri, G. E. (2005). Time varying structural vector autoregressions and monetary policy. *Review of Economic Studies*, 72(3):821–852.

Prüser, J. (2021). The horseshoe prior for time-varying parameter vars and monetary policy. *Journal of Economic Dynamics and Control*, 129:104188.

Ramey, V. A. and Zubairy, S. (2018). Government spending multipliers in good times and in bad: evidence from us historical data. *Journal of Political Economy*, 126(2):850–901.

Reichlin, L., Adam, K., McKibbin, W. J., McMahon, M., Reis, R., Ricco, G., and Weder di Mauro, B. (2021). *The ECB strategy: The 2021 review and its future*. Centre for Economic Policy Research.

Reifschneider, D. and Williams, J. C. (2000). Three lessons for monetary policy in a low-inflation era. *Journal of Money, Credit and Banking*, pages 936–966.

Rogers, J. H., Scotti, C., and Wright, J. H. (2018). Unconventional monetary policy and international risk premia. *Journal of Money, Credit and Banking*, 50(8):1827–1850.

Rossi, B. (2021). Identifying and estimating the effects of unconventional monetary policy:

How to do it and what have we learned? *The Econometrics Journal*, 24(1):C1–C32.

Rubio-Ramirez, J. F., Waggoner, D. F., and Zha, T. (2010). Structural vector autoregressions: Theory of identification and algorithms for inference. *The Review of Economic Studies*, 77(2):665–696.

Rudebusch, G. D. (2001). Is the fed too timid? monetary policy in an uncertain world. *Review of Economics and Statistics*, 83(2):203–217.

Sahuc, J.-G. and Smets, F. (2008). Differences in interest rate policy at the ecb and the fed: An investigation with a medium-scale dsge model. *Journal of Money, Credit and Banking*, 40(2-3):505–521.

Salisu, A. A., Ademuyiwa, I., and Isah, K. O. (2018). Revisiting the forecasting accuracy of phillips curve: the role of oil price. *Energy Economics*, 70:334–356.

Sauer, S. and Sturm, J.-E. (2007). Using taylor rules to understand european central bank monetary policy. *German Economic Review*, 8(3):375–398.

Schularick, M. and Steffen, S. (2020). A protective shield for europe's banks. Technical report, mimeo.

Sims, C. A. (1980). Macroeconomics and reality. *Econometrica*, 48(1):1–48.

Sims, C. A., Waggoner, D. F., and Zha, T. (2008). Methods for inference in large multiple-equation markov-switching models. *Journal of Econometrics*, 146:255–274.

Sims, C. A. and Zha, T. (2006a). Does monetary policy generate recessions? *Macroeconomic Dynamics*, 10(2):231–272.

Sims, C. A. and Zha, T. (2006b). Were there regime switches in us monetary policy? *American Economic Review*, 96(1):54–81.

Sims, E. and Wu, J. C. (2020). Are qe and conventional monetary policy substitutable? *International Journal of Central Banking*, 16(1):195–230.

Smets, F. and Wouters, R. (2005). Comparing shocks and frictions in us and euro area business cycles: a bayesian dsge approach. *Journal of Applied Econometrics*, 20(2):161–183.

Stock, J. H. and Watson, M. W. (2002). Has the business cycle changed and why? *NBER macroeconomics annual*, 17:159–218.

Stroud, J. R., Müller, P., and Polson, N. G. (2003). Nonlinear state-space models with state-dependent variances. *Journal of the American Statistical Association*, 98(462):377–386.

Surico, P. (2007a). The fed's monetary policy rule and us inflation: The case of asymmetric

preferences. *Journal of Economic Dynamics and Control*, 31(1):305–324.

Surico, P. (2007b). The monetary policy of the european central bank. *Scandinavian Journal of Economics*, 109(1):115–135.

Swanson, E. T. (2018). The federal reserve is not very constrained by the lower bound on nominal interest rates. *Brookings Papers on Economic Activity*, 49(Fall):555–572.

Swanson, E. T. (2021). Measuring the effects of federal reserve forward guidance and asset purchases on financial markets. *Journal of Monetary Economics*, 118:32–53.

Swanson, E. T. and Williams, J. C. (2014). Measuring the effect of the zero lower bound on medium-and longer-term interest rates. *American Economic Review*, 104(10):3154–85.

Szczerbowicz, U. (2015). The ecb unconventional monetary policies: have they lowered market borrowing costs for banks and governments? *International Journal of Central Banking*, 11(4):91–127.

Taylor, J. B. (1993). Discretion versus policy rules in practice. In *Carnegie-Rochester conference series on public policy*, volume 39, pages 195–214. Elsevier.

Taylor, J. B. (1999). The robustness and efficiency of monetary policy rules as guidelines for interest rate setting by the european central bank. *Journal of Monetary Economics*, 43(3):655–679.

Tenreyro, S. and Thwaites, G. (2016). Pushing on a string: Us monetary policy is less powerful in recessions. *American Economic Journal: Macroeconomics*, 8(4):43–74.

Tillmann, P. (2020). Monetary policy uncertainty and the response of the yield curve to policy shocks. *Journal of Money, Credit and Banking*, 52(4):803–833.

Trebesch, C. and Zettelmeyer, J. (2018). Ecb interventions in distressed sovereign debt markets: The case of greek bonds. *IMF Economic Review*, 66(2):287–332.

Uhlig, H. (2005). What are the effects of monetary policy on output? results from an agnostic identification procedure. *Journal of Monetary Economics*, 52(2):381–419.

Ullrich, K. (2005). Comparing the fed and the ecb using taylor-type rules. *Applied Economics Quarterly*, 51(3):247–266.

Vissing Jorgensen, A. and Krishnamurthy, A. (2011). The effects of quantitative easing on interest rates: Channels and implications for policy. *Brookings Papers on Economic Activity*, 43(2):215–287.

Wieland, J. F. (2019). Are negative supply shocks expansionary at the zero lower bound?

Journal of Political Economy, 127(3):973–1007.

Wolf, C. K. (2020). Svar (mis) identification and the real effects of monetary policy shocks. *American Economic Journal: Macroeconomics*, 12(4):1–32.

Woodford, M. (2012). Methods of policy accommodation at the interest-rate lower bound. In *Proceedings-Economic Policy Symposium-Jackson Hole*, pages 185–288. Federal Reserve Bank of Kansas City.

Wu, J. C. and Xia, F. D. (2016). Measuring the macroeconomic impact of monetary policy at the zero lower bound. *Journal of Money, Credit and Banking*, 48(2-3):253–291.

Wu, J. C. and Zhang, J. (2019). A shadow rate new keynesian model. *Journal of Economic Dynamics and Control*, 107:103728.

Yellen, J. L. (2011). Unconventional monetary policy and central bank communications. *Board of Governors of the Federal Reserve System (US) Speech*, (Feb 25).